Università di Pisa

Dipartimento di Fisica

Corso di Laurea Magistrale in Fisica

Anno Accademico 2013/2014

Tesi di Laurea Magistrale

Quantum Recovery Operations

Candidato:
Matteo Ippoliti

Relatori:
Prof. Vittorio Giovannetti
Dott. Leonardo Mazza

Abstract

In order to harness the informational power of quantum physics, one must be able to overcome the challenge of *decoherence*. Decoherence is an ubiquitous effect arising from the interaction of a quantum system with its environment. Such interactions generally spoil the quantum coherence of the system, thus degrading its information content.

This thesis deals with the general problem of fighting decoherence in quantum memories. Quantum memories are systems in which a quantum bit can be stored reliably over long periods of time; they represent a necessary intermediate step towards the realization of fully functional quantum computers.

The main focus of the thesis is on the application of *quantum recovery operations* to this general problem. A recovery operation is a physical evolution that tries to undo the effect of a previous noise. Even though decoherence processes are generally irreversible, part of the information that is removed from the original encoding subspace may still be recoverable from other regions of the state space of the memory. Thus, by applying a suitable recovery operation, the fidelity between the encoded state and the recovered one can be improved. By optimizing over all physical recovery operations, a reliable measure for the performance of the quantum memory can be defined.

The thesis is structured as follows. After an introduction to the fundamental concepts in quantum information theory, we define recovery operations and present some results about them, including an upper bound on the optimal recovery fidelity that can be used to evaluate the performance of quantum memory models. We then discuss an application of these concepts, which exploits a suitably engineered form of dissipation to implement a continuous-time version of quantum error correction. Then, after a discussion on how Hamiltonians can be used to protect quantum information, we turn to a second application, which is based on unpaired Majorana modes in condensed matter systems. These exotic quasi-particles have some remarkable properties that suggest they could be used to store quantum information in a way that is immune from local perturbations. We discuss the performance of Majorana-based quantum memories in the open-system scenario, using analytically solvable toy models, and focus on how the results relate to the concepts of *locality* and *parity*, which are generally assumed to underpin the efficacy of Majorana-based quantum memories.

Contents

Abbreviations

CP	**C**ompletely **P**ositive
TP	**T**race **P**reserving
QEC	**Q**uantum **E**rror **C**orrection
QECC	**Q**uantum **E**rror-**C**orrecting **C**ode
CTQEC	**C**ontinuous-**T**ime **Q**uantum **E**rror **C**orrection
ADR	**A**symptotic **D**ecay **R**ate
LRB	**L**ieb-**R**obinson **B**ound

Symbols

$\mathcal{H}_n$	n-qubit Hilbert space
$\mathcal{S}(\mathcal{H})$	space of states (density matrices) on a Hilbert space $\mathcal{H}$
$\mathcal{B}(\mathcal{H})$	algebra of linear operators on a Hilbert space $\mathcal{H}$
$\mathfrak{F}_n$	n-mode fermionic Fock space
ρ	density matrix (qubit)
$\hat{\rho}$	density matrix (larger system)
$\mathbf{1}$, σ_0	identity matrix (qubit)
$\hat{\mathbf{1}}$, I	identity matrix (larger system)
X, Y, Z; σ_1, σ_2, σ_3	Pauli matrices (qubit)
$\boldsymbol{\sigma}$	vector of Pauli matrices (qubit)
$\hat{\sigma}_0^L$, $\hat{\sigma}_1^L$, $\hat{\sigma}_2^L$, $\hat{\sigma}_3^L$	encoded logical matrices (larger system)
$\hat{\boldsymbol{\sigma}}^L$	vector of encoded logical matrices (larger system)
$\mathcal{D}_t$	decoherence channel
$\mathcal{R}$	recovery operation
$\mathcal{L}$	Lindbladian
P	code-space projector
$P_{\mathbf{s}}$	projector onto the $\mathbf{s}$-syndrome subspace
$\hat{a}$, $\hat{a}^\dagger$; $\hat{b}$, $\hat{b}^\dagger$	fermionic (Dirac) operators
$\hat{c}$; $\hat{\gamma}$	fermionic (Majorana) operators
$\hat{P}_f$	fermionic parity operator

Introduction

Quantum-mechanical systems are believed to be more powerful than classical ones at processing information. Several problems exist that a hypothetical *quantum computer* could solve much faster than any imaginable classical device; some of those problems are of great practical importance. However, in order to harness the power of quantum information, the ubiquitous phenomenon of *decoherence* must be dealt with. Decoherence represents a challenge not only for the realization of quantum computers, but also for the more basic task of building a *quantum memory*, i.e. a quantum system that is able to preserve a set of quantum states reliably over long times.

This thesis focuses on the problem of protecting quantum memories from decoherence, and especially on the role that can be played by *recovery operations* in this framework. We study the application of recovery operations to two specific classes of quantum memories: quantum memories based on *dissipation*, and quantum memories that encode information in *unpaired Majorana modes*.

Quantum Information Theory

Quantum Information Theory can be defined as the study of information processing tasks that can be accomplished using quantum mechanical systems [1]. The idea of using quantum mechanics to process information dates back to at least the 1970's [2], and was made popular by Feynman in 1981 [3]. This interest was originally motivated by the problem of simulating quantum physics on a computer. Since the vector $|\psi\rangle$ describing the quantum state of an N-particle system is specified by a number of coefficients that scales *exponentially* with N, simulations on classical computers would be generally inefficient: an exponential amount of classical bits would be needed to track the evolution of all the coefficients. This means that in order to simulate N quantum subsystems, $\mathcal{O}(e^N)$ classical ones are needed. But if the subsystems that constitute the computer were quantum-mechanical, instead of classical, then a polynomial number of them would suffice, thus allowing efficient simulations [4].

The interest in Quantum Information Theory grew considerably when it was realized that quantum computers would be useful not only for the simulation of quantum physics, but also for the solution of classical problems. Some *quantum algorithms* were proven to be faster than their classical counterparts, including Shor's algorithm for factoring prime numbers [5] and Grover's search algorithm [6]. In the following years Quantum Error Correction (QEC) was proven to be possible [7, 8]. QEC is a mechanism based on redundancy; in order to correct the errors that can occur in the elementary constituents of the computer, more elementary constituents must be added, which in turn causes exposition to a higher number of possible errors. It has been shown that, if the error rate of the elementary constituents is lower than a certain threshold, a suitably designed redundant encoding will suppress the error rate of the whole computer. Otherwise, redundancy introduces more errors than it can correct, and the error rate for the whole computer diverges. This result is known as the *fault-tolerance threshold theorem* [9].

Passive Protection from Decoherence

Those discoveries proved that quantum computation is possible, at least in principle: if we were able to manipulate quantum states fast and reliably enough, then fault-tolerant QEC would allow us to overcome the problem of decoherence.

Unfortunately, in most models the accuracy thresholds required for fault-tolerance are very strict, with estimates usually ranging between 10^{-3} and 10^{-6} errors per operation. Present-day experiments are still far from reaching such high accuracies, and it is still unclear whether or not future technological advancements will ever bring the achievable accuracies above the required thresholds: manipulating quantum systems while keeping their quantum coherence intact is generally very difficult. Even "doing nothing" with quantum information is hard: real quantum systems are never exactly closed; interactions with the environment are ubiquitous. Such interactions degrade the quantum coherence of the system, thus making the mere preservation of quantum states a difficult task. This effect is known as *decoherence* and is the foremost adversary of quantum information.

Because of decoherence, the actual realization of a fully functional quantum computer remains an open problem in practice. Moreover, even the preliminary goal of realizing a reliable *quantum memory* is challenging. Even though in principle fault-tolerant quantum error correction provides a solution to this problem, the severe accuracy requirements make it an impractical approach, at least for the foreseeable future. This problem led to the development of several alternative approaches in which information is not protected by the repeated intervention of an external agent, as in the fault-tolerant QEC paradigm, but rather from the physics that governs the hardware. This class of approaches will be denoted generically as *passive*, as opposed to the "active" nature of fault-tolerant QEC.

Passive protection schemes are particularly well suited for the realization of quantum memories: they reproduce the idea of a classical hard drive, in which magnetic interactions protect the encoded information over long times without the need of error correction. They may instead be less suited for the realization of quantum computers, since the physical effects that oppose decoherence may also forbid coherent manipulations.

This thesis focuses on two different approaches for the realization of passive quantum memories. In the first one, a particular form of dissipation is engineered so as to implement an automatic, continuous-time version of QEC. The second approach is based on the recent theoretical discovery of the emergence of unpaired Majorana modes in solid-state systems, whose non-local nature might be beneficial against local perturbations.

Quantum memories based on dissipation

Until recently, dissipation was only associated to noise and decoherence, and thus considered harmful for quantum information. However, it has been realized by Verstraete, Wolf and Cirac [10] that dissipation can also be a useful resource for several information processing tasks, including computation and state-engineering. Their ideas have then been realized in systems of trapped ions [11, 12]. Finally, Pastawski *et al.* provided a general framework for the use of dissipation as a resource for quantum memories [13].

Continuous-time quantum error correction (CTQEC) is much older that those recent works. The first proposal, by Paz and Zurek [14], dates back to 1997, soon after the discovery of QEC. It was originally proposed as a mathematical way of modeling fast repeated QEC operations. In 2005 Sarovar and Milburn proposed a scheme for CTQEC that used a simple cooling process to physically implement the required continuous-time dynamics [15]. CTQEC can thus be seen as a dissipation-based strategy for protecting information. The main disadvantage of CTQEC over more general dissipation-based quantum memories [13] is that the required dissipators are generally non-local, thus making the whole approach non-scalable. Nonetheless, CTQEC provides instances of dissipation-based quantum memories which are interesting by themselves; and provided the underlying QECC is small enough, the physical implementation of CTQEC is probably less demanding than the implementation of standard fault-tolerant QEC in discrete time.

In this thesis we consider the general scheme for translating a stabilizer quantum error-correcting code into a dissipation-based quantum memory, and analyze in detail the two simplest examples. The known results about the simplest instance (the 3-qubit code) are re-derived analytically; then, the 5-qubit perfect code is studied numerically in a way that can be straightforwardly generalized to larger codes by employing enough computational power.

Quantum memories based on Majorana modes

Since the first proposal by Kitaev in 2000 [16], the possibility of employing emergent Majorana zero-modes to store quantum information has gained widespread popularity. Loosely speaking, Majorana modes are "halves" of a regular fermionic Dirac mode; they have never been observed directly because they are usually paired by a mass term to form Dirac modes. However, it has been pointed out [17, 18] that vortices of some peculiar 2-dimensional superconductors may host *unpaired* Majorana modes. The absence of pairing means that two "halves" of a Dirac mode can be arbitrarily far apart from one another. This non-locality, along with the fact that these zero-modes are usually protected by a symmetry or by the topology of the system, has made them very popular candidates as constituents of a quantum memory – though no conclusive result about the efficacy of such schemes is known yet.

Majorana particles are intrinsically interesting, since they would provide the first instance of *non-Abelian anyons* ever observed in nature. This exotic feature, along with the potential applications in quantum information, has made the pursuit of Majorana physics one of the most exciting challenges of both theoretical and experimental condensed matter research [19].

In this thesis we study Majorana-based quantum memories by analyzing toy-models that are simple enough to allow an exact analytical evaluation of the memory performance. From those results, some general conclusions can be drawn about the physical factors that underpin the efficacy of Majorana-based memories.

Outline of the Thesis

This thesis is structured as follows:

1. Chapter 1 provides all the necessary background in Quantum Information theory. It consists of standard textbook material [1] and can be safely skipped by expert readers.

2. Chapter 2 presents the concept of *recovery operation*, which is of central importance for the study of passive quantum memories. Several mathematical tools are introduced, the most important being an upper bound to the amount of information that can be extracted from a memory as a function of time. The material in this Chapter is mostly drawn from [20].

3. Chapter 3 presents the continuous-time implementation of QECCs, in the framework of dissipation-based quantum memories. The Chapter begins with a general introduction to the standard theory of QEC [7], which can be skipped by expert readers. Then the continuous-time version is discussed. The 3-qubit and 5-qubit QECCs are studied in

detail; the known results about the 3-qubit code are re-derived and given a geometric interpretation, while the 5-qubit code is studied numerically.

4. Chapter 4 is a brief review of how Hamiltonians can be used to protect quantum information: an important distinction between two regimes is presented, and the difference between them is illustrated through a concrete example.

5. Chapter 5 discusses Majorana-based quantum memories. After a brief introduction to Majorana modes in condensed matter from both a theoretical and experimental point of view, the encoding of information in a system with unpaired Majorana modes is presented in general. Three toy-models are then introduced and studied analytically using theoretical tools from Chapters 2 and 4. Finally the concepts that are generally assumed to underpin the efficacy of Majorana memories are reviewed critically in light of the memory performance of the toy-models.

6. Chapter 6 summarizes the results of this work and discusses some relevant open problems that may be the focus of future research.

The logical connections between different Chapters are displayed in Figure 1.

Original Content

The material in this thesis is organized in such a way that there is no explicit separation between concepts drawn from the existing literature and original contributions: original parts are inserted whenever required by the logical development of the discussion.

The following list provides references to all the original results in each Chapter.

- In Chapter 2:

  1. The CP criterion for recovery operations (2.5), and its application to the proof of the complete positivity of recoveries induced by "Pauli-like" matrices (§2.3.2).

  2. The optimal recovery operation for a single qubit exposed to a general noise, and the corresponding fidelity (§2.4).

- In Chapter 3:

  1. The recovery fidelity of the 3-qubit bit-flip code subject to an iterated (discrete-time) error-correction procedure, and the corresponding storage time (§3.2.2).

  2. The calculation of the recovery fidelity for the continuous-time implementation of the 3-qubit bit-flip code, in §3.4.2 (the results were already known from e.g. [14], but we present an alternative derivation and discuss the optimality of the result).
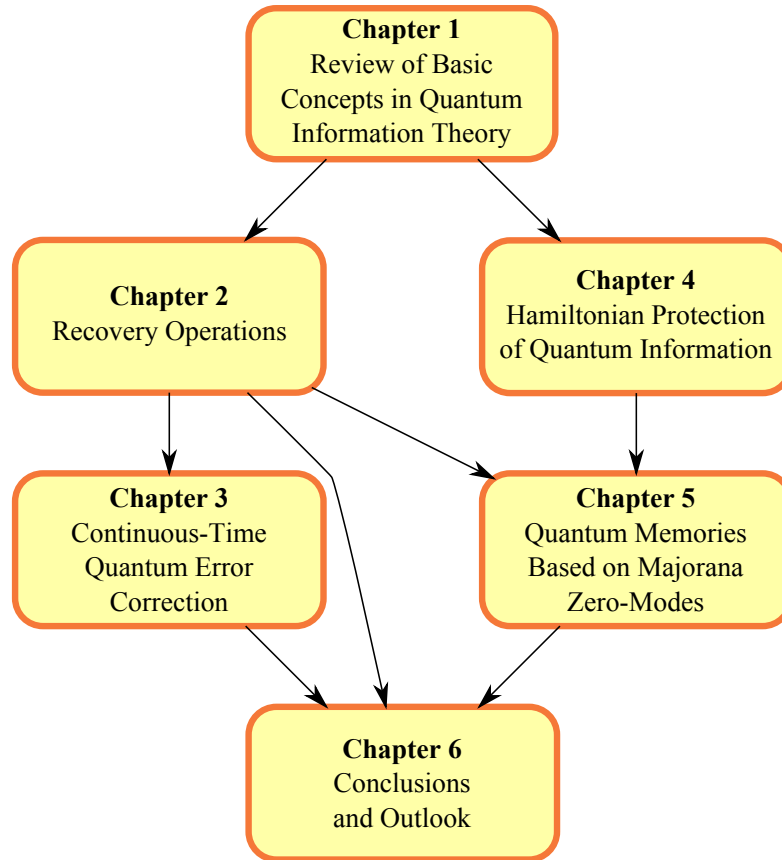
FIGURE 1: concept map of the thesis.

3. The study of fixed and quasi-fixed points of the dynamics for the 3-qubit CTQEC (§3.4.3).

4. The numerical computation of the recovery fidelity for the continuous-time implementation of the 5-qubit QECC (§3.5.3).

- In Chapter 4:

  1. The choice of terminology introduced in §4.1.2 (while the concepts being labeled are not original by themselves, to the best of our knowledge no specific terminology for them can be found in the literature).

  2. The calculations about the memory performance of a minimal Ising chain (§4.2) in both the "decoherence opposition" and the "decoherence prevention" scenarios.

- In Chapter 5:

  1. The discussion of the effective local ground-space dynamics for a system with four distant Majorana zero-modes (§5.2.3).

2. The discussion about the fully-mixed encoding (§5.2.4) and the lower bound on the recovery fidelity (5.53).

3. The discussion of the 8-mode and 12-mode toy models presented in §5.3 and §5.4.

4. The calculation of the memory performance of a quantum memory made of two Kitaev chains under both parity-preserving and non-parity-preserving noise models (§5.5).

- In Appendix E:

  1. The characterization of parity-preserving noise models in terms of their Kraus or Lindblad operators.

The most significant contributions are the following.

1. The microscopic derivation of a Markovian master equation for a pair of Kitaev chains in both fermionic and bosonic environments, and the subsequent evaluation of the performance of such systems as quantum memories: it is shown that, in the large-gap limit, information is preserved in a bosonic environment, while it is lost in a fermionic one (§5.5).

2. An example of the strong dependence of the memory performance on the encoding subspace in a Majorana-based quantum memory. This dependence is observed in a 12-mode toy model, and suggests that long-range correlations in the initial state of the Majorana memory (beyond those strictly needed for the encoding) may be harmful for the encoded information (§5.4).

3. The calculation of the memory performance of the continuous-time (dissipative) implementation of the 5-qubit perfect code (§3.5). The known results were all limited to the 3-qubit code, and thus could only prove protection against the bit-flip noise, which is inherently classical. This result proves that information can be protected against depolarizing noise, which is considered the most aggressive type of quantum noise.

Chapter 1

Review of Basic Concepts in Quantum Information Theory

In this Chapter we provide an elementary introduction to the framework of Quantum Information Theory. In Section 1.1 we define the qubit and derive the geometry of its state space, the Bloch sphere. In Section 1.2 we briefly outline the theory of quantum channels. This provides the mathematical framework for both quantum noise and quantum recovery operations, which will be discussed in depth in Chapter 2. Particular attention is given to Markovian quantum dynamics, since most noise models that will be considered in this thesis are Markovian. Finally, in Section 1.3 two distinguishability measures for quantum states are presented and some of their useful properties are briefly discussed.

1.1 The Quantum Bit

A classical bit of information is a quantity that can be either 0 or 1. This is a rather abstract definition; concretely, a bit must be carried by a physical system. In order to carry a bit of classical information, a system must have (at least) two distinguishable states, that can be labeled as "0" and "1".

By generalizing this notion to a quantum mechanical system, one gets a "quantum bit", or *qubit* [1]. A qubit is the information carried by the state of a two-level system, e.g. a spin-$\frac{1}{2}$ particle. We can label the spin-up state $|\uparrow\rangle$ as $|0\rangle$ and the spin-down state $|\downarrow\rangle$ as $|1\rangle$. These are known as the *computational basis* of the qubit Hilbert space $\mathcal{H}_1$.

1.1.1 Pure and mixed states

Suppose we have a classical bit but we do not know its value with certainty – e.g., we flip a coin without looking at the outcome. This situation can be described as a probabilistic (or statistical) mixture: the state of the coin is "50% heads and 50% tails".

The same applies to a qubit: apart from the intrinsic uncertainty associated to quantum states, in general we have some degree of "classical" ignorance about the state of a quantum system. Suppose we draw a qubit state from an ensemble $E = \{(p_i; |\psi_i\rangle)\}$ (the state is $|\psi_i\rangle$ with probability p_i); this statistical mixture is described by the *density matrix*

$$\rho_E = \sum_i p_i |\psi_i\rangle \langle\psi_i| . \tag{1.1}$$

Density matrices over a Hilbert space $\mathcal{H}$ are linear operators with the following properties:

1. Hermiticity $(\hat{\rho} = \hat{\rho}^\dagger)$,

2. positivity $(\hat{\rho} \geq 0)$,

3. unit trace $(\mathrm{Tr}\,(\hat{\rho}) = 1)$.

Any ensemble state like ρ_E in (1.1) clearly obeys these three requirements. It is also easy to prove the converse – i.e. that any density matrix ρ can be written as ρ_E for an appropriate ensemble E. One such ensemble is given by the eigenvalues and eigenvectors of ρ, though the ensemble representation is not unique.

1.1.2 The Bloch sphere

The space of density matrices over a Hilbert space $\mathcal{H}$ will be denoted by $\mathcal{S}(\mathcal{H})$. If $\mathcal{H}$ has finite dimension d, then $\mathcal{S}(\mathcal{H})$ has dimension $d^2 - 1$. For a qubit, $d = 2$ and therefore $\mathcal{S}(\mathcal{H}_1)$ is a manifold of dimension 3.

In order to gain a geometric picture of this space, it is convenient to represent a general qubit state in terms of Pauli matrices:

$$\sigma_0 = \mathbf{1} = \begin{pmatrix} 1 & 0 \\ 0 & 1 \end{pmatrix}, \quad \sigma_1 = \begin{pmatrix} 0 & 1 \\ 1 & 0 \end{pmatrix}, \quad \sigma_2 = \begin{pmatrix} 0 & -i \\ i & 0 \end{pmatrix}, \quad \sigma_3 = \begin{pmatrix} 1 & 0 \\ 0 & -1 \end{pmatrix}. \tag{1.2}$$

These form a basis (over $\mathbb{C}$) of 2×2 matrices, therefore in general

$$\rho = \frac{1}{2} \sum_{\alpha=0}^{3} r_\alpha \sigma_\alpha. \tag{1.3}$$

Now, Hermiticity requires that $r_\alpha \in \mathbb{R} \ \forall \alpha$; unit trace requires $r_0 = 1$; and positivity requires $\sum_{i=1}^{3} r_i^2 \leq 1$. Therefore

$$\mathcal{S}(\mathcal{H}_1) = \left\{ \frac{\mathbf{1} + \mathbf{r} \cdot \boldsymbol{\sigma}}{2} : |\mathbf{r}| \leq 1 \right\}. \tag{1.4}$$

This is known as the *Bloch sphere*. Its surface ($|\mathbf{r}| = 1$) consists of pure states, i.e. rank-one projectors. The interior consists of mixed states. The center ($\mathbf{r} = 0$) is the *completely mixed state*, the state with minimal information content.

For "qudits" (i.e. d-level systems with $d \geq 3$) or multi-qubit systems, the geometry of $\mathcal{S}(\mathcal{H})$ becomes complicated. For instance, a pair of qubits has a 15-dimensional state space. Comparing this to the 6-dimensional product of two Bloch spheres shows how rich and complicated quantum correlations can be, even in such a simple case [21].

1.2 Quantum Channels

The state of a closed quantum system evolves according to the Schroedinger equation [22]:

$$\frac{d}{dt}\hat{\rho}(t) = -i \left[\hat{H}(t), \hat{\rho}(t) \right] \tag{1.5}$$

The formal solution to this equation is obtained through a time-dependent unitary transformation:

$$\hat{\rho}(t) = \hat{U}(t)\hat{\rho}(0)\hat{U}^\dagger(t), \qquad \hat{U}(t) = T \exp\left[-i \int_0^t d\tau \, \hat{H}(\tau) \right], \tag{1.6}$$

where T denotes time-ordering. However, the time evolution of an *open* quantum system [23] need not be unitary. Let us focus on a subsystem A of a larger closed system $A \otimes B$. The *reduced density matrix* $\hat{\rho}_A(t) \equiv \mathrm{Tr}_B (\hat{\rho}(t))$ evolves according to

$$\hat{\rho}_A(t) = \mathrm{Tr}_B \left(\hat{U}(t)\hat{\rho}(0)\hat{U}^\dagger(t) \right). \tag{1.7}$$

If the initial state $\hat{\rho}(0)$ is completely uncorrelated, i.e. $\hat{\rho}(0) = \hat{\rho}_A(0) \otimes \hat{\rho}_B(0)$, then (1.7) reads

$$\hat{\rho}_A(t) = \mathrm{Tr}_B \left(\hat{U}(t)\hat{\rho}_A(0) \otimes \hat{\rho}_B(0)\hat{U}^\dagger(t) \right) \equiv \Phi_t(\hat{\rho}_A(0)). \tag{1.8}$$

Φ_t is generally *not* a unitary time evolution, i.e. there is no unitary matrix $\hat{U}_A(t)$ acting on subsystem A such that $\hat{\rho}_A(t) = \hat{U}_A(t)\hat{\rho}_A(0)\hat{U}_A^\dagger(t)$.

1.2.1 CPTP maps

The map Φ_t from (1.8) is a linear transformation of the space of density matrices on $\mathcal{H}$, $\mathcal{S}(\mathcal{H})$. The space of density matrices is a sub-manifold of the space of all operators on $\mathcal{H}$, $\mathcal{B}(\mathcal{H})$. A generic *super-operator* (i.e. a linear operator acting on $\mathcal{B}(\mathcal{H})$, like Φ_t), without further constraints, would map $\mathcal{S}(\mathcal{H})$ to a different submanifold of $\mathcal{B}(\mathcal{H})$. Thus, in order to ensure that $\Phi(\mathcal{S}(\mathcal{H})) \subseteq \mathcal{S}(\mathcal{H})$, i.e. that $\Phi(\hat{\rho})$ is a state for every input state $\hat{\rho}$, some constraints must be imposed on Φ.

- (TP) *Trace Preservation*: $\mathrm{Tr}\left(\Phi(\hat{A})\right) = \mathrm{tr}(\hat{A}) \; \forall \, \hat{A} \in \mathcal{B}(\mathcal{H})$;

- (P) *Positivity*: $\Phi(\hat{A}) \geq 0 \; \forall \, \hat{A} \in \mathcal{B}(\mathcal{H})$ such that $\hat{A} \geq 0$.

The necessary condition $\Phi(\mathcal{S}(\mathcal{H})) \subseteq \mathcal{S}(\mathcal{H})$, however, is not sufficient to guarantee that Φ_t corresponds to a physical time evolution. A set of necessary and sufficient constraints is obtained by generalizing (P) to

- (CP) *Complete Positivity*: $(\Phi \otimes \mathcal{I})(\hat{X}) \geq 0 \; \forall \hat{X} \in \mathcal{B}(\mathcal{H} \otimes \mathcal{H}_{\mathrm{aux}})$ such that $\hat{X} \geq 0$, where $\mathcal{H}_{\mathrm{aux}}$ is a generic "auxiliary" Hilbert space and $\mathcal{I}$ is the identity super-operator on $\mathcal{B}(\mathcal{H}_{\mathrm{aux}})$.

The standard example for a super-operator that is (P) but not (CP) is the *transposition* (with respect to a specified basis): $\mathcal{T}(\hat{A}) = \hat{A}^T$ is clearly positive, but it can be shown that $\mathcal{T} \otimes \mathcal{I}$ is not.

The most general process that can occur to a quantum state is therefore described mathematically by a *completely positive, trace-preserving* (CPTP) linear map Φ. Such maps are also called *quantum channels* [1].

A practical way of representing the action of a CPTP map Φ is the *Kraus representation* [24]:

$$\Phi(\hat{\rho}) = \sum_k \hat{M}_k \hat{\rho} \hat{M}_k^\dagger, \tag{1.9}$$

where the $\left\{ \hat{M}_k \right\}$ matrices, called *Kraus operators*, obey the normalization condition

$$\sum_k \hat{M}_k^\dagger \hat{M}_k = \hat{\mathbf{1}}, \tag{1.10}$$

which is needed to ensure the (TP) property.

1.2.2   Markovian dynamics and master equations

The time-evolution of the state of an open quantum system is in general described by a one-parameter family of CPTP maps $\{\mathcal{D}_t : t \geq 0\}$, such that $\hat{\rho}(t) = \mathcal{D}_t\left(\hat{\rho}(0)\right)$. The structure of this family can be arbitrarily complicated, based on the type of interaction with the environment.

There is, however, an interesting class of processes for which $\{\Phi_t : t \geq 0\}$ has the nice mathematical structure of a *semi-group*[1], i.e. $\mathcal{D}_t \circ \mathcal{D}_s = \mathcal{D}_{t+s} \; \forall\, t, s \geq 0$. These processes are called *Markovian* and correspond to the physical scenario in which the environment correlation times are very small compared to the times that characterize the dynamics of the system [23]. This means that the environment has no memory of the previous states of the system; information leaving the system is forever lost.

Under mild continuity assumptions, a one-parameter semi-group can be described in terms of a generator [25]:

$$\mathcal{D}_t = e^{t\mathcal{L}} \quad \forall\, t \geq 0. \tag{1.11}$$

The super-operator $\mathcal{L}$ is called the *Lindbladian*. Imposing the CPTP requirements on $\mathcal{D}_t$ constrains the form of the Lindbladian to the following:

$$\mathcal{L}(\hat{\rho}) = -i[\hat{H}, \hat{\rho}] + \sum_k \left(\hat{L}_k \hat{\rho} \hat{L}_k^\dagger - \frac{1}{2}\left\{ \hat{L}_k^\dagger \hat{L}_k, \hat{\rho} \right\} \right), \tag{1.12}$$

where H is Hermitian and the $\{\hat{L}_k\}$ are generic operators. $\hat{H}$ is obviously identified with the system Hamiltonian, while the $\{\hat{L}_k\}$ are called *Lindblad operators* and represent the dissipative part of the dynamics.

Markovian dynamics can therefore be described by a *master equation* of the general form

$$\frac{d}{dt}\hat{\rho}(t) = \mathcal{L}(\hat{\rho}(t)), \tag{1.13}$$

with $\mathcal{L}$ of the form given in (1.12).

The Lindblad operators and the Hamiltonian are not uniquely determined: $\mathcal{L}$ is invariant under unitary transformations $\hat{L}_k \mapsto \sum_l u_{kl}\hat{L}_l$ (with $\sum_j u_{ij}^* u_{jk} = \delta_{ik}$) and under the family of inhomogeneous transformations

$$\begin{cases} \hat{L}_k \mapsto \hat{L}_k + \alpha_k \hat{\mathbf{1}} \,, \\[2mm] \hat{H} \mapsto \hat{H} + \sum_j \dfrac{\alpha_j^* \hat{L}_j - \alpha_j \hat{L}_j^\dagger}{2i} \,, \end{cases} \tag{1.14}$$

---

[1]It is not a group because every non-trivial element lacks an inverse. This is because the times t and s are required to be positive.

where the $\{\alpha_j\}$ are generic complex numbers. These "gauge fixing" degrees of freedom allow us to take the Lindblad operators traceless and mutually orthogonal, without loss of generality:

$$\mathrm{Tr}\left(\hat{L}_i\right) = 0, \qquad\qquad \mathrm{Tr}\left(\hat{L}_i^\dagger \hat{L}_j\right) = \gamma_i \delta_{ij}. \qquad (1.15)$$

Up to degeneracies in the $\{\gamma_i\}$ coefficients, this choice uniquely specifies the set of Lindblad operators and the Hamiltonian.

1.2.3 Adjoint of a quantum channel

In analogy to the adjoint of an operator $\hat{A} \in \mathcal{B}\left(\mathcal{H}\right)$, one can define the adjoint of a channel $\Phi \in \mathcal{B}\left(\mathcal{B}\left(\mathcal{H}\right)\right)$. While the adjoint of an operator is defined with respect to the Hilbert space Hermitian product on $\mathcal{H}$, i.e. $\langle\phi|\,\hat{A}\psi\rangle = \left\langle\hat{A}^\dagger\phi\,\middle|\,\psi\right\rangle$, the adjoint of a channel is defined in terms of the *Hilbert-Schmidt Hermitian product* on $\mathcal{B}\left(\mathcal{H}\right)$:

$$(\hat{A}, \hat{B})_{HS} = \mathrm{Tr}\left(\hat{A}^\dagger \hat{B}\right). \qquad (1.16)$$

The adjoint of a channel Φ is thus defined as the super-operator Φ^* such that, for all operators $\hat{A}, \hat{B} \in \mathcal{B}\left(\mathcal{H}\right)$, the following holds [1]:

$$\mathrm{Tr}\left(\hat{A}\Phi(\hat{B})\right) = \mathrm{Tr}\left(\Phi^*(\hat{A})\hat{B}\right). \qquad (1.17)$$

Some properties of the adjoint channel that will prove useful are the following.

- If the Kraus operators for Φ are $\left\{\hat{M}_k\right\}$, then those for Φ^* are their adjoints $\left\{\hat{M}_k^\dagger\right\}$.

- Φ is TP if and only if Φ^* is unital (and *vice versa*).

1.3 Distinguishability Measures for Quantum States

In order to develop a theory of information storage and processing, it is crucial to have a way of quantifying the *distinguishability* of two items of information.

In the theory of quantum computation, for instance, one may be interested in implementing a prescribed unitary operation with high accuracy. In order to quantify this accuracy, the output of the real gate must be compared with the output of the ideal one. In the theory of quantum memories, the goal is to store a given quantum state for long times without degrading it. The performance of a quantum memory therefore has to be evaluated in terms of how much the output state is similar to the input state.

In both cases, a measure of distinguishability between quantum states is needed. The two most common measures are the *trace distance* [26] and the *fidelity* [27].

1.3.1 Trace distance

The trace distance between two quantum states $\hat{\rho}$ and $\hat{\sigma}$ is defined as

$$d_{\mathrm{tr}}(\hat{\rho}, \hat{\sigma}) = \frac{1}{2}\mathrm{Tr}(|\hat{\rho} - \hat{\sigma}|), \tag{1.18}$$

where $|\hat{A}| = \sqrt{\hat{A}^\dagger \hat{A}}$. As the name suggests, it is a distance, i.e. it is positive, it equals 0 if and only if the two states are the same, and it obeys the triangular inequality. It is induced by a norm, called the *trace norm*:

$$d_{\mathrm{tr}}(\hat{\rho}, \hat{\sigma}) = \frac{1}{2}\|\hat{\rho} - \hat{\sigma}\|_{\mathrm{tr}}, \qquad \|\hat{A}\|_{\mathrm{tr}} = \mathrm{Tr}(|\hat{A}|) = \max_{\hat{H} \in \mathcal{B}_{\mathrm{op}}} \mathrm{Tr}(\hat{H}\hat{A}) \tag{1.19}$$

The maximization is done over the manifold $\mathcal{B}_{\mathrm{op}}$ of Hermitian matrices with unit operator norm[2]: $\|\hat{H}\|_{\mathrm{op}} = 1$. For any pair of quantum states $\hat{\rho}$ and $\hat{\sigma}$, one has

$$d_{\mathrm{tr}}(\hat{\rho}, \hat{\sigma}) = \frac{1}{2}\|\hat{\rho} - \hat{\sigma}\|_{\mathrm{tr}} \leq \frac{\|\hat{\rho}\|_{\mathrm{tr}} + \|\hat{\sigma}\|_{\mathrm{tr}}}{2} = \frac{\mathrm{Tr}(\hat{\rho}) + \mathrm{Tr}(\hat{\sigma})}{2} = 1, \tag{1.20}$$

so that $d_{\mathrm{tr}}(\hat{\rho}, \hat{\sigma}) \in [0, 1]$. While $d_{\mathrm{tr}}(\hat{\rho}, \hat{\sigma}) = 0$ if and only if $\hat{\rho} = \hat{\sigma}$, it can be shown that $d_{\mathrm{tr}}(\hat{\rho}, \hat{\sigma}) = 1$ if and only if $\mathrm{Tr}(\hat{\rho}\hat{\sigma}) = 0$. This condition (absence of overlap, or Hilbert-Schmidt orthogonality) implies distinguishability[3].

For qubit states one has

$$d_{\mathrm{tr}}\left(\frac{\mathbf{1} + \mathbf{a} \cdot \boldsymbol{\sigma}}{2}, \frac{\mathbf{1} + \mathbf{b} \cdot \boldsymbol{\sigma}}{2}\right) = \frac{1}{4}\mathrm{Tr}(|(\mathbf{a} - \mathbf{b}) \cdot \boldsymbol{\sigma}|) = \frac{|\mathbf{a} - \mathbf{b}|}{2}. \tag{1.21}$$

This is simply half of the Euclidean distance between the corresponding points in the Bloch sphere. Two states have trace distance 1 if and only if they are antipodal, hence distinguishable.

A fundamental property of the trace distance is its *contractivity* under physical evolutions [1]:

$$d_{\mathrm{tr}}(\Phi(\hat{\rho}), \Phi(\hat{\sigma})) \leq d_{\mathrm{tr}}(\hat{\rho}, \hat{\sigma}) \quad \forall \hat{\rho}, \hat{\sigma} \in \mathcal{S}(\mathcal{H}), \tag{1.22}$$

---

[2] The operator norm of a matrix is defined as $\|\hat{H}\|_{\mathrm{op}} = \max_{|\psi\rangle} \left|\frac{\langle\psi|\hat{H}|\psi\rangle}{\langle\psi|\psi\rangle}\right|$, which coincides with the maximum singular value of $\hat{H}$.

[3] If $\hat{\rho}$ and $\hat{\sigma}$ have zero overlap, then they have disjoint supports. Measuring the projector onto the support of $\hat{\rho}$ yields either 0 or 1: if the outcome is 1 then the state is certainly $\hat{\rho}$, otherwise the state is certainly $\hat{\sigma}$. If $\mathrm{Tr}(\hat{\rho}\hat{\sigma}) \neq 0$, no single measurement can discriminate between the two states.

for all CPTP maps Φ. So every physical evolution is a contraction of the metric space $(\mathcal{S}(\mathcal{H}), d_{\mathrm{tr}})$, which implies that it has at least one fixed point:

$$\exists \, \hat{\rho}^* \in \mathcal{S}(\mathcal{H}) : \quad \Phi(\hat{\rho}^*) = \hat{\rho}^*. \tag{1.23}$$

1.3.2 Fidelity

The Uhlmann fidelity [27] between two quantum states $\hat{\rho}$ and $\hat{\sigma}$ is

$$F(\hat{\rho}, \hat{\sigma}) = \left[\mathrm{Tr} \left(\sqrt{\sqrt{\hat{\rho}} \, \hat{\sigma} \, \sqrt{\hat{\rho}}} \right) \right]^2 \tag{1.24}$$

While the trace distance measures how much $\hat{\rho}$ and $\hat{\sigma}$ differ, the fidelity is a measure of how much they are similar:

$$F(\hat{\rho}, \hat{\sigma}) = 1 \iff \hat{\rho} = \hat{\sigma}, \qquad F(\hat{\rho}, \hat{\sigma}) = 0 \iff \mathrm{Tr}\,(\hat{\rho}\hat{\sigma}) = 0. \tag{1.25}$$

The latter condition (zero overlap) again implies that $\hat{\rho}$ and $\hat{\sigma}$ are distinguishable.

If one of the two states is pure, e.g. $\hat{\rho} = |\psi\rangle \langle\psi|$, the definition (1.24) simplifies to

$$F(|\psi\rangle \langle\psi| , \hat{\sigma}) = \langle\psi| \hat{\sigma} |\psi\rangle . \tag{1.26}$$

For qubit states, if one of the states is pure, one has

$$F\left(\frac{\mathbf{1} + \mathbf{a} \cdot \boldsymbol{\sigma}}{2}, \frac{\mathbf{1} + \mathbf{n} \cdot \boldsymbol{\sigma}}{2} \right) = \mathrm{Tr}\left(\frac{\mathbf{1} + \mathbf{a} \cdot \boldsymbol{\sigma}}{2} \frac{\mathbf{1} + \mathbf{n} \cdot \boldsymbol{\sigma}}{2} \right) = \frac{1 + \mathbf{a} \cdot \mathbf{n}}{2}. \tag{1.27}$$

$F = 1$ implies $\mathbf{a} = \mathbf{n}$ (equal states); $F = 0$ implies $\mathbf{a} = -\mathbf{n}$ (antipodal, distinguishable states).

F is obviously not a distance, but can be turned into one by suitable transformations – e.g., $d_{\mathrm{ang}}(\hat{\rho}, \hat{\sigma}) \equiv \arccos(F(\hat{\rho}, \hat{\sigma}))$ is a distance; for a pair of pure states it corresponds to the angle between the two Hilbert space vectors.

Like the trace distance, the fidelity is monotonic under physical evolutions [1]:

$$F(\Phi(\hat{\rho}), \Phi(\hat{\sigma})) \geq F(\hat{\rho}, \hat{\sigma}) \quad \forall \hat{\rho}, \hat{\sigma} \in \mathcal{S}(\mathcal{H}), \tag{1.28}$$

for all CPTP maps Φ. While d_{tr} is monotonically decreasing, F is increasing: both behaviors point to a loss of distinguishability, and therefore of information content.

Another useful property of the fidelity is the *joint concavity* [1]:

$$F\left(\sum_i p_i \hat{\rho}_i, \sum_j p_j \hat{\sigma}_j\right) \geq \sum_i p_i F(\hat{\rho}_i, \hat{\sigma}_i). \tag{1.29}$$

If $\hat{\rho}_i = |\psi_i\rangle \langle\psi_i|$ and $\hat{\sigma}_i = \Phi(\hat{\rho}_i)$ for some quantum channel Φ, then (1.29) becomes

$$F\left(\sum_i p_i |\psi_i\rangle \langle\psi_i|, \Phi\left(\sum_j p_j |\psi_j\rangle \langle\psi_j|\right)\right) \geq \sum_i p_i F(|\psi_i\rangle \langle\psi_i|, \Phi(|\psi_i\rangle \langle\psi_i|))$$

$$= \sum_i p_i \langle\psi_i| \Phi(|\psi_i\rangle \langle\psi_i|) |\psi_i\rangle. \tag{1.30}$$

Chapter 2

Recovery Operations

This Chapter presents the concept of *recovery operation*. We begin by giving the definition and general form of a recovery operation in Section 2.1. In Section 2.2 we discuss a measure for the performance of a recovery operation, the *average recovery fidelity*, and prove an upper bound that is used extensively in the rest of the thesis. We then proceed to define optimal recovery operations in Section 2.3. A "candidate" recovery operation is presented: it saturates the fidelity upper bound, but is not guaranteed to be physical. The complete positivity of a particular class of recovery operations is then proved. A strategy for studying the performance of quantum memory models based on these two observations is briefly outlined. Finally, in Section 2.4 the simple example of a single-qubit "memory" is explicitly analyzed and the exact solution of the optimization problem is discussed in terms of the general concepts introduced in previous Sections.

2.1   General Concept

2.1.1   Definition

We shall use the term *"recovery operation"* to denote a CPTP map that tries to undo the effects of a previous, given noise. This definition is to some extent arbitrary, and may refer to any CPTP mapping between the appropriate state spaces, depending on the framework.

The typical scenario that will be considered in this thesis is the following: an abstract qubit is initially encoded into a physical system, the "memory"; the memory evolves under the effect of perturbations; after some time t, we want to retrieve the original state of the qubit. This requires the choice of a physical mapping between the state space of the memory and the Bloch sphere. This mapping is the recovery operation.
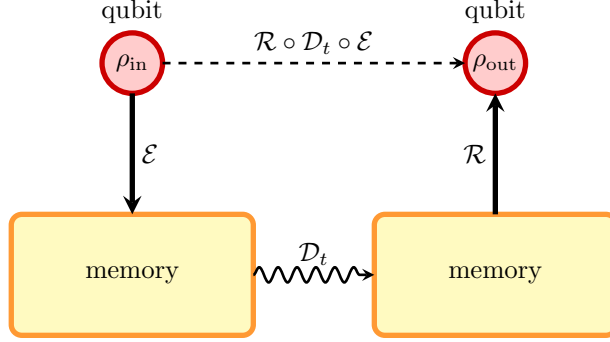
FIGURE 2.1: schematic representation of a quantum memory.

A more mathematically rigorous description is the following.

1. We initially embed the qubit state space $\mathcal{S}(\mathcal{H}_1)$ into a (possibly larger) state space $\mathcal{S}(\mathcal{H}_{\mathrm{sys}})$. The embedding (or encoding) is represented by a CPTP map $\mathcal{E} : \mathcal{S}(\mathcal{H}_1) \to \mathcal{S}(\mathcal{H}_{\mathrm{sys}})$.

2. A given quantum channel $\mathcal{D}_t$, representing the noise or *decoherence*, acts on $\mathcal{S}(\mathcal{H}_{\mathrm{sys}})$.

3. At a given time t we perform a physical operation $\mathcal{R} : \mathcal{S}(\mathcal{H}_{\mathrm{sys}}) \to \mathcal{S}(\mathcal{H}_1)$ such that the output of $\mathcal{R} \circ \mathcal{D}_t \circ \mathcal{E}$ is as close as possible to the input (in a sense that can be made rigorous in terms of the distinguishability measures presented in §1.3).

The procedure is represented in Figure 2.1.

2.1.2 Form of a recovery operation

Recalling the general form of a qubit state (1.4), linearity forces $\mathcal{R}$ to be of the form

$$\mathcal{R}(\hat{\rho}) = \frac{1}{2}\left(\mathbf{1}f_0(\hat{\rho}) + \sum_{\alpha=1}^{3}\sigma_\alpha f_\alpha(\hat{\rho})\right) \qquad \forall \hat{\rho} \in \mathcal{S}\left(\mathcal{H}_{\mathrm{sys}}\right), \qquad (2.1)$$

with f_0, f_1, f_2 and f_3 linear, real-valued functions of $\hat{\rho}$. Now, by the Riesz representation theorem, any linear function can be represented as a Hilbert-Schmidt scalar product with a suitable operator: for each $0 \leq \alpha \leq 3$ there exists an operator $\hat{H}_\alpha$ such that $f_\alpha(\hat{\rho}) \equiv \mathrm{Tr}\left(\hat{H}_\alpha\hat{\rho}\right)$. Real-valuedness forces the $\{\hat{H}_\alpha\}$ to be Hermitian, and trace preservation requires $\hat{H}_0 = \hat{\mathbf{1}}$. Thus the general form of a recovery map is

$$\mathcal{R}(\hat{\rho}) = \frac{1}{2}\left(\mathbf{1}\mathrm{Tr}\left(\hat{\rho}\right) + \sum_{\alpha=1}^{3}\sigma_\alpha\mathrm{Tr}\left(\hat{H}_\alpha\hat{\rho}\right)\right). \qquad (2.2)$$

This is not yet guaranteed to be a CP map. Imposing complete positivity will put additional constraints on the $\{\hat{H}_\alpha : \alpha = 1, 2, 3\}$ operators. For example, it is easy to see that $\|\hat{H}_\alpha\|_{\text{op}} \leq 1$ is a necessary (though insufficient) condition to map the Bloch sphere into itself.

A powerful tool that can be used to check the complete positivity of a quantum channel is the Choi-Jamioulkowski theorem [28]. It establishes an equivalence between the complete positivity of a channel and the positivity of a state, which is much easier to investigate. The Choi-Jamioulkowski state corresponding to a channel Φ acting on $\mathcal{B}(\mathcal{H}_{\text{sys}})$ is

$$\hat{\rho}_{\text{CJ}}^{(\Phi)} = (\Phi \otimes \mathcal{I}) \left(\frac{1}{N} \sum_{i,j=1}^{N} |i\rangle |i\rangle \langle j| \langle j| \right) = \frac{1}{N} \sum_{i,j=1}^{N} \Phi(|i\rangle \langle j|) \otimes |i\rangle \langle j|, \tag{2.3}$$

where $\{|i\rangle : i = 1, \ldots, N\}$ is an orthonormal basis of $\mathcal{H}_{\text{sys}}$.

The Choi-Jamioulkowski state corresponding to a recovery operation $\mathcal{R}$, in the general form (2.2), is thus

$$\begin{aligned}
\hat{\rho}_{\text{CJ}}^{(\mathcal{R})} &= \frac{1}{N} \sum_{i,j=1}^{N} \mathcal{R}(|i\rangle \langle j|) \otimes |i\rangle \langle j| = \frac{1}{2N} \sum_{i,j=1}^{N} \left(\mathbf{1} \delta_{ij} + \sum_{\alpha=1}^{3} \sigma_\alpha \langle j| \hat{H}_\alpha |i\rangle \right) \otimes |i\rangle \langle j| \\
&= \frac{1}{2N} \sum_{i,j=1}^{N} \left(\mathbf{1} \otimes |i\rangle \delta_{ij} \langle j| + \sum_{\alpha=1}^{3} \sigma_\alpha \otimes |i\rangle \hat{H}_\alpha^{ji} \langle j| \right) \\
&= \frac{1}{2N} \left(\mathbf{1} \otimes \hat{\mathbf{1}} + \sum_{\alpha=1}^{3} \sigma_\alpha \otimes \hat{H}_\alpha^T \right).
\end{aligned} \tag{2.4}$$

The transposition is taken with respect to the chosen orthonormal basis $\{|i\rangle : i = 1, \ldots, N\}$. In conclusion from (2.4) we have that $\mathcal{R}$ is a CPTP map if and only if the following operator inequality holds:

$$\mathbf{1} \otimes \hat{\mathbf{1}} + \sum_{\alpha=1}^{3} \sigma_\alpha \otimes \hat{H}_\alpha^T \geq 0. \tag{2.5}$$

The ordered triples $(\hat{H}_1, \hat{H}_2, \hat{H}_3)$ of Hermitian operators that satisfy condition (2.5) are in one-to-one correspondence with physical recovery operations. For a system of n qubits, a recovery operation is specified by three $2^n \times 2^n$ Hermitian matrices, hence by $3(2^n)^2 = 3 \cdot 4^n$ independent parameters. This is a huge number even for a system as small as a pair of qubits ($3 \cdot 4^2 = 48$ parameters) and increases exponentially, thus forbidding a straightforward optimization on the space of all physical recoveries.

2.2   The Average Recovery Fidelity

2.2.1   Definition

In order to decide which recovery operation is the best, a measure of "performance" is needed. This measure must quantify how well the whole Bloch sphere is preserved. A very convenient measure for this purpose is the *average recovery fidelity*:

$$
\begin{aligned}
F_t^{(\mathcal{R})} &= \int d\mu_\phi F\left(|\phi\rangle\langle\phi|, \mathcal{R} \circ \mathcal{D}_t \circ \mathcal{E}\left(|\phi\rangle\langle\phi|\right)\right) \\
&= \int d\mu_\phi \langle\phi|\,\mathcal{R} \circ \mathcal{D}_t \circ \mathcal{E}\left(|\phi\rangle\langle\phi|\right)|\phi\rangle,
\end{aligned}
\tag{2.6}
$$

where $d\mu_\phi$ is the uniform measure on the surface of the Bloch sphere. This is simply an average of the fidelity (1.26) between the input state $|\phi\rangle\langle\phi|$ and the recovered state $\mathcal{R} \circ \mathcal{D}_t \circ \mathcal{E}(|\phi\rangle\langle\phi|)$. This measure only consider the surface of the Bloch sphere, neglecting the mixed states in the interior. This however is not a problem, since by the inequality (1.30) the recovery fidelity for a mixed state is lower-bounded by a convex combination of pure-state recovery fidelities. Therefore averaging over pure input states is enough to characterize the behavior of the whole Bloch sphere $\mathcal{S}\left(\mathcal{H}_1\right)$.

The *optimal recovery fidelity* is

$$
F_t^{\mathrm{opt}} = \max_{\mathcal{R}} F_t^{(\mathcal{R})}.
\tag{2.7}
$$

This quantity only depends on the encoding and on the decoherence channel. Any recovery operation $\mathcal{R}$ such that $F_t^{(\mathcal{R})} = F_t^{\mathrm{opt}}$ will be called an *optimal recovery operation*.

The optimal recovery fidelity (2.7) is a measure of the amount of information still present in the system after a time t. Notice that the optimal recovery operation may be highly impractical, or even technically impossible (e.g. involving highly non-local operations on the system). One can define other measures in order to quantify the amount of information that can be practically recovered by restricting the optimization in (2.7) to a specific sub-class of recovery operations that are considered easy to implement, such as Gaussian maps [29].

Let us derive a more practical formula for (2.6). Let $\hat{\sigma}_\alpha^L$ denote $\mathcal{E}(\sigma_\alpha)$, the embedded logical operators (including $\hat{\sigma}_0^L = \mathcal{E}(\mathbf{1})$). By changing the integration variable from $|\phi\rangle$ to the corresponding Bloch unit vector, one has

$$
\begin{aligned}
F_t^{(\mathcal{R})} &= \int d\mu_\phi \langle\phi|\,\mathcal{R} \circ \mathcal{D}_t \circ \mathcal{E}\left(|\phi\rangle\langle\phi|\right)|\phi\rangle \\
&= \int d\mu_{\mathbf{n}} \mathrm{Tr}\left(\frac{\mathbf{1} + \mathbf{n}\cdot\boldsymbol{\sigma}}{2}\mathcal{R} \circ \mathcal{D}_t\left(\frac{\hat{\sigma}_0^L + \mathbf{n}\cdot\hat{\boldsymbol{\sigma}}^L}{2}\right)\right).
\end{aligned}
\tag{2.8}
$$

The measure $d\mu_{\mathbf{n}}$ over the solid angle is such that $\int d\mu_{\mathbf{n}} 1 = 1$, $\int d\mu_{\mathbf{n}} n_i = 0$ and $\int d\mu_{\mathbf{n}} n_i n_j = \frac{1}{3}\delta_{ij}$; therefore

$$F_t^{(\mathcal{R})} = \mathrm{Tr}\left(\frac{\mathbf{1}}{2}\mathcal{R} \circ \mathcal{D}_t\left(\frac{\hat{\sigma}_0^L}{2}\right)\right) + \frac{1}{3}\sum_{\alpha=1}^{3}\mathrm{Tr}\left(\frac{\sigma_\alpha}{2}\mathcal{R} \circ \mathcal{D}_t\left(\frac{\hat{\sigma}_\alpha^L}{2}\right)\right)$$

$$= \frac{1}{4}\mathrm{Tr}\left(\mathcal{R} \circ \mathcal{D}_t \circ \mathcal{E}(\mathbf{1})\right) + \frac{1}{12}\sum_{\alpha=1}^{3}\mathrm{Tr}\left(\sigma_\alpha \mathcal{R}\left(\mathcal{D}_t\left(\hat{\sigma}_\alpha^L\right)\right)\right). \tag{2.9}$$

Now, since $\mathcal{R}$, $\mathcal{D}_t$ and $\mathcal{E}$ are all trace-preserving channels, $\mathrm{Tr}\left(\mathcal{R} \circ \mathcal{D}_t \circ \mathcal{E}(\mathbf{1})\right) = \mathrm{Tr}(\mathbf{1}) = 2$; thus, recalling the general form of $\mathcal{R}$ (2.2), we have

$$F_t^{(\mathcal{R})} = \frac{1}{2} + \frac{1}{12}\sum_{\alpha=1}^{3}\sum_{\beta=1}^{3}\mathrm{Tr}\left(\sigma_\alpha \frac{1}{2}\mathrm{Tr}\left(\mathcal{D}_t\left(\hat{\sigma}_\alpha^L\right)\hat{H}_\beta\right)\sigma_\beta\right)$$

$$= \frac{1}{2} + \frac{1}{12}\sum_{\alpha=1}^{3}\mathrm{Tr}\left(\mathcal{D}_t\left(\hat{\sigma}_\alpha^L\right)\hat{H}_\alpha\right). \tag{2.10}$$

With analogous techniques one can also compute the fidelity between the encoded state at $t = 0$, $\frac{1}{2}\left(\hat{\sigma}_0^L + \mathbf{n} \cdot \hat{\boldsymbol{\sigma}}^L\right)$, and its time-evolved version $\frac{1}{2}\left(\mathcal{D}_t\left(\hat{\sigma}_0^L\right) + \mathbf{n} \cdot \mathcal{D}_t\left(\hat{\boldsymbol{\sigma}}^L\right)\right)$:

$$F_t^{(\mathcal{I})} = \frac{1}{4}\mathrm{Tr}\left(\hat{\sigma}_0^L \mathcal{D}_t\left(\hat{\sigma}_0^L\right)\right) + \frac{1}{12}\sum_{\alpha=1}^{3}\mathrm{Tr}\left(\mathcal{D}_t\left(\hat{\sigma}_\alpha^L\right)\hat{\sigma}_\alpha^L\right). \tag{2.11}$$

This is denoted by $F_t^{(\mathcal{I})}$ because it corresponds to the trivial recovery operation[1] $\mathcal{R} = \mathcal{I}$.

Remark. While $F_t^{(\mathcal{R})}$ is lower-bounded by $\frac{1}{2}$, $F_t^{(\mathcal{I})}$ can drop to zero. This is because, in the absence of recovery operations, the state at time t can be supported outside the original encoding subspace. Any recovery operation $\mathcal{R}$, instead, forces the state back into the Bloch sphere, thus ensuring at least the "random guess" fidelity of $\frac{1}{2}$ (which is attained by the maximally mixed qubit state $\frac{1}{2}\mathbf{1}$).

2.2.2 Upper bound

Theorem (upper bound on the optimal recovery fidelity). *The optimal recovery fidelity* (2.12) *obeys the following inequality:*

$$F_t^{\mathrm{opt}} \leq \frac{1}{2} + \frac{1}{12}\sum_{\alpha=1}^{3}\left\|\mathcal{D}_t\left(\hat{\sigma}_\alpha^L\right)\right\|_{\mathrm{tr}} \tag{2.12}$$

---

[1]This is a slight abuse of notation, since the identity channel $\mathcal{I}$ does not map $\mathcal{S}\left(\mathcal{H}_{\mathrm{sys}}\right)$ into $\mathcal{S}\left(\mathcal{H}_1\right)$.

Proof. Recalling the definition of the trace norm (1.19), one has that for any two Hermitian matrices $\hat{H}, \hat{X}$

$$\mathrm{Tr}\left(\hat{H}\hat{X}\right) \leq \|\hat{H}\|_{\mathrm{op}} \cdot \|\hat{X}\|_{\mathrm{tr}}. \tag{2.13}$$

Applying this to (2.10), and since the CP condition (2.5) requires $\|\hat{H}_\alpha\|_{\mathrm{op}} \leq 1 \,\forall\alpha$, one has

$$F_t^{(\mathcal{R})} \leq \frac{1}{2} + \frac{1}{12}\sum_{\alpha=1}^{3}\|\hat{H}_\alpha\|_{\mathrm{op}} \cdot \left\|\mathcal{D}_t\left(\hat{\sigma}_\alpha^L\right)\right\|_{\mathrm{tr}} \leq \frac{1}{2} + \frac{1}{12}\sum_{\alpha=1}^{3}\left\|\mathcal{D}_t\left(\hat{\sigma}_\alpha^L\right)\right\|_{\mathrm{tr}}. \tag{2.14}$$

This bound does not depend on $\mathcal{R}$, so a maximization over all physical recoveries yields

$$F_t^{\mathrm{opt}} \leq \frac{1}{2} + \frac{1}{12}\sum_{\alpha=1}^{3}\left\|\mathcal{D}_t\left(\hat{\sigma}_\alpha^L\right)\right\|_{\mathrm{tr}}. \tag{2.15}$$

$$\square$$

There is another way of writing the upper bound (2.12) that makes its geometric meaning clearer:

$$\begin{aligned} F_t^{\mathrm{opt}} &\leq \frac{1}{2} + \frac{1}{12}\sum_{\alpha=1}^{3}\left\|\mathcal{D}_t\left(\frac{\hat{\sigma}_0^L + \hat{\sigma}_\alpha^L}{2}\right) - \mathcal{D}_t\left(\frac{\hat{\sigma}_0^L - \hat{\sigma}_\alpha^L}{2}\right)\right\|_{\mathrm{tr}} \\ &= \frac{1}{2} + \frac{1}{6}\sum_{\alpha=1}^{3}d_{\mathrm{tr}}\left(\mathcal{D}_t\left(\hat{\Psi}_{\alpha+}^L\right); \mathcal{D}_t\left(\hat{\Psi}_{\alpha-}^L\right)\right). \end{aligned} \tag{2.16}$$

$\Psi_{\alpha\pm} = \frac{1\pm\sigma_\alpha}{2}$ is the pure ± 1 eigenstate of σ_α, and $\hat{\Psi}_{\alpha\pm}^L = \mathcal{E}(\Psi_{\alpha\pm})$.

The qualitative interpretation of (2.16) is as follows: a Bloch sphere was embedded into a larger state space, and then subject to some (contractive) deformation; there are many transformations that we can apply in order to try and restore it to its original form, but we are *not* allowed to stretch its diameters. Once, say, the $\hat{x}$ diameter is contracted, an amount of information is inevitably lost. The length of the $\hat{x}$ diameter is measured by the distance of its extremal points, the two antipodal $\hat{x}$ states on the Bloch sphere: $d_{\mathrm{tr}}\left(\mathcal{D}_t\left(\hat{\Psi}_{1+}^L\right); \mathcal{D}_t\left(\hat{\Psi}_{1-}^L\right)\right)$. Each distance is initially equal to 1, so that $F_0^{\mathrm{opt}} = 1$; then, by the contractivity property of the trace distance undec CPTP evolutions [26], the bound (2.16) must decrease, or at most remain constant.

Remark. (2.12) is just an upper bound: it is not guaranteed it can be saturated. This is because the bound depends only on the lengths of the diameters, but not on the angles they form with one another. Consider the following qubit channels: Φ_1, that contracts every σ_α to $\lambda\sigma_\alpha$, and Φ_2, that collapses any σ_α to $\lambda\sigma_3$ (if $\lambda \in [0, \frac{1}{\sqrt{3}}]$, both Φ_1 and Φ_2 are CPTP). Then the $\hat{x}$, $\hat{y}$ and $\hat{z}$ diameters of the Bloch sphere are all contracted from 1 to λ under both channels, and the resulting upper bound is the same: $F^{\mathrm{opt}} \leq \frac{1+\lambda}{2}$. But it is

clear that Φ_2 corrupts information more than Φ_1, by making the three original directions indistinguishable. Indeed, in §2.4 we shall prove a result which implies that the optimal fidelities for Φ_1 and Φ_2 are $\frac{1+\lambda}{2}$ and $\frac{1+\lambda/\sqrt{3}}{2}$ respectively: the former saturates the upper bound, the latter does not.

2.3 Optimal Recovery Operations

2.3.1 Candidate operation

Inequality (2.13) implies that a necessary condition for perfect recoverability of the information is

$$\text{Tr}\left(\hat{H}_\alpha \mathcal{D}_t\left(\hat{\sigma}_\alpha^L\right)\right) = \left\|\mathcal{D}_t\left(\hat{\sigma}_\alpha^L\right)\right\|_{\text{tr}} \quad \forall\,\alpha. \tag{2.17}$$

Now, recalling the definition of the trace norm (1.19) in terms of the "absolute value" of a matrix $|\hat{X}| = \sqrt{\hat{X}^\dagger \hat{X}}$, (2.17) can be re-stated as $\text{Tr}\left(\hat{H}_\alpha \mathcal{D}_t\left(\hat{\sigma}_\alpha^L\right)\right) = \text{Tr}\left(\left|\mathcal{D}_t\left(\hat{\sigma}_\alpha^L\right)\right|\right)$, or

$$\text{Tr}\left(\hat{H}_\alpha \mathcal{D}_t\left(\hat{\sigma}_\alpha^L\right) - \left|\mathcal{D}_t\left(\hat{\sigma}_\alpha^L\right)\right|\right) = 0 \quad \forall\,\alpha. \tag{2.18}$$

An obvious choice at this point is to assume

$$\hat{H}_\alpha = \left|\mathcal{D}_t\left(\hat{\sigma}_\alpha^L\right)\right|\mathcal{D}_t\left(\hat{\sigma}_\alpha^L\right)^{-1} \equiv \text{sign}\left(\mathcal{D}_t\left(\hat{\sigma}_\alpha^L\right)\right) \quad \forall\,\alpha, \tag{2.19}$$

where we introduced the definition of the "sign" of a matrix in analogy with the one for a real number: $\text{sign}(\hat{X}) = |\hat{X}|\hat{X}^{-1}$. In a diagonal basis, one indeed has[2] $\text{sign}\left(\text{diag}\left(\lambda_1, \ldots, \lambda_d\right)\right) = \text{diag}\left(\text{sign}\left(\lambda_1\right), \ldots, \text{sign}\left(\lambda_d\right)\right)$. Another useful way of thinking about the "sign" of matrix is the following. Consider a spectral decomposition of the Hermitian matrix $\hat{X}$,

$$\hat{X} = \sum_{x \in \mathfrak{S}} x\hat{\Pi}(x), \tag{2.20}$$

where $\mathfrak{S}$ is the spectrum of $\hat{X}$ and $\Pi(x)$ is the projector onto the x-eigenspace; then let us split the spectrum into a positive and a negative part: $\mathfrak{S}_+ = \{x \in \mathfrak{S} : x > 0\}$ and $\mathfrak{S}_- = \{x \in \mathfrak{S} : x < 0\}$ (the kernel is irrelevant). The "sign" of $\hat{X}$ can be defined as

$$\text{sign}\left(\hat{X}\right) = \sum_{x \in \mathfrak{S}_+} \hat{\Pi}(x) - \sum_{x \in \mathfrak{S}_-} \hat{\Pi}(x) = \hat{\Pi}^+ - \hat{\Pi}^-, \tag{2.21}$$

i.e. as the projector onto the positive part of $\hat{X}$ minus the projector onto the negative part of $\hat{X}$.

---

[2] For our purposes, $\text{sign}\left(0\right)$ can be defined as 0.

(2.19) then provides a "candidate" optimal recovery operation. The matrices

$$\left\{ \hat{H}_\alpha = \text{sign}\left(\mathcal{D}_t\left(\hat{\sigma}_\alpha^L \right) \right) \right\} \tag{2.22}$$

have operator norm equal to 1, but this is not enough to guarantee that they satisfy the CP criterion (2.5). If they do, then we have a physical recovery operation that saturates the general upper bound, hence it is optimal. Otherwise, no conclusions can be drawn with this argument.

2.3.2 Complete positivity of recovery operations based on "Pauli-like" matrices

Checking the validity of the CP criterion (2.5) is generally difficult. Fortunately there is an interesting class of recovery operations whose complete positivity can be proven in general.

Theorem (Recoveries based on "Pauli-like" matrices are CP) *Consider a recovery map* $\mathcal{R} : \mathcal{S}(\mathcal{H}_{sys}) \mapsto \mathcal{B}(\mathcal{H}_1)$ *in the general form (2.2). Suppose that the* $\left\{ \hat{H}_\alpha \right\}$ *matrices satisfy*

$$\hat{H}_\alpha \hat{H}_\beta = i\varepsilon_{\alpha\beta\gamma} \hat{H}_\gamma, \tag{2.23}$$

$$\left(\hat{H}_\alpha \right)^2 = \hat{\mathbf{1}}. \tag{2.24}$$

Then $\mathcal{R}$ *is CP.*

Proof. From (2.23) we see that the set $\{ \frac{1}{2}\hat{H}_\alpha : \alpha = 1, 2, 3 \}$ obeys the $SU(2)$ Lie algebra:

$$\left[\frac{1}{2}\hat{H}_\alpha, \frac{1}{2}\hat{H}_\beta \right] = i\epsilon_{\alpha\beta\gamma} \frac{1}{2}\hat{H}_\gamma. \tag{2.25}$$

By transposing both sides of (2.25) with respect to an arbitrary basis, we can see that the set $\{ -\frac{1}{2}\hat{H}_\alpha^T : \alpha = 1, 2, 3 \}$ obeys the same algebra; let us therefore give the following definitions:

$$\hat{S}_\alpha = \frac{1}{2}\sigma_\alpha \otimes \hat{\mathbf{1}}, \qquad \hat{L}_\alpha = -\frac{1}{2}\mathbf{1} \otimes \hat{H}_\alpha^T, \qquad \hat{J}_\alpha = \hat{S}_\alpha + \hat{L}_\alpha. \tag{2.26}$$

Then condition (2.5) can be rewritten as follows:

$$\mathbf{1} \otimes \hat{\mathbf{1}} + \sum_{\alpha=1}^{3} (-4)\hat{S}_\alpha \hat{L}_\alpha = \mathbf{1} \otimes \hat{\mathbf{1}} - 4\hat{\mathbf{S}} \cdot \hat{\mathbf{L}} \geq 0. \tag{2.27}$$

Now we can apply the theory of angular momenta, substituting $2\hat{\mathbf{S}} \cdot \hat{\mathbf{L}}$ for $\hat{\mathbf{J}}^2 - \hat{\mathbf{L}}^2 - \hat{\mathbf{S}}^2$ and $\hat{\mathbf{S}}^2$, $\hat{\mathbf{L}}^2$ for $\frac{3}{4}\mathbf{1} \otimes \hat{\mathbf{1}}$; hence the CP condition:

$$\mathbf{1} \otimes \hat{\mathbf{1}} - 2\left(\hat{\mathbf{J}}^2 - \hat{\mathbf{S}}^2 - \hat{\mathbf{L}}^2\right) = \mathbf{1} \otimes \hat{\mathbf{1}} - 2\left(\hat{\mathbf{J}}^2 - \frac{3}{2}\mathbf{1} \otimes \hat{\mathbf{1}}\right)$$
$$= 4(\mathbf{1} \otimes \hat{\mathbf{1}}) - 2\hat{\mathbf{J}}^2 \geq 0. \tag{2.28}$$

From the standard theory of angular momenta we know that $\hat{\mathbf{J}}^2$ has eigenvalues $J(J+1)$, with $J = 0$ (on "singlet" states) or $J = 1$ (on "triplet" states). Either way, $4 - 2J(J+1)$ is non-negative, so $\hat{\rho}_{\mathrm{CJ}}^{(\mathcal{R})}$ is indeed positive and $\mathcal{R}$ is a CPTP channel. $\qquad\square$

Remark. This proof is easily generalized to the case in which $\hat{H}_\alpha^2 \leq \hat{\mathbf{1}}$, i.e. the case in which $\hat{\mathbf{L}}$ involves both "spin-0" and "spin-$\frac{1}{2}$" sub-representations. In the "spin-0" representations one has $\hat{\mathbf{S}} \cdot \hat{\mathbf{L}} = 0$, hence the CP condition $\mathbf{1} \otimes \hat{\mathbf{1}} \geq 0$ is trivially verified; in the "spin-$\frac{1}{2}$" representations the situation is the one discussed above.

2.3.3 Application of the upper bound to the discussion of quantum memory models

We will use the upper bound (2.12) extensively throughout this thesis, especially in Chapter 5. Our approach shall be the following. Given a decoherence process, we shall determine the time-evolved logical matrices matrices $\left\{\mathcal{D}_t\left(\hat{\sigma}_\alpha^L\right)\right\}$, then calculate their trace norm and obtain the upper bound. At this point:

- If the upper bound is low enough to prove a negative result about the memory performance, we are done.

- If the behavior of the upper bound is good (e.g. if it remains constantly equal to 1), we must determine whether or not the bound can be saturated. One way of attaining the bound is by means of the "candidate" recovery operation discussed in §2.3.1.

  - If the matrices (2.19) obey a "Pauli-like" algebra, then by the results of §2.3.2 the candidate recovery is physical, and we have a positive result.

  - Otherwise, our method does not provide any conclusive results about the memory performance.

This approach is summarized in Figure 2.2.
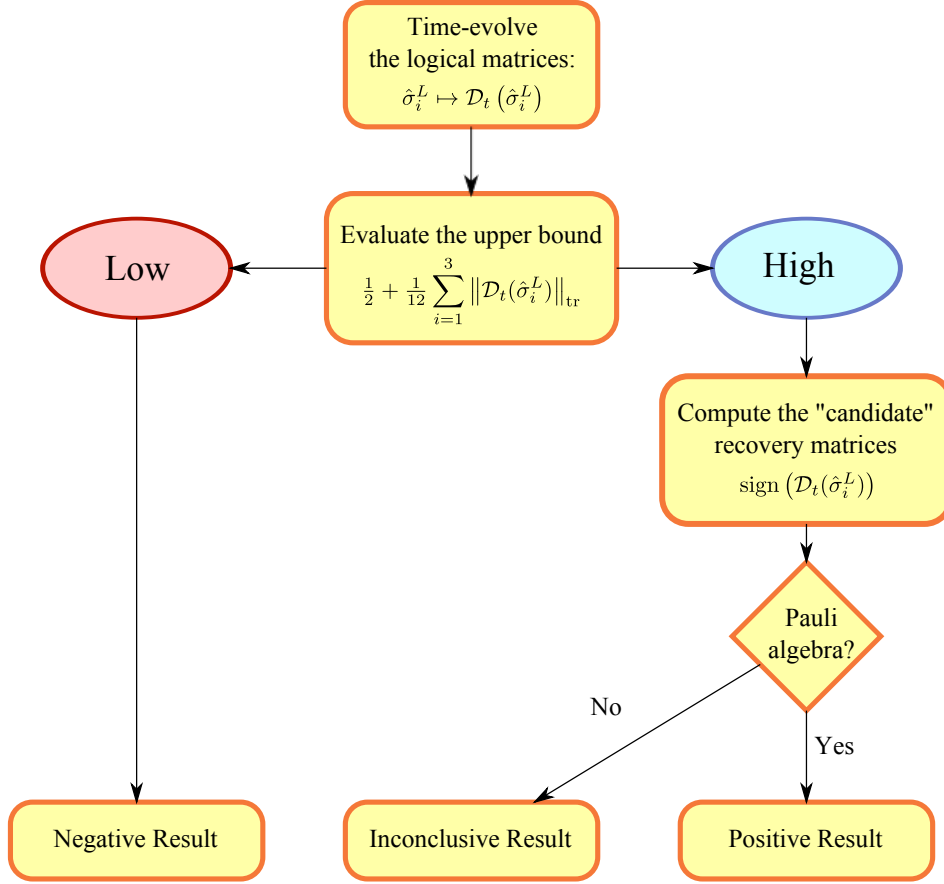
FIGURE 2.2: diagram describing how the upper bound (2.12) and the CP criterion §2.3.2 can be used to discuss the performance of quantum memory models.

2.4   Example: Optimal Recovery Operation for a Single Qubit

We shall conclude this Chapter by explicitly analyzing the simplest framework for recovery operations – the case in which the encoding system is itself a qubit. The problem can be stated as follows: *given a qubit channel $\mathcal{D}_t$, determine the qubit channel $\mathcal{R}$ that maximizes the average recovery fidelity*

$$F_t^{(\mathcal{R})} = \int d\mu_\phi \, \langle\phi| \, \mathcal{R} \circ \mathcal{D}_t \left(|\phi\rangle \langle\phi|\right) |\phi\rangle . \tag{2.29}$$

2.4.1   Single-qubit channels

In this simple case the recovery $\mathcal{R}$ is specified by $3 \cdot 4^1 = 12$ parameters. It is known [30] that these parameters can be conveniently organized as a 3×3 real matrix and a 3×1 real

vector that represent geometrically the action of $\mathcal{R}$ on the Bloch sphere: if Φ is a generic qubit channel, then

$$\Phi\left(\frac{\mathbf{1} + \mathbf{a} \cdot \boldsymbol{\sigma}}{2}\right) = \frac{\mathbf{1} + (M\mathbf{a} + \mathbf{b}) \cdot \boldsymbol{\sigma}}{2}. \tag{2.30}$$

The CP condition for Φ can be expressed as a set of inequalities involving $\mathbf{b}$ and the vector $\boldsymbol{\lambda}$ of singular values of M. Obviously in order to map the Bloch sphere into itself one must have $\max\{\lambda_i\} \le 1$ and $|\mathbf{b}| \le 1$. These conditions however are not sufficient. For $\mathbf{b} = 0$ (unital channels), the conditions on $\boldsymbol{\lambda}$ can be expressed as $\boldsymbol{\lambda} \in \mathcal{T}$, where $\mathcal{T} \subset \mathbb{R}^3$ is the tetrahedron of vertices $\mathcal{V} = \{(1,1,1), (1,-1,-1), (-1,1,-1), (-1,-1,1)\}$. As $|\mathbf{b}|$ expands, the allowed region for $\boldsymbol{\lambda}$ shrinks, until at $|\mathbf{b}| = 1$ the only allowed point is $\boldsymbol{\lambda} = (0,0,0)$ (this extremal case corresponds to amplitude damping channels).

Since in this case both $\mathcal{D}_t$ and $\mathcal{R}$ are qubit channels, this parametrization applies to both of them, thus allowing an exact solution to the problem. For higher-dimensional spaces $(\dim \mathcal{H}_{\mathrm{sys}} = d \ge 2)$, no such convenient parametrizations are known.

2.4.2 Optimal recovery operation and fidelity

Let $\mathcal{D}_t$ be parametrized by M and $\mathbf{b}$, and let us apply a singular value decomposition to M: $M = A^T \Lambda B$, with $A, B \in SO(3)$ and $\Lambda = \mathrm{diag}(\boldsymbol{\lambda})$. Then the optimal recovery operation $\mathcal{R}^{\mathrm{opt}}$ is parametrized by

$$M'_{\mathrm{opt}} = B^T R_{\mathrm{opt}} A, \qquad \mathbf{b}'_{\mathrm{opt}} = 0, \tag{2.31}$$

where R_{opt} is one of the four matrices $\{\mathrm{diag}(\mathbf{v}) : \mathbf{v} \in \mathcal{V}\}$, i.e.

$$I = \mathrm{diag}(1,1,1), \qquad\qquad R_x(\pi) = \mathrm{diag}(1,-1,-1),$$
$$R_y(\pi) = \mathrm{diag}(-1,1,-1), \qquad\qquad R_z(\pi) = \mathrm{diag}(-1,-1,1),$$

to be chosen so as to maximize the quantity $\mathrm{Tr}(R_{\mathrm{opt}}\Lambda) = \mathbf{v} \cdot \boldsymbol{\lambda}$.

The associated recovery fidelity is

$$F^{\mathrm{opt}} = \frac{1}{2} + \frac{1}{6}\mathrm{Tr}(R_{\mathrm{opt}}\Lambda) = \frac{1}{2} + \frac{1}{6}\max_{\mathbf{v} \in \mathcal{V}} \mathbf{v} \cdot \boldsymbol{\lambda}$$
$$= \frac{1}{2} + \frac{1}{6}\sum_{i=1}^{3} |\lambda_i| - \frac{1}{3}\Theta(-\det M)\min_i |\lambda_i|. \tag{2.32}$$

The combination of noise and recovery operation acts as

$$\mathcal{R}^{\mathrm{opt}} \circ \mathcal{D}_t \left(\frac{\mathbf{1} + \mathbf{a} \cdot \boldsymbol{\sigma}}{2}\right) = \frac{1}{2}\left[\mathbf{1} + \left(B^T R_{\mathrm{opt}} \Lambda B \mathbf{a} + B^T R_{\mathrm{opt}} A \mathbf{b}\right) \cdot \boldsymbol{\sigma}\right] \tag{2.33}$$

The matrix acting on **a** is symmetric; the one acting on **b** is orthogonal. The qualitative interpretation of this result is the following: the noise contracts the Bloch sphere along three "principal axes", then rotates it to some other orientation; the best one can do to recover the original states is to rotate the Bloch sphere back to the original orientation. It is impossible to reduce the amount of contraction or the length of the translation vector.

Proof. For a general qubit recovery operation, (2.6) becomes

$$
F^{(\mathcal{R})} = \int d\mu_\phi \langle \phi | \, \mathcal{R} \circ \mathcal{D}_t \left(|\phi\rangle \langle\phi| \right) | \phi \rangle = \int d\mu_\phi \mathrm{Tr} \left(|\phi\rangle \langle\phi| \, \mathcal{R} \circ \mathcal{D}_t \left(|\phi\rangle \langle\phi| \right) \right)
$$
$$
= \int d\mu_\mathbf{n} \mathrm{Tr} \left(\left(\frac{\mathbf{1} + \mathbf{n} \cdot \boldsymbol{\sigma}}{2} \right) \left(\frac{\mathbf{1} + (M'(M\mathbf{n} + \mathbf{b}) + \mathbf{b}') \cdot \boldsymbol{\sigma}}{2} \right) \right)
$$
$$
= \frac{1}{2} \left(1 + \int d\mu_\mathbf{n} \mathbf{n}^T M' M \mathbf{n} \right);
\tag{2.34}
$$

recalling that $\int d\mu_\mathbf{n} n_i n_j = \frac{1}{3} \delta_{ij}$, one has

$$
F^{(\mathcal{R})} = \frac{1}{2} + \frac{1}{6} \mathrm{Tr} \left(M' M \right).
\tag{2.35}
$$

Applying the singular value decomposition $M = A^T \Lambda B$, (2.35) becomes

$$
F^{(\mathcal{R})} = \frac{1}{2} + \frac{1}{6} \mathrm{Tr} \left(M' A^T \Lambda B \right) = \frac{1}{2} + \frac{1}{6} \mathrm{Tr} \left(B M' A^T \Lambda \right) = \frac{1}{2} + \frac{1}{6} \mathrm{Tr} \left(\widetilde{M'} \Lambda \right),
\tag{2.36}
$$

where we defined $\widetilde{M'} = B M' A^T$.

Since by (2.36) $F^{(\mathcal{R})}$ does not depend on $\mathbf{b}'$, we can set $\mathbf{b}' = 0$, so as to maximize the allowed parameter region for $\boldsymbol{\lambda}'$ [30].

Let us apply a singular value decomposition to $\widetilde{M'}$: $\widetilde{M'} = U^T \Lambda' V$, with $U, V \in SO(3)$ and $\Lambda' = \mathrm{diag}\left(\boldsymbol{\lambda}'\right)$. $\boldsymbol{\lambda}' \in \mathcal{T}$ is a vector of allowed singular values for a physical map. It is clear from (2.36) that the dependence of $F_t^{(\mathcal{R})}$ on $\boldsymbol{\lambda}'$ is of the type $F_t^{(\mathcal{R})} = \frac{1}{2} + \mathbf{w} \cdot \boldsymbol{\lambda}'$, for some constant vector $\mathbf{w}$. This means that the function $F_t^{(\mathcal{R})}(\boldsymbol{\lambda}')$ has constant gradient, hence its maxima must lie on the boundaries of the domain $\mathcal{T}$, and namely in the set of vertices[3] $\mathcal{V}$. But then $\widetilde{M'} = U^T \mathrm{diag}\left(\boldsymbol{\lambda}'_\star\right) V$, with $\boldsymbol{\lambda}'_\star \in \mathcal{V}$, is itself orthogonal. Therefore (2.36) yields

$$
F^{\mathrm{opt}} = \frac{1}{2} + \frac{1}{6} \max_{\widetilde{M'} \in SO(3)} \left\{ \sum_{i=1}^3 \widetilde{M'}_{ii} \lambda_i \right\}.
\tag{2.37}
$$

In Appendix A we prove that the set of vectors that are diagonal elements of $SO(3)$ matrices, $\Delta \equiv \{ \mathbf{r} \in \mathbb{R}^3 : r_i = R_{ii} \text{ for some } R \in SO(3) \}$, is none other than the tetrahedron $\mathcal{T}$. Thus

---

[3]If the gradient is orthogonal to a given face of $\mathcal{T}$ and pointing outwards, then the whole face is a manifold of degenerate maximum points; we can choose one of its three vertices. In all other cases the maximum point will be unique and will belong to $\mathcal{V}$.

we can conclude that

$$F^{\text{opt}} = \frac{1}{2} + \frac{1}{6} \max_{\mathbf{v} \in \Delta} \mathbf{v} \cdot \boldsymbol{\lambda} = \frac{1}{2} + \frac{1}{6} \max_{\mathbf{v} \in \mathcal{T}} \mathbf{v} \cdot \boldsymbol{\lambda} = \frac{1}{2} + \frac{1}{6} \max_{\mathbf{v} \in \mathcal{V}} \mathbf{v} \cdot \boldsymbol{\lambda}, \tag{2.38}$$

which is the result we stated in (2.32).

Finally, since $\widetilde{M'}$ is orthogonal and has diagonal elements equal to ± 1, it cannot have off-diagonal elements (otherwise the norm of a column vector would exceed 1); therefore $\widetilde{M'} = \text{diag}\left(\boldsymbol{\lambda}'_\star\right)$, and

$$\begin{cases} M'_{\text{opt}} = B^T \text{diag}\left(\boldsymbol{\lambda}'_\star\right) A, \quad \boldsymbol{\lambda}'_\star \in \mathcal{V} \text{ such that } \boldsymbol{\lambda}'_\star \cdot \boldsymbol{\lambda} = \max_{\mathbf{v} \in \mathcal{V}} \mathbf{v} \cdot \boldsymbol{\lambda}, \\ \mathbf{b}'_{\text{opt}} = 0, \end{cases} \tag{2.39}$$

as stated in (2.31). $\qquad\qquad\square$

Chapter 3

Continuous-Time Quantum Error Correction

In this Chapter the possibility of realizing passive quantum memories via Quantum Error-Correcting Codes (QECCs) is described. An elementary introduction to Quantum Error Correction (QEC) is given in Section 3.1. In Section 3.2 we present the simplest non-trivial example of a QECC, the 3-qubit bit-flip code, and discuss its efficacy at protecting quantum information as measured by the average recovery fidelity. The cases of a single, final recovery step and that of a periodically repeated recovery step are both analyzed. In the high-frequency limit, repeated QEC leads to *continuous-time* QEC (CTQEC). A historical introduction to CTQEC is provided in Section 3.3, along with a discussion of its relation to the general framework of *dissipation-based* quantum memories. Two examples of CTQEC are then studied: the 3-qubit code exposed to a bit-flip noise (Section 3.4) and the 5-qubit perfect code exposed to a depolarizing noise (Section 3.5). In the former case an analytical solution is derived and interpreted geometrically in terms of dynamical fixed points; in the latter case, a numerical solution is presented. The two codes display very similar behaviors.

3.1 Introduction to Quantum Error Correction

3.1.1 The general idea

Suppose that we have a classical bit of information and that we want to store it reliably over long periods of time. The bit must be encoded into a physical system that has at least two classical states, which can be labeled as "0" and "1" respectively. If this system is exposed to noise, in a given unit time there is a non-zero probability p for the system to change its state from "0" to "1", or *vice versa*, thus "flipping" the logical value of the encoded bit.

If p is low enough, this problem is easily solved through redundancy: encoding the logical bit into $2n - 1$ physical bits, and then performing a recovery operation based on majority voting, the probability of retrieving the wrong logical value becomes $\mathcal{O}(p^n)$, since at least n errors must occur to flip a majority of the code bits.

This means that, if the hardware is good enough (i.e. if the error probability p is sufficiently small), one can make the error probability negligible by a simple redundant encoding. This procedure, or some more sophisticated variant thereof, is what makes our classical computation and communication technology so reliable.

The step from classical physics to quantum physics poses some problems to this scheme. First of all, the no-cloning theorem [31] forbids a redundancy like the one used in the classical example – i.e., the mapping $|\psi\rangle \mapsto |\psi\rangle^{\otimes n}$ is unphysical. Secondly, quantum-mechanical measurements cause the collapse of the measured state. This forbids the straightforward application of majority voting rules, in which each bit must be measured individually. Finally, quantum noise comes in a continuum of different forms, unlike its classical counterpart which is basically restricted to bit-flips. The existence of error-correcting procedures that work against infinitely many types of errors is not obvious *a priori*.

Luckily all these problems can be overcome [8, 32]. Quantum states cannot be cloned, but redundant encodings are possible nonetheless: the qubit Hilbert space can be embedded into larger Hilbert spaces, corresponding e.g. to states of several physical qubits. Secondly, by measuring suitable combinations of physical qubits, it is possible to obtain information about the occurrence of errors while leaving the encoded information intact. As for the last problem, it turns out that correcting a finite, discrete set of quantum errors is enough to automatically correct all the continuum of possible errors.

A quantum error-correcting code (QECC) can be formally defined as a subspace C of a Hilbert space, which is usually $\mathcal{H}_n$ for some integer n. The dimension of the *code-space C* is 2^k, $k \leq n$ being the number of encoded (logical) qubits. Sometimes the QECC is defined as the mapping from $\mathcal{H}_k$ into $\mathcal{H}_n$, rather than as the image C of such mapping. P denotes the code-space projector. A QEC procedure consists of a QECC plus a recovery operation $\mathcal{R}$, that maps back $\mathcal{S}(\mathcal{H}_n)$ onto $\mathcal{S}(\mathcal{H}_k)$.

3.1.2 The stabilizer formalism

We shall now describe a very important class of QECCs: the stabilizer codes [33]. In order to do this, some formalism is required.

The *Pauli group* on n qubits is the set

$$G_n = \{1, i, -1, -i\} \times \{I, X, Y, Z\}^{\otimes n} \tag{3.1}$$

with the usual matrix multiplication. The phase factors are needed in order to ensure that the set is closed under multiplication, hence a group. Any two elements of G_n either commute or anti-commute, and every element of G_n squares to either I or $-I$.

If $g_1, \ldots, g_l$ are elements of G_n, $< g_1, \ldots, g_l >$ denotes the subgroup they generate. This is by definition the set of all elements of G that can be obtained by multiplying elements of $\{g_1, \ldots, g_l\}$ with one another, and it is clearly a subgroup of G_n.

Given a subgroup $S \subseteq G_n$, the stabilized subspace $V_S \subseteq \mathcal{H}_n$ is defined as

$$V_S = \{|\psi\rangle \in \mathcal{H}_n : g\,|\psi\rangle = +\,|\psi\rangle \;\forall g \in S\}. \tag{3.2}$$

It is easy to see that V_S is fully specified by a set of generators of S: $g_1, \ldots, g_l$ stabilize $|\psi\rangle$ if and only if the whole $< g_1, \ldots, g_l >$ does. It is also clear that if $-I \in S$, then V_S is trivial, since $-I\,|\psi\rangle = +\,|\psi\rangle$ implies $|\psi\rangle = 0$. From now on it is understood that, whenever we consider a subgroup $S \subseteq G_n$, it does not contain $-I$.

Remark. This constrains S to be an Abelian subgroup. Indeed, since Pauli group operators either commute or anti-commute, in order for S to be non-Abelian there must be at least two anti-commuting elements g_1 and g_2; then we would have $S \ni (g_1 g_2)^3 (g_2 g_1) = -(g_1 g_2)^4$; and since Pauli group operators square to either I or $-I$, $-(g_1 g_2)^4 = -(\pm I)^2 = -I$.

Now consider a subgroup $S \subseteq G_n$ with the above mentioned properties, and its stabilized subspace V_S. This can be regarded as the code-space for a QECC. The code-space projector would be

$$P = \prod_{i=1}^{n-k} \left(\frac{I + g_i}{2} \right), \tag{3.3}$$

where $\{g_1, \ldots, g_{n-k}\}$ is a set of independent generators for S. It can be shown [33] that the dimension of V_S in this case is 2^k: each projector $\frac{I+g_i}{2}$ halves the dimension of the stabilized space; hence the resulting dimension is $2^n \cdot 2^{-(n-k)} = 2^k$. Thus a QECC that stores k logical qubits into n physical ones can be specified by $n - k$ independent and commuting n-qubit Pauli operators. As we will see, this description proves very useful.

3.1.3 Stabilizer codes

The idea of stabilizer codes is to find sets of mutually compatible observables (the stabilizers) that can be measured simultaneously to detect the occurrence of errors on the code, *without perturbing the encoded information*. We shall now see how this task can be accomplished.

Given $n - k$ independent stabilizers $\{g_i\}$, one can always find k more operators $\{\bar{Z}_1, \ldots, \bar{Z}_k\}$ that commute with all the $\{g_i\}$ and with one another [33]. These can be used as logical

Z operators for the encoded qubits. Then one can also find k operators $\{\bar{X}_1, \ldots, \bar{X}_k\}$ that commute with all stabilizers and satisfy

$$[\bar{X}_i, \bar{Z}_j] = 0 \quad \forall\, i \neq j, \qquad\qquad \{\bar{X}_i, \bar{Z}_i\} = 0 \quad \forall\, i. \tag{3.4}$$

These work as logical X operators for the encoded qubits. This means that stabilizer codes are naturally equipped with a set of n-qubit operators whose action on the code-space is exactly that of the logical algebra.

Now, the $\{g_i\}$ and the $\{\bar{Z}_i\}$ together form a set of n commuting observables on the n-qubit system. Each one of them squares to the identity, so their eigenvalues are all ± 1. By diagonalizing simultaneously the set $\{\bar{Z}_1, \ldots \bar{Z}_k, g_1, \ldots, g_{n-k}\}$ one obtains a basis

$$\{|z_1, \ldots z_k; s_1, \ldots s_{n-k}\rangle : z_i \in \{0, 1\}, s_i \in \{0, 1\}\}$$

such that

$$\begin{cases} \bar{Z}_i\,|z_1, \ldots z_k; s_1, \ldots s_{n-k}\rangle = (-1)^{z_i}\,|z_1, \ldots z_k; s_1, \ldots s_{n-k}\rangle, \\ g_j\,|z_1, \ldots z_k; s_1, \ldots s_{n-k}\rangle = (-1)^{s_j}\,|z_1, \ldots z_k; s_1, \ldots s_{n-k}\rangle. \end{cases} \tag{3.5}$$

This representation is very useful, because it factors the logical algebra and the stabilizer algebra. Any vector of the basis is in the form $|\overline{\psi}\rangle \otimes |\mathbf{s}\rangle$, where $|\overline{\psi}\rangle$ is the "logical" part of the vector, and $|\mathbf{s}\rangle$ is the *"syndrome"* part of the vector. The whole Hilbert space $\mathcal{H}_n$ is spanned by several copies of the code-space, each one labeled by a "syndrome string" $\mathbf{s} = (s_1, \ldots, s_{n-k})$. The original code-space is labeled by the trivial syndrome $(0, \ldots, 0)$.

The important thing to notice is that the syndrome $\mathbf{s}$ can be measured without perturbing the logical vector $|\overline{\psi}\rangle$, since the stabilizers commute with the logical algebra. This is the central idea of stabilizer QECCs:

- Finding sets of stabilizers such that the occurrence of any error on up to d qubits[1] just moves the information from the original code-space to one of its copies without damaging it: $|\overline{\psi}\rangle \otimes |\mathbf{0}\rangle \xrightarrow{\text{1 error}} |\overline{\psi}\rangle \otimes |\mathbf{s}\rangle$.

- Obtaining $\mathbf{s}$ by measuring the stabilizers (error detection).

- Taking $|\mathbf{s}\rangle$ back to $|\mathbf{0}\rangle$ by a suitable unitary transformation (error correction).

We shall use the notation $P_\mathbf{s}$ to denote the projector onto the $\mathbf{s}$-syndrome subspace:

$$P_\mathbf{s} = \prod_{i=1}^{n-k} \frac{I + (-1)^{s_i} g_i}{2}. \tag{3.6}$$

This way $P_\mathbf{0}$ coincides with the code-space projector P.

---

[1]d is called the *distance* of the code. The smallest QECCs have $d = 1$; larger and more complicated codes can have larger values of d.

The scheme we outlined above can be summarized by writing the corresponding recovery operation. Let $U_{\mathbf{s}}$ be a unitary that reverts the syndrome vector $|\mathbf{s}\rangle$ to the default value $|\mathbf{0}\rangle$, while leaving the logical vector unchanged: $U_{\mathbf{s}} |\overline{\psi}\rangle \otimes |\mathbf{s}\rangle = |\overline{\psi}\rangle \otimes |\mathbf{0}\rangle$. Then

$$\mathcal{R}(\hat{\rho}) = \sum_{\mathbf{s} \in \{0,1\}^{n-k}} U_{\mathbf{s}} P_{\mathbf{s}} \hat{\rho} P_{\mathbf{s}} U_{\mathbf{s}}^{\dagger}. \tag{3.7}$$

Since $P_{\mathbf{s}} = I_L \otimes |\mathbf{s}\rangle \langle \mathbf{s}|$, the defining property of the $U_{\mathbf{s}}$ matrices implies

$$U_{\mathbf{s}} P_{\mathbf{s}} = U_{\mathbf{s}} (I_L \otimes |\mathbf{s}\rangle \langle \mathbf{s}|) U_{\mathbf{s}}^{\dagger} U_{\mathbf{s}} = (I_L \otimes |\mathbf{0}\rangle \langle \mathbf{0}|) U_{\mathbf{s}} = P U_{\mathbf{s}}. \tag{3.8}$$

This identity can be used to simplify (3.7) to the following form:

$$\mathcal{R}(\hat{\rho}) = \sum_{\mathbf{s} \in \{0,1\}^{n-k}} P U_{\mathbf{s}} \hat{\rho} U_{\mathbf{s}}^{\dagger} P = P \left(\sum_{\mathbf{s} \in \{0,1\}^{n-k}} U_{\mathbf{s}} \hat{\rho} U_{\mathbf{s}}^{\dagger} \right) P. \tag{3.9}$$

This form, while less intuitive, is generally more practical. It also shows clearly that the recovered state belongs to the code-space.

Remark. While in Chapter 2 recovery operations were defined as mappings into $\mathcal{S}(\mathcal{H}_1)$ (the "abstract" qubit state space), in this context it is more practical to treat recovery operations as mappings of $\mathcal{S}(\mathcal{H}_n)$ into itself. The code-space projectors in (3.9) ensure that the two points of view are straightforwardly related.

3.2 The 3-Qubit Bit-Flip Code

Consider the 3-qubit bit-flip code, defined by the following embedding of $\mathcal{H}_1$ into $\mathcal{H}_3$:

$$|0\rangle \mapsto |0_L\rangle = |000\rangle, \qquad\qquad |1\rangle \mapsto |1_L\rangle = |111\rangle. \tag{3.10}$$

This is a stabilizer code: a set of stabilizer generators is for instance $\{Z_1 Z_2, Z_2 Z_3\}$; the logical operators are $\bar{Z} = Z_1 Z_2 Z_3$ and $\bar{X} = X_1 X_2 X_3$. Two stabilizers imply four possible syndromes. To each value of the syndrome corresponds a correcting unitary:

$$(0,0) \mapsto I, \qquad\qquad (0,1) \mapsto X_3,$$
$$(1,0) \mapsto X_1, \qquad\qquad (1,1) \mapsto X_2.$$

The recovery operation (3.9) therefore takes the form

$$\mathcal{R}(\hat{\rho}) = P \hat{\rho} P + \sum_{i=1}^{3} P X_i \hat{\rho} X_i P. \tag{3.11}$$

The encoded logical operators for this code can be immediately derived from (3.10):

$$\hat{\sigma}_0^L = P, \qquad \hat{\sigma}_1^L = P\bar{X}, \qquad \hat{\sigma}_2^L = P\bar{Y}, \qquad \hat{\sigma}_3^L = P\bar{Z}, \qquad (3.12)$$

where $\bar{Y} = \frac{1}{i}\bar{Z}\bar{X} = -Y_1Y_2Y_3$. The projector P ensures that the $\{\hat{\sigma}_\alpha^L\}$ are supported in the code space. Finally from the general definition (3.6) one has

$$P = \frac{I + Z_1Z_2}{2}\frac{I + Z_2Z_3}{2} = \frac{I + Z_1Z_2 + Z_2Z_3 + Z_3Z_1}{4}. \qquad (3.13)$$

3.2.1 Average fidelity (single recovery)

The noise model we consider is a bit-flip noise of strength κ acting identically and independently on each physical qubit. This is represented by a semi-group $\{\phi_t : t \geq 0\}$ of qubit channels defined by

$$\phi_t\left(\frac{\mathbf{1} + \mathbf{a}\cdot\boldsymbol{\sigma}}{2}\right) = \frac{\mathbf{1} + a_1\sigma_1}{2} + e^{-\kappa t}\frac{a_2\sigma_2 + a_3\sigma_3}{2}. \qquad (3.14)$$

We shall now compute the average fidelity (2.9) of the recovery operation (3.11) under the decoherence channel $\mathcal{D}_t = \phi_t^{\otimes 3}$:

$$F^{(\mathcal{R})} = \frac{1}{2} + \frac{1}{12}\sum_{i=1}^{3}\mathrm{Tr}\left(\hat{\sigma}_i^L \mathcal{R} \circ \mathcal{D}_t\left(\hat{\sigma}_i^L\right)\right). \qquad (3.15)$$

$\mathcal{D}_t$ acts on the logical operators as follows:

$$\begin{cases} \mathcal{D}_t\left(\hat{\sigma}_1^L\right) = e^{-2\kappa t}\hat{\sigma}_1^L + \dfrac{1 - e^{-2\kappa t}}{4}\bar{X}, \\[2mm] \mathcal{D}_t\left(\hat{\sigma}_2^L\right) = e^{-\kappa t}\hat{\sigma}_2^L - \dfrac{e^{-\kappa t} - e^{-3\kappa t}}{4}\bar{Y}, \\[2mm] \mathcal{D}_t\left(\hat{\sigma}_3^L\right) = e^{-\kappa t}\hat{\sigma}_3^L - \dfrac{e^{-\kappa t} - e^{-3\kappa t}}{4}\bar{Z}. \end{cases} \qquad (3.16)$$

$\mathcal{R}$ stabilizes the code-space, so that $\mathcal{R}(\hat{\sigma}_i^L) = \hat{\sigma}_i^L$, while

$$\mathcal{R}(I) = 4\hat{\sigma}_0^L, \qquad \mathcal{R}(\bar{X}) = 4\hat{\sigma}_1^L, \qquad \mathcal{R}(\bar{Y}) = -2\hat{\sigma}_2^L, \qquad \mathcal{R}(\bar{Z}) = -2\hat{\sigma}_3^L; \qquad (3.17)$$
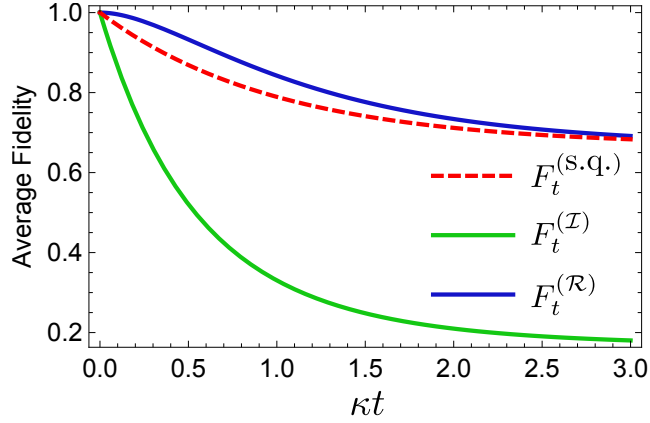
FIGURE 3.1: average fidelity as a function of time for: a single, unencoded qubit ($F_t^{(\mathrm{s.q.})}$, from (3.20)); a 3-qubit code without recovery operation ($F_t^{(\mathcal{I})}$, from (3.21)); a 3-qubit code with QEC recovery operation at read-out ($F_t^{(\mathcal{R})}$, from (3.19)). In each case there is a bit-flip noise of strength κ acting identically and independently on each qubit.

therefore the encoded operators are eigenmodes of the combination $\mathcal{R} \circ \mathcal{D}_t$:

$$
\begin{cases}
\mathcal{R} \circ \mathcal{D}_t \left(\hat{\sigma}_1^L \right) = \hat{\sigma}_1^L, \\[2mm]
\mathcal{R} \circ \mathcal{D}_t \left(\hat{\sigma}_2^L \right) = \left(\dfrac{3e^{-\kappa t} - e^{-3\kappa t}}{2} \right) \hat{\sigma}_2^L, \\[2mm]
\mathcal{R} \circ \mathcal{D}_t \left(\hat{\sigma}_3^L \right) = \left(\dfrac{3e^{-\kappa t} - e^{-3\kappa t}}{2} \right) \hat{\sigma}_3^L.
\end{cases}
\tag{3.18}
$$

Defining $\lambda(t) = \left(\frac{3e^{-\kappa t} - e^{-3\kappa t}}{2} \right)$ and plugging (3.18) into the average fidelity (3.15), we get

$$
F_t^{(\mathcal{R})} = \frac{1}{2} + \frac{1 + 2\lambda(t)}{6} = \frac{2 + \lambda(t)}{3} = 1 - \frac{1}{2}(\kappa t)^2 + \frac{2}{3}(\kappa t)^3 + \mathcal{O}\left((\kappa t)^4 \right).
\tag{3.19}
$$

We can compare the performance of this scheme to the one of a single, unencoded qubit exposed to the same bit-flip noise[2] ϕ_t:

$$
F_t^{(\mathrm{s.q.})} = \frac{2 + e^{-\kappa t}}{3}.
\tag{3.20}
$$

Moreover, in order to evaluate the importance of the recovery operation, one can consider the memory performance of the same QECC without the recovery step (i.e., with $\mathcal{R} = \mathcal{I}$), which can be computed using (2.11):

$$
F_t^{(\mathcal{I})} = \frac{1}{6} + \frac{1}{4}e^{-\kappa t} + \frac{1}{2}e^{-2\kappa t} + \frac{1}{12}e^{-3\kappa t}.
\tag{3.21}
$$

---

[2] The action of ϕ_t on the Bloch sphere is represented by the matrix $\mathrm{diag}\left(1, e^{-\kappa t}, e^{-\kappa t} \right)$. By the results of §2.4, the optimal recovery operation in this case is the identity, and the associated fidelity is (3.20).

The results are plotted in Figure 3.1. The first thing to observe is that in the absence of a recovery operation, the redundant encoding is substantially worse than the trivial one: $F_t^{(\mathcal{I})}$ undergoes a faster decay and asymptotically drops to $\frac{1}{6}$, whereas $F_t^{(\text{s.q.})}$ drops to $\frac{2}{3}$. This shows how important the final recovery operation is: redundant encodings alone merely expose the encoded information to a larger number of possible errors. It takes a clever recovery operation to exploit the potential offered by redundancy.

Another important point that emerges from Figure 3.1 is that, though the 3-qubit encoding followed by the recovery operation outperforms the unencoded qubit, the difference is noticeable only at very short times, since $1 - F_t^{(\mathcal{R})}$ is second-order in κt whereas $1 - F_t^{(\text{s.q.})}$ is first-order. Over long times, the advantage provided by encoding and recovery operations becomes negligible, and both fidelities drop to $\frac{2}{3}$.

3.2.2 Average fidelity (iterated recovery)

As we have seen, QEC is able to protect information very well over short time intervals; over long times, however, the benefits become negligible. In order to protect the encoded information over long times, the recovery step should be iterated periodically. This approach is rather distant from the principles of a "passive" quantum memory, since it requires frequent actions from an external controller. However, as we shall see later, the whole process can be made automatic by means of dissipation. Let us therefore discuss the performance of the 3-qubit QECC under a repeated error-correcting procedure.

Suppose we want to store a qubit state for a time t. Let us split the interval $[0, t]$ into ν equal parts and perform the recovery step at all times $t_k = k\frac{t}{\nu} \equiv k\Delta t$, $k = 1, \ldots, \nu$. The resulting channel is

$$\overline{\mathcal{D}}_{t;\nu \text{ steps}}^{(\mathcal{R})} = (\mathcal{R} \circ \mathcal{D}_{t/\nu})^\nu. \tag{3.22}$$

Its average fidelity can be found immediately recalling (3.18), which stated that the encoded logical matrices $\{\hat{\sigma}_\alpha^L\}$ are eigenmodes of $\mathcal{R} \circ \mathcal{D}_t$:

$$\overline{\mathcal{D}}_{t;\nu \text{ steps}}^{(\mathcal{R})} \left(\hat{\sigma}_\alpha^L \right) = \begin{cases} \hat{\sigma}_\alpha^L & \text{if } \alpha = 0, 1; \\ [\lambda(\Delta t)]^\nu \hat{\sigma}_\alpha^L & \text{if } \alpha = 2, 3. \end{cases} \tag{3.23}$$

Plugging $\overline{\mathcal{D}}_{t;\nu \text{ steps}}^{(\mathcal{R})}$ into the general formula (3.15) in place of $\mathcal{R} \circ \mathcal{D}_t$, one gets

$$\begin{aligned} F_{t;\nu \text{ steps}}^{(\mathcal{R})} &= \frac{1}{2} + \frac{1 + 2[\lambda(\Delta t)]^\nu}{6} \\ &= \frac{2}{3} + \frac{1}{3} \left(\frac{3e^{-\kappa\Delta t} - e^{-3\kappa\Delta t}}{2} \right)^\nu. \end{aligned} \tag{3.24}$$

Here Δt should be interpreted as an experimental parameter, representing the shortest time interval over which the experimenter is technically capable of performing the recovery step $\mathcal{R}$ with high accuracy. The integer ν instead plays the role of a time variable.

In order to evaluate the performance of this scheme, let us compute how many steps it takes for the fidelity to drop below a given threshold F_0 (e.g. 99%). Solving for ν the inequality

$$F^{(\mathcal{R})}_{t;\nu \text{ steps}} = \frac{2}{3} + \frac{1}{3} \left[\lambda(\Delta t) \right]^{\nu} > F_0, \tag{3.25}$$

one has

$$\nu < \nu^*(\Delta t) = \frac{|\log(3F_0 - 2)|}{|\log \lambda(\Delta t)|}. \tag{3.26}$$

The total storage time is therefore

$$T = \nu^*(\Delta t) \cdot \Delta t = |\log(3F_0 - 2)| \frac{\Delta t}{|\log \lambda(\Delta t)|}. \tag{3.27}$$

In the $\kappa \Delta t \to 0$ limit, since $\lambda(\Delta t) \approx 1 - \frac{3}{2}(\kappa \Delta t)^2$, we have

$$T \approx 3(1 - F_0) \frac{\Delta t}{\frac{3}{2}(\kappa \Delta t)^2} = \frac{2(1 - F_0)}{\kappa^2 \Delta t}, \tag{3.28}$$

where we assumed a high fidelity threshold $((1 - F_0) \ll 1)$ and expanded the logarithm to first order. Thus in the limit of continuous error correction the information is frozen. This is an instance of the *quantum Zeno effect* [34], in which frequent measurements cause an effective "freezing" of the dynamics.

From (3.28) we can see that, for $1 - F_0 = \delta \ll 1$, the storage time is $\kappa T \approx 2\delta(\kappa \Delta t)^{-1}$. In order to obtain a significant memory performance ($\kappa T \gg 1$), the time interval Δt must be very small ($\kappa \Delta t \ll \delta$). For instance, if the threshold is set to $F_0 = 99\%$, hundreds of recovery operations must be performed in a unit decoherence time κ^{-1}.

This conclusion points to an interesting direction: *continuous-time quantum error correction.* Obviously any detection-and-correction procedure requires a finite Δt to be implemented reliably, which poses a fundamental limitation to the storage times that can be achieved by the method we described in this Section. But if we consider an error-correcting procedure implemented through a continuous process, such as the ones generally used to describe dissipation, then there is no such limitation *a priori.*

3.3 Continuous-Time QEC and Dissipation-Based Quantum Memories

The idea of continuous-time quantum error correction was first presented in 1997 by Paz and Zurek [14], soon after the discovery of quantum error correction by Shor [7] and the introduction of stabilizer codes by Gottesman [33]. It was used as a way of modeling a discrete-time QEC procedure in the $\Delta t \to 0$ limit [35]. The dissipation-like nature of continuous QEC was regarded only as a technical simplification, without any physical implications.

Some years later the idea was reconsidered from a closed-loop quantum control perspective by Ahn [36] and then by Sarovar and Milburn [37]. Two types of continuous-time procedures for QEC were considered: *indirect-feedback* quantum control (measurements are performed on the system and the outcomes are used by a classical controller to form conditioning signals) and *direct-feedback* quantum control (in which the controller is itself a quantum system coupled to the controlled system). The indirect-feedback scenario is the one that generalizes the "standard" picture of discrete-time QEC, where syndrome measurements are performed and their outcomes are used to choose a correcting unitary. The direct-feedback scenario instead is a continuous-time version of *QEC without measurement* [38]: the syndrome, instead of being measured, is unitarily written on a set of ancillary qubits, which are then used to perform controlled unitary gates on the code qubits. This way the QEC process is fully unitary. At the end of each cycle the ancillas have to be replaced or refreshed to the initial state.

In the paper by Sarovar and Milburn [15] the continuous process was explicitly described as a form of dissipation. The scheme they propose is a continuous-time version of QEC without measurement on the 3-qubit bit-flip code. The main problem in the transition from discrete to continuous time in the framework of QEC without measurement is the re-initialization of ancillary qubits: in the absence of discrete QEC cycles, there are no specified times for refreshing the ancillas. The way out is to assume an *amplitude-damping noise* on the ancillas, i.e. a cooling process that continuously pumps entropy out of the system at a rate comparable to the strength of the interaction Hamiltonian that couples code qubits to ancillary qubits.

Finally, Pastawski *et al.* applied dissipation to the problem of building scalable quantum memories [13]. They consider a many-body quantum system ($N \gg 1$ qubits) in an environment that is engineered so as to produce beneficial effects against other uncontrollable sources of decoherence. The number N of qubits is considered as the amounts of resources used; thus a memory is considered effective if its reliability increases with N. A minimum physical requirement about the "beneficial" dissipation in this framework is *locality*: all Lindblad operators must involve up to k qubits each, with k a constant that does not scale with N, and there must be a way to arrange the N qubits in a d-dimensional lattice structure such that each Lindblad operator is local with respect to the lattice distance. While

numerical evidence for the existence of local dissipation-based quantum memory in $d = 4$ was presented in [13], for $d \leq 3$ the question is still not settled.

A common problem of all schemes based on dissipation is that the required "beneficial" dissipation is generally unnatural, and environment engineering is difficult. Thus one may be led to consider all protocols based on engineered dissipation as mere curiosities. However, an arbitrary Markovian evolution can be simulated with high accuracy using reasonable tools and resources:

- Hamiltonian interactions.

- Single-qubit amplitude-damping channels (cooling processes).

- A polynomial overhead in the number of qubits.

This fact is proved in Appendix C. The peculiar dissipative processes that will be postulated in the next Sections can therefore be simulated with readily available physical resources.

3.4 CTQEC on the 3-Qubit Bit-Flip Code

As an example of the ideas outlined in §3.3, we shall consider the continuous-time implementation of the simplest instance of a QECC, which is again the 3-qubit bit-flip code. Having already studied its discrete-time implementation we will be able to compare the performances of the two versions.

3.4.1 Continuous-time implementation of the recovery operation

Consider the recovery operation $\mathcal{R}$ for the 3-qubit bit-flip code (3.11). Its continuous-time version should produce the following time evolution:

$$\hat{\rho}(t) = e^{-\gamma t} \hat{\rho}(0) + \left(1 - e^{-\gamma t}\right) \mathcal{R}(\hat{\rho}(0)). \tag{3.29}$$

Since $\Phi_t^{(\mathcal{R})} \equiv e^{-\gamma t}\mathcal{I} + (1 - e^{-\gamma t})\mathcal{R}$ is a convex combination of CPTP maps for all $t \geq 0$, it is guaranteed to be CPTP itself. $\Phi_t^{(\mathcal{R})}$ drives the initial state $\hat{\rho}(0)$ to its error-corrected version $\mathcal{R}(\hat{\rho}(0))$ over a time-scale of γ^{-1}.

We will now prove that the time evolution $\Phi_t^{(\mathcal{R})}$ can be derived from a Markovian master equation (1.13). In order to prove this, we shall put the time derivative of (3.29) in a Lindblad form:

$$\frac{d}{dt}\hat{\rho}(t) = -\gamma e^{-\gamma t} \hat{\rho}(0) + \gamma e^{-\gamma t} \mathcal{R}(\hat{\rho}(0)) = \gamma e^{-\gamma t}\left(\mathcal{R}(\hat{\rho}(0)) - \hat{\rho}(0)\right); \tag{3.30}$$

now, from (3.29), we have that $e^{-\gamma t}(\mathcal{R}(\hat{\rho}(0)) - \hat{\rho}(0)) = \mathcal{R}(\hat{\rho}(0)) - \hat{\rho}(t)$ and $\mathcal{R}(\hat{\rho}(0)) = \mathcal{R}(\hat{\rho}(t))$, so that (3.30) becomes

$$\frac{d}{dt}\hat{\rho}(t) = \gamma(\mathcal{R}(\hat{\rho}(0)) - \hat{\rho}(t)) = \gamma(\mathcal{R}(\hat{\rho}(t)) - \hat{\rho}(t)), \tag{3.31}$$

From now on the time dependence of $\hat{\rho}$ is understood. Expanding $\mathcal{R}$ in Kraus form, (3.31) becomes

$$\begin{aligned}
\frac{d}{dt}\hat{\rho} &= \gamma\left(\mathcal{R}(\hat{\rho}) - \hat{\rho}\right) = \gamma\left(P\hat{\rho}P + \sum_{i=1}^{3} PX_i\hat{\rho}X_iP - \hat{\rho}\right) \\
&= \gamma\left(\sum_{\alpha=0}^{3} PX_{\hat{\boldsymbol{\alpha}}}\hat{\rho}X_{\hat{\boldsymbol{\alpha}}}P - \frac{1}{2}\{\hat{\rho}, I\}\right),
\end{aligned} \tag{3.32}$$

where we introduce the shorthand notations $X_{\mathbf{h}} = X_1^{h_1}X_2^{h_2}X_3^{h_3}$ and $(\hat{\boldsymbol{\alpha}})_j = \delta_{\alpha j}$, $j \in \{1, 2, 3\}$. Now, since by construction $\sum_{\mathbf{s}} P_{\mathbf{s}} = I$ and $P_{\mathbf{s}} = U_{\mathbf{s}}PU_{\mathbf{s}}^{\dagger}$, we have $\sum_{\alpha=0}^{3} X_{\hat{\boldsymbol{\alpha}}}PX_{\hat{\boldsymbol{\alpha}}} = I$. Plugged into (3.32), this yields

$$\frac{d}{dt}\hat{\rho} = \gamma\sum_{\alpha=0}^{3}\left(PX_{\hat{\boldsymbol{\alpha}}}\hat{\rho}X_{\hat{\boldsymbol{\alpha}}}P - \frac{1}{2}\{\hat{\rho}, (X_{\hat{\boldsymbol{\alpha}}}P)(PX_{\hat{\boldsymbol{\alpha}}})\}\right), \tag{3.33}$$

which is a master equation in the form (1.13) with Lindblad operators

$$\left\{\sqrt{\gamma}PX_{\hat{\boldsymbol{\alpha}}} : \alpha \in \{0, 1, 2, 3\}\right\}. \tag{3.34}$$

The bit-flip noise, acting identically and independently on each qubit, is represented by the following Lindblad operators:

$$\left\{\sqrt{\frac{\kappa}{2}}X_i : i \in \{1, 2, 3\}\right\}. \tag{3.35}$$

The resulting evolution is Markovian and induced by the sum of the error-inducing and the error-correcting Lindbladians: by joining the sets of Lindblad operators (3.34) and (3.35) we obtain the total set of Lindblad operators,

$$\left\{\hat{L}_1, \dots \hat{L}_7\right\} = \left\{\sqrt{\frac{\kappa}{2}}X_1, \sqrt{\frac{\kappa}{2}}X_2, \sqrt{\frac{\kappa}{2}}X_3, \sqrt{\gamma}P, \sqrt{\gamma}PX_1, \sqrt{\gamma}PX_2, \sqrt{\gamma}PX_3\right\}, \tag{3.36}$$

and the resulting master equation is

$$\frac{d}{dt}\hat{\rho} = \mathcal{L}_{\text{noise}}(\hat{\rho}) + \mathcal{L}_{\text{e.c.}}(\hat{\rho}) = \sum_{k=1}^{7}\left(\hat{L}_k\hat{\rho}\hat{L}_k^\dagger - \frac{1}{2}\left\{\hat{L}_k^\dagger\hat{L}_k, \hat{\rho}\right\}\right)$$

$$= \frac{\kappa}{2}\sum_{i=1}^{3}X_i\hat{\rho}X_i + \gamma\left(P\hat{\rho}P + \sum_{i=1}^{3}PX_i\hat{\rho}X_iP\right) - \left(\frac{3}{2}\kappa + \gamma\right)\hat{\rho}. \tag{3.37}$$

The formal solution to (3.37) is obtained by exponentiation:

$$\mathcal{D}_t = \exp\left[t\left(\mathcal{L}_{\text{noise}} + \mathcal{L}_{\text{e.c.}}\right)\right]. \tag{3.38}$$

3.4.2   Average recovery fidelity

Given the equivalence of each physical qubit in both the initial conditions (code-states are of the type $\alpha\left|000\right\rangle + \beta\left|111\right\rangle$) and the evolution equation (3.37), the evolved state is constrained to the following form:

$$\hat{\rho} \mapsto a(t)\hat{\rho} + b(t)\sum_{i=1}^{3}X_i\hat{\rho}X_i + c(t)\sum_{i=1}^{3}X_i\bar{X}\hat{\rho}\bar{X}X_i + d(t)\bar{X}\hat{\rho}\bar{X}, \tag{3.39}$$

where $\bar{X} \equiv X_1X_2X_3$. It is understood that $\hat{\rho}$ is a code-state: $\hat{\rho} = P\hat{\rho}P$. Let us define the following shorthand notation:

$$\hat{A} = \hat{\rho}, \qquad \hat{B} = \sum_{i=1}^{3}X_i\hat{\rho}X_i, \qquad \hat{C} = \sum_{i=1}^{3}X_i\bar{X}\hat{\rho}\bar{X}X_i, \qquad \hat{D} = \bar{X}\hat{\rho}\bar{X}. \tag{3.40}$$

Loosely speaking, A is an error-free state; B and C are homogeneous sums of states with one and two X errors respectively; and D is the A state affected by an $\bar{X}$ logical error (i.e. an X error on each qubit).

The total Lindbladian (3.37) acts on operators (3.40) as follows:

$$\begin{cases} \mathcal{L}(\hat{A}) = \dfrac{\kappa}{2}\hat{B} - \dfrac{3}{2}\kappa\hat{A}, \\[2mm] \mathcal{L}(\hat{B}) = \left(\dfrac{3}{2}\kappa + 3\gamma\right)\hat{A} - \left(\dfrac{3}{2}\kappa + \gamma\right)\hat{B} + \kappa\hat{C}, \\[2mm] \mathcal{L}(\hat{C}) = \left(\dfrac{3}{2}\kappa + 3\gamma\right)\hat{D} - \left(\dfrac{3}{2}\kappa + \gamma\right)\hat{C} + \kappa\hat{B}, \\[2mm] \mathcal{L}(\hat{D}) = \dfrac{\kappa}{2}\hat{C} - \dfrac{3}{2}\kappa\hat{D}. \end{cases} \tag{3.41}$$

This proves that the ansatz (3.39) is correct: the subspace spanned by $\hat{A}$, $\hat{B}$, $\hat{C}$ and $\hat{D}$ is invariant. The evolution equations for the coefficients $a(t)$, $b(t)$, $c(t)$ and $d(t)$ are found from

$$
\begin{aligned}
\dot{a}\hat{A} + \dot{b}\hat{B} + \dot{c}\hat{C} + \dot{d}\hat{D} &= \mathcal{L}\big(a\hat{A} + b\hat{B} + c\hat{C} + d\hat{D}\big) \\
&= \left[\left(\frac{3}{2}\kappa + 3\gamma\right) b - \frac{3}{2}\kappa a \right] \hat{A} + \left[\frac{\kappa}{2}a - \left(\frac{3}{2}\kappa + \gamma\right) b + \kappa c \right] \hat{B} \\
&\quad + \left[\frac{\kappa}{2}d - \left(\frac{3}{2}\kappa + \gamma\right) c + \kappa b \right] \hat{C} + \left[\left(\frac{3}{2}\kappa + 3\gamma\right) c - \frac{3}{2}\kappa d \right] \hat{D}, \quad (3.42)
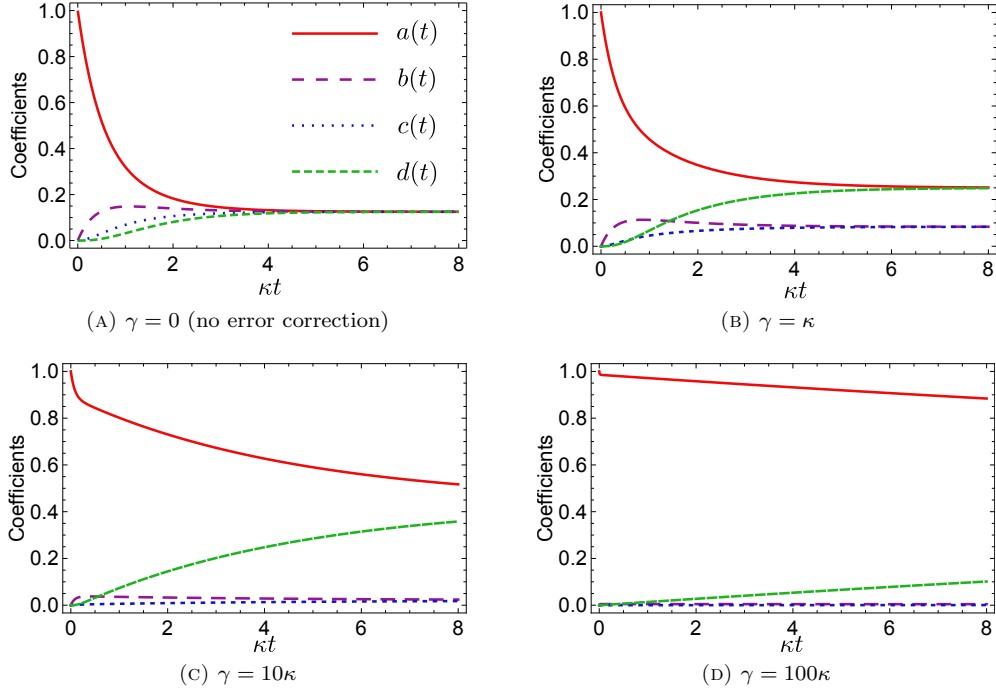\end{aligned}
$$

and read as follows:

$$
\begin{cases}
\dot{a}(t) = \left(\dfrac{3}{2}\kappa + 3\gamma\right) b(t) - \dfrac{3}{2}\kappa a(t), \\[2mm]
\dot{b}(t) = \dfrac{\kappa}{2}a(t) - \left(\dfrac{3}{2}\kappa + \gamma\right) b(t) + \kappa c(t), \\[2mm]
\dot{c}(t) = \dfrac{\kappa}{2}d(t) - \left(\dfrac{3}{2}\kappa + \gamma\right) c(t) + \kappa b(t), \\[2mm]
\dot{d}(t) = \left(\dfrac{3}{2}\kappa + 3\gamma\right) c(t) - \dfrac{3}{2}\kappa d(t);
\end{cases}
\qquad (3.43)
$$

Defining the functions $f^{\pm}(t) \equiv a(t) \pm d(t)$ and $g^{\pm}(t) \equiv b(t) \pm c(t)$, it is easy to see that the four equations (3.43) decouple into two equations involving only f^+ and g^+ and two more equations involving only f^- and g^-. Moreover, $a + 3b + 3c + d = f^+ + 3g^+$ is a constant (corresponding to trace preservation). Thus the system (3.43) can be easily solved, and the solution can be used to compute the exact time evolution of every initially encoded operator ($a(0) = 1$, $b(0) = c(0) = d(0) = 0$). The resulting coefficients as functions of time are plotted in Figure 3.2 for several values of the ratio γ/κ.

In the absence of error correction (Figure 3.2a) all four coefficients converge to the value $\frac{1}{8}$ and the state spreads uniformly over all syndrome subspaces; when the error-correcting dissipator is turned on (Figures 3.2b and 3.2c) the weight outside the code-space, represented by b and c, is suppressed. Finally, in the strong-EC limit (Figure 3.2d) b and c are negligibly small at all times, while a decreases very slowly and d, representing undetectable logical errors, increases at the same rate. In the end logical errors corrupt the information anyway, but it is clear that one can (at least in principle) make the storage time arbitrarily long by increasing γ.

We shall now compute the average fidelity between the initially encoded qubit and its time-evolved counterpart, without performing any additional recovery operation at read-out. In order to avoid ambiguity between the continuously implemented recovery operation $\mathcal{R}$ and any final recovery operation $\mathcal{F}$ that one may perform at read-out, we shall denote the corresponding average fidelity by $F_t^{(\mathcal{R};\mathcal{F})}$.

FIGURE 3.2: the coefficients in formula (3.39) as functions of time, for $\frac{\gamma}{\kappa} = 0, 1, 10, 100$.

If $\hat{\Psi}_{\mathbf{n}}^L = P\hat{\Psi}_{\mathbf{n}}^L P$ is the encoded logical state corresponding to the unit vector $\mathbf{n}$ in the Bloch sphere, i.e. $\hat{\Psi}_{\mathbf{n}}^L = \frac{\hat{\sigma}_0^L + \mathbf{n} \cdot \hat{\boldsymbol{\sigma}}^L}{2}$, one has

$$
\begin{aligned}
F_t^{(\mathcal{R};\mathcal{I})} &= \int d\mu_{\mathbf{n}} \mathrm{Tr}\left(\hat{\Psi}_{\mathbf{n}}^L \mathcal{D}_t\left(\hat{\Psi}_{\mathbf{n}}^L\right)\right) \\
&= \int d\mu_{\mathbf{n}} \mathrm{Tr}\left(\hat{\Psi}_{\mathbf{n}}^L\left(a(t)\hat{\Psi}_{\mathbf{n}}^L + b(t)\sum_{i=1}^{3} X_i \hat{\Psi}_{\mathbf{n}}^L X_i + c(t)\sum_{i=1}^{3} X_i \bar{X}\hat{\Psi}_{\mathbf{n}}^L \bar{X}X_i + d(t)\bar{X}\hat{\Psi}_{\mathbf{n}}^L \bar{X}\right)\right) \\
&= \int d\mu_{\mathbf{n}} \mathrm{Tr}\left(a(t)\hat{\Psi}_{\mathbf{n}}^L + d(t)\hat{\Psi}_{\mathbf{n}}^L \bar{X}\hat{\Psi}_{\mathbf{n}}^L \bar{X}\right),
\end{aligned}
\tag{3.44}
$$

since any X matrix between two encoded operators is annihilated by the code-space projectors ($PX_i P = 0 \ \forall i$). Now, using the fact that $\bar{X}$ acts on the encoded qubit as a bit-flip operator, we get

$$
\begin{aligned}
F_t^{(\mathcal{R};\mathcal{I})} &= \int d\mu_{\mathbf{n}}\left(a(t) + d(t)\mathrm{Tr}\left(\hat{\Psi}_{\mathbf{n}}^L \hat{\Psi}_{R_x(\pi)\mathbf{n}}^L\right)\right) \\
&= a(t) + d(t)\int d\mu_{\mathbf{n}}\frac{1 + n_x^2 - n_y^2 - n_z^2}{2} = a(t) + \frac{1}{3}d(t).
\end{aligned}
\tag{3.45}
$$

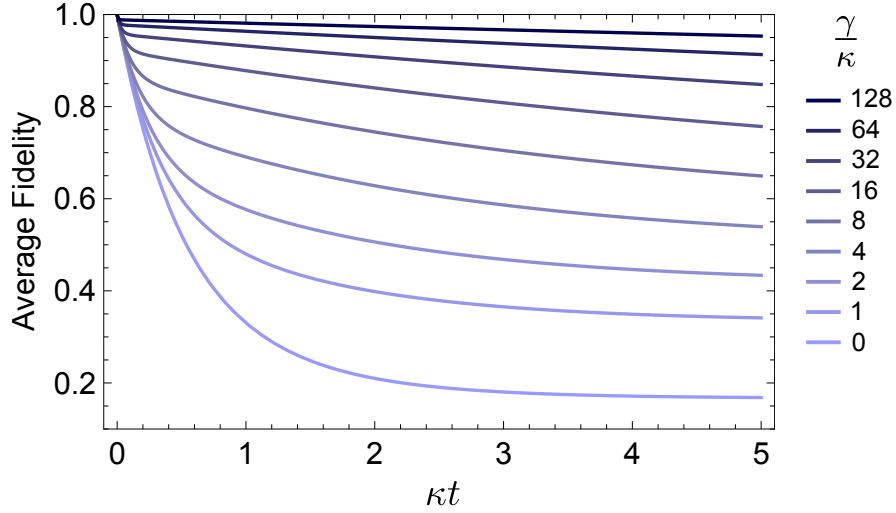A plot of the decay of $F_t^{(\mathcal{R};\mathcal{I})}$ for several values of γ is shown in Figure 3.3.

FIGURE 3.3: decay of the average fidelity $F_t^{(\mathcal{R};\mathcal{I})}$ (3.45) for several values of the ratio $\frac{\gamma}{\kappa}$.

If we perform an additional QEC operation $\mathcal{R}$ at read-out, the recovered state changes according to the following rule:

$$a'(T) = a(T) + 3b(T), \qquad\qquad b'(T) = 0,$$
$$c'(T) = 0, \qquad\qquad d'(T) = d(T) + 3c(T). \qquad (3.46)$$

All the parts of the state are mapped back to the code-space through the shortest path – the parts with a single X error are corrected, so a' gets the b contribution; the parts with two X errors get a third X error, so d' gets the c contribution. This brings the recovery fidelity to

$$F_t^{(\mathcal{R};\mathcal{R})} = a(t) + 3b(t) + c(t) + \frac{1}{3}d(t) = F_t^{(\mathcal{R};\mathcal{I})} + 3b(t) + c(t), \qquad (3.47)$$

which is greater than $F_t^{(\mathcal{R};\mathcal{I})}$ and saturates the upper bound (2.12). Plots of the decay of $F_t^{(\mathcal{R};\mathcal{R})}$ over time are shown in Figure 3.4.

In the strong-EC limit, the b and c coefficients soon become neglibigle; thus the final read-out recovery is useful only for very short times, which is not the range we are interested in. Asymptotically only a and d matter. This is reasonable, since the recovery is being continuously implemented as part of the dynamics; we would thus expect that one additional recovery operation should not change the result significantly – and indeed it does not, and $F_t^{(\mathcal{R};\mathcal{I})}$ is close to optimal. We shall therefore neglect the final read-out recovery step in the following.
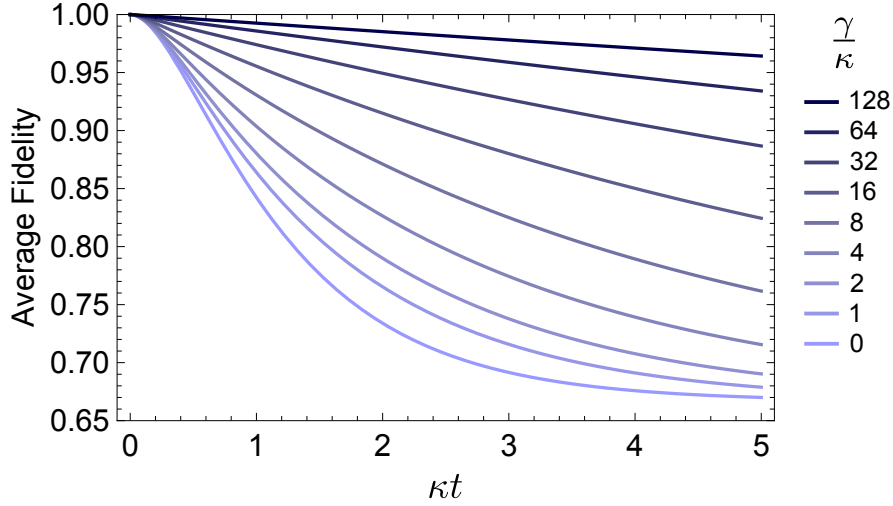
FIGURE 3.4: decay of the average fidelity $F_t^{(\mathcal{R};\mathcal{R})}$ (3.47) for several values of the ratio $\frac{\gamma}{\kappa}$.

3.4.3 Fixed points and asymptotic decay rate

A better understanding of the situation can be gained by studying the dependence of the fixed points and *asymptotic decay rate* (ADR) [39] of $\mathcal{D}_t$ on the parameter $\frac{\gamma}{\kappa}$.

Definition (ADR). The ADR of a Markovian evolution $\mathcal{D}_t = e^{t\mathcal{L}}$ is the lowest (non-zero) decay rate allowed by $\mathcal{D}_t$. More rigorously, it is the minimum of the set

$$\{|\Re(\lambda)| : \Re(\lambda) \neq 0 \text{ and } \mathcal{L}(\hat{\rho}_\lambda) = \lambda\hat{\rho}_\lambda \text{ for some } \hat{\rho}_\lambda\}.$$

If the dynamics is unitary (i.e. $\mathcal{L}$ is purely Hamiltonian) the ADR is undefined. Otherwise it is a strictly positive quantity. It measures the time-scale over which the system reaches its steady state.

Let us consider the master equation (3.37). It is convenient to analyze its Liouville representation $|\dot{\rho}\rangle\rangle = \mathcal{M}_\mathcal{L} |\rho\rangle\rangle$. The Liouville representation is a mathematical way to treat operators as vectors and super-operators as ordinary operators; it is introduced in Appendix B. Applying formula (B.7) to the Lindbladian (3.37), one has

$$\mathcal{M}_\mathcal{L} = \sum_{i=1}^{3} \left(\frac{\kappa}{2} X_i \otimes X_i + \gamma(PX_i) \otimes (PX_i) \right) + \gamma P \otimes P - \left(\frac{3}{2}\kappa + \gamma \right) I \otimes I$$

$$= \left(\frac{\kappa}{2} I \otimes I + \gamma P \otimes P \right) \left(I \otimes I + \sum_{i=1}^{3} X_i \otimes X_i \right) - (2\kappa + \gamma) I \otimes I. \qquad (3.48)$$

Thus the fixed points and the ADR of $\mathcal{D}_t$ can be found by putting the 64×64 matrix $\mathcal{M}_\mathcal{L}$ defined in (3.48) into standard Jordan form. This can be done symbolically on a computer.

eigenvalue	multiplicity
0	2
$-\gamma$	6
$-(\gamma + 1)$	22
$-(\gamma + 2)$	24
$-(\gamma + 3)$	6
$-\dfrac{\gamma + 4 + \sqrt{(\gamma + 4)^2 - 12}}{2}$	2
$-\dfrac{\gamma + 4 - \sqrt{(\gamma + 4)^2 - 12}}{2}$	2

TABLE 3.1: eigenvalues of the 3-qubit Lindbladian involving bit-flip noise and continuous error correction ($\kappa = 1$).

The result is that all Jordan blocks are trivial, i.e. $\mathcal{M}_\mathcal{L}$ can be put in diagonal form, and the 64 eigenvalues are listed in Table 3.1. In the strong QEC limit ($\gamma \gg \kappa$) one has:

- Two independent fixed points, corresponding to zero eigenvalues (one such fixed point is required by contractivity, while the other is a genuine property of the dynamics).

- 60 modes that decay over a short time scale $\sim \gamma^{-1}$.

- Two modes that decay over a long time scale $\sim \gamma\kappa^{-2}$, corresponding to the last entry in Table 3.1,

$$-\frac{(\gamma + 4\kappa) - \sqrt{(\gamma + 4\kappa)^2 - 12\kappa^2}}{2} = -\frac{\gamma + 4\kappa}{2}\left(1 - \sqrt{1 - \frac{12\kappa^2}{(\gamma + 4\kappa)^2}}\right)$$
$$= -\frac{3\kappa^2}{\gamma} + \mathcal{O}\left(\frac{\kappa^3}{\gamma^2}\right). \tag{3.49}$$

The latter modes are stable in the limit of infinitely strong QEC, or equivalently in the absence of noise. For large but finite values of $\frac{\gamma}{\kappa}$, they are the slowest decaying modes, which define the ADR:

$$\Delta = \frac{\gamma + 4\kappa - \sqrt{(\gamma + 4\kappa)^2 - 12\kappa^2}}{2} \sim 3\frac{\kappa^2}{\gamma}. \tag{3.50}$$

Stable modes. The two stable modes are easy to find. First of all, the subspace spanned by I and P is invariant under the action of the Lindbladian (3.37):

$$\begin{cases} \mathcal{L}[I] = \sum_{i=1}^{3}\left(\frac{\kappa}{2}I + \gamma P\right) + \gamma P - \left(\frac{3}{2}\kappa + \gamma\right)I = \gamma(4P - I), \\ \mathcal{L}[P] = \sum_{i=1}^{3}\left(\frac{\kappa}{2}X_i P X_i + \gamma P X_i P X_i P\right) + \gamma P - \left(\frac{3}{2}\kappa + \gamma\right)P = \frac{\kappa}{2}(I - 4P). \end{cases} \tag{3.51}$$

Hence $\mathcal{L}[aI + bP] = \left(a\gamma - b\frac{\kappa}{2}\right)(4P - I)$ is zero for $b = 2\frac{\gamma}{\kappa}a$. Normalizing the trace of the linear combination to 2, we have the first fixed point:

$$\hat{\sigma}_0^* = \frac{1}{2}\frac{\kappa I + 2\gamma P}{2\kappa + \gamma}.\tag{3.52}$$

In the strong QEC limit, this approximates the $\hat{\sigma}_0^L$ operator. By the same reasoning it can be seen that $\bar{X}$ and $P\bar{X}P$ can be combined to form a fixed point:

$$\begin{cases} \mathcal{L}[\bar{X}] = \gamma(4P\bar{X}P - \bar{X}), \\ \mathcal{L}[P\bar{X}P] = \dfrac{\kappa}{2}(\bar{X} - 4P\bar{X}P), \end{cases}\tag{3.53}$$

thus $\mathcal{L}(a\bar{X} + bP\bar{X}P)$ is zero for $b = 2\frac{\gamma}{\kappa}a$, and the second fixed point is

$$\sigma_1^* = \frac{1}{2}\frac{\kappa\bar{X} + 2\gamma P\bar{X}P}{2\kappa + \gamma}.\tag{3.54}$$

The normalization is chosen so that $\|\hat{\sigma}_1^*\|_{\mathrm{tr}} = 2$. In the strong QEC limit, $\hat{\sigma}_1^*$ approximates $\hat{\sigma}_1^L$.

Slowly-decaying modes. The other two modes of interest are those that, though not fixed, decay very slowly in the $\gamma \gg \kappa$ limit. These two modes are expected to approximate $\hat{\sigma}_2^L$ and $\hat{\sigma}_3^L$. It is easy to see that the subspace spanned by $\bar{Z}$ and $P\bar{Z}P$ is invariant under the action of the Lindbladian:

$$\begin{cases} \mathcal{L}[\bar{Z}] = -(3\kappa + \gamma)\bar{Z} - 2\gamma P\bar{Z}P, \\ \mathcal{L}[P\bar{Z}P] = -\dfrac{\kappa}{2}\bar{Z} - \kappa P\bar{Z}P, \end{cases}\tag{3.55}$$

so that

$$\mathcal{L}[a\bar{Z} + bP\bar{Z}P] = -\left((3\kappa + \gamma)a + \frac{\kappa}{2}b\right)\bar{Z} - (2\gamma a + \kappa b)P\bar{Z}P.\tag{3.56}$$

The eigenvalue problem restricted to this subspace,

$$\begin{pmatrix} -(3\kappa + \gamma) & -\frac{\kappa}{2} \\ -2\gamma & -\kappa \end{pmatrix}\begin{pmatrix} a \\ b \end{pmatrix} = \lambda\begin{pmatrix} a \\ b \end{pmatrix},\tag{3.57}$$

can be solved to obtain the eigenvalues

$$\lambda_\pm^* = \frac{-(\gamma + 4\kappa) \pm \sqrt{\gamma^2 + 8\kappa\gamma + 4\kappa^2}}{2}.\tag{3.58}$$

The one with the $+$ sign is the ADR. The corresponding slowly-decaying mode is

$$\hat{\sigma}_3^* = \frac{\left(2\kappa + \gamma + \sqrt{\gamma^2 + 8\kappa\gamma + 4\kappa^2}\right) P\bar{Z}P - \bar{Z}}{4\kappa + \gamma + \sqrt{\gamma^2 + 8\kappa\gamma + 4\kappa^2}}. \tag{3.59}$$

In the strong QEC limit this approximates $\hat{\sigma}_3^L$. Finally, the same reasoning can be applied to $\bar{Y}$ and $P\bar{Y}P$, since the only property of $\bar{Z}$ that was used in this derivation (its anti-commutation with X_1, X_2 and X_3) is shared by $\bar{Y}$. Therefore

$$\hat{\sigma}_2^* = \frac{\left(2\kappa + \gamma + \sqrt{\gamma^2 + 8\kappa\gamma + 4\kappa^2}\right) P\bar{Y}P - \bar{Y}}{4\kappa + \gamma + \sqrt{\gamma^2 + 8\kappa\gamma + 4\kappa^2}} \tag{3.60}$$

completes the set of independent "quasi-fixed" operators.

Qualitative behavior of the encoded qubit. $\mathcal{S}(\mathcal{H}_3)$ is a large manifold: it has (real) dimension $4^3 - 1 = 63$. The Bloch sphere is a 3-manifold, and so is its encoded image. The encoding therefore takes place in a tiny sub-manifold of the available state space. As we have seen, 60 out of the 63 dimension of $\mathcal{S}(\mathcal{H}_3)$ decay over a short time-scale $\sim \gamma^{-1}$. Of the remaining three dimensions, one is exactly stable and two decay over a long time scale $\Delta^{-1} \sim \gamma\kappa^{-2}$. This defines a quasi-stable 3-manifold

$$\mathcal{Q} = \left\{ \frac{\hat{\sigma}_0^* + \mathbf{r} \cdot \hat{\boldsymbol{\sigma}}^*}{2} : \mathbf{r} \in \mathbb{R}^3 \text{ such that } \hat{\sigma}_0^* + \mathbf{r} \cdot \hat{\boldsymbol{\sigma}}^* \geq 0 \right\} \subset \mathcal{S}(\mathcal{H}_3). \tag{3.61}$$

$\mathcal{Q}$ is generally *not* aligned with the encoded Bloch sphere. It is if and only if $\gamma = \infty$ (i.e. $\kappa = 0$). If γ is large but finite, there will be a small "tilt" between the two 3-manifolds.

The first part of the time evolution therefore is a sudden collapse of the encoded Bloch sphere onto $\mathcal{Q}$, i.e. a sudden suppression of all non-protected modes involved in the original encoding. This process causes a small fidelity loss of order $\frac{\kappa}{\gamma}$ (the angle between the two manifolds) in a short time interval $\sim \gamma^{-1}$, so that in the the initial slope of F_t is approximately independent of γ. This explains the behavior of the fidelity curves in Figure 3.3.

After this transient, when all non-fixed modes have been suppressed, the dynamics is confined to the sub-manifold $\mathcal{Q}$. The decoherence process takes the form of an effective bit-flip channel whose strength is the ADR, $\Delta \propto \kappa^2 \gamma^{-1}$.

s	$U_\mathbf{s}$	s	$U_\mathbf{s}$	s	$U_\mathbf{s}$	s	$U_\mathbf{s}$
0000	I	0100	Z_5	1000	X_2	1100	X_3
0001	X_1	0101	Z_2	1001	Z_4	1101	Y_2
0010	Z_3	0110	X_4	1010	Z_1	1110	Y_3
0011	X_5	0111	Y_5	1011	Y_1	1111	Y_4

TABLE 3.2: correction unitaries for the 5-qubit perfect code. $\mathbf{s}$ is the 4-bit syndrome string obtained by measuring the stabilizers, and $U_\mathbf{s}$ is the prescribed unitary operation that resets $\mathbf{s}$ to (0000).

3.5 CTQEC on the 5-Qubit Perfect Code

3.5.1 The 5-qubit perfect code

The 3-qubit QECC we studied in the previous Section is not a completely satisfactory example, since it is only able to correct a "classical" noise like the bit-flip. It would not be able to protect quantum information against a general combination of bit-flip and phase-flip errors. In this Section we are thus going to consider the simplest QECC that is capable of correcting *every* single-qubit error, which is the 5-qubit perfect code discovered by Laflamme [40].

The 5-qubit perfect code is a stabilizer code defined by the following stabilizer operators:

$$\begin{cases} g_1 = X_1 Z_2 Z_3 X_4 \\ g_2 = X_2 Z_3 Z_4 X_5 \\ g_3 = X_1 X_3 Z_4 Z_5 \\ g_4 = Z_1 X_2 X_4 Z_5 \end{cases} \tag{3.62}$$

There are $2^4 = 16$ possible syndromes: one is associated to the absence of any error; the other 15 correspond to an X, Y or Z error occurring on any one of the 5 qubits. The prescribed correction operations are shown in Table 3.2.

The logical operators are $\bar{Z} = Z_1 Z_2 Z_3 Z_4 Z_5$ and $\bar{X} = X_1 X_2 X_3 X_4 X_5$; the codewords can be found by solving the eigenvector problem $g_i \ket{\psi} = + \ket{\psi} \; \forall i$ and $\bar{Z} \ket{\psi} = \pm \ket{\psi}$.

The code detects all single-qubit and 2-qubit errors. It corrects single-qubit errors, while in general the correction of 2-qubit errors fails (e.g. the $X_1 Z_3$ error would be detected but misinterpreted as a single-qubit X_5 error, and corrected accordingly; the resulting gate would be $X_1 Z_3 X_5 = \bar{Z} g_1 g_2 g_4$, that is an undetectable logical phase-flip).

3.5.2 Continuous-time implementation of the recovery operation

The recovery operation for the 5-qubit QECC is the obtained from the general form (3.9), with the $U_{\mathbf{s}}$ unitaries given in Table 3.2. Its continuous implementation is given by the family of channels

$$\Phi_t^{(\mathcal{R})} = e^{-\gamma t}\mathcal{I} + (1 - e^{-\gamma t})\mathcal{R} \tag{3.63}$$

As we have seen for the 3-qubit code (3.33), this semi-group of channels is the solution of a Markovian master equation with Lindblad operators $\left\{\sqrt{\gamma}PU_{\mathbf{s}}\right\}$.

The noise model we shall consider is a uniform depolarizing channel with strength κ, acting identically and independently on each qubit:

$$\Phi_t = \phi_t^{\otimes 5}, \qquad \phi_t\left(\frac{\mathbf{1} + \mathbf{a}\cdot\boldsymbol{\sigma}}{2}\right) = \frac{\mathbf{1} + e^{-\kappa t}\mathbf{a}\cdot\boldsymbol{\sigma}}{2}. \tag{3.64}$$

This channel is produced by a Markovian master equation whose Lindblad operators are $\left\{\sqrt{\frac{\kappa}{2}}\sigma_a^{(i)}\right\}$, with $\sigma_a^{(i)}$ representing the Pauli matrix σ_a acting on the i-th qubit.

The decoherence channel resulting from the combination of depolarizing noise and continuous-time error correction is formally given by

$$\mathcal{D}_t = \exp\left[t\left(\mathcal{L}_{\text{noise}} + \mathcal{L}_{\text{e.c.}}\right)\right]. \tag{3.65}$$

While for the 3-qubit QECC an analytical computation was feasible, the 5-qubit QECC requires a numerical treatment.

3.5.3 Numerical computation of the recovery fidelity

Since $\mathcal{L}$ is a matrix of size $4^5 = 1024$, a straightforward computation of the exponential (3.65) is hard. Equivalently, the master equation $\frac{d}{dt}\hat{\rho} = \mathcal{L}(\hat{\rho})$ is a system of 1024 coupled differential equations, whose numerical solution is difficult.

To overcome these problems we shall use an approximate techinque based on the Trotter expansion [41]:

$$e^{\hat{A}+\hat{B}} = \lim_{N\to\infty}\left(e^{A/N}e^{B/N}\right)^N, \tag{3.66}$$

valid for every pair of operators $\hat{A}$, $\hat{B}$. This formula can be used to approximate the exponential of two non-commuting operators (or super-operators, as in our case): a first approximation is

$$e^{\hat{A}+\hat{B}} = \left(e^{\hat{A}/N} e^{\hat{B}/N}\right)^N + \mathcal{O}\left(\frac{1}{N}\right). \tag{3.67}$$

This approximation can be improved by symmetrizing the product in brackets [42]:

$$e^{\hat{A}+\hat{B}} = \left(e^{\hat{A}/2N} e^{\hat{B}/N} e^{\hat{A}/2N}\right)^N + \mathcal{O}\left(\frac{1}{N^2}\right). \tag{3.68}$$

Let us define the "approximate evolution operators"

$$\mathcal{D}_t^{(N)} = \left(e^{\frac{t}{2N}\mathcal{L}_{\text{noise}}} e^{\frac{t}{N}\mathcal{L}_{\text{e.c.}}} e^{\frac{t}{2N}\mathcal{L}_{\text{noise}}}\right)^N = \left(\Phi_{t/2N} \circ \Phi_{t/N}^{(\mathcal{R})} \circ \Phi_{t/2N}\right)^N$$
$$= \left[e^{-\gamma t/N}\Phi_{t/N} + \left(1 - e^{-\gamma t/N}\right)\Phi_{t/2N} \circ \mathcal{R} \circ \Phi_{t/2N}\right]^N. \tag{3.69}$$

Their average fidelity (with a trivial read-out $\mathcal{I}$) is

$$\widetilde{F}_{t;N}^{(\mathcal{R};\mathcal{I})} \equiv \frac{1}{4}\text{Tr}\left(\hat{\sigma}_0^L \mathcal{D}_t^{(N)}\left(\hat{\sigma}_0^L\right)\right) + \frac{1}{12}\sum_{\alpha=1}^{3}\text{Tr}\left(\hat{\sigma}_\alpha^L \mathcal{D}_t^{(N)}\left(\hat{\sigma}_\alpha^L\right)\right). \tag{3.70}$$

Clearly the approximation becomes exact in the $N \to \infty$ limit:

$$\lim_{N\to\infty} \widetilde{F}_{t;N}^{(\mathcal{R};\mathcal{I})} = F_t^{(\mathcal{R};\mathcal{I})}. \tag{3.71}$$

For all practical purposes, a good approximation can be obtained by computing $\widetilde{F}_{t;N}^{(\mathcal{R};\mathcal{I})}$ for a large but finite value of N. In order for the approximation to be good, each partial channel must be very close to the identity. This means that both κt and γt must be much smaller than N. Being typically interested in the strong-EC limit, the condition for a good approximation is $N \gg \gamma t$.

The numerical results are presented in Figure 3.5. We considered six evolutions corresponding to values of $\frac{\gamma}{\kappa}$ within the strong-QEC limit ($\gamma \gtrsim 100\kappa$). For each one we computed $\widetilde{F}_{t;N}^{(\mathcal{R};\mathcal{I})}$ for ten equally spaced values of t in the range $[0; 5 \cdot 10^{-3}\kappa^{-1}]$, and for $N \in \{10, 15, 20, 25, 30\}$. We then extrapolated the $N \to \infty$ limit by fitting the N^{-2} scaling. In Figure 3.6 this technique is shown to provide a reliable result for the channel with the highest γt among those considered.

The qualitative behavior is the same as the one we found for the 3-qubit code: there is an initial transient in which the rate of information loss does not depend on the QEC strength γ; then, after a time interval $\sim \gamma^{-1}$ (which is very short in the strong QEC limit), the timescale for the decay becomes very long ($\sim \gamma\kappa^{-2}$). The $\gamma = 0$ channel (a purely depolarizing channel with no QEC) was also added to Figure 3.5 to provide a comparison.

FIGURE 3.5: decay of the average fidelity $F_t^{(\mathcal{R};\mathcal{I})}$ for the 5-qubit perfect code subject to depolarizing noise of strength κ and continuous error correction of strength γ (computed numerically via second-order Trotter expansion), for several values of the ratio $\frac{\gamma}{\kappa}$.
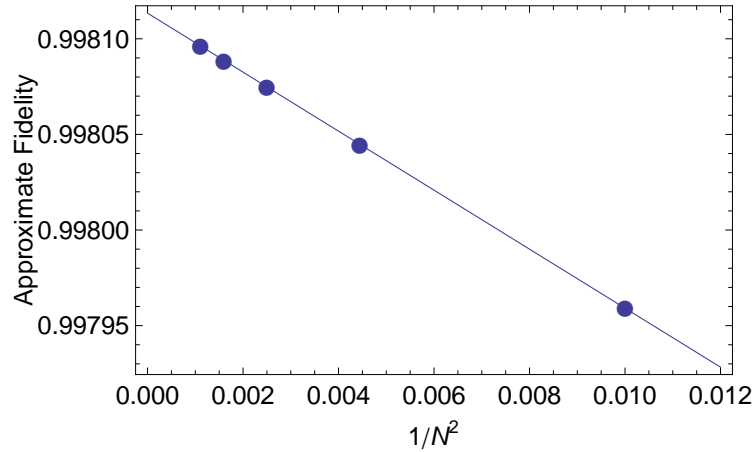
FIGURE 3.6: scaling of $\widetilde{F}_{t;N}^{(\mathcal{R};\mathcal{I})}$ with the number of steps N in the Trotter approximation, for the $\gamma = 2000\kappa$, $t = 0.005\kappa^{-1}$ channel. In this case $\gamma t = 10$, which is the highest value among the points plotted in Figure 3.5. The $N \to \infty$ limit can be extrapolated from the fit. In order to obtain a reliable fit, values of N as small as 30 suffice, even though $\frac{\gamma t}{N} = \frac{1}{3}$ is not very small by itself.
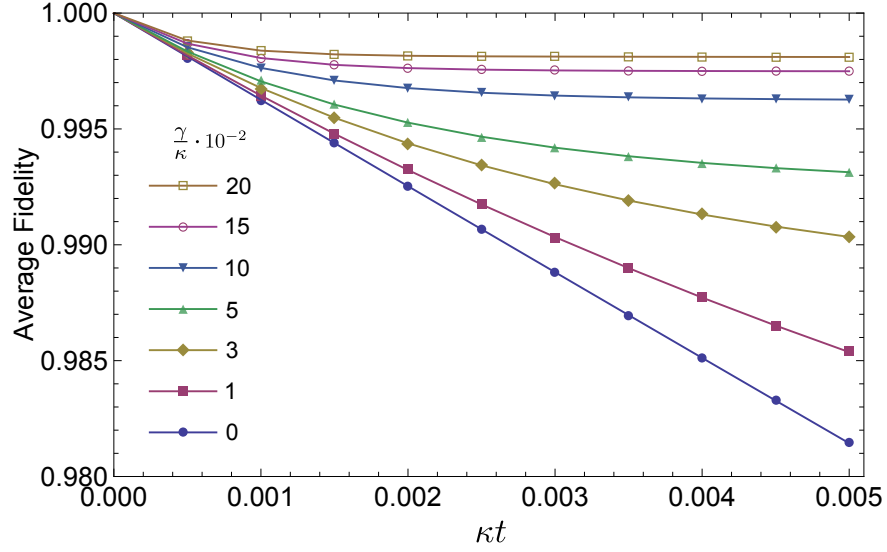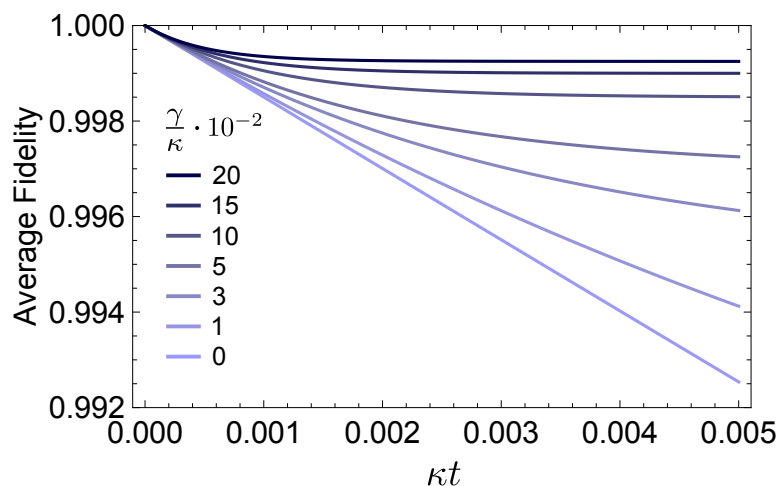
FIGURE 3.7: decay of the average fidelity $F_t^{(\mathcal{R};\mathcal{I})}$ for the 3-qubit code subject to bit-flip noise of strength κ and continuous error correction of strength γ, for several values of the ratio $\frac{\gamma}{\kappa}$. The function $F_t^{(\mathcal{R};\mathcal{I})}$ is the same as the one shown in Figure 3.3; this plot focuses on shorter times and higher values of γ, in order to allow a comparison with Figure 3.5.

3.5.4 Conclusion

This analysis shows explicitly that the continuous-time version of a perfect QECC works against the depolarizing noise, which is generally considered the most destructive kind of noise. Moreover it is a specifically quantum noise, involving bit-flips, phase-flips and bit-phase-flips. This proves that the analytical results of Section 3.4 for the 3-qubit QECC are not due to the classical form of the noise, and that the general approach we outlined can be generalized to larger codes.

This is not surprising, since the continuous-time implementation of QEC can be seen as the limit of a discrete-time implementation, which is known to be effective. Nevertheless, the similarity between the 3-qubit and 5-qubit cases is remarkable (see Figures 3.5 and 3.7). This similarity suggests that similar results should hold for the continuous-time implementation of any stabilizer code.

Chapter 4

Hamiltonian Protection of Quantum Information

In this Chapter we discuss how Hamiltonians can be used to protect quantum information from decoherence. In Section 4.1, after a general introduction to the topic, a distinction between two types of Hamiltonian protection of information is presented. The two types of protection are dubbed "opposition" and "prevention" of decoherence, respectively. Section 4.2 provides a simple example of this distinction: the memory performance of spin chain chain is discussed in both scenarios, and the Ising Hamiltonian is proven to be effective in one case and ineffective in the other.

4.1 General Framework

4.1.1 "Self-correcting" quantum memories

The idea of protecting quantum information at the hardware level, by turning stabilizer codes into Hamiltonians that would penalize errors, was first presented by Kitaev in [43]. The idea was motivated by the analogy with classical magnetic memories, where a redundant encoding and a suitable interaction between the constituents makes the information resilient to noise without the need of any EC procedure.

The specific model proposed by Kitaev was later ruled out as a candidate for a "self-correcting" quantum memory, as it cannot protect information from thermal noise [44], and several limitations to this general scheme have been pointed out [45, 46]; on the other hand, positive results were claimed for 4-dimensional systems with local interactions [47]

and for 2-dimensional and 3-dimensional systems with long-range interactions [48, 49]. The search for "self-correcting" quantum memories is ongoing [50].

4.1.2 "Opposing" and "preventing" decoherence

When discussing the effectiveness of Hamiltonian protection of quantum information, an important distinction has to be made:

- Simply adding the Hamiltonian term to the master equation that describes the evolution of the system, leaving all the dissipators unchanged, may protect the encoded information. In this case we shall say that the Hamiltonian is *opposing* the given decoherence.

- Introducing the Hamiltonian from the beginning in the microscopic derivation of the master equation may damp the dissipators or change their form. If this modification of the dissipators protects the encoded information, then we will say that the Hamiltonian is *preventing* decoherence.

From this point of view, Chapter 3 dealt with strategies for *opposing decoherence* using dissipators. There is a general argument showing that dissipators are better suited than Hamiltonians for this task [13]: a dissipator represents the occurrence of stochastic errors, hence in general it will add entropy to the system; while another dissipator can in principle pump this entropy out of the system (e.g. by a cooling process), a Hamiltonian can only move this entropy around the system. The best a Hamiltonian can do is to concentrate all the entropy into a specific subsystem, leaving the rest of the system unharmed; but eventually there will be too much entropy in the system and the memory will fail.

What makes Hamiltonians more interesting is their ability to *prevent* decoherence. Starting from an extended system that includes the memory and its environment, under some assumptions about the nature of the interactions, the form of the initial state, and the environment correlation times, one can derive a Markovian master equation for the evolution of the system's reduced density matrix. If the extended system is governed by a Hamiltonian $\hat{H}_{\text{tot}} = \hat{H}_{\text{sys}} + \hat{H}_{\text{env}} + \hat{H}_{\text{int}}$, the presence of $\hat{H}_{\text{sys}}$ damps all the "quantum jumps" that require crossing a gap. Therefore a suitably engineered Hamiltonian should be able to reduce the error probability.

4.2 An Example: Minimal Ising Chain

We will now analyze a simple example in order to illustrate the distinction between decoherence "prevention" and "opposition". The example is based on a minimal Ising chain, i.e.

three spins coupled to one another by a ferromagnetic (ZZ) interaction, each one exposed to a bit-flip noise. Intuitively, a high ferromagnetic gap should forbid bit-flips and therefore protect the encoded information. However, as we will see, this only holds at the "prevention" level, and not at the "opposition" level. This means that the ferromagnetic interaction is completely ineffective against a *given* bit-flip noise; it can only damp the bit-flip operators if we include it from the beginning of the derivation.

4.2.1 Ineffective opposition to decoherence

We will first consider a three-spin system with a ferromagnetic Hamiltonian

$$\hat{H}_{\text{sys}} = -JZ_1Z_2 - JZ_2Z_3 - JZ_3Z_1 =$$
$$= JI - 4J\frac{I + Z_1Z_2 + Z_2Z_3 + Z_3Z_1}{4} = J(I - 4P) \tag{4.1}$$

P is the code-space projector for the 3-qubit QECC, introduced in (3.13). On each spin acts identically and independently a bit-flip noise, represented by the Lindblad operator $\sqrt{\frac{\kappa}{2}}X$, so that the overall Lindbladian is

$$\mathcal{L}[\hat{\rho}] = -i[\hat{H}_{\text{sys}}, \hat{\rho}] + \mathcal{L}_{\text{noise}}(\hat{\rho}) = 4iJ[P, \hat{\rho}] + \frac{\kappa}{2}\sum_{i=1}^{3}\left(X_i\hat{\rho}X_i - \hat{\rho}\right). \tag{4.2}$$

Let us relabel the standard basis $\{|i\rangle \otimes |j\rangle \otimes |k\rangle : i, j, k \in \{0, 1\}\}$ as $\{|n\rangle : n \in \{1, \ldots 8\}\}$, by identifying the binary triple (i, j, k) with the number $n = 4i + 2j + k + 1$. In this basis the projector P is an 8×8 matrix whose only non-zero entries are in positions $(1, 1)$ and $(8, 8)$:

$$P = \text{diag}\,(1, 0, 0, 0, 0, 0, 0, 1) \tag{4.3}$$

Let us also introduce the following parametrization for 8×8 Hermitian matrices:

$$\hat{\rho} = \begin{pmatrix} a & \mathbf{v}^\dagger & b \\ \mathbf{v} & C & \mathbf{w} \\ b^* & \mathbf{w}^\dagger & d \end{pmatrix}, \tag{4.4}$$

where $a, d \in \mathbb{R}$, $b \in \mathbb{C}$, $\mathbf{v}, \mathbf{w} \in \mathbb{C}^6$, and C is a 6×6 Hermitian matrix. Encoded logical states, or code-states, correspond to $\mathbf{v} = \mathbf{w} = C = 0$, $a, d \in [0, 1]$, $a + d = 1$, and $|b| \leq 1$.

Lemma *The time-evolution induced by* (4.2) *on a code-state is not influenced by the Hamiltonian* $\hat{H}_{sys}$.

Proof. Consider the commutator $[P, \hat{\rho}]$ in (4.2). Left and right multiplication by P act on $\hat{\rho}$ as follows:

$$P\hat{\rho} = \begin{pmatrix} a & \mathbf{v}^\dagger & b \\ 0 & 0 & 0 \\ b^* & \mathbf{w}^\dagger & d \end{pmatrix}, \qquad \hat{\rho}P = \begin{pmatrix} a & 0 & b \\ \mathbf{v} & 0 & \mathbf{w} \\ b^* & 0 & d \end{pmatrix}, \qquad (4.5)$$

so that

$$[P, \hat{\rho}] = \begin{pmatrix} 0 & \mathbf{v}^\dagger & 0 \\ -\mathbf{v} & 0 & -\mathbf{w} \\ 0 & \mathbf{w}^\dagger & 0 \end{pmatrix}. \qquad (4.6)$$

The Hamiltonian $\hat{H}_{\mathrm{sys}}$ can have an influence on the time evolution of $\hat{\rho}$ only if matrix elements corresponding to $\mathbf{v}$ or $\mathbf{w}$ are non-vanishing. Assuming the initial condition is a code-state, such parameters are initially zero. In order to prove that they stay equal to zero at all times, consider the following subspaces of $\mathcal{B}(\mathcal{H}_3)$:

$$\begin{cases} \Delta = \mathrm{Span}\{\sigma_{a_1} \otimes \sigma_{a_2} \otimes \sigma_{a_3} : a_1, a_2, a_3 \in \{0, 3\}\}, \\ \overline{\Delta} = \mathrm{Span}\{\sigma_{a_1} \otimes \sigma_{a_2} \otimes \sigma_{a_3} : a_1, a_2, a_3 \in \{1, 2\}\}. \end{cases} \qquad (4.7)$$

Δ is the subspace of diagonal matrices, whereas $\overline{\Delta}$ consists of "anti-diagonal" matrices, i.e. matrices $\hat{\rho}$ whose only non-zero entries lie on the transverse diagonal:

$$\overline{\Delta} \ni \hat{\rho} = \begin{pmatrix} 0 & & \rho_{1,8} \\ & \cdot^{\cdot^{\cdot}} & \\ \rho_{8,1} & & 0 \end{pmatrix}. \qquad (4.8)$$

Both Δ and $\overline{\Delta}$ are invariant under the time-evolution induced by the Lindbladian (4.2): it is easy to verify that

$$\mathcal{L}[\sigma_{a_1} \otimes \sigma_{a_2} \otimes \sigma_{a_3}] = -\frac{\kappa}{2}\left(3 - \sum_{i=1}^{3}(-1)^{\delta_{a_i,2}+\delta_{a_i,3}}\right)\sigma_{a_1} \otimes \sigma_{a_2} \otimes \sigma_{a_3}. \qquad (4.9)$$

This proves that $\mathcal{D}_t\left(\Delta \oplus \overline{\Delta}\right) \subseteq \Delta \oplus \overline{\Delta}$. Since all code-states belong to $\Delta \oplus \overline{\Delta}$, if $\hat{\rho}(0)$ is a code-state then $\hat{\rho}(t) \in \Delta \oplus \overline{\Delta} \ \forall t$. This concludes the proof, since all matrices of $\Delta \oplus \overline{\Delta}$ have $\mathbf{v} = \mathbf{w} = 0$. $\qquad \square$

Since $\hat{H}_{\mathrm{sys}}$ has no effect whatsoever on the time-evolution of encoded logical states, the coherence time of the memory is independent from J; hence there is no opposition to decoherence.
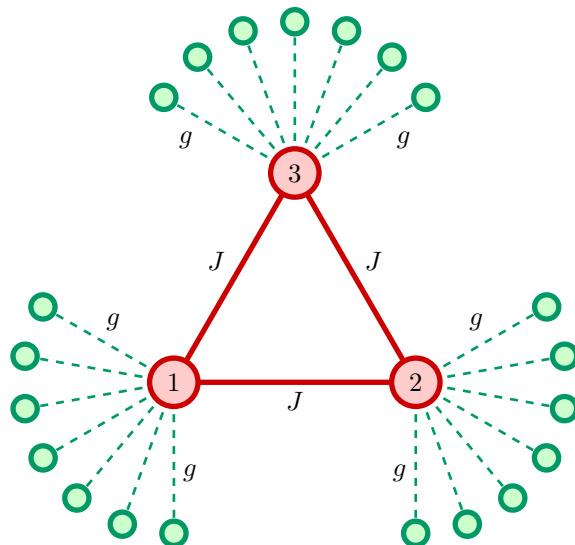
FIGURE 4.1:   schematic representation of the minimal Ising chain exposed to a local spin environment. The large circles labeled by $1, 2, 3$ are the system spins; the smaller circles are environment spins. Lines represent Hamiltonian interactions.

4.2.2   Effective prevention of decoherence

We will now consider the same system, but instead of adding the Ising Hamiltonian term to a given noise, we shall provide a microscopic derivation of a master equation starting from a system-environment Hamiltonian interaction.

Definition of the model.   The system is made of three spins with the Ising Hamiltonian (4.1). Each of the three spins is coupled to a distinct environment made of N spins. The situation is illustrated in Figure 4.1.

Each environment is governed by the same type of Hamiltonian:

$$\hat{H}_{\text{env},i} = \sum_{j=1}^{N} \frac{\omega_{i,j}}{2} Z_{i,j}. \tag{4.10}$$

$Z_{i,j}$ is the Pauli Z operator acting on the jth spin of the ith environment, and the $\{\omega_{i,j}\}$ are random energy gaps, which we assume to be independently and identically distributed according to a probability density function $f(E)$.

Finally, each environment is coupled to one of the system spins through the following interaction Hamiltonian:

$$\hat{H}_{\text{int},i} = g \sum_{j=1}^{N} X_i X_{i,j}. \tag{4.11}$$

Let $\hat{H}_{\text{env}} \equiv \sum_{i=1}^{3} \hat{H}_{\text{env},i}$ and $\hat{H}_{\text{int}} \equiv \sum_{i=1}^{3} \hat{H}_{\text{int},i}$; then the total Hamiltonian governing system and environment is

$$\hat{H}_{\text{tot}} = \hat{H}_{\text{sys}} + \hat{H}_{\text{env}} + \hat{H}_{\text{int}}. \tag{4.12}$$

Derivation of a master equation. We assume that the environment is initially in the fully mixed state, $\hat{\rho}_{\text{env}}(0) \propto I$ (which can be seen as a thermal state with $T = \infty$). The system instead starts from a generic state $\hat{\rho}_{\text{sys}}(0)$. The reduced density matrix of the system evolves according to

$$\hat{\rho}_{\text{sys}}(t) = \frac{\text{Tr}_{\text{env}}\left(\mathcal{D}_t\left(\hat{\rho}_{\text{sys}}(0) \otimes I_{\text{env}}\right)\right)}{\text{Tr}_{\text{env}}\left(I_{\text{env}}\right)}. \tag{4.13}$$

The evolution (4.13) is generally not Markovian because the finite size of the environment allows some memory effects: information that left the system can return after a finite amount of time. However, if we consider a very large environment that is very weakly coupled to the system, within some reasonable physical assumptions the evolution becomes Markovian, and the corresponding master equation can be derived from $\hat{H}_{\text{sys}}$, $\hat{H}_{\text{env}}$ and $\hat{H}_{\text{int}}$. The derivation is carried out in Appendix D.

In the notation of the Appendix, one has $\hat{A}_i = gX_i$. The interaction-picture evolution of such operators is

$$\hat{A}_i(t) = e^{it\hat{H}_{\text{sys}}} \hat{A}_i e^{-it\hat{H}_{\text{sys}}} = e^{-i4Jt}gPX_i + g(I - P)X_i(I - P) + e^{i4Jt}gX_iP, \tag{4.14}$$

so that the Fourier components are

$$\begin{cases} \hat{A}_i(-4J) = gPX_i, \\ \hat{A}_i(0) = g(I - P)X_i(I - P), \\ \hat{A}_i(4J) = gX_iP. \end{cases} \tag{4.15}$$

The B operators are $B_i = \sum_{j=1}^{N} X_{i,j}$. Their interaction-picture evolution is

$$\hat{B}_i(t) = e^{i\sum_{k=1}^{N} \frac{1}{2}\omega_{i,k}tZ_{i,k}} \sum_{j=1}^{N} X_{i,j} e^{-i\sum_{k=1}^{N} \frac{1}{2}\omega_{i,k}tZ_{i,k}} = \sum_{j=1}^{N} e^{i\omega_{i,j}tZ_{i,j}} X_{i,j}; \tag{4.16}$$

now, using the formula $e^{i\mathbf{v}\cdot\boldsymbol{\sigma}} = \cos(v)\mathbf{1} + i\sin(v)\frac{\mathbf{v}}{v}\cdot\boldsymbol{\sigma}$, (4.16) becomes

$$\begin{aligned} \hat{B}_i(t) &= \sum_{j=1}^{N} \left(\cos(\omega_{i,j}t)I + i\sin(\omega_{i,j}t)Z_{i,j}\right) X_{i,j} \\ &= \sum_{j=1}^{N} \left(\cos(\omega_{i,j}t)X_{i,j} - \sin(\omega_{i,j}t)Y_{i,j}\right). \end{aligned} \tag{4.17}$$

The environment correlation function defined in (D.11) in our case is

$$K_{ij}(t) = \frac{\mathrm{Tr}_{\mathrm{env}}\left(\hat{B}_i(t)\hat{B}_j(0)\right)}{\mathrm{Tr}_{\mathrm{env}}\left(I_{\mathrm{env}}\right)} = \delta_{ij}\sum_{k=1}^{N}\cos(\omega_{i,k}t). \tag{4.18}$$

The function that determines the Lindblad operators in the master equation (D.18) is

$$\gamma_{ij}(\omega) = \int_{-\infty}^{\infty} dt \; e^{i\omega t} K_{ij}(t) = \delta_{ij}\sum_{k=1}^{N}\int_{-\infty}^{\infty} dt \; e^{i\omega t}\cos(\omega_{i,k}t)$$

$$= \pi\delta_{ij}\sum_{k=1}^{N}\left(\delta(\omega - \omega_{i,k}) + \delta(\omega + \omega_{i,k})\right). \tag{4.19}$$

This function must be averaged over the ensemble of energy gaps of the environment spins, $\{\omega_{i,k}\}$, which we assume to be independently and identically distributed according to a probability density function $f(E)$:

$$\langle\gamma_{ij}(\omega)\rangle = \int\left(\prod_{k=1}^{N} d\omega_{i,k} f(\omega_{i,k})\right)\gamma_{ij}(\omega) = \pi N\delta_{ij}\left(f(\omega) + f(-\omega)\right) \tag{4.20}$$

Lindblad operators. Matrix (4.20) is already diagonal in the i,j indices, therefore the resulting Lindblad operators (D.20) are simply

$$\left\{\hat{L}_{i,\omega}\right\} = \left\{\sqrt{\langle\gamma_{ii}(\omega)\rangle}\hat{A}_i(\omega)\right\}$$

$$= \left\{\left[\pi N g^2(f(\omega) + f(-\omega))\right]^{\frac{1}{2}} X_i(\omega) : \; i \in \{1, 2, 3\}, \; \omega \in \{-4J, 0, +4J\}\right\} \tag{4.21}$$

Finally, we shall take the weak-coupling limit, i.e. we shall consider a large number of environment spins interacting very weakly with the system. This limit ensures the Markovian nature of the resulting process, and provides a physical motivation for the average (4.20). Mathematically, the weak-coupling limit consists in the limits $N \to \infty$ and $g \to 0$, with the product $\pi g^2 N \equiv \kappa^2$ kept constant. Recalling the form of the $\left\{\hat{A}(\omega)\right\}$ operators from (4.15), we get the explicit form of the Lindblad operators:

$$\begin{cases} \hat{L}_{i,-4J} = \kappa\sqrt{f(4J) + f(-4J)}X_i P, \\ \hat{L}_{i,0} = \kappa\sqrt{2f(0)}(I - P)X_i(I - P), \\ \hat{L}_{i,4J} = \kappa\sqrt{f(4J) + f(-4J)}P X_i. \end{cases} \tag{4.22}$$

Renormalization of the Hamiltonian. The "Lamb-shift Hamiltonian" (D.19) is

$$\hat{H}_{LS} = -\sum_{i,j=1}^{3} \sum_{\omega \in \{0, \pm 4J\}} \langle S_{ij}(\omega) \rangle \, \hat{A}_j(\omega)^\dagger \hat{A}_j(\omega)$$

$$= -g^2 \sum_{i,j=1}^{3} \Bigg(\langle S_{ij}(-4J) \rangle \, X_j P X_i + \langle S_{ij}(4J) \rangle \, P X_j X_i P$$

$$+ \langle S_{ij}(0) \rangle \, (I - P) X_j (I - P) X_i (I - P) \Bigg). \tag{4.23}$$

The $S(\omega)$ matrices are defined in (D.16). We have

$$S_{ij}(0) = \frac{1}{2i} \int_{-\infty}^{\infty} dt \, \text{sign}(t) \, K_{ij}(t) = \frac{1}{2i} \sum_{k=1}^{N} \int_{-\infty}^{\infty} dt \, \text{sign}(t) \cos(\omega_{i,k} t) = 0 \tag{4.24}$$

and

$$S_{ij}(\pm 4J) = \frac{1}{2i} \int_{-\infty}^{\infty} dt \, e^{\pm i4Jt} \text{sign}(t) \, K_{ij}(t) = \frac{\delta_{ij}}{2i} \sum_{k=1}^{N} \int_{-\infty}^{\infty} dt \, e^{\pm i4Jt} \text{sign}(t) \cos(\omega_{i,k} t)$$

$$= \frac{\delta_{ij}}{2} \sum_{k=1}^{N} \left(\mathcal{P} \frac{1}{\pm 4J + \omega_{i,k}} + \mathcal{P} \frac{1}{\pm 4J - \omega_{i,k}} \right), \tag{4.25}$$

where $\mathcal{P}$ denotes the Cauchy principal part. Therefore $\langle S_{ij}(0) \rangle = 0$ and

$$\langle S_{ij}(\pm 4J) \rangle = \delta_{ij} \frac{N}{2} \int_{-\infty}^{+\infty} dE \, f(E) \left(\mathcal{P} \frac{1}{E \pm 4J} - \mathcal{P} \frac{1}{E \mp 4J} \right)$$

$$= \pm \delta_{ij} \left(\fint_{-\infty}^{+\infty} dE \, \frac{f(E)}{E + 4J} - \fint_{-\infty}^{+\infty} dE \, \frac{f(E)}{E - 4J} \right) \equiv \pm \delta_{ij} \lambda(J), \tag{4.26}$$

where the slashes denote the principal part of the integrals and $\lambda(J)$ is a shorthand notation for the expression in brackets (which has dimensions of $[\text{energy}]^{-1}$). With these results it can be shown that the Lamb-shift Hamiltonian (4.23) becomes

$$\hat{H}_{LS} = 3g^2 \lambda(J) \big[P - (I - P) \big]. \tag{4.27}$$

This is a renormalization of the energy levels of the original system Hamiltonian (4.1): the ground energy level is increased by $3g^2 \lambda(J)$, while the excited level decreases by the same amount; both eigenspaces are left unchanged and no degeneracies are lifted.

Conclusion. The effective dynamics of the 3-qubit system is governed by the Lindbladian

$$\mathcal{L}_{\text{tot}}(\hat{\rho}) = -i \left[(J + 6g^2 \lambda(J)) P, \hat{\rho} \right] + \sum_{j=1}^{3} \sum_{\omega \in \{0, \pm 4J\}} \left(\hat{L}_{\omega,j} \hat{\rho} \hat{L}_{\omega,j}^\dagger - \frac{1}{2} \left\{ \hat{L}_{\omega,j}^\dagger \hat{L}_{\omega,j}, \hat{\rho} \right\} \right). \tag{4.28}$$

It can be seen from (4.22) that

- Lindblad operators $\{\hat{L}_{i,0}\}$ annihilate the code-space and act only on its orthogonal complement, with strength $\kappa^2 f(0)$;

- Lindblad operators $\{\hat{L}_{i,\pm 4J}\}$ connect the code-space and its orthogonal complement, thus causing errors, and have strength $\kappa^2 f(4J)$.

The spectrum of energy gaps of bath spins $f(E)$ generally has a cut-off energy Ω, above which it drops exponentially:

$$f(E)\big|_{E \gg \Omega} \lesssim e^{-E/\Omega}. \tag{4.29}$$

Thus by taking $J \gg \Omega$, one can arbitrarily suppress the $\{\hat{L}_{i,\pm 4J}\}$ operators. From (4.26) it is clear that the "Lamb shift" energy correction $\lambda(J)$ vanishes as $J \to \infty$. Finally, the $\{\hat{L}_{i,0}\}$ Lindblad operators are innocuous on encoded states. Therefore an initially encoded state is completely frozen in the large-gap limit, and we can conclude that the Ising Hamiltonian effectively prevents decoherence in this system.

Chapter 5

Quantum Memories Based on Majorana Zero-Modes

In this Chapter we shall discuss quantum memories based on fermionic systems that host unpaired Majorana modes using the techniques developed in the previous Chapters. The first part of the Chapter (Sections 5.1 and 5.2) introduces the key ideas and illustrates them through simple examples. The second part (Sections 5.3 through 5.6) analyzes several quantum memory toy-models.

The idea of unpaired Majorana modes in condensed matter theory is introduced in Section 5.1, along with a brief review of the status of experimental searches. Section 5.2 discusses the encoding of a qubit in a fermionic system with unpaired Majorana modes. In this framework, particle-number parity arises naturally as a key concept, and we link it to the memory performance within a simple approximation.

In the second part of the Chapter, several toy-models of Majorana-based quantum memories are presented and discussed. In Section 5.3 a minimal model allowing local, Markovian, parity-preserving noise is introduced. It consists of eight Majorana modes. Its memory performance is evaluated under both parity-preserving and non-parity-preserving noise models. In Section 5.4 four more Majorana modes are added to the system, thus allowing different encoding choices. Two encodings are tested and the resulting memory performances are shown to be very different. This difference is explained in terms of locality. Section 5.5 presents a more realistic model, the Kitaev chain, and discusses its performance as a quantum memory under both parity-preserving and non-parity-preserving noise models. Finally, in Section 5.6 the concepts that are generally believed to ensure the protection of information in a Majorana-based quantum memory are critically reviewed, in light of the results obtained from the toy-models.

5.1 Majorana "Fermions" in Condensed Matter Systems

In 1937 Ettore Majorana discovered his famous wave equation describing spin-$\frac{1}{2}$ fermions that are their own antiparticles [51]. As of yet, no elementary particles have been found that obey the Majorana equation – though the nature of neutrino masses and of dark matter is still unclear, which potentially leaves room for Majorana mass terms in some extensions of the Standard Model of particle physics. However, in the last fifteen years Majorana fermions have been gaining a remarkable popularity in a completely different setting: condensed matter physics [52]. In this setting, they are not fundamental particles, but rather *quasiparticles*, emerging from the collective behavior of electrons in solid-state systems. Remarkably, in two spatial dimensions Majorana quasiparticles are predicted to exhibit *non-Abelian anyonic statistics*: hence the term "Majorana fermions" is misleading, and the more neutral label "Majorana modes" is preferred.

Loosely speaking, a Majorana quasiparticle is an equal, coherent superposition of an electron and a hole. Normally, such quasiparticles are not observed because they combine pairwise to form ordinary electrons or holes; they can be observed individually only if they are somehow *unpaired*.

It has been known since the late 1990's that vortices of chiral 2-dimensional p-wave superconductors can host unpaired Majorana modes [17, 18, 53]. This fact became of interest for quantum information theory after the proposal by Kitaev of a supposedly decoherence-free qubit based on unpaired Majorana modes [16]. This proposal, along with the inherently interesting physics that such exotic quasiparticles would exhibit, boosted the experimental searches for unpaired Majorana modes in condensed matter systems [19].

In this Section we shall provide a short introduction to Majorana modes in condensed matter physics: in §5.1.1 we introduce the formalism of Majorana modes; then in §5.1.2 we present the Kitaev chain as a simple, solvable toy-model which displays unpaired Majorana modes; finally, in §5.1.3 we briefly review the status of experimental searches.

5.1.1 Dirac and Majorana modes

Consider a fermionic systems consisting of N Dirac modes. The creation and annihilation operators for the N modes are $\left\{ \hat{a}_i, \, \hat{a}_i^\dagger : i \in \{1, \ldots N\} \right\}$. These operators obey the canonical anti-commutation relations:

$$\{\hat{a}_i, \hat{a}_j\} = 0, \qquad\qquad \{\hat{a}_i^\dagger, \hat{a}_j\} = \delta_{i,j}\hat{\mathbf{1}}. \tag{5.1}$$

The state space for the system is the fermionic N-mode Fock space $\mathfrak{F}_N$, spanned by orthonormal basis vectors

$$|n_1, \ldots n_N\rangle = \left(\hat{a}_1^\dagger\right)^{n_1} \cdots \left(\hat{a}_N^\dagger\right)^{n_N} |\Omega\rangle, \tag{5.2}$$

where $|\Omega\rangle$ is the vacuum state and each n_i is either 0 or 1. The dimension of $\mathfrak{F}_N$ is thus 2^N.

Remark. The order of the creation operators in (5.2) has to be specified in order to avoid sign ambiguity.

The fermionic system can equivalently be described using *Majorana operators*:

$$\hat{c}_{r,1} = \hat{a}_r + \hat{a}_r^\dagger, \qquad\qquad \hat{c}_{r,2} = \frac{\hat{a}_r - \hat{a}_r^\dagger}{i}. \tag{5.3}$$

The $\{\hat{c}_{r,j}\}$ operators obey the algebra

$$\{\hat{c}_{r,j}, \hat{c}_{s,k}\} = 2\delta_{r,s}\delta_{j,k}\hat{1}, \tag{5.4}$$

which can be straightforwardly proved using the canonical anti-commutation relations (5.1). Majorana operators have several properties that make them a convenient choice for some types of calculations:

- They are self-adjoint.

- They square to $\hat{1}$, thus their eigenvalues are either $+1$ or -1.

- They are traceless.

- They can all be treated on the same footing[1].

The following is a summary of useful relations between the Dirac and Majorana formalisms:

$$\hat{a}_r = \frac{\hat{c}_{r,1} + i\hat{c}_{r,2}}{2}, \qquad\qquad \hat{a}_r^\dagger = \frac{\hat{c}_{r,1} - i\hat{c}_{r,2}}{2}, \tag{5.5}$$

$$\hat{a}_r^\dagger\hat{a}_r = \hat{n}_r = \frac{\hat{1} + i\hat{c}_{r,1}\hat{c}_{r,2}}{2}, \qquad\qquad \hat{a}_r\hat{a}_r^\dagger = \hat{1} - \hat{n}_r = \frac{\hat{1} - i\hat{c}_{r,1}\hat{c}_{r,2}}{2}, \tag{5.6}$$

$$(-1)^{\hat{n}_r} = \hat{1} - 2\hat{n}_r = -i\hat{c}_{r,1}\hat{c}_{r,2}. \tag{5.7}$$

Remark. The Majorana operators $\{\hat{c}_{r,j} : r \in \{1, \ldots N\}, j \in \{1, 2\}\}$ generate the whole algebra $\mathcal{B}(\mathfrak{F}_N)$.

---

[1] The $\{\hat{c}_{r,1}\}$ and $\{\hat{c}_{r,2}\}$ operators are completely equivalent; one could relabel $\hat{c}_{r,1} \mapsto \hat{c}'_{2r-1}$ and $\hat{c}_{r,2} \mapsto \hat{c}'_{2r}$, and the algebra (5.4) would be invariant under orthogonal transformations of the vector $(\hat{c}'_1, \ldots \hat{c}'_{2N})$.

Proof. The monomials $\hat{\mu}[\boldsymbol{\alpha}] \equiv (\hat{c}_{1,1})^{\alpha_{1,1}} \cdots (\hat{c}_{N,2})^{\alpha_{N,2}}$, parametrized by binary $2N$-tuples $\boldsymbol{\alpha} \in \{0,1\}^{2N}$, are orthogonal in the Hilbert-Schmidt Hermitian product:

$$\text{Tr}\left(\hat{\mu}[\boldsymbol{\alpha}]^{\dagger}\hat{\mu}[\boldsymbol{\beta}]\right) = \delta_{\boldsymbol{\alpha},\boldsymbol{\beta}}\dim(\mathfrak{F}_N). \tag{5.8}$$

This provides a set of 2^{2N} independent operators. Since $2^{2N} = \dim(\mathfrak{F}_N)^2 = \dim(\mathcal{B}(\mathfrak{F}_N))$, the operators must also be a complete set, hence a basis. $\qquad\square$

5.1.2 The Kitaev chain

Until recently, the Majorana formalism presented in §5.1.1 was considered a useful theoretical tool without any concrete physical meaning. This is because, loosely speaking, a Majorana operator represents only *half* of a fermionic degree of freedom – one needs two Majorana modes to obtain a Dirac mode. These "half fermions" were expected to always combine into single, local Dirac modes.

However it was shown by Kitaev [16] that in some physical scenarios one can actually obtain *unpaired* Majorana modes. The pairing between Majorana modes corresponds to the occupation energy of the corresponding Dirac mode. Therefore, unpaired Majorana modes must also be zero-energy modes of the system Hamiltonian. Thus the terms *"unpaired Majorana mode"* and *"Majorana zero-mode"* will be used interchangeably.

We shall review Kitaev's model for two reasons:

1. It provides a simple example of a condensed matter system hosting Majorana zero-modes, and

2. We will analyze its performance as a quantum memory in §5.5.

The model. Consider a one-dimensional system consisting of L sites, with open boundary conditions. Each site hosts a Dirac mode $\hat{a}_r$, $r \in \{1, \ldots L\}$. The Hamiltonian involves hopping terms, superconducting pair creation/annihilation terms, and chemical potential terms:

$$\hat{H} = \sum_{r=1}^{L-1}\left(-t(\hat{a}_r^{\dagger}\hat{a}_{r+1} + \hat{a}_{r+1}^{\dagger}\hat{a}_r) + \Delta\hat{a}_r\hat{a}_{r+1} + \Delta^*\hat{a}_{r+1}^{\dagger}\hat{a}_r^{\dagger}\right) + \mu\sum_{r=1}^{L}\left(\hat{a}_r^{\dagger}\hat{a}_r - \frac{1}{2}\hat{\mathbf{1}}\right). \tag{5.9}$$

Any complex phase in the parameter Δ can be absorbed by a suitable redefinition of the $\hat{a}_r$ operators, thus all parameters can be assumed real. The form of (5.9) in terms of Majorana operators is

$$\hat{H} = \sum_{r=1}^{L-1}\left(\frac{\Delta-t}{2}i\hat{c}_{r,1}\hat{c}_{r+1,2} + \frac{\Delta+t}{2}i\hat{c}_{r,2}\hat{c}_{r+1,1}\right) + \mu\sum_{r=1}^{L}\frac{i}{2}\hat{c}_{r,1}\hat{c}_{r,2} \tag{5.10}$$
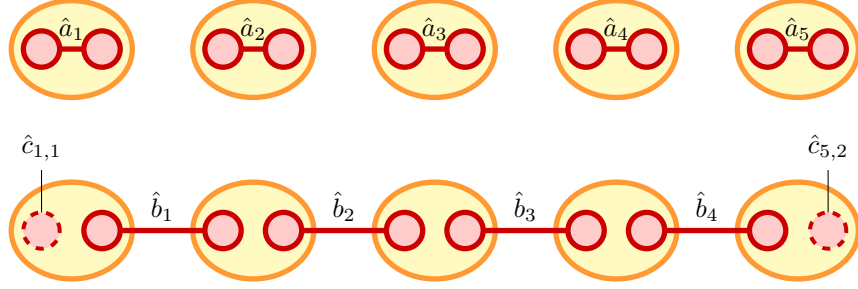
FIGURE 5.1: the two phases of the Kitaev chain ($L = 5$). Top: trivial phase (5.11). Bottom: topological phase (5.12) with unpaired edge modes. The ellipses represent the sites of the chain. The smaller circles represent Majorana modes. Segments joining Majorana modes represent the pairing into a Dirac mode.

If $t = \Delta = 0$ and $\mu > 0$, the Hamiltonian (up to additive constants) is

$$\hat{H}_1 = \mu \sum_{r=1}^{L} \hat{a}_r^\dagger \hat{a}_r, \tag{5.11}$$

and the vacuum state $|\Omega\rangle$ is a non-degenerate ground state. On the other hand, if $t = \Delta > 0$ and $\mu = 0$, one has

$$\hat{H}_2 = t \sum_{r=1}^{L-1} i\hat{c}_{r,2}\hat{c}_{r+1,1} = t \sum_{r=1}^{L-1} \hat{b}_r^\dagger \hat{b}_r, \tag{5.12}$$

where we introduced the "bond" Dirac modes

$$\hat{b}_r = \frac{\hat{c}_{r,2} + i\hat{c}_{r+1,1}}{2}, \qquad\qquad \hat{b}_r^\dagger = \frac{\hat{c}_{r,2} - i\hat{c}_{r+1,1}}{2}. \tag{5.13}$$

Majorana zero-modes. Hamiltonians (5.11) and (5.12) are very similar. The difference between them is that, while $\hat{H}_1$ pairs the two Majorana modes of each site, $\hat{H}_2$ pairs Majorana modes from adjacent sites. This difference is illustrated in Figure 5.1. The most remarkable property of (5.12) is that the two Majorana edge-modes $\hat{c}_{1,1}$ and $\hat{c}_{L,2}$ are *unpaired*. These are the zero-energy Majorana modes that are sought by the experimental condensed matter community. They define a Dirac mode, $\hat{n}_0 \equiv \frac{\hat{\mathbf{1}} + i\hat{c}_{1,1}\hat{c}_{L,2}}{2}$, which has zero occupation energy and is de-localized over the two distant edges of the chain.

The presence of $\hat{n}_0$ causes all the spectrum of $\hat{H}_2$ to be (at least) two-fold degenerate, since the occupation number $\hat{n}_0$ has no effect on the energy level; specifically, for the two-fold degenerate ground states one can choose $\left|\psi_{GS}^{(0)}\right\rangle$ and $\left|\psi_{GS}^{(1)}\right\rangle$, defined by

$$\hat{b}_r \left|\psi_{GS}^{(i)}\right\rangle = 0 \; \forall \, r, i, \qquad \hat{n}_0 \left|\psi_{GS}^{(0)}\right\rangle = 0, \qquad \hat{n}_0 \left|\psi_{GS}^{(1)}\right\rangle = \left|\psi_{GS}^{(1)}\right\rangle. \tag{5.14}$$

Equivalently, the two ground states are distinguished by the value of of the *fermionic number-parity operator*:

$$\hat{P}_f = \prod_{r=1}^{L}(-i\hat{c}_{r,1}\hat{c}_{r,2}). \tag{5.15}$$

By an appropriate permutation of the Majorana modes, and recalling (5.7), one has $\hat{P}_f = (-1)^{\hat{n}_0}\prod_{r=1}^{L-1}(-1)^{\hat{b}_r^\dagger\hat{b}_r}$, so that

$$\hat{P}_f\left|\psi_{GS}^{(0)}\right\rangle = +\left|\psi_{GS}^{(0)}\right\rangle, \qquad\qquad \hat{P}_f\left|\psi_{GS}^{(1)}\right\rangle = -\left|\psi_{GS}^{(1)}\right\rangle. \tag{5.16}$$

It can be shown [16] that the original Hamiltonian (5.9) (with $\Delta = t$) is in a *topological phase* with degenerate ground states for $|\mu| < 2|t|$. These ground states have some features that make them appealing candidates as logical states for a quantum memory, the most interesting one being the *topological robustness* of their degeneracy [54]. A topologically robust degeneracy is one that cannot be lifted by any *local* Hamiltonian perturbation in the thermodynamic limit ($L \to \infty$). At finite size, an exponentially small splitting $\mathcal{O}(e^{-L})$ is allowed. Therefore in a closed-system scenario (i.e. under Hamiltonian perturbations) the states are protected from dephasing[2].

This property is extremely remarkable, but does not guarantee *a priori* that Majorana zero-modes would effectively protect quantum information from external perturbations. Testing the validity of "topological protection" and "parity protection" in an open quantum system scenario is the general goal of Sections 5.3 through 5.5.

5.1.3 Experimental searches for Majorana zero-modes

Several strategies for engineering and detecting the elusive Majorana zero-modes have been proposed [19, 55]. Currently the most promising and experimentally viable proposals involve nanowires with strong spin-orbit coupling and proximity-induced superconductivity [56, 57, 58, 59].

Proximity with a 2-dimensional or 3-dimensional superconductor is necessary in order to produce the Δ terms in the Hamiltonian (5.9), because superconductivity is impossible in one dimension at finite temperature. Moreover, the Hamiltonian (5.9) contains *spinless* fermions; it is quite clear that if two spin components were allowed, then in the topological phase each edge would host *two* Majorana modes, which might combine into a single Dirac mode. Therefore one spin component must be "frozen". This can normally be accomplished

---

[2] If the two logical states of a qubit have energy levels that differ by a random gap δE, then the unitary evolution attaches a random phase of $e^{-i\,\delta Et}$ to coherence terms like $|0\rangle\langle1|$; averaging over the random values of δE yields a suppression of coherence terms and thus a loss of quantum information. The process is known as *dephasing*.

by means of a magnetic field. However, if we isolated, say, the spin-up component of the nanowire electrons with a magnetic field, then in order to obtain the required Δ terms we would need an exotic *p*-wave superconductor[3]. Remarkably, the desired effect can be obtained also with ordinary, *s*-wave superconductors, through a combination of spin-orbit coupling and a transverse magnetic field.

Evidence for Majorana zero-modes in this type of devices has been recently claimed [60, 61]. An anomalous peak in the conductance of the nanowire is observed at zero bias voltage; the peak is present for a wide range of experimental parameters and fits the predictions based on the presence of Majorana edge modes [62, 63]. This evidence may not yet be conclusive [64]; more investigations are needed for an unambiguous detection.

However, while the conclusive detection of Majorana physics in superconducting systems in the near future appears very likely, the step from detection to coherent manipulation of Majorana modes is far from trivial, and will probably require a much longer time.

5.2 Encoding a Qubit in a Fermionic System with Majorana Zero-Modes

In this Section we discuss how a qubit can be encoded in the even-parity sector[4] of a fermionic system with unpaired Majorana modes. §5.2.1 presents some general concepts about parity in fermionic systems, including the superselection rule on fermionic parity. The details of the qubit encoding are provided in §5.2.2. Finally, in §5.2.3 and §5.2.4 we discuss the memory performance of such encoding within some simplifying assumptions: in the former we project the dynamics onto the ground-space, and consider recovery operations that act on the zero-modes only; in the latter, we consider the real dynamics of the whole system and allow arbitrary recovery operations, at the expense of a simplified encoding and an *ad hoc* assumption about the decoherence process.

5.2.1 The role of parity

Superselection rule on fermionic parity. Consider a fermionic system and let $\hat{n}$ be the associated particle number operator:

$$\hat{n} = \sum_i \hat{a}_i^\dagger \hat{a}_i. \tag{5.17}$$

---

[3] Hamiltonian terms of the form $\hat{a}_\uparrow^\dagger \hat{a}_\uparrow$ would be necessary. Such terms corresponds to a Cooper pair in a spin triplet state.

[4]There is nothing special about even parity; we might as well have chosen the odd-parity sector. The important point is that the parity operator must have a fixed value on the encoded states.

Let $|n\rangle$ denote an eigenstate of $\hat{n}$ with eigenvalue $n \in \mathbb{N}$: $\hat{n}|n\rangle = n|n\rangle$. There is a general theorem, known as *fermionic parity superselection rule* [65], that forbids *coherent superpositions* of eigenstates $|n\rangle$ and $|n'\rangle$ such that n and n' have different parity. For instance, the state $\frac{1}{\sqrt{2}}(|1\rangle + |4\rangle)$ is unphysical. This is because a rotation of 2π about any axis produces a minus sign for each occupied fermionic mode, so that $\hat{R}_{2\pi}|n\rangle = (-1)^n |n\rangle$; hence the trivial operation $\hat{R}_{2\pi}$ would map $|1\rangle + |4\rangle$ to $-|1\rangle + |4\rangle$, which is an inequivalent vector.

However, *statistical mixtures* of states with different parities are allowed: for instance, $\hat{\rho} = \frac{1}{2}|1\rangle\langle 1| + \frac{1}{2}|4\rangle\langle 4|$ is invariant under the action of $\hat{R}_{2\pi}$, since

$$\hat{R}_{2\pi}\hat{\rho}\hat{R}_{2\pi}^{\dagger} = \frac{1}{2}(-1)|1\rangle\langle 1|(-1) + \frac{1}{2}(+1)|4\rangle\langle 4|(+1) = \hat{\rho}. \tag{5.18}$$

But *coherence terms* between the even and odd sectors are forbidden: $|1\rangle\langle 4| \xrightarrow{\hat{R}_{2\pi}} -|1\rangle\langle 4|$. Therefore physical density matrices must be block-diagonal, with blocks corresponding to the even and odd sectors:

$$\hat{\rho} = \begin{pmatrix} p\hat{\rho}_{\text{even}} & 0 \\ 0 & (1-p)\hat{\rho}_{\text{odd}} \end{pmatrix}, \qquad \text{Tr}(\hat{\rho}_{\text{even}}) = \text{Tr}(\hat{\rho}_{\text{odd}}) = 1, \qquad p \in [0,1]. \tag{5.19}$$

$\hat{R}_{2\pi}$ is none other than the fermionic parity operator, $\hat{P}_f$, introduced in (5.15). The superselection rule can be stated as follows: a state $\hat{\rho}$ is physical if and only if $\hat{P}_f\hat{\rho}\hat{P}_f = +\hat{\rho}$, or equivalently if and only if $\left[\hat{P}_f, \hat{\rho}\right] = 0$.

Since each Majorana operator $\hat{c}$ anti-commutes with $\hat{P}_f$, every physical state $\hat{\rho}$ must be a linear combination of even-degree monomials – i.e., products of an even number of $\hat{c}$ operators. We shall adopt a somewhat misleading terminology and label this type of operators as *"bosonic"*, even though they have nothing to do with bosons. Conversely, linear combinations of odd-degree monomials will be labeled as *"fermionic"*. This choice of terms avoids the ambiguity between even-degree and even-number operators: the former shall be called "bosonic", the latter simply "even".

In conclusion, one has

$$\hat{P}_f\hat{O}\hat{P}_f = \begin{cases} +\hat{\rho} & \text{if } \hat{O} \text{ is bosonic}, \\ -\hat{\rho} & \text{if } \hat{O} \text{ is fermionic}; \end{cases} \tag{5.20}$$

and all operators $\hat{O} \in \mathcal{B}(\mathfrak{F}_N)$ can be written as a sum of a bosonic and a fermionic part:

$$\hat{O} = \overbrace{\frac{\hat{O} + \hat{P}_f\hat{O}\hat{P}_f}{2}}^{\text{bosonic}} + \overbrace{\frac{\hat{O} - \hat{P}_f\hat{O}\hat{P}_f}{2}}^{\text{fermionic}}. \tag{5.21}$$

"Average parity" of a mixed state. As shown in (5.19), for every physical state[5] $\hat{\rho}$ we have $\hat{\rho} = p\hat{\rho}_{\text{even}} + (1-p)\hat{\rho}_{\text{odd}}$, $p \in [0,1]$. This decomposition can also be obtained as follows:

$$\hat{\rho} = \left(\frac{\hat{\mathbf{1}} + \hat{P}_f}{2}\right)\hat{\rho} + \left(\frac{\hat{\mathbf{1}} - \hat{P}_f}{2}\right)\hat{\rho}$$

$$= \left(\frac{\hat{\mathbf{1}} + \hat{P}_f}{2}\right)\hat{\rho}\left(\frac{\hat{\mathbf{1}} + \hat{P}_f}{2}\right) + \left(\frac{\hat{\mathbf{1}} - \hat{P}_f}{2}\right)\hat{\rho}\left(\frac{\hat{\mathbf{1}} - \hat{P}_f}{2}\right), \qquad (5.22)$$

where the second equality comes from the fact that $[\hat{P}_f, \hat{\rho}] = 0$ (because $\hat{\rho}$ is bosonic) and $\hat{P}_f^2 = \hat{\mathbf{1}}$. Then, introducing the even-parity and odd-parity projectors $\hat{\Pi}^{\pm} = \frac{\hat{\mathbf{1}} \pm \hat{P}_f}{2}$, a comparison between (5.19) and (5.22) yields

$$p\hat{\rho}_{\text{even}} = \hat{\Pi}^+ \hat{\rho}\, \hat{\Pi}^+, \qquad\qquad (1-p)\hat{\rho}_{\text{odd}} = \hat{\Pi}^- \hat{\rho}\, \hat{\Pi}^-. \qquad (5.23)$$

Thus bosonic operators can be further divided into *even* and *odd* operators:

$$\hat{P}_f\hat{\rho} = \hat{\rho}\hat{P}_f = \begin{cases} +\hat{\rho} & \text{if } \hat{\rho} \text{ is even,} \\ -\hat{\rho} & \text{if } \hat{\rho} \text{ is odd.} \end{cases} \qquad (5.24)$$

Applying (5.22), the *average parity* of a state $\hat{\rho}$ can be expressed as

$$\left\langle \hat{P}_f \right\rangle = \text{Tr}\left(\hat{P}_f\hat{\rho}\right) = \text{Tr}\left(p\hat{\rho}_{\text{even}} - (1-p)\hat{\rho}_{\text{odd}}\right) = 2p - 1. \qquad (5.25)$$

For the fully mixed state $2^{-N}\hat{\mathbf{1}}$ one has $p\hat{\rho}_{\text{even}} = \Pi^+(2^{-N}\hat{\mathbf{1}})\Pi^+$, so that $p = \text{Tr}\left(2^{-N}\Pi^+\right) = \frac{1}{2}$. This is intuitive, since the fully mixed state is an equal mixture of pure states with all particle numbers. If the code-space is chosen inside the subspace of even operators, then the initial value of $\langle \hat{P}_f \rangle$ is $+1$. Therefore, a decoherence process mapping the code-space to the completely mixed state would imply a decay of the average parity from 1 to 0.

This particular example displays a correlation between the decay of average parity and the loss of information. This correlation between parity preservation and protection of information is believed to be rather general and goes by the name of *parity-protected quantum information* [66, 67]: it is assumed that, as long as the parity remains well-defined, a Majorana-based quantum memory should work; on the other hand, if the noise involves particle loss or contamination, the memory is expected to fail. We shall return on this concept in the following Sections.

---

[5]We recall that physical states for fermions are positive, unit-trace bosonic operators.

5.2.2 Encoding a qubit in the even-parity sector

Consider a fermionic system that hosts four unpaired Majorana modes $\{\hat{m}_1, \hat{m}_2, \hat{m}_3, \hat{m}_4\}$ that are far apart from one another. We can combine them to form two non-local Dirac modes:

$$\begin{cases} \hat{g}_0 = \dfrac{\hat{m}_1 + i\hat{m}_2}{2}, & \hat{g}_0^\dagger = \dfrac{\hat{m}_1 - i\hat{m}_2}{2}, \\ \hat{d}_0 = \dfrac{\hat{m}_3 + i\hat{m}_4}{2}, & \hat{d}_0^\dagger = \dfrac{\hat{m}_3 - i\hat{m}_4}{2}. \end{cases} \tag{5.26}$$

The other fermionic degrees of freedom that constitute the system are paired into gapped Dirac eigenmodes $\{\hat{a}_i\}$.

Let us encode the logical qubit in the following pair of orthogonal states:

$$\begin{cases} |0_L\rangle = |\Omega\rangle, \\ |1_L\rangle = \hat{d}_0^\dagger \hat{g}_0^\dagger |\Omega\rangle. \end{cases} \tag{5.27}$$

$|\Omega\rangle$ is the vacuum state of the fermionic system.

Remark. Two Majorana modes are not enough to encode a qubit: $|\Omega\rangle$ and $\hat{g}_0^\dagger |\Omega\rangle$ have different parities, thus coherent superpositions are forbidden by the fermionic parity super-selection rule. Such states can be used to encode a classical bit, but not a qubit. With four modes instead there is a non-trivial even-parity sector, which allows the encoding of a full qubit.

Let $\hat{\rho}_{\mathrm{enc}}$ denote the ground-space projector: $\hat{\rho}_{\mathrm{enc}} = \prod_i \hat{a}_i \hat{a}_i^\dagger$. The logical Pauli operators corresponding to the encoding (5.27) are

$$\begin{cases} \hat{\sigma}_0^L = |0_L\rangle\langle 0_L| + |1_L\rangle\langle 1_L| = \dfrac{1}{2}(\hat{\mathbf{1}} - \hat{m}_1\hat{m}_2\hat{m}_3\hat{m}_4)\,\hat{\rho}_{\mathrm{enc}}; \\[2mm] \hat{\sigma}_1^L = |0_L\rangle\langle 1_L| + h.c. = \dfrac{i}{2}(\hat{m}_2\hat{m}_3 + \hat{m}_1\hat{m}_4)\,\hat{\rho}_{\mathrm{enc}}; \\[2mm] \hat{\sigma}_2^L = -i\,|0_L\rangle\langle 1_L| + h.c. = -\dfrac{i}{2}(\hat{m}_1\hat{m}_3 - \hat{m}_2\hat{m}_4)\,\hat{\rho}_{\mathrm{enc}}; \\[2mm] \hat{\sigma}_3^L = |0_L\rangle\langle 0_L| - |1_L\rangle\langle 1_L| = -\dfrac{i}{2}(\hat{m}_1\hat{m}_2 + \hat{m}_3\hat{m}_4)\,\hat{\rho}_{\mathrm{enc}}. \end{cases} \tag{5.28}$$

Remark. Denoting the ground-space by G and the projector onto its even-parity sector by $\hat{\Pi}_G^+ = \frac{1}{2}(\hat{\mathbf{1}} + \hat{P}_f^G)\hat{\rho}_{\mathrm{enc}} = \frac{1}{2}(\hat{\mathbf{1}} - \hat{m}_1\hat{m}_2\hat{m}_3\hat{m}_4)\hat{\rho}_{\mathrm{enc}}$, the encoded Pauli operators (5.28) can be written as

$$\begin{cases} \hat{\sigma}_0^L = \hat{\Pi}_G^+, & \hat{\sigma}_1^L = \Pi_G^+\,(i\hat{m}_2\hat{m}_3)\,\hat{\Pi}_G^+, \\ \hat{\sigma}_2^L = \Pi_G^+\,(-i\hat{m}_1\hat{m}_3)\,\hat{\Pi}_G^+, & \hat{\sigma}_3^L = \Pi_G^+\,(-i\hat{m}_1\hat{m}_2)\,\hat{\Pi}_G^+. \end{cases} \tag{5.29}$$

Notation (5.29) makes our choice of parity sector explicit, and displays the Pauli algebra of the encoded operators more clearly. Moreover, it relates the encoding (5.28) to the one that

is most frequently used in the literature [66], which is

$$\hat{\sigma}_0^L = \hat{\rho}_{\text{enc}}, \qquad \hat{\sigma}_1^L = i\hat{m}_2\hat{m}_3\hat{\rho}_{\text{enc}}, \qquad \hat{\sigma}_2^L = -i\hat{m}_1\hat{m}_3\hat{\rho}_{\text{enc}}, \qquad \hat{\sigma}_3^L = -i\hat{m}_1\hat{m}_2\hat{\rho}_{\text{enc}}. \qquad (5.30)$$

The encoding (5.30), though algebraically simpler than (5.29), has undefined parity, and is therefore less suited to study parity protection.

5.2.3 Effective local dynamics in the ground space

We shall now study the memory performance that can be achieved through the encoding (5.28) by applying a recovery operation only on the zero-modes $\{\hat{m}_1, \ldots \hat{m}_4\}$. This constraint is physically motivated, since it is reasonable to assume that the zero-modes (having already been manipulated for the initial encoding) should be accurately controllable by the experimenter, whereas a general recovery operation that involves the whole system might be technically difficult to implement.

Because of this restriction, we do not need to consider the whole decoherence channel $\mathcal{D}_t$. It suffices to define the effective ground-space channel $\widetilde{\mathcal{D}}_t$ by averaging over the non-zero energy sector S:

$$\widetilde{\mathcal{D}}_t(\hat{\rho}_0) = \text{Tr}_S\left(\mathcal{D}_t\left(\hat{\rho}_0\right)\right) \quad \forall\, \hat{\rho}_0 \in \mathcal{S}\left(G\right). \qquad (5.31)$$

Constraints from locality and parity preservation. If $\mathcal{D}_t$ is parity-preserving and local, then some useful properties hold. Those properties are discussed in Appendices E and F. Let us recall two of them here:

- The Lieb-Robinson bound (LRB) for pairs of distant fermionic operators,

$$\left\|\left\{\mathcal{D}_t\left(\hat{O}_A\right), \hat{O}_B\right\}\right\|_{\text{op}} \leq cV\left\|\hat{O}_A\right\|_{\text{op}}\left\|\hat{O}_B\right\|_{\text{op}} e^{-\frac{d_{AB}-vt}{\xi}}. \qquad (5.32)$$

- The clustering property for pairs of distant operators:

$$\mathcal{D}_t^*\left(\hat{O}_A\hat{O}_B\right) \simeq \mathcal{D}_t^*\left(\hat{O}_A\right)\mathcal{D}_t^*\left(\hat{O}_B\right). \qquad (5.33)$$

The notation is as follows: $\hat{O}_A$, $\hat{O}_B$ are operators located on distant regions A and B of the system; d_{AB} is the distance between such regions, and V is their size; v, ξ and c are model-dependent constants. Finally $\mathcal{D}_t^*$ is the adjoint[6] of channel $\mathcal{D}_t$. The LRB (5.32) represents the fact that local dynamics propagates correlations with a finite group velocity, that defines an effective light-cone[7]. The clustering property (5.33) holds as long as the

---

[6] The adjoint of a quantum channels was defined in equation (1.17).

[7] While in relativistic field theories correlations outside the light cone are strictly forbidden by causality, in this setting exponentially small tails are allowed.

space-like slices of the light-cones do not intersect, with an error that is exponentially small in $\frac{d_{AB} - vt}{\xi}$. (5.33) is related to the clustering of expectation values of distant observables on uncorrelated states,

$$
\begin{aligned}
\left\langle \hat{O}_A \hat{O}_B \right\rangle_t &= \mathrm{Tr}\left(\hat{O}_A \hat{O}_B \mathcal{D}_t \left(\hat{\rho}_A \hat{\rho}_B \right) \right) = \mathrm{Tr}\left(\mathcal{D}_t^* \left(\hat{O}_A \hat{O}_B \right) \hat{\rho}_A \hat{\rho}_B \right) \\
&\simeq \mathrm{Tr}\left(\mathcal{D}_t^* \left(\hat{O}_A \right) \hat{\rho}_A \mathcal{D}_t^* \left(\hat{O}_B \right) \hat{\rho}_B \right) = \left\langle \hat{O}_A \right\rangle_t \left\langle \hat{O}_B \right\rangle_t .
\end{aligned}
\tag{5.34}
$$

The effective ground-space channel $\widetilde{\mathcal{D}}_t$ inherits the relevant locality properties from $\mathcal{D}_t$. By applying the LRB (5.32) to two fermionic monomials $\hat{m}_i$ and $\hat{m}_j$, $i \neq j$, we can see that, for t small enough,

$$
\left\{ \widetilde{\mathcal{D}}_t(\hat{m}_i), \hat{m}_j \right\} \simeq 0 \ \forall j \neq i \qquad \Longrightarrow \qquad \widetilde{\mathcal{D}}_t(\hat{m}_i) \simeq \lambda_i(t) \hat{m}_i,
\tag{5.35}
$$

where $0 \leq \lambda_i(t) \leq 1$ (because of the contractivity of the trace norm, (1.22)), while the clustering property (5.33) implies

$$
\widetilde{\mathcal{D}}_t^*(\hat{m}_i \mathcal{F}[\{\hat{m}_j\}_{j \neq i}]) \simeq \widetilde{\mathcal{D}}_t^*(\hat{m}_i) \widetilde{\mathcal{D}}_t^*(F[\{\hat{m}_j\}_{j \neq i}])
\tag{5.36}
$$

for any monomial $\mathcal{F}[\{\hat{m}_j\}_{j \neq i}]$ in the three modes $\{\hat{m}_j : j \neq i\}$.

With these ingredients, and by further requiring unitality of $\mathcal{D}_t$, it is easy to prove that

$$
\widetilde{\mathcal{D}}_t(\hat{m}_1^{\alpha_1} \hat{m}_2^{\alpha_2} \hat{m}_3^{\alpha_3} \hat{m}_4^{\alpha_4}) \simeq \prod_{j=1}^4 \left(\widetilde{\mathcal{D}}_t(\hat{m}_j) \right)^{\alpha_j} \simeq \left(\prod_{j=1}^4 \lambda_j(t)^{\alpha_j} \right) \hat{m}_1^{\alpha_1} \hat{m}_2^{\alpha_2} \hat{m}_3^{\alpha_3} \hat{m}_4^{\alpha_4},
\tag{5.37}
$$

up to LRB corrections (that vanish in the thermodynamic limit).

Recovery fidelity. Let us assume for simplicity that $\lambda_i(t) = \lambda(t) \ \forall i$. Then the upper bound on the optimal recovery fidelity (2.12) for $\widetilde{\mathcal{D}}_t$ can be easily evaluated. One has for instance

$$
\begin{aligned}
\left\| \widetilde{\mathcal{D}}_t \left(\hat{\sigma}_1^L \right) \right\|_{\mathrm{tr}} &= \frac{1}{2} \left\| \widetilde{\mathcal{D}}_t(i\hat{m}_2 \hat{m}_3 + i\hat{m}_1 \hat{m}_4) \right\|_{\mathrm{tr}} \simeq \frac{\lambda^2(t)}{2} \| i\hat{m}_2 \hat{m}_3 + i\hat{m}_1 \hat{m}_4 \|_{\mathrm{tr}} \\
&= \lambda^2(t) \left\| \hat{\sigma}_1^L \right\|_{\mathrm{tr}} = 2\lambda^2(t),
\end{aligned}
\tag{5.38}
$$

and the same holds for $\hat{\sigma}_2^L$ and $\hat{\sigma}_3^L$; thus the upper bound reads

$$
F_t^{\mathrm{opt}} \leq \frac{1}{2} + \frac{1}{12} \sum_{i=1}^3 \left\| \mathcal{D}_t \left(\hat{\sigma}_i^L \right) \right\|_{\mathrm{tr}} = \frac{1 + \lambda^2(t)}{2}.
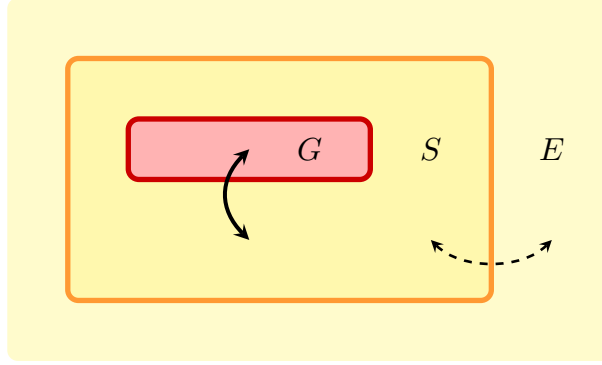\tag{5.39}
$$

FIGURE 5.2: partition of the system considered in §5.2.3. G represent the zero-energy sector; S represents the other modes of the fermionic system; E is a generic environment. Even in the absence of system-environment tunneling processes (dashed arrow), there can still be tunneling processes between S and G (solid arrow). Such processes generally change the the average ground-space parity $\left\langle \hat{P}_f^G \right\rangle$.

Since sign $\left(\lambda^2(t) \hat{\sigma}_i^L \right) = \hat{\sigma}_i^L$, the candidate optimal recovery operation is the one induced by the original logical matrices $\left\{ \hat{\sigma}_\alpha^L \right\}$. Their Pauli algebra ensures that the candidate recovery map is physical, hence the bound (5.39) is saturated.

Remark. The upper bound (5.39) refers to the effective ground-space dynamics, hence it bounds the result that can be attained by operating *on the zero-modes only*. This limitation has a strong physical and experimental motivation: a recovery operation that involves the zero-modes only should be technically much simpler to implement than one involving the whole system. Obviously, though, by operating on the whole system one may be able to achieve higher fidelities.

Fidelity and parity preservations. Recalling that $\hat{P}_f^G = -\hat{m}_1 \hat{m}_2 \hat{m}_3 \hat{m}_4$ is the fermionic parity operator (5.15) restricted to the ground space, the average ground-space parity of a state $\hat{\rho}(0)$ that is initially encoded in the even-parity sector evolves as follows:

$$\left\langle \hat{P}_f^G \right\rangle_t = \mathrm{Tr} \left(\hat{P}_f^G \hat{\rho}(t) \right) = \mathrm{Tr} \left(\hat{P}_f^G \widetilde{\mathcal{D}}_t \left(\hat{\rho}(0) \right) \right) \simeq \mathrm{Tr} \left(\widetilde{\mathcal{D}}_t^* \left(\hat{P}_f^G \right) \hat{\rho}(0) \right)$$

$$\simeq \left(\prod_{i=1}^4 \lambda_i(t) \right) \mathrm{Tr} \left(\hat{P}_f^G \hat{\rho}(0) \right) = \lambda^4(t) \left\langle \hat{P}_f^G \right\rangle_0 = \lambda^4(t). \tag{5.40}$$

We used the diagonal form (5.37) to prove that $\widetilde{\mathcal{D}}_t \simeq \widetilde{\mathcal{D}}_t^*$, up to LRB corrections. Comparing (5.39) and (5.40) we can conclude that

$$F_t^{\mathrm{opt}} = \frac{1}{2} \left(1 + \sqrt{\left\langle \hat{P}_f^G \right\rangle_t} \right), \tag{5.41}$$

up to the usual LRB corrections (which vanish in the thermodynamic limit).

Equation (5.41) shows a remarkable instance of parity protection of quantum information: no local perturbations can degrade the encoded information without altering the average parity of the ground space.

Remark. From the fact that $\mathcal{D}_t$ is parity-preserving (meaning that $\mathcal{D}_t^*(\hat{P}_f) = \hat{P}_f \ \forall t$) one cannot deduce that $\widetilde{\mathcal{D}}_t^*(\hat{P}_f^G) = \hat{P}_f^G$. In terms of particle tunneling, preserving $\hat{P}_f$ corresponds to forbidding single-particle tunneling events between the system and the environment; nonetheless, single particles *are* allowed to tunnel between the ground space G and the rest of the system S, thus changing $\hat{P}_f^G$ and $\hat{P}_f^S$. A schematic picture of the situation is given in Figure 5.2. If a physical mechanism forbade single-particle tunneling between S and G in some specific settings, however, the survival of the encoded information would be automatically ensured by (5.41).

5.2.4 Fully mixed encoding

In some situations the discussion of §5.2.3 may yield unsatisfactory results, i.e. by operating on the zero-modes only one might be able to recover only a small fraction of the information. It would therefore be interesting to consider the whole fermionic system, without tracing over the non-zero energy sector S. However the evaluation of the memory performance in the general case is too complicated. We shall therefore add some convenient assumptions in order to gain at least some insight into the problem.

Encoding subspace.   While we defined the encoded operators (5.28) via a ground-space projector $\hat{\rho}_{\text{enc}}$, the simplest choice from an algebraic point of view would be to replace the projector with the completely mixed state: $\hat{\rho}_{\text{enc}} \propto \hat{\mathbf{1}}$. Unfortunately this state has undefined parity, being a statistical mixture of pure states with all allowed particle numbers (both even and odd). It is therefore convenient to drop the even-parity-sector encoding (5.29) and choose the algebraically simpler version (5.29), which we recall here:

$$\hat{\sigma}_0^L = \hat{\rho}_{\text{enc}}, \qquad \hat{\sigma}_1^L = i\hat{m}_2\hat{m}_3\hat{\rho}_{\text{enc}}, \qquad \hat{\sigma}_2^L = -i\hat{m}_1\hat{m}_3\hat{\rho}_{\text{enc}}, \qquad \hat{\sigma}_3^L = -i\hat{m}_1\hat{m}_2\hat{\rho}_{\text{enc}}. \qquad (5.42)$$

In order to have $\left\|\hat{\sigma}_\alpha^L\right\|_{\text{tr}} = 2$, the normalization in $\hat{\rho}_{\text{enc}} \propto \hat{\mathbf{1}}$ must be set to $\hat{\rho}_{\text{enc}} = 2^{-(N-1)}\hat{\mathbf{1}}$.

Contrary to equation (5.35), with other Majorana modes available the zero-modes are not necessarily eigenmodes of the decoherence channel. However, the local nature of the dynamics implies (through the Lieb-Robinson bound (5.32)) that $\mathcal{D}_t$ can only "smear out" the zero-modes locally, within a pseudo-light-cone; as long as the different light cones do not overlap, some useful algebraic properties are retained. The situation is illustrated in Figure 5.3.

We shall now make our first simplifying assumption. The clustering property (5.33) is proven in Appendix F in the Heisenberg picture, i.e. for the adjoint channel $\mathcal{D}_t^*$, but the
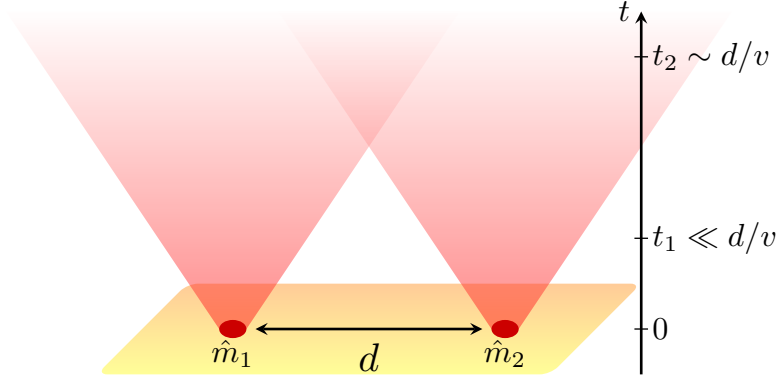
FIGURE 5.3: effect of the Lieb-Robinson bound on the time evolution of two distant Majorana modes $\hat{m}_1$, $\hat{m}_2$. Local dynamics propagates correlation with a finite group velocity v: the two modes $\mathcal{D}_t(\hat{m}_1)$ and $\mathcal{D}_t(\hat{m}_2)$ are approximately confined within pseudo-light cones. At times such that the space-like slices of the light-cones are well separated (t_1) the clustering property (5.33) holds; at later times (t_2) it fails.

same proof straightforwardly applies to the channel $\mathcal{D}_t$, provided its Lindblad operators are normal[8]. Assuming that (F.17) holds in our case, the Majorana modes essentially retain their anti-commutativity at short times:

$$\{\mathcal{D}_t(\hat{m}_i), \mathcal{D}_t(\hat{m}_j)\} = \mathcal{D}_t(\hat{m}_i)\mathcal{D}_t(\hat{m}_j) + \mathcal{D}_t(\hat{m}_j)\mathcal{D}_t(\hat{m}_i) \simeq \mathcal{D}_t(\hat{m}_i\hat{m}_j) + \mathcal{D}_t(\hat{m}_j\hat{m}_i)$$

$$= \mathcal{D}_t(\{\hat{m}_i, \hat{m}_j\}) = 0 \text{ if } i \neq j. \tag{5.43}$$

A consequence of this fact is that

$$\mathcal{D}_t\left(\hat{\sigma}_1^L\right)\mathcal{D}_t\left(\hat{\sigma}_2^L\right) \simeq \left(i\mathcal{D}_t(\hat{m}_2)\mathcal{D}_t(\hat{m}_3)\,2^{-(N-1)}\right)\left(-i\mathcal{D}_t(\hat{m}_1)\mathcal{D}_t(\hat{m}_3)\,2^{-(N-1)}\right)$$

$$\simeq -\mathcal{D}_t(\hat{m}_2)\mathcal{D}_t(\hat{m}_1)\left(\mathcal{D}_t(\hat{m}_3)\right)^2 2^{-2(N-1)} \simeq \mathcal{D}_t(\hat{m}_1\hat{m}_2)\left(\mathcal{D}_t(\hat{m}_3)\right)^2 2^{-2(N-1)}$$

$$= i\mathcal{D}_t\left(\hat{\sigma}_3^L\right)\left(\mathcal{D}_t(\hat{m}_3)\right)^2 2^{-(N-1)} \tag{5.44}$$

(the factor of $2^{-(N-1)}$ comes from the normalization of $\hat{\rho}_{\mathrm{enc}} \propto \hat{\mathbf{1}}$). Analogous relations hold for the other pairs of encoded Pauli matrices. Therefore, if

$$\left(\mathcal{D}_t(\hat{m}_i)\right)^2 \simeq \lambda^2(t)\hat{\mathbf{1}} \tag{5.45}$$

for some function $0 \leq \lambda(t) \leq 1$, the evolved Pauli matrices continue to obey a "Pauli-like" algebra (up to Lieb-Robinson corrections):

$$\mathcal{D}_t\left(\hat{\sigma}_\alpha^L\right)\mathcal{D}_t\left(\hat{\sigma}_\beta^L\right) \simeq i\varepsilon_{\alpha\beta\gamma}2^{-(N-1)}\lambda^2(t)\mathcal{D}_t\left(\hat{\sigma}_\gamma^L\right). \tag{5.46}$$

---

[8] A normal operator is one that commutes with its adjoint: $[L, L^\dagger] = 0$. This includes Hermitian and unitary operators as particular cases.

Multiplying both sides of (5.46) by $2^{2(N-1)}\lambda^{-4}(t)$, we see that the operators $\left\{\frac{2^{N-1}}{\lambda^2(t)}\mathcal{D}_t\left(\hat{\sigma}_\alpha^L\right)\right\}$ obey the original Pauli algebra. Moreover, each of them squares to the identity: for instance,

$$\left(\frac{2^{N-1}}{\lambda^2(t)}\mathcal{D}_t\left(\hat{\sigma}_1^L\right)\right)^2 \simeq \frac{1}{\lambda^4(t)}i\mathcal{D}_t\left(\hat{m}_2\right)\mathcal{D}_t\left(\hat{m}_3\right)i\mathcal{D}_t\left(\hat{m}_2\right)\mathcal{D}_t\left(\hat{m}_3\right)$$

$$\simeq \frac{1}{\lambda^4(t)}\left(\mathcal{D}_t\left(\hat{m}_2\right)\right)^2\left(\mathcal{D}_t\left(\hat{m}_3\right)\right)^2 = \hat{\mathbf{1}}. \tag{5.47}$$

By the results of §2.3.2, those operators define a CP recovery operation. This recovery operation is optimal, since $2^{N-1}\lambda^{-2}(t)\mathcal{D}_t\left(\hat{\sigma}_\alpha^L\right) = \text{sign}\left(\mathcal{D}_t\left(\hat{\sigma}_\alpha^L\right)\right)$. Therefore the optimal recovery fidelity saturates the upper bound (2.12):

$$F_{\text{mix};t}^{\text{opt}} = \frac{1}{2} + \frac{1}{12}\sum_{\alpha=1}^3 \left\|\mathcal{D}_t\left(\hat{\sigma}_\alpha^L\right)\right\|_{\text{tr}} = \frac{1}{2} + \frac{1}{12}\sum_{\alpha=1}^3 \text{Tr}\left(\left(2^{N-1}\lambda^{-2}(t)\mathcal{D}_t\left(\hat{\sigma}_\alpha^L\right)\right)\mathcal{D}_t\left(\hat{\sigma}_\alpha^L\right)\right)$$

$$= \frac{1}{2} + \frac{1}{12}\sum_{\alpha=1}^3 2^{-(N-1)}\lambda^2(t)\text{Tr}\left(\text{sign}\left(\mathcal{D}_t\left(\hat{\sigma}_\alpha^L\right)\right)^2\right) = \frac{1+\lambda^2(t)}{2}. \tag{5.48}$$

The remarkable point about this result is that it is completely determined by the local action of the noise on each Majorana zero-mode, parametrized by $\lambda(t)$. There is no need for the noise to correlate distant zero-modes; perturbing each one individually is enough to degrade the encoded information. Also, the similarity between (5.48) and (5.39) should be noted, though the time-dependent parameter $\lambda(t)$ has slightly different meanings in the two settings[9].

This result about the maximally mixed encoding (5.48) can be used to prove a *lower bound* to the optimal recovery fidelity achievable through a pure encoding. Let $\overline{\mathcal{R}}_t$ be the optimal recovery operation for the maximally mixed encoding, i.e.

$$\overline{\mathcal{R}}_t(\hat{\rho}) = \frac{1}{2}\left(\text{Tr}\left(\hat{\rho}\right)\mathbf{1} + \sum_{\alpha=1}^3 \text{Tr}\left(\hat{\rho}2^{N-1}\lambda^{-2}(t)\mathcal{D}_t\left(\hat{\sigma}_\alpha^L\right)\right)\sigma_\alpha\right). \tag{5.49}$$

Then the following inequality holds:

$$F_{\text{mix};t}^{\text{opt}} = F_{\text{mix};t}^{(\overline{\mathcal{R}}_t)} = 2^{-(N-2)}\sum_{n_3=0}^1 \cdots \sum_{n_N=0}^1 F_{\underline{n};t}^{(\overline{\mathcal{R}}_t)} \leq 2^{-(N-2)}\sum_{n_3=0}^1 \cdots \sum_{n_N=0}^1 F_{\underline{n};t}^{\text{opt}}, \tag{5.50}$$

where $\{n_3,\ldots,n_N\}$ are the occupation numbers of the $N-2$ non-zero-energy Dirac modes that compose the system along with the four Majorana zero-modes, and $F_{\underline{n};t}$ is the fidelity obtained through a pure-state encoding with occupation numbers $\underline{n} = (n_3,\ldots n_N)$. (5.50)

---

[9]In (5.48) $\lambda(t)$ is defined via $\mathcal{D}_t\left(\hat{m}_i\right)^2 = \lambda^2(t)\hat{\mathbf{1}}$, while in (5.39) the definition is $\widetilde{\mathcal{D}}_t(\hat{m}_i) = \lambda(t)\hat{m}_i$. In the latter case one generally obtains a smaller parameter, and thus recovers less information.

holds because the encoding operation

$$\mathcal{E}_{\hat{\rho}_{\text{enc}}} \left(\frac{\mathbf{1} + \mathbf{v} \cdot \boldsymbol{\sigma}}{2} \right) = \frac{\hat{\sigma}_0^L + \mathbf{v} \cdot \hat{\boldsymbol{\sigma}}^L}{2} \tag{5.51}$$

is linear in $\hat{\rho}_{\text{enc}}$ (which is implicit in the definitions of $\hat{\sigma}_0^L$ and $\hat{\boldsymbol{\sigma}}^L$, (5.42)); therefore

$$\begin{aligned}
F_{\text{mix};t}^{(\overline{\mathcal{R}}_t)} &= \int d\mu_{\mathbf{v}} \text{Tr} \left(\frac{\mathbf{1} + \mathbf{v} \cdot \boldsymbol{\sigma}}{2} \overline{\mathcal{R}}_t \circ \mathcal{D}_t \circ \mathcal{E}_{\text{mix}} \left(\frac{\mathbf{1} + \mathbf{v} \cdot \boldsymbol{\sigma}}{2} \right) \right) \\
&= 2^{-(N-2)} \sum_{n_3=0}^{1} \cdots \sum_{n_N=0}^{1} \int d\mu_{\mathbf{v}} \text{Tr} \left(\frac{\mathbf{1} + \mathbf{v} \cdot \boldsymbol{\sigma}}{2} \overline{\mathcal{R}}_t \circ \mathcal{D}_t \circ \mathcal{E}_{\underline{n}} \left(\frac{\mathbf{1} + \mathbf{v} \cdot \boldsymbol{\sigma}}{2} \right) \right) \\
&= 2^{-(N-2)} \sum_{n_3=0}^{1} \cdots \sum_{n_N=0}^{1} F_{\underline{n};t}^{(\overline{\mathcal{R}}_t)}.
\end{aligned} \tag{5.52}$$

The meaning of (5.50) is that under these hypotheses (that distant operators "cluster" (F.17) and that time-evolved Majorana modes square to c-numbers (5.45)) there is *at least* a pure encoding that performs *at least* as well as the maximally mixed one. Thus one has the following lower bound on the optimal recovery fidelity that can be achieved through pure encodings:

$$\max_{\underline{n}} F_{\underline{n};t}^{\text{opt}} \geq F_{\text{mix};t}^{\text{opt}} = \frac{1 + \lambda^2(t)}{2} \tag{5.53}$$

This lower bound may be used together with the upper bound (2.12) to constrain the optimal recovery fidelity allowed by a given system.

Remark. The result (5.53) depends critically on the *ad hoc* assumption (5.45), which is a strong and rather arbitrary requirement. Instances in which (5.45) holds include the case in which each $\hat{m}_i$ is an eigenmode of $\mathcal{D}_t$ (which is however satisfactorily treated with the approach described in §5.2.3), and the case in which $\mathcal{D}_t(\hat{m}_i)$ is a linear combination of single Majorana modes[10], with no cubic or higher-degree terms. The clustering property (5.43) is also proved only in the case of normal Lindblad operators, which excludes some potentially interesting noise models; though as far as we know it may hold more generally.

5.3 Toy Model of a Quantum Memory with Eight Majorana Modes

We shall now start the analysis of quantum memory toy-models based on Majorana zero-modes. In this Section we will study a model based on eight modes. The model is introduced

---

[10] In this case (5.45) can be proven by straightforwardly generalizing the identity $(\alpha \hat{m}_1 + \beta \hat{m}_2)^2 = \alpha^2 \hat{m}_1^2 + \beta^2 \hat{m}_2^2 + \alpha\beta \{\hat{m}_1, \hat{m}_2\} = (\alpha^2 + \beta^2)\hat{\mathbf{1}}$.
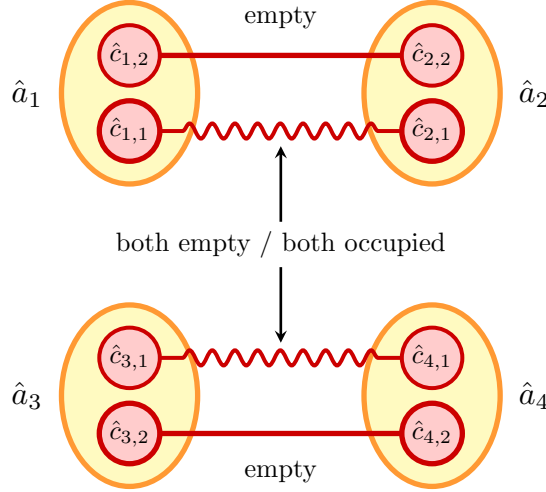
FIGURE 5.4: schematic representation of the encoding in the 8-mode model. The qubit is encoded into the non-local Dirac modes corresponding to wavy lines. The Dirac modes corresponding to straight lines are always initialized empty.

in §5.3.1, and its memory performance is evaluated under both non-parity-preservng (§5.3.2) and parity-preserving (§5.3.3) local noise models.

5.3.1 Definition of the model

Let us consider a system consisting of four Dirac modes located far apart from one another. No other modes are present. Each Dirac mode can be described as a pair of Majorana modes. If we assume the system Hamiltonian to be zero, each one of the eight Majorana modes is a zero-mode, and thus unpaired. Therefore one can (at least in principle) choose a Majorana mode from each site to perform the non-local qubit encoding (5.28), while initializing the other four modes in some vacuum state $\hat{\rho}_{\mathrm{enc}}$. The noise is assumed to couple only same-site Majorana modes. A schematic representation of the encoding is given in Figure 5.4

Though very unrealistic, this model is interesting because some important properties, including locality and parity preservation, can be imposed *exactly*. It is therefore interesting from a theoretical point of view to investigate the extent to which such features protect the encoded information, even in an unrealistic setting.

Let $\hat{a}_r^\dagger, \hat{a}_r$ denote the creation (annihilation) operators for the four Dirac modes. $r \in \{1, 2, 3, 4\}$ labels the site. The notation for the Majorana modes is the one introduced in (5.3):

$$\hat{c}_{r,1} = \hat{a}_r + \hat{a}_r^\dagger, \qquad\qquad \hat{c}_{r,2} = i(\hat{a}_r^\dagger - \hat{a}_r). \qquad (5.54)$$

Four of them, say the $\{\hat{c}_{r,1}\}$, will be used to encode the qubit; the other four will be initialized in the state

$$\hat{\rho}_{\text{enc}} = \frac{\hat{\mathbf{1}} - i\hat{c}_{1,2}\hat{c}_{2,2}}{2} \frac{\hat{\mathbf{1}} - i\hat{c}_{3,2}\hat{c}_{4,2}}{2}. \tag{5.55}$$

The encoded Pauli operators defined in (5.28) for this model take the following form:

$$\begin{cases} \hat{\sigma}_0^L = \dfrac{1}{2}(\hat{\mathbf{1}} - \hat{c}_{1,1}\hat{c}_{2,1}\hat{c}_{3,1}\hat{c}_{4,1})\hat{\rho}_{\text{enc}}, \\[2mm] \hat{\sigma}_1^L = \dfrac{i}{2}(\hat{c}_{2,1}\hat{c}_{3,1} + \hat{c}_{1,1}\hat{c}_{4,1})\hat{\rho}_{\text{enc}}, \\[2mm] \hat{\sigma}_2^L = \dfrac{i}{2}(\hat{c}_{2,1}\hat{c}_{4,1} - \hat{c}_{1,1}\hat{c}_{3,1})\hat{\rho}_{\text{enc}}, \\[2mm] \hat{\sigma}_3^L = -\dfrac{i}{2}(\hat{c}_{1,1}\hat{c}_{2,1} + \hat{c}_{3,1}\hat{c}_{4,1})\hat{\rho}_{\text{enc}}. \end{cases} \tag{5.56}$$

5.3.2 Memory performance under a non-parity-preserving noise

We shall first consider a noise model that describes tunneling processes of individual fermions between the system and an environment, thus altering the system parity $\hat{P}_f$. We prove that the optimal recovery fidelity F_t^{opt} in this case is smaller than $\frac{1+e^{-\Gamma t}}{2}$, where Γ is a parameter related to the rate of the tunneling events: thus all the encoded information is lost over a time scale determined by the local details of the noise, and no protection is provided by the non-local encoding.

Noise model. The tunneling processes can be modeled by Lindblad operators $\sqrt{\gamma}\hat{a}_r$ (draining particles out of the memory at a rate γ), and $\sqrt{\delta}\hat{a}_r^\dagger$ (pumping particles into the memory at a rate δ). The total Lindbladian is the sum of four single-site Lindbladians: $\mathcal{L}(\hat{\rho}) = \sum_{r=1}^4 \mathcal{L}_r(\hat{\rho})$, with

$$\begin{aligned} \mathcal{L}_r(\hat{\rho}) &= \left(\gamma\hat{a}_r\hat{\rho}\hat{a}_r^\dagger + \delta\hat{a}_r^\dagger\hat{\rho}\hat{a}_r - \frac{1}{2}\left\{\hat{\rho}, \gamma\hat{a}_r^\dagger\hat{a}_r + \delta\hat{a}_r\hat{a}_r^\dagger\right\} \right) \\ &= \frac{\gamma+\delta}{4}(\hat{c}_{r,1}\hat{\rho}\hat{c}_{r,1} + \hat{c}_{r,2}\hat{\rho}\hat{c}_{r,2} - 2\hat{\rho}) + i\frac{\gamma-\delta}{4}(\hat{c}_{r,2}\hat{\rho}\hat{c}_{r,1} - \hat{c}_{r,1}\hat{\rho}\hat{c}_{r,2} - \{\hat{\rho}, \hat{c}_{r,1}\hat{c}_{r,2}\}) \end{aligned} \tag{5.57}$$

Lindbladians corresponding to different sites commute ($\mathcal{L}_i(\mathcal{L}_j(\hat{\rho})) = \mathcal{L}_j(\mathcal{L}_i(\hat{\rho})) \ \forall i, j$), thus they induce mutually commuting decoherence channels:

$$\mathcal{D}_t = \exp\left(t\sum_{r=1}^4 \mathcal{L}_r\right) = \prod_{r=1}^4 e^{t\mathcal{L}_r} = \mathcal{D}_t^{(1)} \circ \mathcal{D}_t^{(2)} \circ \mathcal{D}_t^{(3)} \circ \mathcal{D}_t^{(4)}, \tag{5.58}$$

with $\mathcal{D}_t^{(r)} = e^{t\mathcal{L}_r}$. Therefore in order to calculate $\mathcal{D}_t$ it suffices to focus on a single site and then compose the four commuting $\mathcal{D}_t^{(r)}$ partial channels.

	ν_r		
	0	1	2
bosonic	$\mathcal{A}_r$	$\mathcal{B}_r$	$\mathcal{C}_r$
fermionic	$\mathcal{C}_r$	$\mathcal{B}_r$	$\mathcal{A}_r$

TABLE 5.1: partition of all monomials of the algebra into the three subsets $\mathcal{A}_r$, $\mathcal{B}_r$, $\mathcal{C}_r$. ν_r denotes the number of Majorana operators of the set $\{\hat{c}_{r,1}, \hat{c}_{r,2}\}$ that appear in the monomial.

Decoherence channel. In order to compute the action of $\mathcal{D}_t^{(r)}$ on all operators, we shall divide the set of monomials of the system algebra into three subsets:

- $\mathcal{A}_r$, including all monomials $\hat{A}$ such that $[\hat{A}, \hat{c}_{r,1}] = [\hat{A}, \hat{c}_{r,2}] = 0$.

- $\mathcal{B}_r$, including all monomials $\hat{B}$ such that $[\hat{B}, \hat{c}_{r,1}] = \{\hat{B}, \hat{c}_{r,2}\} = 0$ or $\{\hat{B}, \hat{c}_{r,1}\} = [\hat{B}, \hat{c}_{r,2}] = 0$.

- $\mathcal{C}_r$, including all monomials $\hat{C}$ such that $\{\hat{C}, \hat{c}_{r,1}\} = \{\hat{C}, \hat{c}_{r,2}\} = 0$.

A simple rule for determining the "type" of a given monomial is illustrated in Table 5.1.

It is easy to see from the definitions of the three subsets and from the Lindbladian (5.57) that

$$\begin{cases} \mathcal{L}_r(\hat{A}) = (\delta - \gamma)\hat{A} i\hat{c}_{r,1}\hat{c}_{r,2} & \forall \hat{A} \in \mathcal{A}_r, \\ \mathcal{L}_r(\hat{B}) = -\dfrac{\gamma + \delta}{2}\hat{B} & \forall \hat{B} \in \mathcal{B}_r, \\ \mathcal{L}_r(\hat{C}) = -(\gamma + \delta)\hat{C} & \forall \hat{C} \in \mathcal{C}_r. \end{cases} \qquad (5.59)$$

Type $\mathcal{B}_r$ and $\mathcal{C}_r$ monomials are eigenmodes of $\mathcal{D}_t^{(r)}$, while type $\mathcal{A}_r$ monomials mix with type $\mathcal{C}_r$ ones:

$$\begin{cases} \mathcal{D}_t^{(r)}(\hat{A}) = \hat{A}\left(\hat{1} + \dfrac{\delta - \gamma}{\gamma + \delta}\left(1 - e^{-(\gamma+\delta)t}\right)i\hat{c}_{r,1}\hat{c}_{r,2}\right) & \forall \hat{A} \in \mathcal{A}_r, \\ \mathcal{D}_t^{(r)}(\hat{B}) = e^{-(\gamma+\delta)t/2}\hat{B} & \forall \hat{B} \in \mathcal{B}_r, \\ \mathcal{D}_t^{(r)}(\hat{C}) = e^{-(\gamma+\delta)t}\hat{C} & \forall \hat{C} \in \mathcal{C}_r. \end{cases} \qquad (5.60)$$

Each partial channel $\mathcal{D}_t^{(r)}$ either damps the monomial (type $\mathcal{B}_r$ or $\mathcal{C}_r$) or attaches to it an operator $\hat{\rho}_r'(t) \equiv \hat{1} + \frac{\delta-\gamma}{\gamma+\delta}\left(1 - e^{-(\gamma+\delta)t}\right)i\hat{c}_{r,1}\hat{c}_{r,2}$ (type $\mathcal{A}_r$).

Remark. If $\hat{\rho}$ is a monomial in $\mathcal{A}_s$ and, for instance, $\hat{\rho} \in \mathcal{B}_r$ for some $s \neq r$, then $\mathcal{D}_t^{(s)}(\hat{\rho}) = \hat{\rho}\hat{\rho}_s'(t)$ is a linear combination of two monomials, $\hat{\rho}$ and $\hat{\rho}i\hat{c}_{r,1}\hat{c}_{r,2}$, that *still* belong to $\mathcal{B}_r$ at all times (because none of the relevant parameters in Table 5.1 are changed by multiplication with $i\hat{c}_{r,1}\hat{c}_{r,2}$). This means, more generally, that the partitions based on all sites $s \neq r$ are invariant under $\mathcal{D}_t^{(r)}$. Therefore, in order to compute the time evolution of any monomial of the algebra, one just has to determine the type of the monomial with respect to the

four partitions obtained by considering different sites, $r = 1, 2, 3, 4$, and then attach to the original monomial the four factors prescribed by (5.60) (in an arbitrary order since they mutually commute).

Recovery fidelity. In order to evaluate the upper bound on the recovery fidelity (2.12), the trace norms of the evolved logical operators must be computed. Let us start from $\hat{\sigma}_1^L$, as defined in (5.56):

$$
\begin{aligned}
\hat{\sigma}_1^L &= \frac{1}{8}\Big[(i\hat{c}_{2,1}\hat{c}_{3,1} + i\hat{c}_{1,1}\hat{c}_{4,1})(\hat{\mathbf{1}} - i\hat{c}_{1,2}\hat{c}_{2,2})(\hat{\mathbf{1}} - i\hat{c}_{3,2}\hat{c}_{4,2})\Big] \\
&= \frac{1}{8}\Big[i\hat{c}_{2,1}\hat{c}_{3,1} + i\hat{c}_{1,1}\hat{c}_{4,1} - \hat{c}_{1,2}\hat{c}_{2,1}\hat{c}_{2,2}\hat{c}_{3,1} + \hat{c}_{1,1}\hat{c}_{1,2}\hat{c}_{2,2}\hat{c}_{4,1} + \hat{c}_{2,1}\hat{c}_{3,1}\hat{c}_{3,2}\hat{c}_{4,2} \\
&\quad - \hat{c}_{1,1}\hat{c}_{3,2}\hat{c}_{4,1}\hat{c}_{4,2} + i\hat{c}_{1,2}\hat{c}_{2,1}\hat{c}_{2,2}\hat{c}_{3,1}\hat{c}_{3,2}\hat{c}_{4,2} + i\hat{c}_{1,1}\hat{c}_{1,2}\hat{c}_{2,2}\hat{c}_{3,2}\hat{c}_{4,1}\hat{c}_{4,2}\Big].
\end{aligned}
\tag{5.61}
$$

The eight monomials in brackets can be classified using the first row of Table 5.1 (since they are all bosonic). For instance, the first one is of type $(\mathcal{A}_1\mathcal{B}_2\mathcal{B}_3\mathcal{A}_4)$, hence its time evolution is obtained by attaching a factor of $e^{-(\gamma+\delta)t}\hat{\rho}_1'(t)\hat{\rho}_4'(t)$. Applying this technique to all eight monomials in (5.61), and defining $\Gamma = \gamma + \delta$ for brevity, one gets

$$
\begin{aligned}
\mathcal{D}_t\left(\hat{\sigma}_1^L\right) &= \frac{e^{-\Gamma t}}{8}\Big[i\hat{c}_{2,1}\hat{c}_{3,1}\hat{\rho}_1'\hat{\rho}_4' + i\hat{c}_{1,1}\hat{c}_{4,1}\hat{\rho}_2'\hat{\rho}_3' + e^{-\Gamma t}\big(-\hat{c}_{1,2}\hat{c}_{2,1}\hat{c}_{2,2}\hat{c}_{3,1}\hat{\rho}_4' \\
&\quad + \hat{c}_{1,1}\hat{c}_{1,2}\hat{c}_{2,2}\hat{c}_{4,1}\hat{\rho}_3' + \hat{c}_{2,1}\hat{c}_{3,1}\hat{c}_{3,2}\hat{c}_{4,2}\hat{\rho}_1' - \hat{c}_{1,1}\hat{c}_{3,2}\hat{c}_{4,1}\hat{c}_{4,2}\hat{\rho}_2'\big) \\
&\quad + e^{-2\Gamma t}\big(i\hat{c}_{1,2}\hat{c}_{2,1}\hat{c}_{2,2}\hat{c}_{3,1}\hat{c}_{3,2}\hat{c}_{4,2} + i\hat{c}_{1,1}\hat{c}_{1,2}\hat{c}_{2,2}\hat{c}_{3,2}\hat{c}_{4,1}\hat{c}_{4,2}\big)\Big].
\end{aligned}
\tag{5.62}
$$

The presence of $\hat{\rho}'$ operators makes it impossible to diagonalize all the monomials that compose $\mathcal{D}_t\left(\hat{\sigma}_1^L\right)$ simultaneously. This makes an analytical computation of the trace norm difficult. Figure 5.5 shows the results of numerical calculations, by which is clear that the dependence on the $\frac{\delta}{\gamma}$ ratio (at fixed Γ) is unimportant as far as the memory performance is concerned.

We shall therefore focus on the analytically solvable case $\gamma = \delta$, in which particles flow in and out of the system at equal rates. In this case $\hat{\rho}_r'(t) = \hat{\mathbf{1}}\ \forall r, \forall t$, and (5.62) becomes

$$
\mathcal{D}_t\left(\hat{\sigma}_1^L\right) = \frac{e^{-\Gamma t}}{8}(i\hat{c}_{2,1}\hat{c}_{3,1} + i\hat{c}_{1,1}\hat{c}_{4,1})\left(\hat{\mathbf{1}} - e^{-\Gamma t}i\hat{c}_{1,2}\hat{c}_{2,2}\right)\left(\hat{\mathbf{1}} - e^{-\Gamma t}i\hat{c}_{3,2}\hat{c}_{4,2}\right).
\tag{5.63}
$$

By diagonalizing the complete set of commuting observables $i\hat{c}_{1,1}\hat{c}_{2,1}$, $i\hat{c}_{3,1}\hat{c}_{4,1}$, $i\hat{c}_{1,2}\hat{c}_{2,2}$, $i\hat{c}_{3,2}\hat{c}_{4,2}$, one has

$$
\begin{aligned}
\left\|\mathcal{D}_t\left(\hat{\sigma}_1^L\right)\right\|_{\mathrm{tr}} &= \frac{e^{-\Gamma t}}{8}\sum_{a,b,c,d=\pm 1}|a+b|\cdot\left|1 - e^{-\Gamma t}c\right|\cdot\left|1 - e^{-\Gamma t}d\right| \\
&= \frac{e^{-\Gamma t}}{2}\left(\sum_{c=\pm 1}\left|1 - e^{-\Gamma t}c\right|\right)^2 = 2e^{-\Gamma t}.
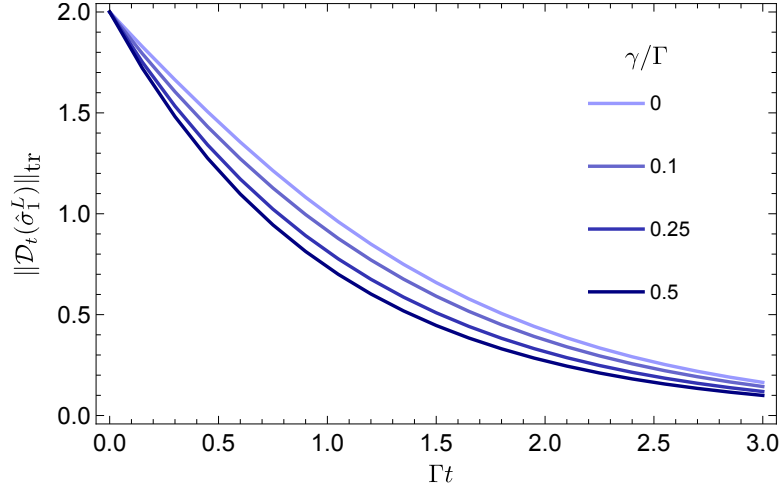\end{aligned}
\tag{5.64}
$$

FIGURE 5.5: decay of the trace norm of $\mathcal{D}_t\left(\hat{\sigma}_1^L\right)$, from (5.62), for several values of the ratio $\frac{\gamma}{\Gamma}$. The trace norm is invariant under $\frac{\gamma}{\Gamma} \mapsto 1 - \frac{\gamma}{\Gamma}$. Thus $\gamma/\Gamma = 0.5$ yields an extremal curve, corresponding to the worst case.

By a completely analogous procedure the same result for $\hat{\sigma}_2^L$ and $\hat{\sigma}_3^L$ can be proven. Therefore, in the $\gamma = \delta$ case, the upper bound on the recovery fidelity is

$$F_t{}^{\text{opt}} \leq \frac{1 + e^{-\Gamma t}}{2}. \tag{5.65}$$

In light of the numerical data in Figure 5.5, the bound should slightly improve for $\delta \neq \gamma$ (at fixed $\gamma + \delta$), though not significantly.

The upper bound (5.65) is enough to prove a negative result about the memory performance. All the encoded information is lost over a time scale Γ^{-1}, which is completely specified by the local properties of the noise (namely, the tunneling rates); no protection whatsoever is provided by the non-local encoding.

5.3.3 Memory performance under a parity-preserving noise

We shall now turn to a parity-preserving noise model, and prove that the memory performance in this case is only marginally better than it was in the previous one, with F_t^{opt} upper-bounded by $\frac{2+e^{-4\gamma t}}{3}$. Namely, we find that a classical bit of information is protected, but all quantum coherence is lost over a time scale dictated by the local properties of the noise (represented by the coefficient γ), with no advantages over a local encoding. Therefore no parity protection is observed in this case.

Noise model. By the results of Appendix E, a parity-preserving Markovian process must have purely bosonic Lindblad operators. By further requiring *locality*, few possibilities are

left: the only local, bosonic monomials on site r are $i\hat{c}_{r,1}\hat{c}_{r,2}$ and $\hat{1}$. Thus the most general Lindblad operator is

$$\hat{L}_r = \alpha_r \hat{1} + \beta_r i \hat{c}_{r,1}\hat{c}_{r,2}, \quad \alpha_r,\, \beta_r \in \mathbb{C}. \tag{5.66}$$

However, using the "gauge fixing" freedom on the choice of Lindblad operators (1.15), it is possible to assume without loss of generality $\beta_r = \sqrt{\gamma_r} \in \mathbb{R}$, and to remove the part proportional to $\hat{1}$ by introducing the effective Hamiltonian

$$\hat{H}'_r = \Im(\alpha_r)\beta_r i \hat{c}_{r,1}\hat{c}_{r,2} \equiv \mu_r \left(2\hat{a}_r^\dagger \hat{a}_r - \hat{1}\right), \tag{5.67}$$

where we defined the "chemical potential" $\mu_r \equiv 2\Im(\alpha_r)\beta_r$. The resulting master equation is

$$\frac{d}{dt}\hat{\rho}(t) = \sum_{r=1}^{4} \mathcal{L}_r(\hat{\rho}), \tag{5.68}$$

$$\mathcal{L}_r(\hat{\rho}) = -i\frac{\mu_r}{2}\left[i\hat{c}_{r,1}\hat{c}_{r,2}, \hat{\rho}\right] + \gamma_r \left(\hat{c}_{r,1}\hat{c}_{r,2}\hat{\rho}\hat{c}_{r,2}\hat{c}_{r,1} - \hat{\rho}\right). \tag{5.69}$$

Decoherence channel. Since $[\mathcal{L}_i, \mathcal{L}_j] = 0$, we have

$$\mathcal{D}_t = \exp\left(t\sum_{r=1}^{4}\mathcal{L}_r\right) = \prod_{r=1}^{4} e^{t\mathcal{L}_r} \equiv \mathcal{D}_t^{(1)} \circ \mathcal{D}_t^{(2)} \circ \mathcal{D}_t^{(3)} \circ \mathcal{D}_t^{(4)}, \tag{5.70}$$

like we had in the fermionic case (5.58). Thus the dynamics can be completely solved by studying a single site.

It is easy to see that $\hat{1}$ and $i\hat{c}_{r,1}\hat{c}_{r,2}$ are fixed points of $\mathcal{D}_t^{(r)}$. As for the fermionic monomials, we have

$$\begin{aligned}
\mathcal{L}_r(\hat{c}_{s,j}) &= \delta_{rs}\left(\frac{\mu_r}{2}[\hat{c}_{r,1}\hat{c}_{r,2}, \hat{c}_{r,j}] + \gamma_r\left(\hat{c}_{r,1}\hat{c}_{r,2}\hat{c}_{r,j}\hat{c}_{r,2}\hat{c}_{r,1} - \hat{c}_{r,j}\right)\right) \\
&= \delta_{rs}\left(\mu_r\hat{c}_{r,1}\hat{c}_{r,2} - 2\gamma_r\hat{1}\right)\hat{c}_{r,j} \\
&= \begin{cases} \delta_{rs}\left(-\mu_r\hat{c}_{r,2} - 2\gamma_r\hat{c}_{r,1}\right) & \text{if } j = 1, \\ \delta_{rs}\left(\mu_r\hat{c}_{r,1} - 2\gamma_r\hat{c}_{r,2}\right) & \text{if } j = 2. \end{cases}
\end{aligned} \tag{5.71}$$

Thus the subspace spanned by $\hat{c}_{r,1}$ and $\hat{c}_{r,2}$ is invariant under each $\mathcal{D}_t^{(r)}$.

Remark. This proves an exact, infinite-distance Lieb-Robinson bound: bosonic (fermionic) operators on distant sites exactly commute (anti-commute) at all times.

Let us now compute the time evolution of general local fermionic operators $\xi(0)\hat{c}_{r,1}+\eta(0)\hat{c}_{r,2}$. From (5.71), one has

$$\begin{pmatrix} \dot{\xi}(t) \\ \dot{\eta}(t) \end{pmatrix} = -\begin{pmatrix} 2\gamma_r & -\mu_r \\ \mu_r & 2\gamma_r \end{pmatrix}\begin{pmatrix} \xi(t) \\ \eta(t) \end{pmatrix}. \tag{5.72}$$

The solution is found by exponentiation:

$$\begin{pmatrix} \xi(t) \\ \eta(t) \end{pmatrix} = \exp\left(-t\begin{pmatrix} 2\gamma_r & -\mu_r \\ \mu_r & 2\gamma_r \end{pmatrix}\right)\begin{pmatrix} \xi(0) \\ \eta(0) \end{pmatrix} =$$

$$= e^{-2\gamma_r t}\begin{pmatrix} \cos\mu_r t & \sin\mu_r t \\ -\sin\mu_r t & \cos\mu_r t \end{pmatrix}\begin{pmatrix} \xi(0) \\ \eta(0) \end{pmatrix}. \tag{5.73}$$

There is an exponential damping over a time-scale $(2\gamma_r)^{-1}$ and a rotation within the subspace at a frequency μ_r.

Recovery fidelity. In order to evaluate the upper bound on the recovery fidelity (2.12), one has to compute the time-evolved logical operators $\left\{\mathcal{D}_t\left(\hat{\sigma}_i^L\right)\right\}$. There are two observations that can be made in order to make such computation easier:

- From (5.73) it can be seen that the Hamiltonian part and the dissipative part of the dynamics commute[11]; thus the Hamiltonian induces a unitary evolution that can be exactly inverted, with no effect on the optimal recovery fidelity. For this reason one can set $\mu_r = 0 \ \forall\, r$ without loss of generality.

- The decoherence channel is parity-preserving, hence its Kraus operators are bosonic by the results of Appendix E; therefore $\mathcal{D}_t\left(\hat{P}_f\hat{\rho}\right) = \hat{P}_f\mathcal{D}_t\left(\hat{\rho}\right) \ \forall\,\hat{\rho}$. Logic operators (5.56) consist of eight monomials each, but they can be simplified by conveniently introducing parity projectors: e.g.,

$$\hat{\sigma}_1^L = \frac{1}{8}(i\hat{c}_{2,1}\hat{c}_{3,1} + i\hat{c}_{1,1}\hat{c}_{4,1})(\hat{\mathbf{1}} - i\hat{c}_{1,2}\hat{c}_{2,2})(\hat{\mathbf{1}} - i\hat{c}_{3,2}\hat{c}_{4,2})$$

$$= \frac{1}{4}\left(i\hat{c}_{2,1}\hat{c}_{3,1} + i\hat{c}_{1,1}\hat{c}_{4,1} - i\hat{c}_{2,1}\hat{c}_{3,1}i\hat{c}_{1,2}\hat{c}_{2,2} - i\hat{c}_{2,1}\hat{c}_{3,1}i\hat{c}_{3,2}\hat{c}_{4,2}\right)\hat{\Pi}^+. \tag{5.74}$$

Now, since $\mathcal{D}_t$ is transparent to the even-parity projector $\hat{\Pi}^+ = \frac{\hat{\mathbf{1}}+\hat{P}_f}{2}$, one just has to time-evolve four monomials, instead of eight.

---

[11] Equation (5.73) deals with fermionic monomials, whereas bosonic monomials are stabilized by each part of the dynamics separately: the action of the Hamiltonian commutes with that of the dissipation on every monomial, and thus on all the algebra.

In light of these observations, we have

$$
\begin{aligned}
\mathcal{D}_t \left(\hat{\sigma}_1^L \right) &= \mathcal{D}_t \left(\frac{i\hat{c}_{2,1}\hat{c}_{3,1} + i\hat{c}_{1,1}\hat{c}_{4,1} - i\hat{c}_{2,1}\hat{c}_{3,1}i\hat{c}_{1,2}\hat{c}_{2,2} - i\hat{c}_{2,1}\hat{c}_{3,1}i\hat{c}_{3,2}\hat{c}_{4,2}}{4} \right) \hat{\Pi}^+ \\
&= \frac{1}{4} \Big[i\mathcal{D}_t \left(\hat{c}_{2,1} \right) \mathcal{D}_t \left(\hat{c}_{3,1} \right) + i\mathcal{D}_t \left(\hat{c}_{1,1} \right) \mathcal{D}_t \left(\hat{c}_{4,1} \right) \\
&\qquad - i\hat{c}_{2,1}\mathcal{D}_t \left(\hat{c}_{3,1} \right) \mathcal{D}_t \left(i\hat{c}_{1,2} \right) \hat{c}_{2,2} - i\mathcal{D}_t \left(\hat{c}_{2,1} \right) \hat{c}_{3,1}i\hat{c}_{3,2}\mathcal{D}_t \left(\hat{c}_{4,2} \right) \Big] \hat{\Pi}^+ . \qquad (5.75)
\end{aligned}
$$

Now, from (5.73) we have $\mathcal{D}_t \left(\hat{c}_r \right) = e^{-2\gamma_r t}\hat{c}_r \ \forall r$; assuming for simplicity that $\gamma_r = \gamma \ \forall r$, (5.75) yields $\mathcal{D}_t \left(\hat{\sigma}_1^L \right) = e^{-4\gamma t}\mathcal{D}_t \left(\hat{\sigma}_1^L \right)$. Then

$$
\left\| \mathcal{D}_t \left(\hat{\sigma}_1^L \right) \right\|_{\mathrm{tr}} = \left\| e^{-4\gamma t}\hat{\sigma}_1^L \right\|_{\mathrm{tr}} = 2e^{-4\gamma t}. \qquad (5.76)
$$

The same holds for $\hat{\sigma}_2^L$, since it can be obtained from $\hat{\sigma}_1^L$ by swapping the labels of sites $r = 3$ and $r = 4$ (some signs have to be adjusted, but they do not change substantially the previous derivation). At this point we do not even need to consider $\hat{\sigma}_3^L$ in order to prove the claimed result: since $\left\| \mathcal{D}_t \left(\hat{\sigma}_3^L \right) \right\|_{\mathrm{tr}} \leq 2$, the upper bound (2.12) reads

$$
F_t^{\mathrm{opt}} \leq \frac{1}{2} + \frac{1}{3}e^{-4\gamma t} + \frac{1}{12} \left\| \mathcal{D}_t \left(\hat{\sigma}_3^L \right) \right\|_{\mathrm{tr}} \leq \frac{2}{3} + \frac{1}{3}e^{-4\gamma t}. \qquad (5.77)
$$

This suffices to prove a negative result about the memory performance. Quantum coherence of the encoded information is completely lost over a time scale of $(4\gamma)^{-1}$, which depends only on the local properties of the noise. It can be shown that $\left\| \mathcal{D}_t \left(\hat{\sigma}_3^L \right) \right\|_{\mathrm{tr}} = 2 \ \forall t$, so that classical information encoded in $\hat{\sigma}_3^L$ is preserved, but this fact is only due to the peculiar noise model[12]. The non-locality of encoded information, by itself, does not provide any protection, even in the case of a parity-preserving noise.

5.4 Toy-Model of a Quantum Memory with Twelve Majorana Modes

We shall now consider a slightly more complicated model, in which a Majorana mode is added to each of the four sites in the 8-mode model studied in the previous Section. This extension allows different choices for the encoding subspaces, so that we can study the effects of such choices on the memory performance under a parity-preserving noise model.

We introduce the model in §5.4.1. We then present the two encodings and evaluate their memory performances in §5.4.2 and §5.4.3. Finally we discuss the results in §5.4.4.

---

[12] It would also happen for a local encoding, like $\hat{\sigma}_3^L = -\frac{i}{8}(\hat{c}_{1,1}\hat{c}_{1,2} + \hat{c}_{2,1}\hat{c}_{2,2})(\hat{\mathbf{1}} - i\hat{c}_{3,1}\hat{c}_{3,2})(\hat{\mathbf{1}} - i\hat{c}_{4,1}\hat{c}_{4,2})$.
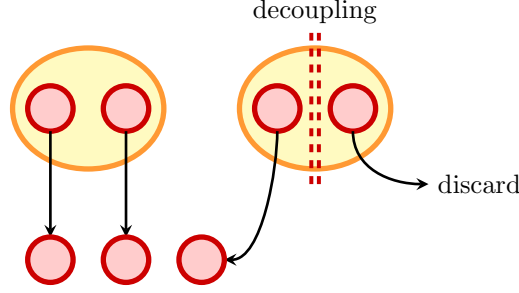
FIGURE 5.6: the groups of three Majorana modes used in §5.4 can in principle be obtained from two neighboring Dirac modes, provided one of the four corresponding Majorana modes is fully decoupled from the others. The decoupling must hold for the full dynamics, including the dissipation.

5.4.1 Definition of the model

The system consists of twelve Majorana modes, which are divided to form four groups of three; the groups are far apart from one another, so that no Hamiltonian or Lindbladian terms can couple them. In itself this model has no physical meaning, since Majorana modes come in pairs, not in triplets; however, it can be considered as an effective description of a physical situation. Consider a system of two ordinary Dirac fermions, and suppose that their dynamics is such that a Majorana mode is decoupled from the other three. Then one can effectively discard the decoupled mode, and use the remaining three as building blocks for the quantum memory model (Figure 5.6).

We shall use the following notation:

- $\{\hat{c}_{r,j} : r \in \{1, 2, 3, 4\} ; j \in \{0, 1, 2\}\}$ are the Majorana modes. r labels the different "groups" while j labels the modes within a given group.

- $\left\{\hat{a}_r = \frac{1}{2}(\hat{c}_{r,0} + i\hat{c}_{r,1})\right\}$ are "site" Dirac modes.

- $\left\{\hat{b}_r = \frac{1}{2}(\hat{c}_{r,1} + i\hat{c}_{r,2})\right\}$ are "bond" Dirac modes.

It is assumed that $\hat{c}_{r,0}$ and $\hat{c}_{r,1}$ come from the same physical site, while $\hat{c}_{r,2}$ comes from a neighboring site; hence the noise is allowed to couple $\hat{c}_{r,0}$ and $\hat{c}_{r,1}$, but does not act on $\hat{c}_{r,2}$.

The noise model we shall consider is essentially the same one that we considered in §5.3.3: parity-preserving, local Markovian noise represented by Lindblad operators

$$\hat{L}_r = \sqrt{\gamma} i \hat{c}_{r,0} \hat{c}_{r,1}. \tag{5.78}$$

The action of the single-site Lindbladian $\mathcal{L}_r$ on a state $\hat{\rho}$ reads

$$\mathcal{L}_r(\hat{\rho}) = \gamma \left(i\hat{c}_{r,0}\hat{c}_{r,1} \hat{\rho} i\hat{c}_{r,0}\hat{c}_{r,1} - \hat{\rho} \right) = \gamma \left(\hat{c}_{r,0}\hat{c}_{r,1} \hat{\rho} \hat{c}_{r,1}\hat{c}_{r,0} - \hat{\rho} \right). \tag{5.79}$$

The total Lindbladian is $\mathcal{L} = \sum_{r=1}^{4} \mathcal{L}_r$.

Since the Lindbladians pertaining to different groups commute with one another, it suffices to focus on a single group.

5.4.2 Encoding in the ground space of a local Hamiltonian

Let us consider the usual encoding (5.28), with $\hat{c}_{r,0}$ in place of $\hat{m}_r$ and the following choice of encoding projector:

$$\hat{\rho}_{\text{enc}} = \prod_{r=1}^{4} \hat{b}_r \hat{b}_r^\dagger = \prod_{r=1}^{4} \frac{\hat{\mathbf{1}} - i\hat{c}_{r,1}\hat{c}_{r,2}}{2}. \tag{5.80}$$

$\hat{\rho}_{\text{enc}}$ corresponds to the ground-space projector of the following local Hamiltonian:

$$\hat{H} = \frac{\epsilon}{2} \sum_{r=1}^{4} i\hat{c}_{r,1}\hat{c}_{r,2} = \epsilon \sum_{r=1}^{4} \hat{b}_r^\dagger \hat{b}_r + \text{const.} \tag{5.81}$$

The encoding is represented in Figure 5.7.

We will now prove that:

1. The upper bound (2.12) is trivial, i.e. it reads $F_t^{\text{opt}} \leq 1 \; \forall t$.

2. The candidate recovery operation is CP, hence physical.

Therefore $F_t^{\text{opt}} = 1 \; \forall t$, which means that the information is perfectly recoverable at all times.

Upper bound on the recovery fidelity. The logical operators $\left\{\hat{\sigma}_\alpha^L\right\}$ in this encoding are sums of monomials of the form $\hat{c}_{r,0}^\alpha (i\hat{c}_{r,1}\hat{c}_{r,2})^\beta$. The action of (5.79) on such monomials is

$$\mathcal{L}_r \left[(\hat{c}_{r,0})^\alpha (i\hat{c}_{r,1}\hat{c}_{r,2})^\beta\right] = -2\gamma(1 - \delta_{\alpha\beta})(\hat{c}_{r,0})^\alpha (i\hat{c}_{r,1}\hat{c}_{r,2})^\beta. \tag{5.82}$$

The solution of the master equation for this class of monomials is therefore

$$\begin{cases} \mathcal{D}_t\left(\hat{\mathbf{1}}\right) = \hat{\mathbf{1}}, & \mathcal{D}_t\left(\hat{c}_{r,0}\right) = e^{-2\gamma t}\hat{c}_{r,0}, \\ \mathcal{D}_t\left(i\hat{c}_{r,1}\hat{c}_{r,2}\right) = e^{-2\gamma t}i\hat{c}_{r,1}\hat{c}_{r,2}, & \mathcal{D}_t\left(\hat{c}_{r,0}\,i\hat{c}_{r,1}\hat{c}_{r,2}\right) = \hat{c}_{r,0}\,i\hat{c}_{r,1}\hat{c}_{r,2}. \end{cases} \tag{5.83}$$
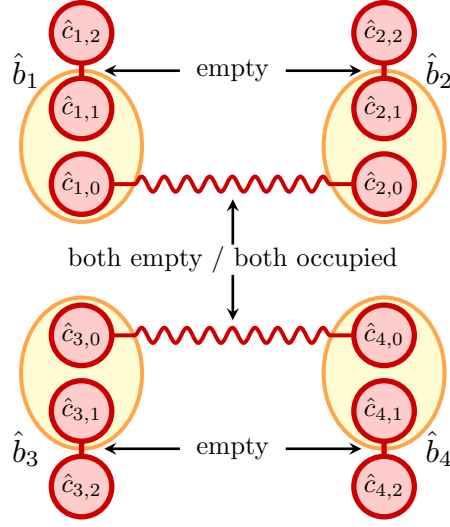
FIGURE 5.7: 12-mode model, encoding in the ground space of a local Hamiltonian. The ellipses represent the action of local, parity-preserving noise. Dirac modes corresponding to straight lines are always initialized empty. The qubit is encoded into the non-local Dirac modes corresponding to wavy lines.

As a consequence of (5.83), we have

$$
\begin{cases}
\mathcal{D}_t\left(\hat{b}_r\hat{b}_r^\dagger\right) = \dfrac{\hat{\mathbf{1}} - e^{-2\gamma t}i\hat{c}_{r,1}\hat{c}_{r,2}}{2}, \\[2ex]
\mathcal{D}_t\left(\hat{c}_{r,0}\hat{b}_r\hat{b}_r^\dagger\right) = \hat{c}_{1,0}\dfrac{e^{-2\gamma t}\hat{\mathbf{1}} - i\hat{c}_{r,1}\hat{c}_{r,2}}{2}.
\end{cases}
\tag{5.84}
$$

By applying (5.84) one can compute the time evolution of every encoded logical operator. In this case the three logical operators are all equivalent (i.e. related to one another by a suitable relabeling of the sites), thus in order to evaluate the upper bound (2.12) it suffices to time-evolve a single one of them, say $\hat{\sigma}_3^L$.

It can be shown that the trace norm of $\mathcal{D}_t\left(\hat{\sigma}_3^L\right)$ is $\left\|\mathcal{D}_t\left(\hat{\sigma}_3^L\right)\right\|_{\mathrm{tr}} = 2\ \forall t$. An easy way to prove this result is by taking the $t \to \infty$ limit: in this limit, (5.84) reads

$$
\mathcal{D}_\infty\left(\hat{b}_r\hat{b}_r^\dagger\right) = \frac{\hat{\mathbf{1}}}{2}, \qquad\qquad \mathcal{D}_\infty\left(\hat{c}_{1,0}\hat{b}_r\hat{b}_r^\dagger\right) = -\frac{i}{2}\hat{c}_{1,0}\hat{c}_{1,1}\hat{c}_{1,2}.
\tag{5.85}
$$

Thus, by applying the exact clustering property (F.17) (which holds because the Lindblad operators are Hermitian, hence normal), one gets

$$
\begin{aligned}
\mathcal{D}_\infty\left(\hat{\sigma}_3^L\right) &= -\frac{i}{2}\left[\mathcal{D}_\infty\left(\hat{c}_{1,0}\hat{b}_1\hat{b}_1^\dagger\,\hat{c}_{2,0}\hat{b}_2\hat{b}_2^\dagger\,\hat{b}_3\hat{b}_3^\dagger\,\hat{b}_4\hat{b}_4^\dagger\right) + \mathcal{D}_\infty\left(\hat{b}_1\hat{b}_1^\dagger\,\hat{b}_2\hat{b}_2^\dagger\,\hat{c}_{3,0}\hat{b}_3\hat{b}_3^\dagger\,\hat{c}_{4,0}\hat{b}_4\hat{b}_4^\dagger\right)\right] \\[2ex]
&= -\frac{1}{32}\left(i\hat{c}_{1,0}\hat{c}_{2,0}\,i\hat{c}_{1,1}\hat{c}_{1,2}\,\hat{c}_{2,1}\hat{c}_{2,2} + i\hat{c}_{3,0}\hat{c}_{4,0}\,i\hat{c}_{3,1}\hat{c}_{3,2}\,i\hat{c}_{4,1}\hat{c}_{4,2}\right).
\end{aligned}
\tag{5.86}
$$

By simultaneously diagonalizing the complete set of commuting observables $\{i\hat{c}_{1,0}\hat{c}_{2,0}, i\hat{c}_{3,0}\hat{c}_{4,0}\}$ $\cup\ \{i\hat{c}_{r,1}\hat{c}_{r,2} : r \in \{1,\ldots 4\}\}$, we get

$$\left\|\mathcal{D}_\infty(\hat{\sigma}_3^L)\right\|_{\mathrm{tr}} = \sum_{a,b,c=\pm 1}\sum_{d,e,f=\pm 1} \frac{1}{32}\left|abc+def\right| = 2. \tag{5.87}$$

Since $\left\|\mathcal{D}_t\left(\hat{\sigma}_3^L\right)\right\|_{\mathrm{tr}}$ is a monotonically decreasing function of time, (5.87) implies that

$$\left\|\mathcal{D}_t\left(\hat{\sigma}_3^L\right)\right\|_{\mathrm{tr}} = 2\ \forall\, t, \tag{5.88}$$

which is what we wanted to prove.

We thus obtain a trivial upper bound: $F_t^{\mathrm{opt}} \leq 1$. This does not yet imply perfect recoverability of the information, because the "candidate" recovery operation might not be physical (i.e. CP).

Perfect recoverability of the information. It is easy to verify that the expressions for $\mathcal{D}_\infty\left(\hat{\sigma}_2^L\right)$ and $\mathcal{D}_\infty\left(\hat{\sigma}_1^L\right)$ are identical to (5.86), up to swapping some pairs of site indices. Hence the $\left\{\mathcal{D}_\infty(\hat{\sigma}_\alpha^L)\right\}$ matrices obey the following "Pauli-like" algebra:

$$\mathcal{D}_\infty(\hat{\sigma}_\alpha^L)\mathcal{D}_\infty(\hat{\sigma}_\beta^L) = \frac{i}{16}\varepsilon_{\alpha\beta\gamma}\mathcal{D}_\infty(\hat{\sigma}_\gamma^L), \tag{5.89}$$

which means that the matrices $\{16\mathcal{D}_\infty(\hat{\sigma}_\alpha^L)\}$ obey the original Pauli algebra.

Another fact that is easily seen from (5.86) is that the spectrum of $\mathcal{D}_\infty(\hat{\sigma}_\alpha^L)$ consists of three distinct eigenvalues, $\left\{+\frac{1}{16}, 0, -\frac{1}{16}\right\}$; 0 is 32-fold degenerate, and corresponds to the annihilation of the odd-parity sector by the even-parity projector, while each $\pm\frac{1}{16}$ is 16-fold degenerate. Since all non-zero eigenvalues have equal absolute value (1/16), we have

$$\mathrm{sign}\left(\mathcal{D}_\infty(\hat{\sigma}_\alpha^L)\right) = 16\mathcal{D}_\infty(\hat{\sigma}_\alpha^L). \tag{5.90}$$

By the results of §2.3.2, the recovery induced by the $\left\{16\mathcal{D}_\infty(\hat{\sigma}_\alpha^L)\right\}$ is CP (hence physical) and saturates the upper bound. Since the bound in this case was proven to be trivial ($F_t^{\mathrm{opt}} \leq 1$ $\forall\, t$), we have $F_\infty^{\mathrm{opt}} = 1$; therefore the information is perfectly recoverable at $t = \infty$, and hence at all intermediate times.

5.4.3 Encoding in the ground space of a non-local Hamiltonian

We shall now consider the same system with a different encoding, defined by the projector

$$\hat{\rho}_{\mathrm{enc}} = \prod_{j=1,2} \frac{\hat{\mathbf{1}} - i\hat{c}_{1,j}\hat{c}_{2,j}}{2}\frac{\hat{\mathbf{1}} - i\hat{c}_{3,j}\hat{c}_{4,j}}{2}. \tag{5.91}$$
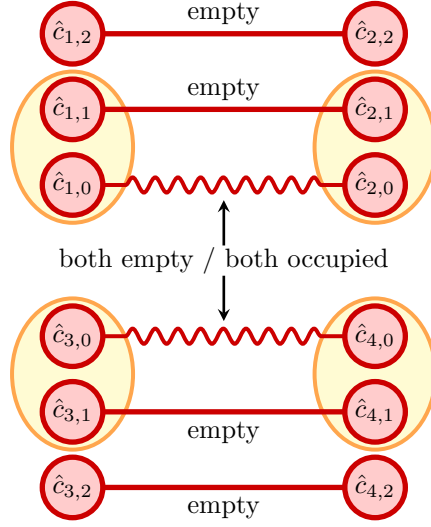
FIGURE 5.8: 12-mode model, encoding in the ground space of a non-local Hamiltonian. The ellipses represent the action of local, parity-preserving noise. Dirac modes corresponding to straight lines are always initialized empty. The qubit is encoded into the non-local Dirac modes corresponding to wavy lines.

This is the ground-space projector of a non-local Hamiltonian that couples site 1 with site 2 and site 3 with site 4 (Figure 5.8). It is therefore of limited physical interest by itself, but it is nonetheless a mathematically legitimate encoding that can be used to probe the effect of additional non-local correlations on the memory performance.

The non-local correlations in the encoding (5.91) make $\hat{\sigma}_3^L$ inequivalent to $\hat{\sigma}_1^L$ and $\hat{\sigma}_2^L$. It can be shown by the same methods used in the previous Section that

$$\left\| \mathcal{D}_t \left(\hat{\sigma}_1^L \right) \right\|_{\mathrm{tr}} = \left\| \mathcal{D}_t \left(\hat{\sigma}_2^L \right) \right\|_{\mathrm{tr}} = 2 e^{-4\gamma t}, \qquad\qquad \left\| \mathcal{D}_t \left(\hat{\sigma}_3^L \right) \right\|_{\mathrm{tr}} = 2. \qquad (5.92)$$

By plugging the results of (5.92) in the general upper bound on the recovery fidelity (2.12) one gets

$$F_t^{\mathrm{opt}} \leq \frac{1}{2} + \frac{1 + 2 e^{-4\gamma t}}{6} = \frac{2}{3} + \frac{1}{3} e^{-4\gamma t}. \qquad (5.93)$$

This is exactly the same result that was derived for the 8-mode model in (5.77). It is indeed clear that, with the encoding choice (5.91), we are merely juxtaposing the four Majorana modes $\{\hat{c}_{r,2} : r \in \{1, \ldots 4\}\}$ to the 8-mode model. Since the new Majorana modes are decoupled from the old ones and completely inert, the memory performance cannot change.

5.4.4 Dependence of the memory performance on the encoding state

In this Section we have seen that the same quantum memory model can display completely different behaviors depending on the choice of the encoding subspace:

- The encoding projector $\hat{\rho}_{\text{enc}}$ from (5.80), which projects onto the ground-space of a *local* Hamiltonian, allows perfect recovery of the encoded information at all times.

- The encoding projector $\hat{\rho}_{\text{enc}}$ from (5.91), which projects onto the ground-space of a *non-local* Hamiltonian, exposes the encoded qubit to a complete dephasing, thus degrading all quantum coherence over a time scale that depends only on the local noise parameter γ.

This result can be interpreted as an effect of long-range correlations. The relation between entanglement and non-locality [68] has been known since the dawn of quantum theory, with the EPR paradox [69]; it looks therefore reasonable to assume that the locality requirements for a Majorana-based quantum memory must address not only the dynamics, but also the encoding, i.e. the correlations that are initially present in the state of the quantum memory. Additional long-range correlations, beyond the minimal amount required by the encoding, seem to expose the encoded information to decoherence.

5.5 The Kitaev Chain as a Quantum Memory

In this Section we consider a system made of two Kitaev chains[13] as a quantum memory and evaluate its performance when it is exposed to a fermionic environment (§5.5.1) and a bosonic one (§5.5.2). In both cases a Markovian master equation is derived microscopically in the weak-coupling approximation described in Appendix D.

Notation. The notation for the fermionic modes of the chain shall be the following:

- $\{\hat{a}_r : r \in \{1, \dots L\}\}$ are the L "site" Dirac modes of the first chain.

- $\{\hat{a}_r : r \in \{L + 1, \dots 2L\}\}$ are the L "site" Dirac modes of the second chain.

- To each "site" Dirac mode $\hat{a}_r$ correspond the two Majorana modes $\hat{c}_{r,1}, \hat{c}_{r,2}$. $\hat{c}_{1,1}$ and $\hat{c}_{L,2}$ are the zero-energy edge modes of the first chain; $\hat{c}_{L+1,1}$ and $\hat{c}_{2L,2}$ are those of the second chain.

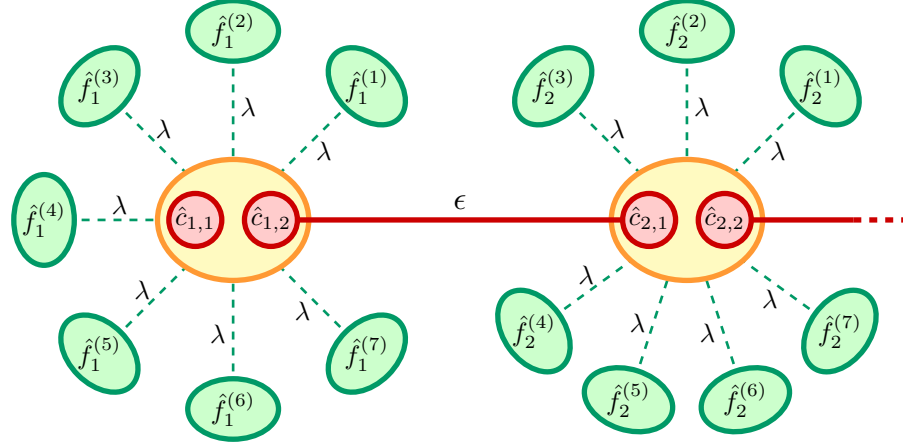[13]The Kitaev chain was introduced in §5.1.2.

FIGURE 5.9: schematic representation of the noise model considered in §5.5.1. Two sites of the Kitaev chain are showed (large ellipses); each environment is made of N Dirac modes (small ellipses; $N = 7$ in the figure). Solid lines represent the Kitaev Hamiltonian couplings; dashed lines represent tunneling interactions with the environment.

- $\left\{ \hat{b}_r : r \in \{1, \ldots L-1, L+1, \ldots 2L-1\} \right\}$ are the "bond" Dirac modes:

$$\hat{b}_r = \frac{\hat{c}_{r,2} + i\hat{c}_{r+1,1}}{2}. \tag{5.94}$$

The notation for the environment degrees of freedom will be specified separately for each noise model.

5.5.1 Fermionic environment

We shall first consider the two chains exchanging particles locally with a fermionic environment, within a Markovian approximation, and prove that the optimal recovery fidelity at time t is upper-bounded by $\frac{1}{2}\left(1 + e^{-4g^2 f(0)t}\right)$, where g is an effective coupling constant and $f(0)$ is the spectral density of gapless environment fermions. Provided the environment is not gapped, the information is entirely lost over a time scale dictated by the local properties of the environment and of the interactions; no scaling with the chain size is observed.

Noise model. Let us consider a fermionic environment interacting with the chains through a tunneling Hamiltonian. Each site of each chain interacts with a distinct set of N environment modes (see Figure 5.9). The notation for environment fermionic modes is the following:

- $\left\{ \hat{f}_r^{(n)} : r \in \{1, \ldots 2L\}, \, n \in \{1, \ldots N\} \right\}$ are the environment Dirac modes that interact with the site mode $\hat{a}_r$.

- To each Dirac mode $\hat{f}_r^{(n)}$ correspond the two Majorana modes $\hat{\gamma}_{r,1}^{(n)}, \hat{\gamma}_{r,2}^{(n)}$.

The two chains are assumed to be well separated, and thus fully decoupled. Let us start by considering a single chain: $r \in \{1, \ldots, L\}$. The Hamiltonian governing the extended system (chain and environment) is the sum of $\hat{H}_{\text{sys}}$, which is the Kitaev Hamiltonian (5.12); $\hat{H}_{\text{env}}$, acting on the environment; and $\hat{H}_{\text{int}}$, that describes tunneling processes between system and environment:

$$\begin{cases} \hat{H}_{\text{sys}} = \epsilon \sum_{r=1}^{L-1} \hat{b}_r^\dagger \hat{b}_r = \frac{\epsilon}{2} \sum_{r=1}^{L-1} i\hat{c}_{r,2}\hat{c}_{r+1,1} + \text{const.}, \\[2mm] \hat{H}_{\text{env}} = \sum_{r=1}^{L} \sum_{n=1}^{N} \omega_{r,n} \left(\hat{f}_r^{(n)}\right)^\dagger \hat{f}_r^{(n)} = \sum_{r=1}^{L} \sum_{n=1}^{N} \frac{\omega_{r,n}}{2} i\hat{\gamma}_{r,1}^{(n)}\hat{\gamma}_{r,2}^{(n)} + \text{const.}, \\[2mm] \hat{H}_{\text{int}} = -\lambda \sum_{r=1}^{L} \sum_{n=1}^{N}(\hat{a}_r^\dagger \hat{f}_r^{(n)} + h.c.) = \frac{\lambda}{2} \sum_{r=1}^{L} \sum_{n=1}^{N}(-i\hat{c}_{r,1}\hat{\gamma}_{r,2}^{(n)} + i\hat{c}_{r,2}\hat{\gamma}_{r,1}^{(n)}). \end{cases} \quad (5.95)$$

$\{\omega_{r,n}\}$ are the values of the energy gaps for environment fermions; we will assume that they are independently and identically distributed random variables with a probability density function $f(E)$. λ is a real parameter[14] representing a tunneling amplitude.

Derivation of the master equation. We will now derive a Markovian master equation for the Kitaev chain, following the approach presented in Appendix D.

The interaction Hamiltonian in (5.95) can be writeen, in the language of Appendix D, as

$$\hat{H}_{\text{int}} = \sum_{r=1}^{L} \sum_{s=1,2} \hat{A}_{r,s}\hat{B}_{r,s}: \qquad \hat{A}_{r,s} = \hat{c}_{r,s}, \qquad \hat{B}_{r,s} = \frac{\lambda}{2} \sum_{s'=1,2} (\sigma_2)_{ss'} \sum_{n=1}^{N} \hat{\gamma}_{r,s'}^{(n)}. \quad (5.96)$$

The interaction-picture environment operators are

$$\hat{B}_{r,s}(t) = \frac{\lambda}{2} \sum_{n=1}^{N} \sum_{s'=1}^{2} e^{i\hat{H}_{\text{int}}t}(\sigma_2)_{ss'}\hat{\gamma}_{r,s'}^{(n)}e^{-i\hat{H}_{\text{int}}t} = \frac{\lambda}{2} \sum_{n=1}^{N} \sum_{s'=1}^{2} e^{i\omega_{r,n}t\, i\hat{\gamma}_{r,1}^{(n)}\hat{\gamma}_{r,2}^{(n)}}(\sigma_2)_{ss'}\hat{\gamma}_{r,s'}^{(n)}$$

$$= \frac{\lambda}{2} \sum_{n=1}^{N} \sum_{s'=1}^{2} (\sigma_2)_{ss'} \left(\cos(\omega_{r,n}t) + i\sin(\omega_{r,n}t)i\hat{\gamma}_{r,1}^{(n)}\hat{\gamma}_{r,2}^{(n)}\right) \hat{\gamma}_{r,s'}^{(n)}. \quad (5.97)$$

Noting that $i\hat{\gamma}_{r,1}^{(n)}\hat{\gamma}_{r,2}^{(n)}\hat{\gamma}_{r,s'}^{(n)} = \sum_{s''=1}^{2} (\sigma_2)_{s's''}\gamma_{r,s''}^{(n)}$, we can rewrite (5.97) as

$$\hat{B}_{r,s}(t) = \frac{\lambda}{2} \sum_{n=1}^{N} \sum_{s''=1}^{2} (\cos(\omega_{r,n}t)(\sigma_2)_{s,s''} + i\sin(\omega_{r,n}t)\delta_{s,s''}) \hat{\gamma}_{r,s''}^{(n)}. \quad (5.98)$$

---

[14] Any complex phase in λ can be "gauged" away by redefining the $\hat{f}$ operators.

The correlation function defined in (D.11) is

$$
\begin{aligned}
K_{r,s;r',s'}(t) &= \frac{\mathrm{Tr}_{\mathrm{env}}\left(\hat{B}_{r,s}(t)\hat{B}_{r',s'}(0)\right)}{\mathrm{Tr}_{\mathrm{env}}\left(\hat{\mathbf{1}}_{\mathrm{env}}\right)} \\
&= \frac{\lambda^2}{4}\sum_{n,n'=1}^{N}\sum_{j,j'=1}^{2}\left(\cos(\omega_{r,n}t)(\sigma_2)_{s,j} + i\sin(\omega_{r,n}t)\delta_{s,j}\right)(\sigma_2)_{s',j'}\frac{\mathrm{Tr}_{\mathrm{env}}\left(\hat{\gamma}_{r,j}^{(n)}\hat{\gamma}_{r',j'}^{(n')}\right)}{\mathrm{Tr}_{\mathrm{env}}\left(\hat{\mathbf{1}}_{\mathrm{env}}\right)} \\
&= \frac{\lambda^2}{4}\delta_{r,r'}\sum_{n=1}^{N}\left(\cos(\omega_{r,n}t)(\sigma_2\sigma_2^T)_{ss'} + i\sin(\omega_{r,n}t)(\sigma_2^T)_{ss'}\right).
\end{aligned}
\tag{5.99}
$$

Since $\sigma_2^T = -\sigma_2$ and $(\sigma_2)^2 = \sigma_0$, this simplifies to

$$
K_{r,s;r',s'}(t) = -\frac{\lambda^2}{4}\delta_{r,r'}\sum_{n=1}^{N}\left(e^{i\omega_{r,n}t\,\sigma_2}\right)_{ss'}.
\tag{5.100}
$$

Averaging over the bath gap spectrum yields

$$
\langle K_{r,s;r',s'}(t)\rangle = -\frac{N\lambda^2}{4}\delta_{rr'}\int dE f(E)\left(e^{iEt\,\sigma_2}\right)_{ss'}.
\tag{5.101}
$$

This is easily diagonalized – the eigenvectors are $\frac{1}{\sqrt{2}}(A_{r,1}\pm iA_{r,2})$ and the corresponding eigenvalues are $-\frac{N\lambda^2}{4}e^{\pm iEt}$. Finally, the Fourier transformation of (5.101) is

$$
\begin{aligned}
\langle\gamma_{r,r'}^{\pm}(\omega)\rangle &= \int_{-\infty}^{\infty}d\tau\langle K_{rr'}^{\pm}(\tau)\rangle e^{i\omega\tau} = -\frac{N\lambda^2}{4}\delta_{rr'}\int_{-\infty}^{\infty}d\tau\int dE f(E)e^{\pm iE\tau} \\
&= -\frac{N\lambda^2}{4}\delta_{rr'}\int dE f(E)2\pi\delta(\omega\pm E) = -\frac{\pi N\lambda^2}{2}\delta_{rr'}f\left(\mp\omega\right).
\end{aligned}
\tag{5.102}
$$

The Lindblad operators are obtained by taking the weak coupling limit ($N\to\infty$, $\lambda\to 0$) while keeping $\pi N\lambda^2/2 = g^2$ constant. They are

$$
\left\{\sqrt{2g^2 f(-\omega)}\hat{a}_r(\omega),\ \sqrt{2g^2 f(\omega)}\hat{a}_r^\dagger(\omega) : r\in\{1,\dots L\}\right\}.
\tag{5.103}
$$

In general $f(E)$ has a cut-off energy Ω above which it drops exponentially: $f(E)|_{E\gg\Omega}\lesssim e^{-E/\Omega}$. Thus the only Lindblad operators that matter in the $\epsilon\gg\Omega$ limit are

$$
\left\{\sqrt{2g^2 f(0)}\hat{a}_r(0),\ \sqrt{2g^2 f(0)}\hat{a}_r^\dagger(0) : r\in\{1,\dots,L\}\right\}.
\tag{5.104}
$$

Now, it is clear that the $\omega = 0$ part of a "bulk" mode $\hat{a}_r^{(\dagger)}(0)$ is zero. For an edge mode like $\hat{a}_1$ one has instead a non-zero static component:

$$e^{it\hat{H}_{\text{sys}}}\hat{a}_1 e^{-it\hat{H}_{\text{sys}}} = e^{i\frac{\epsilon}{2}t\hat{c}_{1,2}\hat{c}_{2,1}}\frac{\hat{c}_{1,1} + i\hat{c}_{1,2}}{2}e^{-i\frac{\epsilon}{2}t\hat{c}_{1,2}\hat{c}_{2,1}} = \frac{\hat{c}_{1,1}}{2} + ie^{i\epsilon t\hat{c}_{1,2}\hat{c}_{2,1}}\frac{\hat{c}_{1,2}}{2}$$

$$= \frac{\hat{c}_{1,1}}{2} + i\cos(\epsilon t)\frac{\hat{c}_{1,2}}{2} - \sin(\epsilon t)\frac{\hat{c}_{2,1}}{2}. \tag{5.105}$$

Therefore $\hat{a}_1(0) = \frac{1}{2}\hat{c}_{1,1}$. Analogously, for the other edge, $\hat{a}_L(0) = \frac{i}{2}\hat{c}_{L,2}$.

In the $\epsilon \to \infty$ limit, therefore, the only non-vanishing Lindblad operators are[15] $\sqrt{g^2 f(0)}\hat{c}_{1,1}$ and $\sqrt{g^2 f(0)}\hat{c}_{L,2}$

As for the Lamb-shift Hamiltonian, the only term that does not get suppressed by a large gap is

$$\langle S_{r,s;r',s'}(0)\rangle = \frac{1}{2i}\int_{-\infty}^{+\infty} dt\,\text{sign}\,(t)\,\langle K_{r,r';s,s'}(t)\rangle$$

$$= -\frac{N\lambda^2}{8i}\delta_{rr'}\int_{-\infty}^{+\infty}dt\int_{-\infty}^{+\infty}dE f(E)\text{sign}\,(t)\left(e^{iEt\,\sigma_2}\right)_{ss'}. \tag{5.106}$$

Diagonalizing it in the same way as $\gamma_{r,s;r',s'}$ was diagonalized, one gets

$$\left\langle S_{r,r'}^{\pm}(0)\right\rangle = -\frac{N\lambda^2}{8i}\delta_{rr'}\int_{-\infty}^{+\infty}dE f(E)\int_{-\infty}^{+\infty}dt\,\text{sign}\,(t)\,e^{\pm iEt}$$

$$= \pm\frac{N\lambda^2}{4}\delta_{rr'}\fint_{-\infty}^{+\infty}dE\frac{f(E)}{E}, \tag{5.107}$$

where $\fint$ denotes the Cauchy principal part of the integral. While the coefficient itself may be ill-defined[16] (depending on the behavior of f), the resulting Lamb-shift Hamiltonian vanishes:

$$\lim_{\epsilon\to\infty}\hat{H}_{LS} = \sum_{r,r'=1}^{L}\sum_{\sigma=\pm}\left\langle S_{r,r'}^{\sigma}(0)\right\rangle\hat{A}_{r'}^{\sigma}(0)\hat{A}_r^{\sigma}(0)$$

$$= \sum_{r=1}^{L}\left\langle S_{r,r}^{+}(0)\right\rangle\left(\left(\hat{A}_r^{+}(0)\right)^2 - \left(\hat{A}_r^{-}(0)\right)^2\right), \tag{5.108}$$

where the second equality comes from the fact that $\left\langle S_{r,r}^{-}(0)\right\rangle = -\left\langle S_{r,r}^{+}(0)\right\rangle$, which is clear from (5.107). Then, since $\hat{A}_r^{+} = \sqrt{2}\hat{a}_r$, one has $\hat{A}_r^{+}(0) = \sqrt{2}\hat{a}_r(0)$, which is either zero or a Majorana edge mode (squaring to $\hat{\mathbf{1}}$). Analogous considerations apply to $\hat{A}_r^{-}(0)$. Therefore the term in brackets in (5.108) vanishes, and so does $\lim_{\epsilon\to\infty}\hat{H}_{LS}$.

---

[15] A factor of $\sqrt{2}$ comes from the fact that each Lindblad operator appears twice, because $\hat{a}_1(0) = \hat{a}_1^{\dagger}(0)$ and $\hat{a}_L(0) = -\hat{a}_1(0)$. The minus sign is irrelevant as the Lindbladian is quadratic in the Lindblad operators.

[16] The weak-coupling limit, which involves $N \to \infty$ and thus makes $f(E)$ a *continuous* spectrum, instead of a sum of δ functions, should be taken *after* all the calculations are done to avoid this type of problems. If one regards $f(E)$ as a sum of δ functions, then (5.107) is well defined, and $\hat{H}_{LS}$ vanishes for all finite values of N.

Memory performance. The resulting master equation for the two-chain system in the large-gap limit is

$$\frac{d}{dt}\hat{\rho}(t) = -i\left[\hat{H}_{\text{sys}}, \hat{\rho}\right] + \sum_{(r,j)\in\{\text{edges}\}} g^2 f(0)\big(\hat{c}_{r,j}\hat{\rho}\hat{c}_{r,j} - \hat{\rho}\big). \tag{5.109}$$

Assuming a ground-space encoding, and therefore neglecting the Hamiltonian part of the dynamics, the action of the Lindbladian $\mathcal{L}$ on a given monimial $\hat{\mu}$ is $\mathcal{L}\left(\hat{\mu}\right) = -2\nu g^2 f(0)\hat{\mu}$, where ν is the number of Majorana edge-modes involved by $\hat{\mu}$. Since the logical operators $\left\{\hat{\sigma}_\alpha^L\right\}$ are sums of monomials with $\nu = 2$, they are globally damped by a factor of $e^{-4g^2 f(0)t}$, and the upper bound on the recovery fidelity (2.12) is

$$F_t^{\text{opt}} = \frac{1}{2} + \frac{1}{2}e^{-4g^2 f(0)t}. \tag{5.110}$$

The storage time for the encoded information therefore does not scale with the chain length L. No topological protection of quantum information is observed.

Remark. If the environment has no zero-modes, i.e. if $f(0) = 0$, then there is no dissipation at all in the large gap limit, and the storage time diverges.

5.5.2 Bosonic environment

We shall now turn to a Markovian bosonic environment, consisting of spins, and prove a positive result about the memory performance of the pair of Kitaev chains. In the limit of large gap in the chain Hamiltonian, all harmful perturbations are suppressed; those that remain are innocuous on the ground-space encoding. Therefore the encoded qubit survives indefinitely.

Noise model. The setting is the same as the one considered in the fermionic case (§5.5.1), except for the fact that each mode of the chain $\hat{a}_r$ interacts with spins, instead of fermions. Each site mode has a distinct environment made of N spins, $\{\boldsymbol{\sigma}_{r,n} : n \in \{1, \dots, N\}\}$, where $\boldsymbol{\sigma}_{r,n} = (X_{r,n}, Y_{r,n}, Z_{r,n})$ are the Pauli operators for the nth spin of the rth environment.

The Hamiltonian governing the extended system (Kitaev chain and spin environment) is the sum of $\hat{H}_{\text{sys}}$, which is the Kitaev Hamiltonian (5.12); $\hat{H}_{\text{env}}$, acting on the spins; and $\hat{H}_{\text{int}}$,

coupling the chain to the spins.

$$
\begin{cases}
\hat{H}_{\text{sys}}\epsilon \sum_{r=1}^{L-1} \hat{b}_r^\dagger \hat{b}_r = \dfrac{\epsilon}{2} \sum_{r=1}^{L-1} i\hat{c}_{r,2}\hat{c}_{r+1,1} + \text{const.} \\[2ex]
\hat{H}_{\text{env}} = \sum_{r=1}^{L} \sum_{n=1}^{N} \dfrac{\omega_{r,n}}{2} Z_{r,n}, \\[2ex]
\hat{H}_{\text{int}} = -\lambda \sum_{r=1}^{L} \sum_{n=1}^{N} \hat{a}_r^\dagger \hat{a}_r X_{r,n} = -\lambda \sum_{r=1}^{L} \sum_{n=1}^{N} i\hat{c}_{r,1}\hat{c}_{r,2} X_{r,n} + \text{const.}
\end{cases}
\tag{5.111}
$$

$\{\omega_{r,n}\}$ are the values of the energy gaps of the environment spins. We will assume that they are independently and identically distributed random variables with a probability density function $f(E)$.

Derivation of the master equation. We shall briefly show how to compute the functions that are needed in order to perform the derivation in Appendix D.

The decomposition of $\hat{H}_{\text{int}}$ is as follows:

$$
\hat{H}_{\text{int}} = \sum_{r=1}^{L} \hat{A}_r \hat{B}_r, \qquad \hat{A}_r = i\hat{c}_{r,1}\hat{c}_{r,2}, \qquad \hat{B}_r = -\lambda \sum_{n=1}^{N} X_{r,n}
\tag{5.112}
$$

The interaction-picture $\hat{B}_r(t)$ operators are

$$
\hat{B}_r(t) = -\lambda e^{it\hat{H}_{\text{env}}} \sum_{n=1}^{N} X_{r,n} e^{-it\hat{H}_{\text{env}}} = -\lambda \sum_{n=1}^{N} e^{i\omega_{r,n} t\, Z_{r,n}} X_{r,n}
$$

$$
= -\lambda \sum_{n=1}^{N} \left(\cos(\omega_{r,n}t) X_{r,n} - \sin(\omega_{r,n}t) Y_{r,n} \right).
\tag{5.113}
$$

The correlation function defined in (D.11) is

$$
K_{r,r'}(t) = \frac{\text{Tr}_{\text{env}} \left(\hat{B}_r(t)\hat{B}_{r'}(0) \right)}{\text{Tr}_{\text{env}} \left(I_{\text{env}} \right)} = \lambda^2 \sum_{n,n'=1}^{N} \frac{\text{Tr}_{\text{env}} \left(\left(\cos(\omega_{r,n}t)X_{r,n} - \sin(\omega_{r,n}t)Y_{r,n} \right) X_{r',n'} \right)}{\text{Tr}_{\text{env}} \left(I_{\text{env}} \right)}
$$

$$
= \lambda^2 \delta_{r,r'} \sum_{n=1}^{N} \cos(\omega_{r,n}t).
\tag{5.114}
$$

Averaging over the bath gap spectrum yields

$$
\langle K_{rr'}(t) \rangle = N\lambda^2 \delta_{r,r'} \int dE f(E) \cos(Et),
\tag{5.115}
$$

whose Fourier transform is

$$\langle \gamma_{rr'}(\omega) \rangle = \int_{-\infty}^{\infty} d\tau \langle K_{rr'}(\tau) \rangle e^{i\omega\tau} = N\lambda^2 \delta_{r,r'} \int_{-\infty}^{\infty} d\tau \int dE f(E) \cos(E\tau)$$

$$= \pi N\lambda^2 \delta_{rr'} \int dE f(E) \left(\delta(\omega + E) + \delta(\omega - E) \right)$$

$$= \pi N\lambda^2 \delta_{r,r'} \left(f(\omega) + f(-\omega) \right) \tag{5.116}$$

By taking the $N \to \infty$ and $\lambda \to 0$ limits, with $\pi N\lambda^2 = g^2$ kept constant (weak-coupling limit), we finally obtain the set of Lindblad operators:

$$\left\{ \sqrt{g^2(f(\omega) + f(-\omega))} \hat{A}_r(\omega) : r \in \{1, \ldots, L\} \right\} \tag{5.117}$$

The only Lindblad operators that are not suppressed in the $\epsilon \to \infty$ limit are

$$\left\{ g\sqrt{2f(0)}(i\hat{c}_{r,1}\hat{c}_{r,2})(0) : r \in \{1, \ldots, L\} \right\}. \tag{5.118}$$

The Fourier components of $i\hat{c}_{r,1}\hat{c}_{r,2}$ can be determined by computing its time evolution under $\hat{H}_{\text{sys}}$. If site r lies in the "bulk" of the chain, i.e. $r \in \{2, \ldots L-1\}$, then, letting $\hat{n}_r^{(b)} = \hat{b}_r^\dagger \hat{b}_r$ be the number operator for the rth bond mode, we have

$$e^{it\hat{H}_{\text{sys}}} i\hat{c}_{r,1}\hat{c}_{r,2} e^{-it\hat{H}_{\text{sys}}} = i\hat{c}_{r,1}\hat{c}_{r,2} e^{-i\,2t\epsilon\,(\hat{n}_{r-1}^{(b)} + \hat{n}_r^{(b)} - \hat{1})}$$

$$= i\hat{c}_{r,1}\hat{c}_{r,2} \left[e^{-i\,2\epsilon t} \hat{n}_{r-1}^{(b)} \hat{n}_r^{(b)} + e^{i\,2\epsilon t} \left(\hat{1} - \hat{n}_{r-1}^{(b)} \right) \left(\hat{1} - \hat{n}_r^{(b)} \right) \right.$$

$$\left. + \left(\hat{1} - \hat{n}_{r-1}^{(b)} \right) \hat{n}_r^{(b)} + \hat{n}_{r-1}^{(b)} \left(\hat{1} - \hat{n}_r^{(b)} \right) \right]. \tag{5.119}$$

There are two oscillating components at $\omega = \pm 2\epsilon$ and a static component:

$$(i\hat{c}_{r,1}\hat{c}_{r,2})(0) = i\hat{c}_{r,1}\hat{c}_{r,2} \left[\left(\hat{1} - \hat{n}_{r-1}^{(b)} \right) \hat{n}_r^{(b)} + \hat{n}_{r-1}^{(b)} \left(\hat{1} - \hat{n}_r^{(b)} \right) \right]$$

$$= \frac{i}{2} \hat{c}_{r,1}\hat{c}_{r,2} - \frac{i}{2} \hat{c}_{r-1,2}\hat{c}_{r+1,1}. \tag{5.120}$$

If site r is an edge of the chain, e.g. $r = 1$, then

$$e^{it\hat{H}_{\text{sys}}} i\hat{c}_{1,1}\hat{c}_{1,2} e^{-it\hat{H}_{\text{sys}}} = i\hat{c}_{1,1}\hat{c}_{1,2} e^{-i\,t\epsilon\,i\hat{c}_{1,2}\hat{c}_{2,1}} = \cos(\epsilon t) i\hat{c}_{1,1}\hat{c}_{1,2} + \sin(\epsilon t) i\hat{c}_{1,1}\hat{c}_{2,1}$$

$$= i\hat{c}_{1,1} \left(e^{i\epsilon t} \hat{b}_1^\dagger + e^{-i\epsilon t} \hat{b}_1 \right) \tag{5.121}$$

There are only $\omega = \pm \epsilon$ oscillating components, therefore $(i\hat{c}_{1,1}\hat{c}_{1,2})(0) = 0$. The same conclusion applies to $r = L$.

The only Lindblad operators that are not suppressed in the $\epsilon \to \infty$ limit are therefore

$$\left\{ \sqrt{\frac{g^2 f(0)}{2}} (i\hat{c}_{r,1}\hat{c}_{r,2})(0) : r \in \{2, \dots L-1\} \right\} \tag{5.122}$$

As for the Lamb-shift Hamiltonian, it can be shown by same method applied to the fermionic case that it vanishes in the large-gap limit.

Memory performance. Lindblad operators (5.122) are innocuous on a ground-space encoding. As can be seen from the first form of (5.120), $(i\hat{c}_{r,1}\hat{c}_{r,2})(0)$ acts non-trivially only on states with *exactly one* excitation in the bond modes $\left\{ \hat{b}_{r-1}, \hat{b}_r \right\}$. On such states, it moves the excitation from one bond to the other. All other states, including in particular those in the ground space, are annihilated.

The ground-space encoding is therefore stabilized by both the Hamiltonian $\hat{H}_{\text{sys}}$ and the Lindblad operators (5.122); thus in the $\epsilon \to \infty$ limit the dynamics is trivial and information is stored indefinitely.

For finite values of ϵ much larger than the cut-off energy of the bath gap spectrum Ω, the main source of decoherence is represented by edge operators (5.121), whose Fourier frequencies are $\omega = \pm\epsilon$. The $\omega = \pm 2\epsilon$ parts of "bulk" operators are a higher-order correction:

$$f(2\epsilon) \sim e^{-2\epsilon/\Omega} \sim (f(\epsilon))^2 \quad \text{if} \quad \epsilon \gg \Omega. \tag{5.123}$$

A qualitative understanding of the decoherence process can be gained in terms of bond excitations. The operators (5.121) create excitations in the bond modes near the edges by exchanging an energy ϵ with the environment (which makes the process unlikely if ϵ is large); then, operators (5.120) can propagate the excitations without further energy exchanges. The $\omega = \pm 2\epsilon$ components of (5.119), on the other hand, can create pairs of excitations in two adjacent bonds in the bulk of the chain. This requires exchanging an energy of 2ϵ with the environment. Thus the creation of bulk excitations is much less likely than the creation of edge excitations.

5.6 Conclusions

The models analyzed in Sections 5.3, 5.4 and 5.5 can be used to test the validity of some conjectures about Majorana-based quantum memories. The results are summarized in Table 5.2.

It is widely believed that information stored non-locally into distant Majorana zero-modes should be protected against local perturbations. While this is true for closed systems under

	Lindblad operators	
	fermionic	bosonic
8 modes	✗	✗
12 modes	✗	✗/✓
Kitaev chain	✗	✓

TABLE 5.2: summary of the results obtained in §5.3, 5.4 and 5.5 about the performances of different Majorana memory toy-models. ✗ denotes a failure of protection, i.e. no advantage over a local enconding; ✓ denotes perfect recoverability of the information; "✗/✓" means that both behaviors are displayed under different choices of encoding subspace.

Hamiltonian perturbations, the models we analyzed show that this strategy is not always effective in open-system scenarios.

Particle exchanges with the environment, represented by "fermionic" Lindblad operators, are generally able to couple directly to the Majorana zero-modes. Even though no coherent action on the different zero-modes is allowed, in all the toy-models we examined we found that this coupling degrades the encoded information over a time-scale determined by the local details of the system-environment interaction. Thus, even in the thermodynamic limit (arbitrarily separated sites in the 8-mode and 12-mode models, or infinitely long Kitaev chains), the use of de-localized fermionic modes yields no benefit over a simple local encoding.

Even when single-particle exchanges are forbidden, the memory performance is not guaranteed to be satisfactory. The 12-mode model is the most interesting one in this respect, as it shows completely different results depending on the chosen encoding subspace. The ground space of a *non-local* Hamiltonian was shown to provide no protection, while the ground space of a *local* Hamiltonian allowed perfect recoverability of information at all times.

We did not find any models such that, choosing $\hat{\rho}_{\text{enc}}$ as the ground-space projector of a local Hamiltonian and assuming a parity-preserving Markovian noise, the encoded qubit would not be protected. This suggests that not only the locality of *interactions* should be stressed, but also that of *correlations* in the initial state. Additional long-range correlations beyond those strictly required seem to spoil the memory performance.

Finally, parity preservation does not guarantee a satisfactory memory performance, but it definitely appears to be a necessary condition. This, if proven in a general and rigorous way, would pose a fundamental limitation on the domain of applicability of Majorana-based quantum memories – the protection would work only against a particular class of noise models. It is however argued in [66] that at low temperatures, in a superconducting device, the main source of decoherence would be represented by Cooper pair tunneling, with only a small fraction of individual electrons in the environment. This would provide an important class of systems for which Majorana-based protection might be effective in the open-system scenario.

Chapter 6

Conclusion and Outlook

6.1 The Importance of Recovery Operations

Several works in the existing literature on quantum memories discuss the problem of keeping quantum states fixed, and evaluate the performance of quantum memory models accordingly, i.e. by simply comparing the initial and final states of the quantum memory. That approach, though physically motivated, is not completely satisfactory, because it leaves room for false-negative results: information may still be present in the large state space of the quantum memory, though not in the sub-manifold in which it was originally encoded.

The use of non-trivial recovery operations avoids such false-negative results: the optimal recovery fidelity is by construction a *bona fide* measure of the amount of information present in the memory. In this thesis we discuss a specific instance (§5.4.2) in which a discussion based on the optimal recovery fidelity proves necessary: the fidelity between the initially encoded states and the time-evolved ones drops to a very small value after a short time – which could be naively interpreted as a bad memory performance; however, all the information can be exactly recovered at all times via a non-trivial operation.

It is therefore crucial to include the optimization over physical recovery operations in the study of quantum memory models. While it would be desirable to find quantum systems that are capable of "freezing" a qubit, so that no recovery operation is required for their correct operation, it should be emphasized that this class of systems does not encompass the whole domain of functional quantum memories. It is entirely possible, on the contrary, that such systems form a very rare subclass. It would thus be unreasonable to dismiss all other functional quantum memory models by ignoring non-trivial recovery operation.

One interesting direction for future work on quantum recovery operations is the restriction to particular classes of "simple" operations, i.e. time evolutions that can be obtained with

physically inexpensive resources, such as nearest-neighbor interactions. The optimal recovery fidelity is a good measure of the amount of information that is present in the system, but it may be impractical (or technically impossible) to actually retrieve all the information. Therefore in some cases a discussion based on e.g. the optimal *gaussian* recovery fidelity [20] may have more practical relevance than one based on the optimal recovery fidelity itself.

6.2 Dissipation as a Resource for Quantum Memories

In Chapter 3 we discussed continuous-time quantum error correction as a strategy to preserve qubit states over long periods of time. One remarkable aspect of this strategy is that it employs dissipation as a resource: more specifically, it uses suitably engineered forms of dissipation in order to oppose other types of dissipation that would otherwise degrade the encoded information.

In recent years dissipation has been proven to be a powerful resource for quantum information applications, including state engineering and computation [10]. Quantum error correction and quantum memories are no exception [13, 15]. The discussion of Appendix C, based on [13], proves that the physical resources needed to engineer an arbitrary form of Markovian dissipation are rather inexpensive: a small number of ancillary qubits, simple cooling processes[1] and Hamiltonian interactions. These resources are considered less expensive than the fast, reliable unitary operations that are required by many quantum information protocols, including standard, discrete-time quantum error correction.

In this thesis we studied simple instances of "dissipative quantum memories" based on quantum error-correcting codes: the recovery operation defined by the error correction procedure is implemented continuously in time by means of dissipation; the two dissipative processes (the one modeling noise and the one modeling error correction) work against each other, and the resulting balance depends on how strong is the error-correcting dissipation with respect to the noise. In the strong error-correction regime, the storage time for the encoded qubit scales approximately linearly with the error correction strength. Thus, at least in principle, we can store a qubit with a fidelity threshold of, say, 99.9% for as long as we like, by simply tuning the strength of the error-correcting dissipation to the required value. In every real implementation, however, there will be a technical limitation to the strength that can be attained, which poses a fundamental limitation to this type of schemes[2].

We studied the dissipative implementation of the 3-qubit bit-flip code and the 5-qubit perfect code. The former had already been studied in [14], while the results about the latter are entirely original. For the 3-qubit code, we considered a bit-flip noise; we derived an analytical expression for the average recovery fidelity in the case of trivial read-out, and proved

---

[1]Technically, single-qubit *amplitude damping channels*.
[2]This limitation should however be weaker than the corresponding one for discrete-time quantum error correction.

that in the strong error correction regime that fidelity is nearly optimal (i.e. continuous-time quantum error correction causes an effective "freezing" of the encoded states, and no further recovery operation is needed at read-out). For the 5-qubit code, we considered a depolarizing noise and followed a numerical approach based on the Trotter expansion. We found results that are remarkably similar to those derived (analytically) for the 3-qubit code. This represents a proof of principle that the depolarizing noise, generally considered the most aggressive type of quantum noise, can be effectively fought with dissipation-based strategies.

The results we presented about the 5-qubit code can be straightforwardly generalized to any stabilizer code. However, increasing the number of qubits makes numerical computations more difficult, since the dimension of the state space scales exponentially; thus there is a technical limit to the size of quantum codes that can be studied in this way. Moreover, the Hamiltonians that must be implemented in order to simulate the action of the error-correcting dissipators are highly non-local. Thus, while we may reasonably expect future implementations of continuous-time quantum error correction on three or five qubits, the dissipative versions of larger codes are less likely to ever become experimentally testable.

This problem might however be partially overcome. *Operator* (or *subsystem*) quantum error correction [70] can reduce the weight of stabilizers by introducing convenient "gauge qubits" into the code. A continuous-time implementation of operator quantum error correction may therefore yield to experimentally viable dissipation-based memories with a larger number of qubits. Increasing the size of the code would yield several benefits, such as the encoding of two or more logical qubits, or the ability to detect and correct d-qubit errors, for some $d > 1$. Thus, continuous-time operator quantum error correction may be a way to overcome some limits of the analysis presented in Chapter 3.

Finally, all schemes based on a single, global recovery operation $\mathcal{R}$ are subject to an important limitation that was pointed out by Pastawski *et al.* [13]. By considering a *"stochastic unraveling"* of the master equation $\dot{\rho} = \gamma(\mathcal{R}(\rho) - \rho)$, one sees that on average a time interval $\Delta t \sim \gamma^{-1}$ must elapse before the first recovery step occurs; in this time interval, an n-qubit code undergoes on average $n\kappa\Delta t \sim n\frac{\kappa}{\gamma}$ errors. If this number is too large, the first occurrence of the recovery operation fails and so does the quantum memory. Thus, in order to protect the encoded information, one needs to set $\frac{\gamma}{\kappa} \gg n$, i.e. larger codes require stronger error-correcting noise to work properly. This is a fundamental limitation to the scalability of the approach.

Because of this general limitation, the existence of *scalable* quantum memories based on dissipation is a non-trivial open problem. Pastawski *et al.* [13] gave numerical evidence for the existence of a non-zero error threshold for a local, scalable, dissipative quantum memory based on the 4-dimensional toric code, and similar results have been proven very recently for a 2-dimensional toric code controlled by a classical cellular automaton [71]. This type of schemes looks therefore very promising.

6.3 Passive Protection of Information through Majorana Zero-Modes

Because of their remarkable physical properties, including non-Abelian anyonic statistics, Majorana "fermions"[3] have gained great popularity in the condensed matter community in recent years. Their non-local nature led many theorists to believe that they could be used to protect quantum information from local perturbations. This belief, though never proven in the open-system scenario, has enjoyed widespread acceptance, especially in the experimental literature. In this thesis we tested the extent to which the assumption is correct in some simple, analytically solvable models, relating the results to the concepts of *locality* and *parity*.

The first conclusion that emerges from such models is that the *preservation of number-parity* seems to be a necessary condition. This means that the tunneling of single fermions (or the coherent tunneling of any odd number of them) between the system and the environment must be forbidden:

- Noise models that involve single-particle tunneling are allowed to couple directly to the zero-modes alone. This causes the memory to fail in constant time, without any benefit from the non-local encoding. Moreover, the very absence of a gap makes the zero-modes particularly vulnerable.

- Parity-preserving noise, on the other hand, cannot involve a zero-mode alone (as that would not preserve number parity). This leaves room for the protection of information, but does not ensure it. Different memory performances are shown to be possible under this class of noise models.

The second conclusion is that *locality* is a fundamental requirement not only for the dynamics, which was to be expected, but also for the initial state of the quantum memory. Indeed, there are in general many ways to encode a qubit state in a Majorana-based memory, which can be though of as ground spaces of different Hamiltonians (sharing the same zero-modes, but generally differing on the non-zero energy sector). We showed an example in which a Majorana-based memory exposed to a parity-preserving local noise succeeds or fails at protecting the information depending on whether the encoding space is defined by a *local* or *non-local* Hamiltonian (§5.4). This effect can be interpreted in terms of additional long-range entanglement spoiling the local nature of the noise: no long-range correlations beyond those strictly required by the encoding should be present in the initial state of the memory. The role of the encoding subspace in the context of Majorana-based memories has never been investigated so far, and it would be interesting to study other more realistic models and test the validity of our interpretation based on locality.

---

[3]Because of their anyonic statistics, Majorana quasiparticles in condensed matter systems are not fermions. More accurate terms include "unpaired Majorana modes", "Majorana zero-modes" and "Majorana bound states".

Finally, we derived a positive result about the memory performance of a pair of Kitaev chains exposed to parity-preserving, local Markovian dynamics, in the limit of a large gap in the chain Hamiltonian. We derived the Markovian master equation in the weak-coupling limit, starting from a Hamiltonian interaction with a bosonic bath, and showed that the resulting Markovian dynamics does not degrade the encoded information. The physical factors that seem to underpin this positive results are:

- Locality of the dynamics (both Hamiltonian and dissipative).

- Encoding in the ground space of a local Hamiltonian.

- Large Hamiltonian gap.

One limitation of this result is the fact that the modeling of the Kitaev chains and of the dissipative process is not completely realistic: the Kitaev chain is an effective description of a more complicated system, namely a semiconductor nanowire with proximity-induced superconductivity; and a local noise can be much more complicated than the one we considered, e.g. coupling several neighboring sites instead of dephasing a single one. An interesting direction for future investigation may be the adaptation of the techniques presented in this thesis to more complicated and realistic models.

Also, a numerical study about the finite-gap behavior of the optimal recovery fidelity might prove very interesting. Under Hamiltonian perturbations, the storage time scales exponentially with the length of the chain: it would be interesting to compare the Hamiltonian scenario to the dissipative one.

More generally, a detailed understanding of Majorana-based memories, including a list of necessary and sufficient physical requirements and quantitative criteria, is still missing. As the experimental pursuit for Majorana fermions progresses, a parallel progress in the theoretical understanding of their potential for quantum information is in order. The optimal recovery operations, as shown in this thesis, are the appropriate tools to pursue this task.

Appendix A

Diagonal Elements of $SO(3)$ Matrices

In this Appendix we prove a lemma that is used in §2.4.

Lemma (diagonal elements of $SO(3)$ matrices). *The set of possible diagonals of $SO(3)$ matrices,*

$$\Delta \equiv \left\{ \mathbf{v} \in \mathbb{R}^3 : v_i = R_{ii} \text{ for some } R \in SO(3) \right\}, \tag{A.1}$$

is the tetrahedron $\mathcal{T}$ of vertices $(1,1,1)$, $(1,-1,-1)$, $(-1,1,-1)$ and $(-1,-1,1)$.

Proof. Let us start by recalling that a general 3-dimensional rotation can be parametrized by three Euler angles:

$$R = \begin{pmatrix} \cos\zeta & -\sin\zeta & 0 \\ \sin\zeta & \cos\zeta & 0 \\ 0 & 0 & 1 \end{pmatrix} \begin{pmatrix} 1 & 0 & 0 \\ 0 & \cos\chi & -\sin\chi \\ 0 & \sin\chi & \cos\chi \end{pmatrix} \begin{pmatrix} \cos\eta & -\sin\eta & 0 \\ \sin\eta & \cos\eta & 0 \\ 0 & 0 & 1 \end{pmatrix} =$$

$$= \begin{pmatrix} \cos\zeta\cos\eta - \sin\zeta\sin\eta\cos\chi & \dots & \dots \\ \dots & \cos\zeta\cos\eta\cos\chi - \sin\zeta\sin\eta & \dots \\ \dots & \dots & \cos\chi \end{pmatrix}. \tag{A.2}$$

From this parametrization we see that the general $\mathbf{v} \in \Delta$ is

$$\mathbf{v} = \begin{pmatrix} \cos\zeta\cos\eta - \sin\zeta\sin\eta\cos\chi \\ \cos\zeta\cos\eta\cos\chi - \sin\zeta\sin\eta \\ \cos\chi \end{pmatrix}. \tag{A.3}$$

Then we can apply the trigonometric identities $\cos\zeta\cos\eta = \frac{1}{2}(\cos(\zeta+\eta)+\cos(\zeta-\eta))$ and $\sin\zeta\sin\eta = -\frac{1}{2}(\cos(\zeta+\eta)-\cos(\zeta-\eta))$ and define $\alpha = \zeta+\eta, \beta = \zeta-\eta$ in order to rewrite the general $\mathbf{v} \in \Delta$ as follows:

$$\mathbf{v} = \begin{pmatrix} \frac{1}{2}(\cos\alpha+\cos\beta) + \frac{1}{2}(\cos\alpha-\cos\beta)\cos\chi \\ \frac{1}{2}(\cos\alpha+\cos\beta)\cos\chi + \frac{1}{2}(\cos\alpha-\cos\beta) \\ \cos\chi \end{pmatrix} = \begin{pmatrix} \cos\alpha\frac{1+\cos\chi}{2} + \cos\beta\frac{1-\cos\chi}{2} \\ \cos\alpha\frac{1+\cos\chi}{2} - \cos\beta\frac{1-\cos\chi}{2} \\ \cos\chi \end{pmatrix}. \quad \text{(A.4)}$$

Finally let us parametrize $\mathcal{T}$ as the set of convex combinations of its vertices: let $a,b,c,d \in [0,1]$ be such that $a+b+c+d = 1$; then a general point in $\mathcal{T}$ can be written as

$$\mathbf{v} = a\begin{pmatrix} +1 \\ +1 \\ +1 \end{pmatrix} + b\begin{pmatrix} +1 \\ -1 \\ -1 \end{pmatrix} + c\begin{pmatrix} -1 \\ +1 \\ -1 \end{pmatrix} + d\begin{pmatrix} -1 \\ -1 \\ +1 \end{pmatrix} = \begin{pmatrix} a+b-c-d \\ a-b+c-d \\ a-b-c+d \end{pmatrix}. \quad \text{(A.5)}$$

Now, equating (A.5) and (A.4) we can prove the two inclusions $\mathcal{T} \subseteq \Delta$ and $\Delta \subseteq \mathcal{T}$.

1. Assuming $a,b,c,d \in [0,1]$ and $a+b+c+d = 1$, one can solve for $\cos(\alpha)$, $\cos(\beta)$ and $\cos(\chi)$ to find

$$\begin{cases} \cos\chi = a-b-c+d, \\ \cos\alpha = \dfrac{2(a-d)}{1+a-b-c+d} = \dfrac{2(a-d)}{2a+2d} = \dfrac{a-d}{a+d}, \\ \cos\beta = \dfrac{2(b-c)}{1-a+b+c-d} = \dfrac{2(b-c)}{2b+2c} = \dfrac{b-c}{b+c}. \end{cases} \quad \text{(A.6)}$$

It is easy to see that each cosine lies in $[-1,1]$, so that the three Euler angles α, β and χ are well defined, and every point of $\mathcal{T}$ belongs to Δ.

2. Solving a, b, c and $d = 1-a-b-c$, one gets

$$\begin{cases} a = \dfrac{(1+\cos\alpha)(1+\cos\chi)}{4}, & b = \dfrac{(1+\cos\beta)(1-\cos\chi)}{4}, \\ c = \dfrac{(1-\cos\beta)(1-\cos\chi)}{4}, & d = \dfrac{(1-\cos\alpha)(1+\cos\chi)}{4}. \end{cases} \quad \text{(A.7)}$$

Each parameter is clearly non-negative, and clearly not larger than 1, and it is easy to see that $a+b+c+d = 1$. Therefore every point of Δ belongs to $\mathcal{T}$.

Both inclusions being proven, we can conclude that $\Delta = \mathcal{T}$. $\qquad\square$

Appendix B

Liouville Representation for Super-Operators

The Liouville representation is a mathematical way to describe linear operators as vectors and super-operators as matrices acting on them. The idea is the following: if $\{|i\rangle : i \in \{1, \dots N\}\}$ is an orthonormal basis of the Hilbert space $\mathcal{H}$, then each operator $\hat{A} \in \mathcal{B}(\mathcal{H})$ can be identified with a vector of $\mathcal{H}^{\otimes 2}$ as follows:

$$\hat{A} = \sum_{i,j=1}^{N} A_{ij} |i\rangle \langle j| \mapsto \left|\hat{A}\right\rangle\!\rangle = \sum_{i,j=1}^{N} A_{ij} |i\rangle \otimes |j\rangle \in \mathcal{H}^{\otimes 2}. \tag{B.1}$$

The double angle bracket is used to distinguish "super-kets" (vectors of $\mathcal{H}^{\otimes 2}$) from ordinary kets (vectors of $\mathcal{H}$).

Mathematically, (B.1) amounts to the statement that $\mathcal{B}(\mathcal{H})$ and $\mathcal{H} \otimes \mathcal{H}$ are isomorphic, which is true if $\mathcal{H}$ is finite-dimensional[1]. This fact can be used to perform some convenient manipulations with super-operators. Since super-operators are elements of $\mathcal{B}(\mathcal{B}(\mathcal{H}))$, they act on "super-kets" of $\mathcal{B}(\mathcal{H})$ as ordinary matrices:

$$|\Phi(\hat{\rho})\rangle\!\rangle = \mathcal{M}_\Phi \, |\hat{\rho}\rangle\!\rangle, \qquad\qquad \mathcal{M}_\Phi \in \mathcal{B}\left(\mathcal{H}^{\otimes 2}\right). \tag{B.2}$$

Lemma (ABC rule). *The Liouville representation of a product of three operators $\hat{A}$, $\hat{B}$ and $\hat{C}$ obeys the following rule:*

$$\left|\hat{A}\hat{B}\hat{C}\right\rangle\!\rangle = \left(\hat{A} \otimes \hat{C}^T\right) \left|\hat{B}\right\rangle\!\rangle. \tag{B.3}$$

---

[1]It is always true that $\mathcal{B}(\mathcal{H}) \cong \mathcal{H} \otimes \mathcal{H}^*$; if $\mathcal{H}$ is finite-dimensional, one also has $\mathcal{H} \cong \mathcal{H}^*$.

Proof.

$$\left(\hat{A} \otimes \hat{C}^T\right) \left|\hat{B}\right\rangle\!\rangle = \sum_{i,j,k,l,m,n} A_{ij} C_{lk} B_{mn}(|i\rangle \langle j| \otimes |k\rangle \langle l|) |m\rangle \otimes |n\rangle$$

$$= \sum_{ijkl} A_{ij} B_{jl} C_{lk} |i\rangle \otimes |k\rangle = \sum_{i,k=1}^N \left(\hat{A}\hat{B}\hat{C}\right)_{ik} |i\rangle \otimes |k\rangle = \left|\hat{A}\hat{B}\hat{C}\right\rangle\!\rangle. \quad \text{(B.4)}$$

$\square$

The "ABC rule" can also be applied to pairs of operators by conveniently including an identity operator:

$$\left|\hat{A}\hat{B}\right\rangle\!\rangle = \begin{cases} \left|\hat{A}\hat{B}I\right\rangle\!\rangle = \left(\hat{A} \otimes I\right) \left|\hat{B}\right\rangle\!\rangle, \\ \left|I\hat{A}\hat{B}\right\rangle\!\rangle = \left(I \otimes \hat{B}^T\right) \left|\hat{A}\right\rangle\!\rangle. \end{cases} \quad \text{(B.5)}$$

Applying identities (B.3) and (B.5) to the case of a Lindbladian super-operator

$$\mathcal{L}(\hat{\rho}) = -i[\hat{H}, \hat{\rho}] + \sum_k \left(\hat{L}_k \hat{\rho} \hat{L}_k^\dagger - \frac{1}{2}\left\{\hat{\rho}, \hat{L}_k^\dagger \hat{L}_k\right\}\right), \quad \text{(B.6)}$$

we obtain

$$\mathcal{M}_\mathcal{L} = -i\left(\hat{H} \otimes I + I \otimes \hat{H}^T\right) + \sum_k \left(\hat{L}_k \otimes \hat{L}_k^* - \frac{1}{2}I \otimes \hat{L}_k^T \hat{L}_k^* - \frac{1}{2}\hat{L}_k^\dagger \hat{L}_k \otimes I\right). \quad \text{(B.7)}$$

Appendix C

Approximating Arbitrary Master Equations with Hamiltonians and Damped Qubits

In Chapter 3 we discuss the power of dissipation as a tool to protect quantum information. In the examples that we consider, the environment acts on the system through very peculiar Lindblad operators, each one involving several qubits. From an experimental point of view, it is not clear *a priori* whether such complicated and unnatural dissipative process can be engineered.

In this Appendix we shall see how arbitrary dissipative processes can be simulated using relatively inexpensive physical resources, such as Hamiltonian interactions and single-qubit cooling processes [10, 13].

Let us consider for simplicity a noise represented by a single Lindblad operator. Then the following theorem holds.

Theorem (simulation of target master equations). *The target master equation*

$$\frac{d}{dt}\hat{\rho} = \gamma \left(\hat{L}\hat{\rho}\hat{L}^\dagger - \frac{1}{2}\left\{ \hat{L}^\dagger\hat{L}, \hat{\rho} \right\} \right), \tag{C.1}$$

where $Tr\left(L^\dagger L\right) = 1$, *can be approximated by using an ancillary qubit subject to an amplitude-damping noise of strength* χ *and engineering the system-ancilla Hamiltonian*

$$\hat{H}_{SA} = \frac{\sqrt{\chi\gamma}}{2}\left(\hat{L}\otimes\sigma^+ + \hat{L}^\dagger\otimes\sigma^-\right). \tag{C.2}$$

Proof. The full master equation governing the system and the ancilla is

$$\frac{d}{dt}\hat{\rho}_{SA} = -i\omega\left[\hat{L}_S\sigma_A^+ + \hat{L}_S^\dagger\sigma_A^-, \hat{\rho}_{SA}\right] + \chi\left(\sigma_A^-\hat{\rho}_{SA}\sigma_A^+ - \frac{1}{2}\left\{\sigma_A^+\sigma_A^-, \hat{\rho}_{SA}\right\}\right), \tag{C.3}$$

where we set $\omega = \frac{\sqrt{\gamma\chi}}{2}$ for brevity. Let us define the matrices $\hat{\rho}_{00}$, $\hat{\rho}_{01}$, $\hat{\rho}_{10}$ and $\hat{\rho}_{11}$ by

$$\hat{\rho}_{ij} = {}_A\langle i|\,\hat{\rho}_{SA}\,|j\rangle_A\,, \tag{C.4}$$

so that $\hat{\rho}_S \equiv \text{Tr}_A\left(\hat{\rho}_{SA}\right) = \hat{\rho}_{00} + \hat{\rho}_{11}$. (C.3) is equivalent to the following system:

$$\begin{cases} \dfrac{d}{dt}\hat{\rho}_{00} = -i\omega\hat{L}^\dagger\hat{\rho}_{10} + i\omega\hat{\rho}_{01}\hat{L} + \chi\hat{\rho}_{11}, \\[2mm] \dfrac{d}{dt}\hat{\rho}_{01} = -i\omega\hat{L}^\dagger\hat{\rho}_{11} + i\omega\hat{\rho}_{00}\hat{L}^\dagger - \dfrac{\chi}{2}\hat{\rho}_{01}, \\[2mm] \dfrac{d}{dt}\hat{\rho}_{11} = -i\omega\hat{L}\hat{\rho}_{01} + i\omega\hat{\rho}_{10}\hat{L}^\dagger - \chi\hat{\rho}_{11}. \end{cases} \tag{C.5}$$

Notice that while $\hat{\rho}_{00}$ and $\hat{\rho}_{11}$ are self-adjoint, one has $\hat{\rho}_{01}^\dagger = \hat{\rho}_{10}$. The equation for $\hat{\rho}_{10}$ is thus omitted. The following integral representation for $\hat{\rho}_{01}$ and $\hat{\rho}_{11}$ holds:

$$\hat{\rho}_{01}(t) = e^{-\chi t/2}\hat{\rho}_{01}(0) + i\omega\int_0^t d\tau\, e^{-\chi\tau/2}\left(\hat{L}^\dagger\hat{\rho}_{11}(t-\tau) - \hat{\rho}_{00}(t-\tau)\hat{L}^\dagger\right), \tag{C.6}$$

$$\hat{\rho}_{11}(t) = e^{-\chi t}\hat{\rho}_{11}(0) + i\omega\int_0^t d\tau\, e^{-\chi\tau}\left(\hat{L}\hat{\rho}_{01}(t-\tau) - \hat{\rho}_{10}(t-\tau)\hat{L}^\dagger\right). \tag{C.7}$$

By initializing the ancilla in the $|0\rangle$ state, one has $\hat{\rho}_{01}(0) = \hat{\rho}_{11}(0) = 0$, so that

$$\begin{aligned} \|\hat{\rho}_{01}(t)\|_{\text{op}} &\leq \omega\int_0^t d\tau\, e^{-\chi\tau/2}\left\|\hat{L}^\dagger\hat{\rho}_{11}(t-\tau) - \hat{\rho}_{00}(t-\tau)\hat{L}^\dagger\right\|_{\text{op}} \\ &\leq \omega\int_0^t d\tau\, e^{-\chi\tau/2}\left\|\hat{L}^\dagger\right\|_{\text{op}}\cdot\left(\|\hat{\rho}_{00}(t-\tau)\|_{\text{op}} + \|\hat{\rho}_{11}(t-\tau)\|_{\text{op}}\right) \\ &\leq \omega\int_0^t d\tau\, e^{-\chi\tau/2} = \frac{2\omega}{\chi}\int_0^{\chi t/2} d\theta\, e^{-\theta} \leq \frac{2\omega}{\chi} \end{aligned} \tag{C.8}$$

(the third inequality comes from the fact that $\left\|\hat{L}^\dagger\right\|_{\text{op}} \leq \left\|\hat{L}^\dagger\right\|_{\text{tr}} = 1$). Analogously,

$$\|\hat{\rho}_{11}(t)\|_{\text{op}} \leq \omega \int_0^t d\tau e^{-\chi\tau} \left\|\hat{L}\hat{\rho}_{01}(t-\tau) - \hat{\rho}_{10}(t-\tau)\hat{L}^\dagger\right\|_{\text{op}}$$
$$\leq \omega \int_0^t d\tau e^{-\chi\tau} \|\hat{L}\|_{\text{op}} \cdot 2\|\hat{\rho}_{01}(t-\tau)\|_{\text{op}} \leq \left(\frac{2\omega}{\chi}\right)^2. \tag{C.9}$$

Assuming $\epsilon = \frac{2\omega}{\chi} \ll 1$, one has that $\hat{\rho}_{01}$ and $\hat{\rho}_{11}$ are both small at all times, bounded by ϵ and ϵ^2 respectively. Now, by using integration by parts on (C.6) one gets

$$\hat{\rho}_{01}(t) = i\omega \int_0^t d\tau e^{-\chi\tau/2} \left(\hat{L}^\dagger \hat{\rho}_{11}(t-\tau) + \frac{2}{\chi} \frac{d}{ds}\hat{\rho}_{00}(s)\Big|_{s=t-\tau} \hat{L}^\dagger \right)$$
$$+ i\epsilon\hat{\rho}_{00}(t)\hat{L}^\dagger - i\epsilon e^{-\chi t/2}\hat{\rho}_{00}(0)\hat{L}^\dagger. \tag{C.10}$$

Substituting $\frac{d}{ds}\hat{\rho}_{00}(s)$ with its expression (C.5), we see that the integral term is $\mathcal{O}(\epsilon^2)$, so that after an initial transient

$$\hat{\rho}_{01}(t) \simeq i\epsilon\hat{\rho}_{00}(t)\hat{L}^\dagger. \tag{C.11}$$

By an analogous reasoning one has

$$\hat{\rho}_{11}(t) \simeq -i\frac{\epsilon}{2}\left(\hat{L}\hat{\rho}_{01}(t) - \hat{\rho}_{10}(t)\hat{L}^\dagger\right) \simeq \epsilon^2 \hat{L}\hat{\rho}_{00}(t)\hat{L}^\dagger. \tag{C.12}$$

Now, since $\hat{\rho}_{11}$ is small with respect to $\hat{\rho}_{00}$, the reduced density matrix $\hat{\rho}_S = \text{Tr}_A\left(\hat{\rho}_{SA}\right)$ is well approximated by $\hat{\rho}_{00}$, and from (C.5) we can conclude that

$$\frac{d}{dt}\hat{\rho}_S \simeq \frac{d}{dt}\hat{\rho}_{00} = -i\omega\hat{L}^\dagger\hat{\rho}_{10} + i\omega\hat{\rho}_{01}\hat{L} + \chi\hat{\rho}_{11}$$
$$\simeq -i\omega\hat{L}^\dagger(-i\epsilon\hat{L}\hat{\rho}_{00}) + i\omega(i\epsilon\hat{\rho}_{00}\hat{L}^\dagger)\hat{L} + \chi\epsilon^2\hat{L}\hat{\rho}_{00}\hat{L}^\dagger$$
$$= \frac{4\omega^2}{\chi}\left(\hat{L}\hat{\rho}_{00}\hat{L}^\dagger - \frac{1}{2}\left\{\hat{\rho}_{00}, \hat{L}^\dagger\hat{L}\right\}\right). \tag{C.13}$$

The choice $\omega = \frac{\sqrt{\gamma\chi}}{2}$ ensures that the strength of the effective dissipation is γ. The condition $\epsilon \ll 1$ becomes $\sqrt{\frac{\gamma}{\chi}} \ll 1$. $\qquad\square$

A more rigorous version of this derivation, complete with error estimates, is provided in [13].

In order to simulate dissipative processes with multiple Lindblad operators, more ancillas must be added (one ancilla for each Lindblad operator).

Appendix D

Microscopic Derivation of a Markovian Master Equation in the Weak-Coupling Limit

This derivation follows the one presented in [23], §3.3.1.

We have a system and an environment, governed by a total Hamiltonian $\hat{H}_{\text{tot}} = \hat{H}_{\text{sys}} + \hat{H}_{\text{env}} + \hat{H}_{\text{int}}$. We are interested in a particular limit in which the dynamics of the reduced density matrix of the system becomes Markovian. What follows is a derivation of the form of the resulting master equation, given $\hat{H}_{\text{sys}}$, $\hat{H}_{\text{env}}$, and $\hat{H}_{\text{int}}$.

We shall work in the interaction picture: let $\hat{H}_I(t) \equiv e^{i(\hat{H}_{\text{sys}}+\hat{H}_{\text{env}})t} \hat{H}_{\text{int}} e^{-i(\hat{H}_{\text{sys}}+\hat{H}_{\text{env}})t}$; then

$$\frac{d}{dt}\hat{\rho}(t) = -i[\hat{H}_I(t), \hat{\rho}(t)]. \tag{D.1}$$

Integrating this equation we get $\hat{\rho}(t) = \hat{\rho}(0) - i \int_0^t ds [\hat{H}_I(s), \hat{\rho}(s)]$, which can be substituted into the right-hand side of (D.1) to obtain

$$\frac{d}{dt}\hat{\rho}(t) = -i[\hat{H}_I(t), \hat{\rho}(0)] - \int_0^t ds \left[\hat{H}_I(t), [\hat{H}_I(s), \hat{\rho}(s)] \right]. \tag{D.2}$$

Here we invoke the Born approximation ($\hat{\rho}(t) \approx \hat{\rho}_{\text{sys}}(t) \otimes \hat{\rho}_{\text{env}}(0)$, which removes memory effects of the environment) and the Markov approximation ($\hat{\rho}_{\text{sys}}(s) \approx \hat{\rho}_{\text{sys}}(t)$, which removes any dependence on the previous history of the system). Furthermore, let us assume for the moment that the first term in (D.2) vanishes:

$$\text{Tr}_{\text{env}} \left([\hat{H}_I(t), \hat{\rho}(0)] \right) = 0 \tag{D.3}$$

(we shall prove it later). Under these simplifying assumptions, (D.2) becomes

$$\frac{d}{dt}\hat{\rho}_{\text{sys}}(t) \simeq -\int_0^t ds\, \text{Tr}_{\text{env}}\left(\left[\hat{H}_I(t), [\hat{H}_I(s), \hat{\rho}_{\text{sys}}(t) \otimes \hat{\rho}_{\text{env}}]\right]\right). \tag{D.4}$$

In order to get a semi-group solution, the dependence on the initial condition ($t = 0$) must be removed. We shall change the variable of integration from s to $s' = t - s$, and integrate on the range $(0, \infty)$ (instead of $(0, t)$):

$$\frac{d}{dt}\hat{\rho}_{\text{sys}}(t) \simeq -\int_0^\infty ds'\, \text{Tr}_{\text{env}}\left(\left[\hat{H}_I(t), [\hat{H}_I(t - s'), \hat{\rho}_{\text{sys}}(t) \otimes \hat{\rho}_{\text{env}}]\right]\right). \tag{D.5}$$

Now let us define the traceless[1], Hermitian operators $\left\{\hat{A}_\alpha\right\}$ and $\left\{\hat{B}_\alpha\right\}$, acting on the system and on the environment respectively, such that $\hat{H}_{\text{int}} = \sum_\alpha \hat{A}_\alpha \otimes \hat{B}_\alpha$. Let us also write down a Fourier decomposition of the operators $\left\{\hat{A}_\alpha\right\}$:

$$\hat{A}_\alpha(t) = e^{-it\hat{H}_{\text{sys}}}\hat{A}_\alpha e^{it\hat{H}_{\text{sys}}} = \sum_\omega \hat{A}_\alpha(\omega)e^{-i\omega t}. \tag{D.6}$$

Applying this decomposition, we have

$$\hat{H}_I(t) = \sum_{\alpha,\omega} e^{-i\omega t}\hat{A}_\alpha(\omega) \otimes \hat{B}_\alpha(t), \qquad \hat{B}_\alpha(t) = e^{i\hat{H}_{\text{env}}t}\hat{B}_\alpha e^{-i\hat{H}_{\text{env}}t}. \tag{D.7}$$

We are now in a position to prove (D.3):

$$\text{Tr}_{\text{env}}\left([\hat{H}_I(t), \hat{\rho}(0)]\right) = \sum_{\alpha,\omega} e^{-i\omega t}\text{Tr}_{\text{env}}\left([\hat{A}_\alpha(\omega) \otimes \hat{B}_\alpha(t), \hat{\rho}_{\text{sys}}(0) \otimes \hat{\rho}_{\text{env}}]\right)$$

$$= \sum_{\alpha,\omega} e^{-i\omega t}[\hat{A}_\alpha(\omega), \hat{\rho}_{\text{sys}}(0)]\text{Tr}\left(\hat{B}_\alpha(t)\hat{\rho}_{\text{env}}\right) = 0, \tag{D.8}$$

assuming $\text{Tr}\left(\hat{B}_\alpha\hat{\rho}_{\text{env}}\right) = 0$, which holds in particular for the choice we always adopt in this thesis, i.e. $\hat{\rho}_{\text{env}} \propto I$.

The decomposition (D.6), plugged into (D.5), yields

$$\frac{d}{dt}\hat{\rho}_{\text{sys}}(t) = -\sum_{\alpha,\omega}\sum_{\alpha',\omega'}\int_0^\infty ds\, e^{-i\omega t}e^{-i\omega'(t-s)}$$

$$\text{Tr}_{\text{env}}\left(\left[\hat{A}_\alpha(\omega) \otimes \hat{B}_\alpha(t), [\hat{A}_{\alpha'}(\omega') \otimes \hat{B}_{\alpha'}(t - s), \hat{\rho}_{\text{sys}}(t) \otimes \hat{\rho}_{\text{env}}]\right]\right); \tag{D.9}$$

---

[1] They can be assumed traceless up to a redefinition of $\hat{H}_{\text{sys}}$ or $\hat{H}_{\text{env}}$: e.g. one can write $\hat{A}_1 \otimes \hat{B}_1 = (\hat{A}_1 - \alpha I_{\text{sys}}) \otimes \hat{B}_1 + \alpha I_{\text{sys}} \otimes \hat{B}_1$ and absorb the last term into $\hat{H}_{\text{env}}$. A suitable choice of α annihilates the trace of $\hat{A}_1$.

and, expanding the nested commutators,

$$
\begin{aligned}
\frac{d}{dt}\hat{\rho}_{\text{sys}}(t) = -\sum_{\alpha,\omega}\sum_{\alpha',\omega'}\int_0^\infty ds\, e^{-i\omega t}e^{-i\omega'(t-s)}\Big(& \hat{A}_\alpha(\omega)\hat{A}_{\alpha'}(\omega')\hat{\rho}_{\text{sys}}(t)\text{Tr}\left(\hat{B}_\alpha(t)\hat{B}_{\alpha'}(t-s)\hat{\rho}_{\text{env}}\right) \\
& - \hat{A}_\alpha(\omega)\hat{\rho}_{\text{sys}}(t)\hat{A}_{\alpha'}(\omega')\text{Tr}\left(\hat{B}_\alpha(t)\hat{\rho}_{\text{env}}\hat{B}_{\alpha'}(t-s)\right) \\
& - \hat{A}_{\alpha'}(\omega')\hat{\rho}_{\text{sys}}(t)\hat{A}_\alpha(\omega)\text{Tr}\left(\hat{B}_{\alpha'}(t-s)\hat{\rho}_{\text{env}}\hat{B}_\alpha(t)\right) \\
& + \hat{\rho}_{\text{sys}}(t)\hat{A}_{\alpha'}(\omega')\hat{A}_\alpha(\omega)\text{Tr}\left(\hat{\rho}_{\text{env}}\hat{B}_{\alpha'}(t-s)\hat{B}_\alpha(t)\right)\Big).
\end{aligned}
\tag{D.10}
$$

Now let us define the environment correlation function

$$
K_{\alpha\beta}(s) = \text{Tr}\left(\hat{B}_\alpha(t)\hat{B}_\beta(t-s)\hat{\rho}_{\text{env}}\right),
\tag{D.11}
$$

which does not depend on t because of time translation invariance. (D.10) involves the Fourier transform of $\Theta(s)K_{\alpha\beta}(s)$,

$$
\Gamma_{\alpha\beta}(\omega') \equiv \int_{-\infty}^\infty ds\,\Theta(s)K_{\alpha\beta}(s)e^{i\omega' s} = \int_0^\infty ds\,K_{\alpha\beta}(s)e^{i\omega' s}.
\tag{D.12}
$$

Assuming $[\hat{\rho}_{\text{env}}, \hat{B}_\alpha(t)] = 0\,\forall\alpha, t$, which holds in particular for $\hat{\rho}_{\text{env}} \propto I$, we can rewrite (D.10) as

$$
\begin{aligned}
\frac{d}{dt}\hat{\rho}_{\text{sys}}(t) = -\sum_{\alpha,\omega}\sum_{\beta,\omega'}e^{-i(\omega+\omega')t}\Gamma_{\alpha\beta}(\omega')\big(& \hat{A}_\alpha(\omega)\hat{A}_\beta(\omega')\hat{\rho}_{\text{sys}}(t) + \hat{\rho}_{\text{sys}}(t)\hat{A}_\beta(\omega')\hat{A}_\alpha(\omega) \\
& - \hat{A}_\alpha(\omega)\hat{\rho}_{\text{sys}}(t)\hat{A}_\beta(\omega') - \hat{A}_\beta(\omega')\hat{\rho}_{\text{sys}}(t)\hat{A}_\alpha(\omega)\big)
\end{aligned}
\tag{D.13}
$$

At this point we invoke the *rotating wave approximation*, and neglect all terms of the sum with $\omega + \omega' \neq 0$:

$$
\begin{aligned}
\frac{d}{dt}\hat{\rho}_{\text{sys}}(t) = \sum_{\alpha,\beta}\sum_\omega\Gamma_{\alpha\beta}(\omega)\big(& \hat{A}_\alpha(\omega)\hat{\rho}_{\text{sys}}(t)\hat{A}_\beta(-\omega) + \hat{A}_\beta(-\omega)\hat{\rho}_{\text{sys}}(t)\hat{A}_\alpha(\omega) \\
& - \hat{A}_\alpha(\omega)\hat{A}_\beta(-\omega)\hat{\rho}_{\text{sys}}(t) - \hat{\rho}_{\text{sys}}(t)\hat{A}_\beta(-\omega)\hat{A}_\alpha(\omega)\big)
\end{aligned}
\tag{D.14}
$$

By relabeling some dummy indices, (D.14) becomes

$$
\begin{aligned}
\frac{d}{dt}\hat{\rho}_{\text{sys}}(t) = \sum_{\alpha,\beta}\sum_\omega\big(& (\Gamma_{\alpha\beta}(\omega) + \Gamma_{\beta\alpha}(-\omega))\hat{A}_\alpha(\omega)\hat{\rho}_{\text{sys}}(t)\hat{A}_\beta(-\omega) \\
& - \Gamma_{\beta\alpha}(-\omega)\hat{A}_\beta(-\omega)\hat{A}_\alpha(\omega)\hat{\rho}_{\text{sys}}(t) - \Gamma_{\alpha\beta}(\omega)\hat{\rho}_{\text{sys}}(t)\hat{A}_\beta(-\omega)\hat{A}_\alpha(\omega)\big\}.
\end{aligned}
\tag{D.15}
$$

Now let

$$
\begin{cases}
\Gamma_{\alpha\beta}(\omega) + \Gamma_{\beta\alpha}(-\omega) = \int_{-\infty}^{+\infty} ds\, e^{i\omega s}\mathrm{Tr}\left(\hat{B}_\alpha(s)\hat{B}_\beta(0)\hat{\rho}_{\mathrm{env}}\right) \equiv \gamma_{\alpha\beta}(\omega), \\
\Gamma_{\alpha\beta}(\omega) - \Gamma_{\beta\alpha}(-\omega) = \int_{-\infty}^{+\infty} ds\, \mathrm{sign}\,(s)\, e^{i\omega s}\mathrm{Tr}\left(\hat{B}_\alpha(s)\hat{B}_\beta(0)\hat{\rho}_{\mathrm{env}}\right) \equiv 2iS_{\alpha\beta}(\omega).
\end{cases}
\tag{D.16}
$$

Both $\gamma(\omega)$ and $S(\omega)$ are Hermitian matrices. Plugging these definitions into (D.15) we get

$$
\frac{d}{dt}\hat{\rho}_{\mathrm{sys}}(t) = \sum_{\alpha,\beta}\sum_{\omega}\left(\gamma_{\alpha\beta}(\omega)\hat{A}_\alpha(\omega)\hat{\rho}_{\mathrm{sys}}(t)\hat{A}_\beta(-\omega) - \frac{1}{2}\gamma_{\alpha\beta}(\omega)\left\{\hat{A}_\beta(-\omega)\hat{A}_\alpha(\omega), \hat{\rho}_{\mathrm{sys}}(t)\right\}\right.
$$
$$
\left. + iS_{\alpha\beta}(\omega)\left[\hat{A}_\beta(-\omega)\hat{A}_\alpha(\omega), \hat{\rho}_{\mathrm{sys}}(t)\right]\right).
\tag{D.17}
$$

The term involving the commutator yields the so-called "Lamb-shift Hamiltonian" contribution, which is a renormalization of the original system Hamiltonian, while the remaining terms can cast into Lindblad form by diagonalizing the $\gamma(\omega)$ matrices, and using the fact that $\hat{A}(-\omega) = \left(\hat{A}(\omega)\right)^\dagger$:

$$
\frac{d}{dt}\hat{\rho}_{\mathrm{sys}}(t) = -i[\hat{H}_{LS}, \hat{\rho}_{\mathrm{sys}}(t)] + \sum_{\alpha,\omega}\left(\hat{L}_{\alpha,\omega}\hat{\rho}_{\mathrm{sys}}(t)\hat{L}_{\alpha,\omega}^\dagger - \frac{1}{2}\left\{\hat{L}_{\alpha,\omega}^\dagger\hat{L}_{\alpha,\omega}, \hat{\rho}_{\mathrm{sys}}(t)\right\}\right),
\tag{D.18}
$$

finally, going back from the interaction representation to the Schroedinger picture, the original system Hamiltonian $\hat{H}_{\mathrm{sys}}$ must be added to $\hat{H}_{LS}$.

In conclusion: if we start from $\hat{H}_{\mathrm{sys}}$, $\hat{H}_{\mathrm{env}}$ and $\hat{H}_{\mathrm{int}} = \sum_\alpha \hat{A}_\alpha \otimes \hat{B}_\alpha$, the final Hamiltonian will be

$$
\hat{H}_{\mathrm{sys}} + \hat{H}_{LS} = \hat{H}_{\mathrm{sys}} - \sum_{\alpha,\beta}\sum_{\omega}S_{\alpha\beta}(\omega)\hat{A}_\beta(\omega)^\dagger\hat{A}_\alpha(\omega),
\tag{D.19}
$$

while the Lindblad operators representing the dissipative part of the dynamics will be

$$
\hat{L}_{\alpha,\omega} = \sum_\beta \sqrt{d_{\alpha\alpha}(\omega)}c_{\alpha\beta}(\omega)\hat{A}_\beta(\omega),
\tag{D.20}
$$

where, for each ω, $c(\omega)$ is the unitary matrix that diagonalizes $\gamma(\omega)$ to $d(\omega)$: $\gamma(\omega) = c(\omega)^\dagger d(\omega)c(\omega)$. $\qquad\square$

Remark. This derivation is formulated for spin systems. In the Thesis we apply it to fermionic systems as well. The main difference between the two cases is that fermionic operators do not have a tensor structure, hence system operators may anti-commute with environment operators. It can be shown, however, that the derivation works anyway, with minor sign adjustments.

Appendix E

Parity-Preserving Noise Models

In this Appendix we prove two lemmas about parity-preserving noise models. One is about general quantum channels, the other about Markovian dynamics. These lemmas are used in §5.3 through §5.5 to constrain the parity-preserving noise models to which the Majorana memory toy-models are exposed.

Lemma (parity-preserving channels). *A quantum channel Φ is parity-preserving (PP) if and only if its Kraus operators are all "bosonic" (BK).*

Proof.

- (BK) $\implies$ (PP): the Kraus operators $\left\{ \hat{M}_k \right\}$ commute with $\hat{P}_f$, therefore

$$\left\langle \hat{P}_f \right\rangle_{\Phi(\hat{\rho})} = \text{Tr}\left(\hat{P}_f \Phi(\hat{\rho}) \right) = \text{Tr}\left(\Phi^*(\hat{P}_f)\hat{\rho} \right) = \sum_k \text{Tr}\left(\hat{M}_k^\dagger \hat{P}_f \hat{M}_k \hat{\rho} \right)$$

$$= \text{Tr}\left(\sum_k \hat{M}_k^\dagger \hat{M}_k \hat{P}_f \hat{\rho} \right); \tag{E.1}$$

  by invoking the Kraus completeness relation (1.10) one has $\left\langle \hat{P}_f \right\rangle_{\Phi(\hat{\rho})} = \left\langle \hat{P}_f \right\rangle_{\hat{\rho}}$.

- (PP) $\implies$ (BK): we have

$$\text{Tr}\left(\hat{P}_f \hat{\rho} \right) = \text{Tr}\left(\hat{P}_f \Phi(\hat{\rho}) \right) = \text{Tr}\left(\Phi^*(\hat{P}_f)\hat{\rho} \right) \tag{E.2}$$

for all physical states $\hat{\rho}$, i.e. for all bosonic operators. Let us consider a generic operator $\hat{\mu}$; (E.2) must hold for its bosonic part:

$$\text{Tr}\left(\hat{P}_f \frac{\hat{\mu} + \hat{P}_f \hat{\mu}\hat{P}_f}{2}\right) = \text{Tr}\left(\Phi^*\left(\hat{P}_f\right) \frac{\hat{\mu} + \hat{P}_f \hat{\mu}\hat{P}_f}{2}\right), \qquad (E.3)$$

which can be rewritten by isolating $\hat{\mu}$:

$$\text{Tr}\left(\hat{\mu}\left(2\hat{P}_f - \Phi^*(\hat{P}_f) - \hat{P}_f \Phi^*(\hat{P}_f)\hat{P}_f\right)\right) = 0 \qquad \forall \hat{\mu} \in \mathcal{B}\left(\mathfrak{F}_N\right). \qquad (E.4)$$

By taking $\hat{\mu} = \left(2\hat{P}_f - \Phi^*(\hat{P}_f) - \hat{P}_f \Phi^*(\hat{P}_f)\hat{P}_f\right)^\dagger$, we can see that the Hilbert-Schmidt norm of the operator in brackets vanishes; hence we must have

$$2 \cdot \hat{\mathbf{1}} - \hat{P}_f \Phi^*(\hat{P}_f) - \Phi^*(\hat{P}_f)\hat{P}_f = 2 \cdot \hat{\mathbf{1}} - \sum_k \left(\hat{P}_f \hat{M}_k^\dagger \hat{P}_f \hat{M}_k + \hat{M}_k^\dagger \hat{P}_f \hat{M}_k \hat{P}_f\right) = 0. \quad (E.5)$$

Decomposing the Kraus operators $\left\{\hat{M}_k\right\}$ into their fermionic and bosonic parts, and recalling the Kraus completeness relation (1.10), one gets

$$\sum_k \left[2\left(\hat{M}_k^b + \hat{M}_k^f\right)^\dagger \left(\hat{M}_k^b + \hat{M}_k^f\right) - \left(\hat{M}_k^b - \hat{M}_k^f\right)^\dagger \left(\hat{M}_k^b + \hat{M}_k^f\right)\right.$$

$$\left. -\left(\hat{M}_k^b + \hat{M}_k^f\right)^\dagger \left(\hat{M}_k^b - \hat{M}_k^f\right)\right] = 0. \qquad (E.6)$$

The bosonic and fermionic parts of this expression must vanish separately; considering the bosonic part one gets

$$\sum_k \left(\hat{M}_k^f\right)^\dagger \hat{M}_k^f = 0. \qquad (E.7)$$

Taking the trace of (E.7), and recalling the definition of the Hilbert-Schmidt norm $\|\hat{A}\|_2 = \sqrt{\text{Tr}\left(\hat{A}^\dagger \hat{A}\right)}$, we can conclude that

$$\sum_k \left(\|\hat{M}_k^f\|_2\right)^2 = 0 \implies \|\hat{M}_k^f\|_2 = 0 \,\forall k \implies \hat{M}_k^f = 0 \,\forall k, \quad (E.8)$$

hence all Kraus operators are purely bosonic.

$$\square$$

Lemma (parity-preserving Markovian dynamics). *Let $\mathcal{L}$ be a Lindbladian and $\mathcal{D}_t = e^{t\mathcal{L}}$ be the associated decoherence process. $\mathcal{D}_t$ is parity preserving (PP) if and only if the Lindblad operators that define $\mathcal{L}$ are all bosonic (BL).*

Proof.

- (PP) $\implies$ (BL): the conservation of average parity yields

$$\frac{d}{dt}\left\langle \hat{P}_f \right\rangle_t = \mathrm{Tr}\left(\hat{P}_f \mathcal{L}(\hat{\rho}(t)) \right) = \mathrm{Tr}\left(\mathcal{L}^*(\hat{P}_f)\hat{\rho}(t) \right) = 0 \,\forall\, t. \tag{E.9}$$

This must hold for every physical state $\hat{\rho}$, hence for all bosonic operators; it must therefore hold for the bosonic part of a generic operator $\hat{\mu}$:

$$\mathrm{Tr}\left(\mathcal{L}^*(\hat{P}_f)\frac{\hat{\mu} + \hat{P}_f\hat{\mu}\hat{P}_f}{2} \right) = \frac{1}{2}\mathrm{Tr}\left(\hat{\mu}\left(\mathcal{L}^*(\hat{P}_f) + \hat{P}_f\mathcal{L}^*(\hat{P}_f)\hat{P}_f \right) \right) = 0. \tag{E.10}$$

Therefore we must have

$$\hat{P}_f\mathcal{L}^*(\hat{P}_f) + \mathcal{L}^*(\hat{P}_f)\hat{P}_f = 0. \tag{E.11}$$

Using the same techniques that led to the proof of the previous lemma, one gets $\sum_k \left(\hat{L}_k^f \right)^\dagger \hat{L}_k^f = 0$, and thus

$$\sum_k \mathrm{Tr}\left(\left(\hat{L}_k^f \right)^\dagger \hat{L}_k^f \right) = \sum_k \left(\|\hat{L}_k^f\|_2 \right)^2 = 0. \tag{E.12}$$

This proves that $\hat{L}_k^f = 0 \,\forall\, k$, i.e. that all Lindblad operators must be bosonic.

- (BL) $\implies$ (PP): expressing $\frac{d}{dt}\left\langle \hat{P}_f \right\rangle_t$ as in (E.9), by the (BL) property one has $\mathcal{L}^*(\hat{P}_f) = \hat{P}_f\mathcal{L}^*(\hat{\mathbf{1}})$; then, since $\mathcal{L}^*(\hat{\mathbf{1}}) = \sum_k \hat{L}_k^\dagger \hat{L}_k - \frac{1}{2}\left\{ \hat{\mathbf{1}}, \hat{L}_k^\dagger \hat{L}_k \right\} = 0$,

$$\frac{d}{dt}\left\langle \hat{P}_f \right\rangle_t = \mathrm{Tr}\left(\hat{\rho}\mathcal{L}^*(\hat{P}_f) \right) = \mathrm{Tr}\left(\hat{\rho}\hat{P}_f\mathcal{L}^*(\hat{\mathbf{1}}) \right) = 0. \tag{E.13}$$

Thus $\left\langle \hat{P}_f \right\rangle_t$ is constant and $\mathcal{D}_t$ is parity-preserving.

$\square$

Appendix F

Local Noise Models

F.1 Lieb-Robinson Bound for Spins

It has been known since the 1970's that two-point correlations in spin systems propagate with an effective group velocity [72]. Mathematically, this statement is known as the *Lieb-Robinson bound* (LRB) [73]. LRBs have proven to be powerful tools for quantum many-body physics [74]. Their validity was also recently established in experiments with cold atoms [75].

Theorem (closed spin systems). *Let Λ be a spin lattice, and let $A, B \subset \Lambda$ be two disjoint regions separated by a distance d_{AB}; if the system is governed by a* local *Hamiltonian $\hat{H}$, then for every pair of operators $\hat{O}_A$, $\hat{O}_B$ supported on regions A and B the following holds:*

$$\left\| \left[\hat{O}_A(t), \hat{O}_B(0) \right] \right\|_{op} \leq cV \|\hat{O}_A\|_{op} \|\hat{O}_B\|_{op} \exp\left(-\frac{d_{AB} - vt}{\xi} \right), \qquad \text{(F.1)}$$

where V is the size of the largest region and c, v, ξ are model-dependent constants.

The physical meaning of (F.1) is that the effect of local interactions is to "spread" correlations within an effective light-cone, defined by the group velocity v. However, while in a relativistic quantum field theory signaling outside the c light-cone is strictly forbidden by causality, (F.1) allows exponentially small tails outside the v effective light-cone. The parameter ξ defines the characteristic decay length of those tails.

The original formulation of the LRB (F.1) deals with short-range Hamiltonian interactions. However, the scope of the result was recently extended to encompass Markovian quantum dynamics [76].

Theorem (open spin systems, Markovian dynamics). *Let Λ be a spin lattice, and let $A, B \subset \Lambda$ be two disjoint regions separated by a distance d_{AB}; if the system is governed by a Lindbladian $\mathcal{L} = \sum_{X \subseteq \Lambda} \mathcal{L}_X$, with each $\mathcal{L}_X$ represented by Lindblad operators supported*

on region X, and $\mathcal{L}_X = 0$ *for all regions X of diameter greater that some fixed distance d,
then the following holds:*

$$\left\| \left[\mathcal{D}_t\left(\hat{O}_A\right), \hat{O}_B \right] \right\|_{op} \leq cV \|\hat{O}_A\|_{op} \|\hat{O}_B\|_{op} \exp\left(-\frac{d_{AB} - vt}{\xi} \right), \qquad (F.2)$$

with $\mathcal{D}_t = e^{t\mathcal{L}}$.

F.2 Lieb-Robinson Bound for Fermions

Consider a fermionic system on a lattice Λ, with a Dirac mode $\hat{a}_i$ on each site of the lattice.
The LRB for closed spin systems (F.1) can be straightforwardly generalized to pairs of distant
"bosonic" operators on the fermionic lattice [77]. Since Hamiltonians are necessarily bosonic,
all the commutation properties for distant operators that are used in the derivation of (F.1)
hold in this case as well. Moreover, by exchanging all commutators with anti-commutators,
a similar bound for pairs of distant "fermionic" operators can be proven.

Theorem (closed fermionic systems). *Let Λ be a fermionic lattice, and let $A, B \subset \Lambda$
be two disjoint regions separated by a distance d_{AB}; if the system is governed by a* local
*Hamiltonian $\hat{H}$, then for every pair of bosonic operators $\hat{O}_A^b$, $\hat{O}_B^b$ supported on regions A
and B one has*

$$\left\| \left[\hat{O}_A^b(t), \hat{O}_B^b \right] \right\|_{op} \leq cV \|\hat{O}_A^b\|_{op} \|\hat{O}_B^b\|_{op} \exp\left(-\frac{d_{AB} - vt}{\xi} \right); \qquad (F.3)$$

*analogously, for every pair of fermionic operators $\hat{O}_A^f$, $\hat{O}_B^f$ supported on regions A and B,
one has*

$$\left\| \left\{ \hat{O}_A^f(t), \hat{O}_B^f \right\} \right\|_{op} \leq cV \|\hat{O}_A^f\|_{op} \|\hat{O}_B^f\|_{op} \exp\left(-\frac{d_{AB} - vt}{\xi} \right). \qquad (F.4)$$

For the case of Markovian decoherence no general theorem is yet known. This is because,
unlike Hamiltonians which are necessarily bosonic, Lindblad operators are allowed to be
fermionic (e.g. tunneling processes from the environment may be represented by $\hat{L} \propto \hat{a}^\dagger$).
The failure of commutativity between distant operators invalidates the known proofs.

However, in the simple case of purely bosonic Lindblad operators (which by the results
of Appendix E corresponds to parity-preserving noise models), the derivation of the LRB
for open spin systems (F.2) applies entirely, if $\hat{O}_A$ and $\hat{O}_B$ are both bosonic. Exchanging
commutators with anti-commutators, the case in which $\hat{O}_A$ and $\hat{O}_B$ are both fermionic is
covered as well. Thus the LRBs (F.3) and (F.4) hold in the open-system scenario as well,
provided all Lindblad operators are bosonic.

Theorem (open fermionic systems, Markovian parity-preserving dynamics). *Let* Λ *be a fermionic lattice, and let* $A, B \subset \Lambda$ *be two disjoint regions separated by a distance* d_{AB}; *if the system is governed by a Lindbladian* $\mathcal{L} = \sum_{X \subseteq \Lambda} \mathcal{L}_X$, *with each* $\mathcal{L}_X$ *represented by* bosonic *Lindblad operators supported on region* X, *and* $\mathcal{L}_X = 0$ *for all regions* X *of diameter greater that some fixed distance* d, *then for every pair of bosonic operators* $\hat{O}_A^b$, $\hat{O}_B^b$ *supported on regions* A *and* B *one has*

$$\left\| \left[\mathcal{D}_t \left(\hat{O}_A^b \right), \hat{O}_B^b \right] \right\|_{op} \leq cV \|\hat{O}_A^b\|_{op} \|\hat{O}_B^b\|_{op} \exp\left(-\frac{d_{AB} - vt}{\xi} \right); \tag{F.5}$$

analogously, for every pair of fermionic operators $\hat{O}_A^f$, $\hat{O}_B^f$ *supported on regions* A *and* B, *one has*

$$\left\| \left\{ \mathcal{D}_t \left(\hat{O}_A^f \right), \hat{O}_B^f \right\} \right\|_{op} \leq cV \|\hat{O}_A^f\|_{op} \|\hat{O}_B^f\|_{op} \exp\left(-\frac{d_{AB} - vt}{\xi} \right). \tag{F.6}$$

F.3 Clustering Property of Distant Operators

Theorem (open spin systems, Heisenberg picture). *Consider a spin lattice* Λ *and two operators* $\hat{O}_A$ *and* $\hat{O}_B$ *supported on distant regions* $A, B \subset \Lambda$. *Assuming the dynamics is Markovian and described by local Lindblad operators, then the following* clustering property *holds:*

$$\left\| \mathcal{D}_t^* \left(\hat{O}_A \hat{O}_B \right) - \mathcal{D}_t^* \left(\hat{O}_A \right) \mathcal{D}_t^* \left(\hat{O}_B \right) \right\|_{op} \leq c'V \|\hat{O}_A\|_{op} \|\hat{O}_B\|_{op} e^{-\frac{d_{AB} - 2vt}{2\xi}}, \tag{F.7}$$

where $\mathcal{D}_t^*$ *is the adjoint of the decoherence channel* $\mathcal{D}_t = e^{t\mathcal{L}}$.

Remark. Equation (F.7) means that

$$\mathcal{D}_t^* \left(\hat{O}_A \hat{O}_B \right) \simeq \mathcal{D}_t^* \left(\hat{O}_A \right) \mathcal{D}_t^* \left(\hat{O}_B \right), \tag{F.8}$$

up to LRB corrections, which are small as long as the space-like sections of the effective light-cones of regions A and B do not overlap.

Proof. This proof is based on the one provided in [76]. Let $\mathcal{L}$ be the Lindbladian that induces $\mathcal{D}_t$. Let us split Λ into three parts, as in Figure F.1: $\tilde{A}$, $\tilde{B}$ and R, where $A \subset \tilde{A}$, $B \subset \tilde{B}$, and R is a strip thick enough that each Lindblad operator is supported either in $\tilde{A} \cup R$ or in $\tilde{B} \cup R$ (i.e. a Lindblad operator cannot couple $\tilde{A}$ and $\tilde{B}$ directly). Let

$$\mathcal{L}_R = \sum_{\substack{X: \\ X \cap R \neq \emptyset}} \mathcal{L}_X, \qquad \mathcal{L}_0 = \mathcal{L} - \mathcal{L}_R, \qquad \mathcal{L}(\eta) = \mathcal{L}_0 + \eta \mathcal{L}_R. \tag{F.9}$$
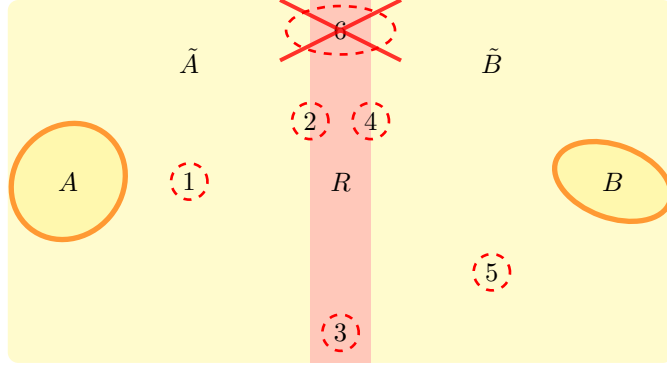
FIGURE F.1: partition of the system used to prove the clustering property for distant operators. The system is partitioned into three regions: $\tilde{A}$, that includes A; $\tilde{B}$, that includes B; and R, a strip that separates $\tilde{A}$ from $\tilde{B}$. The dashed circles represent local contributions to the Lindbladian: regions of types 1 and 5 contribute to $\mathcal{L}_0$; regions of types 2, 3 and 4 contribute to $\mathcal{L}_R$. R is taken thick enough to ensure that no contributions to the Lindbladian come from regions of type 6 (intersecting both $\tilde{A}$ and $\tilde{B}$).

Let $\mathcal{D}_t^{(\eta)} = e^{t\mathcal{L}(\eta)}$ for brevity. This defines a family of quantum channels parametrized by η: for $\eta = 0$ the regions A and B are separated by a barrier R in which no dynamics takes place; increasing η the dynamics in R is turned on, and for $\eta = 1$ one gets the original channel $\mathcal{D}_t^{(1)} \equiv \mathcal{D}_t$.

Equation (F.7) can be proven starting from the fact that $\mathcal{D}_t^{(0)*}$ obeys the following *exact* clustering property:

$$\mathcal{D}_t^{(0)*}\left(\hat{O}_A \hat{O}_B\right) = \mathcal{D}_t^{(0)*}\left(\hat{O}_A\right) \mathcal{D}_t^{(0)*}\left(\hat{O}_B\right), \tag{F.10}$$

which shall be proven separately, and using the following integral representation:

$$\mathcal{D}_t^* = e^{t\mathcal{L}^*} = e^{t\mathcal{L}_0^*} + \int_0^1 d\eta \frac{\partial}{\partial \eta} e^{t\mathcal{L}(\eta)^*} = e^{t\mathcal{L}_0^*} + \int_0^1 d\eta \int_0^t d\beta e^{(t-\beta)\mathcal{L}(\eta)^*} \mathcal{L}_R^* e^{\beta \mathcal{L}(\eta)^*}$$

$$= \mathcal{D}_t^{(0)*} + \int_0^1 d\eta \int_0^t d\beta \mathcal{D}_{t-\beta}^{(\eta)*} \circ \mathcal{L}_R^* \circ \mathcal{D}_\beta^{(\eta)*}. \tag{F.11}$$

Let us denote the second term as $\mathcal{F}_t$. Then following bound holds:

$$\left\|\mathcal{F}_t(\hat{O}_A)\right\|_{\text{op}} \leq \int_0^1 d\eta \int_0^t d\beta \left\|\mathcal{D}_{t-\beta}^{(\eta)*} \circ \mathcal{L}_R^* \circ \mathcal{D}_\beta^{(\eta)*}(\hat{O}_A)\right\|_{\text{op}}$$

$$\leq \int_0^1 d\eta \int_0^t d\beta \left\|\mathcal{L}_R^* \circ \mathcal{D}_\beta^{(\eta)*}(\hat{O}_A)\right\|_{\text{op}}$$

$$\leq \|\mathcal{L}_R^*\|_{\text{op}} \|\hat{O}_A\|_{\text{op}} cV \exp\left(-\frac{d_{AB} - 2vt}{2\xi}\right). \tag{F.12}$$

The second inequality follows from the contractivity of quantum channels; as for the third one, the Markovian LRB (F.2) is invoked to bound the amplitude of $\mathcal{D}_\beta^{(\eta)}(\hat{O}_A)$ in the support

of $\mathcal{L}_R^*$ (which is a distance $\sim \frac{d_{AB}}{2}$ from A). The same reasoning applies to $\hat{O}_B$ and to the product $\hat{O}_A \hat{O}_B$. Finally, applying the exact clustering property (F.10), one has

$$
\left\| \mathcal{D}_t \left(\hat{O}_A \hat{O}_B \right) - \mathcal{D}_t \left(\hat{O}_A \right) \mathcal{D}_t \left(\hat{O}_B \right) \right\|_{\mathrm{op}} = \left\| \mathcal{F}_t \left(\hat{O}_A \hat{O}_B \right) - \mathcal{F}_t \left(\hat{O}_A \right) \mathcal{D}_t^{(0)} \left(\hat{O}_B \right) \right.
$$
$$
\left. - \mathcal{D}_t^{(0)} \left(\hat{O}_A \right) \mathcal{F}_t \left(\hat{O}_B \right) + \mathcal{F}_t \left(\hat{O}_A \right) \mathcal{F}_t \left(\hat{O}_B \right) \right\|_{\mathrm{op}}
$$
$$
\leq 4 \|\mathcal{L}_R\|_{\mathrm{op}} \|\hat{O}_A\|_{\mathrm{op}} \|\hat{O}_B\|_{\mathrm{op}} c V \exp\left(-\frac{d_{AB} - 2vt}{2\xi} \right),
$$
$$(\mathrm{F.13})$$

which is precisely (F.7) after redefining $c' = c\|\mathcal{L}_R\|_{\mathrm{op}}$. $\qquad\square$

We shall now separately prove formula (F.10), which was a key step in the previous proof.

Lemma (exact clustering property) *The channel $\mathcal{D}_t^{(0)*} = e^{t\mathcal{L}^*(0)}$ obeys an exact version of the clustering property* (F.7), *i.e.*

$$
\mathcal{D}_t^{(0)*} \left(\hat{O}_A \hat{O}_B \right) = \mathcal{D}_t^{(0)*} \left(\hat{O}_A \right) \mathcal{D}_t^{(0)*} \left(\hat{O}_B \right). \tag{F.14}
$$

Proof. Consider a Lindbladian $\mathcal{L}_X$ consisting of Lindblad operators $\left\{ \hat{L}_{X,k} \right\}$ supported on $X \subset \Lambda$ and an operator $\hat{O}_Y$ supported on $Y \subset \Lambda$. If $X \cap Y = \emptyset$, then $\mathcal{L}_X^*(\hat{O}_Y) = \hat{O}_Y \mathcal{L}_X^*(\hat{\mathbf{1}})$ (because $\hat{O}_Y$ commutes with all the $\{L_{X,k}\}$). But $\mathcal{L}_X^*(\hat{\mathbf{1}}) = \sum_k (\hat{L}_{X,k}^\dagger \hat{L}_{X,k} - \hat{L}_{X,k}^\dagger \hat{L}_{X,k}) = 0$. Thus, decomposing $\mathcal{L}_0 = \mathcal{L}_{\tilde{A}} + \mathcal{L}_{\tilde{B}}$, one has that $\mathcal{L}^*(\hat{O}_A) = \mathcal{L}_{\tilde{A}}^*(\hat{O}_A)$ and $\mathcal{L}^*(\hat{O}_B) = \mathcal{L}_{\tilde{B}}^*(\hat{O}_B)$. As a consequence, the Leibniz rule applies to the product of any two operators on opposite sides of R:

$$
\mathcal{L}_0^* \left(\hat{O}_{\tilde{A}} \hat{O}_{\tilde{B}} \right) = \mathcal{L}_{\tilde{A}}^* \left(\hat{O}_{\tilde{A}} \right) \hat{O}_{\tilde{B}} + \hat{O}_{\tilde{A}} \mathcal{L}_{\tilde{B}}^* \left(\hat{O}_{\tilde{B}} \right) = \mathcal{L}_0^* \left(\hat{O}_{\tilde{A}} \right) \hat{O}_{\tilde{B}} + \hat{O}_{\tilde{A}} \mathcal{L}_0^* \left(\hat{O}_{\tilde{B}} \right). \tag{F.15}
$$

It follows that, since $\mathcal{L}_{\tilde{A}}^*(\hat{O}_A)$ ($\mathcal{L}_{\tilde{B}}^*(\hat{O}_B)$) is still supported in $\tilde{A}$ ($\tilde{B}$),

$$
\mathcal{D}_t^{(0)*} \left(\hat{O}_A \hat{O}_B \right) = \sum_{k=0}^\infty \frac{t^k}{k!} (\mathcal{L}_0^*)^k \left(\hat{O}_A \hat{O}_B \right) = \sum_{k=0}^\infty \frac{t^k}{k!} \sum_{q=0}^k \binom{k}{q} (\mathcal{L}_0^*)^q \left(\hat{O}_A \right) (\mathcal{L}_0^*)^{k-q} \left(\hat{O}_B \right)
$$
$$
= \sum_{q,j=0}^\infty \frac{t^{q+j}}{q!j!} (\mathcal{L}_0^*)^q \left(\hat{O}_A \right) (\mathcal{L}_0^*)^j \left(\hat{O}_B \right) = \mathcal{D}_t^{(0)*} \left(\hat{O}_A \right) \mathcal{D}_t^{(0)*} \left(\hat{O}_B \right), \tag{F.16}
$$

where the index j was defined as $k - q$. $\qquad\square$

The result can be generalized to Schroedinger-picture channels as well, under an additional hypothesis.

Theorem (open spin systems, Schroedinger picture). *Consider a spin lattice Λ and two operators $\hat{O}_A$ and $\hat{O}_B$ supported on distant regions $A, B \subset \Lambda$. Assuming the dynamics is Markovian and described by local and* normal *Lindblad operators, then the following clustering property* holds:

$$\mathcal{D}_t\left(\hat{O}_A \hat{O}_B\right) \simeq \mathcal{D}_t\left(\hat{O}_A\right) \mathcal{D}_t\left(\hat{O}_B\right), \tag{F.17}$$

up to LRB corrections.

Proof. The only property of the Heisenberg picture that was used in the previous proof is the fact that the adjoint of a Lindbladian always annihilates the identity: $\mathcal{L}^*(\hat{\mathbf{1}}) = 0$. This holds as well in the Schroedinger picture, provided all Lindblad operators are normal: $\mathcal{L}(\hat{\mathbf{1}}) = \sum_k \left[\hat{L}_k, \hat{L}_k^\dagger\right] = 0$. $\qquad\qquad\square$

Remark 1. The assumption of normal Lindblad operators is necessary: it is very easy to provide counter-examples to (F.17) using e.g. ladder operators $\sigma^\pm$ as Lindblad operators.

Remark 2. The whole discussion can be straightforwardly mapped from a spin framework to a fermionic one, provided all Lindblad operators are bosonic. This additional assumption is necessary since otherwise the Jordan-Wigner transformation that implements this mapping would yield non-local Lindblad operators, thus invalidating the key assumption of locality.

Acknowledgements

Bibliography

[1] M. A. Nielsen and I. L. Chuang. *Quantum Computation and Quantum Information.* Cambridge University Press, 2000.

[2] R. S. Ingarden. Quantum information theory. *Reports on Mathematical Physics*, 10 (1):43 – 72, 1976. ISSN 0034-4877. URL `http://www.sciencedirect.com/science/article/pii/0034487776900057`.

[3] R. P. Feynman. Simulating physics with computers. *International Journal of Theoretical Physics*, 21(6-7):467–488, 1982. ISSN 0020-7748. URL `http://dx.doi.org/10.1007/BF02650179`.

[4] D. Deutsch. Quantum theory, the Church-Turing principle and the universal quantum computer. *Proceedings of the Royal Society of London. A. Mathematical and Physical Sciences*, 400(1818):97–117, 1985. URL `http://rspa.royalsocietypublishing.org/content/400/1818/97.abstract`.

[5] P. W. Shor. Algorithms for quantum computation: discrete logarithms and factoring. In *Foundations of Computer Science, 1994 Proceedings., 35th Annual Symposium on*, pages 124–134, Nov 1994.

[6] L. K. Grover. A fast quantum mechanical algorithm for database search. In *Proceedings of the Twenty-eighth Annual ACM Symposium on Theory of Computing*, STOC '96, pages 212–219, New York, NY, USA, 1996. ACM. ISBN 0-89791-785-5. URL `http://doi.acm.org/10.1145/237814.237866`.

[7] P. W. Shor. Scheme for reducing decoherence in quantum computer memory. *Phys. Rev. A*, 52:R2493–R2496, Oct 1995. URL `http://link.aps.org/doi/10.1103/PhysRevA.52.R2493`.

[8] A. R. Calderbank and P. W. Shor. Good quantum error-correcting codes exist. *Phys. Rev. A*, 54:1098–1105, Aug 1996. URL `http://link.aps.org/doi/10.1103/PhysRevA.54.1098`.

[9] D. Aharonov and M. Ben-Or. Fault-tolerant quantum computation with constant error. In *Proceedings of the Twenty-ninth Annual ACM Symposium on Theory of Computing*, STOC '97, pages 176–188, New York, NY, USA, 1997. ACM. ISBN 0-89791-888-6. URL `http://doi.acm.org/10.1145/258533.258579`.

[10] F. Verstraete, M. M. Wolf, and J. I. Cirac. Quantum computation and quantum-state engineering driven by dissipation. *Nature Physics*, 3:633 – 636, 2009. URL `http://www.nature.com/nphys/journal/v5/n9/abs/nphys1342.html`.

[11] J. T. Barreiro, M. Muller, P. Schindler, D. Nigg, T. Monz, M. Chwalla, M. Hennrich, C. F. Roos, P. Zoller, and R. Blatt. An open-system quantum simulator with trapped ions. *Nature*, 470:486 – 491, 2011. URL `http://www.nature.com/nature/journal/v470/n7335/abs/10.1038-nature09801-unlocked.html`.

[12] S. Diehl, E. Rico, M. A. Baranov, and P. Zoller. Topology by dissipation in atomic quantum wires. *Nature Physics*, 7:971 – 977, 2011. URL `http://www.nature.com/nphys/journal/v7/n12/abs/nphys2106.html`.

[13] F. Pastawski, L. Clemente, and J. I. Cirac. Quantum memories based on engineered dissipation. *Phys. Rev. A*, 83:012304, Jan 2011. URL `http://link.aps.org/doi/10.1103/PhysRevA.83.012304`.

[14] J. P. Paz and W. H. Zurek. Continuous error correction. *Proceedings of the Royal Society of London. Series A: Mathematical, Physical and Engineering Sciences*, 454 (1969):355–364, 1998. URL `http://rspa.royalsocietypublishing.org/content/454/1969/355.abstract`.

[15] M. Sarovar and G. J. Milburn. Continuous quantum error correction by cooling. *Phys. Rev. A*, 72:012306, Jul 2005. URL `http://link.aps.org/doi/10.1103/PhysRevA.72.012306`.

[16] A. Y. Kitaev. Unpaired Majorana fermions in quantum wires. *Physics-Uspekhi*, 44 (10S):131, 2001. URL `http://stacks.iop.org/1063-7869/44/i=10S/a=S29`.

[17] N. Read and D. Green. Paired states of fermions in two dimensions with breaking of parity and time-reversal symmetries and the fractional quantum Hall effect. *Phys. Rev. B*, 61:10267–10297, Apr 2000. URL `http://link.aps.org/doi/10.1103/PhysRevB.61.10267`.

[18] G. E. Volovik. Fermion zero modes on vortices in chiral superconductors. *Journal of Experimental and Theoretical Physics Letters*, 70(9):609–614, 1999. ISSN 0021-3640. URL `http://dx.doi.org/10.1134/1.568223`.

[19] J. Alicea. New directions in the pursuit of Majorana fermions in solid state systems. *Reports on Progress in Physics*, 75(7):076501, 2012. URL `http://stacks.iop.org/0034-4885/75/i=7/a=076501`.

[20] L. Mazza, M. Rizzi, M. D. Lukin, and J. I. Cirac. Robustness of quantum memories based on Majorana zero modes. *Phys. Rev. B*, 88:205142, Nov 2013. URL `http://link.aps.org/doi/10.1103/PhysRevB.88.205142`.

[21] I. Bengtsson and K. Zyczkowski. *Geometry of Quantum States*. Cambridge University Press, 2006.

[22] J. J. Sakurai. *Modern Quantum Mechanics*. Addison-Wesley, 1993.

[23] H. P. Breuer and F. Petruccione. *The theory of open quantum systems*. Oxford University Press, Great Clarendon Street, 2002.

[24] K. Kraus, A. Bohm, J. D. Dollard, and W. H. Wootters, editors. *States, Effects, and Operations Fundamental Notions of Quantum Theory*, volume 190 of *Lecture Notes in Physics, Berlin Springer Verlag*, 1983.

[25] G. Lindblad. On the generators of quantum dynamical semigroups. *Communications in Mathematical Physics*, 48(2):119–130, 1976. URL `http://dx.doi.org/10.1007/BF01608499`.

[26] A. Gilchrist, N. K. Langford, and M. A. Nielsen. Distance measures to compare real and ideal quantum processes. *Phys. Rev. A*, 71:062310, Jun 2005. URL `http://link.aps.org/doi/10.1103/PhysRevA.71.062310`.

[27] R. Jozsa. Fidelity for mixed quantum states. *Journal of Modern Optics*, 41(12):2315–2323, 1994. URL `http://dx.doi.org/10.1080/09500349414552171`.

[28] M. D. Choi. Completely positive linear maps on complex matrices. *Linear Algebra and its Applications*, 10(3):285 – 290, 1975. ISSN 0024-3795. URL `http://www.sciencedirect.com/science/article/pii/0024379575900750`.

[29] C. Weedbrook, S. Pirandola, R. Garcia-Patron, N. J. Cerf, T. C. Ralph, J. H. Shapiro, and S. Lloyd. Gaussian quantum information. *Rev. Mod. Phys.*, 84:621–669, May 2012. URL `http://link.aps.org/doi/10.1103/RevModPhys.84.621`.

[30] M. B. Ruskai, S. Szarek, and E. Werner. An analysis of completely-positive trace-preserving maps on $\mathcal{M}_2$. *Linear Algebra and its Applications*, 347(1–3):159 – 187, 2002. ISSN 0024-3795. URL `http://www.sciencedirect.com/science/article/pii/S002437950100547X`.

[31] W. K. Wootters and W. H. Zurek. A single quantum cannot be cloned. *Nature*, 299:802–803, Oct 1982. URL `http://www.nature.com/nature/journal/v299/n5886/abs/299802a0.html`.

[32] D. A. Lidar and T. A. Brun. *Quantum Error Correction*. Cambridge University Press, 2013. ISBN 9780521897877.

[33] D. Gottesman. Stabilizer codes and quantum error correction. *Caltech PhD Thesis*, 1997. URL `http://arxiv.org/abs/quant-ph/9705052`.

[34] W. M. Itano, D. J. Heinzen, J. J. Bollinger, and D. J. Wineland. Quantum Zeno effect. *Phys. Rev. A*, 41:2295–2300, Mar 1990. URL `http://link.aps.org/doi/10.1103/PhysRevA.41.2295`.

[35] D. V. Averin and R. Fazio. Active suppression of decoherence in Josephson-junction qubits. *Journal of Experimental and Theoretical Physics Letters*, 78(10):664–668, 2003. ISSN 0021-3640. URL `http://dx.doi.org/10.1134/1.1644314`.

[36] C. Ahn, A. C. Doherty, and A. J. Landahl. Continuous quantum error correction via quantum feedback control. *Phys. Rev. A*, 65:042301, Mar 2002. URL `http://link.aps.org/doi/10.1103/PhysRevA.65.042301`.

[37] M. Sarovar and G. J. Milburn. Continuous quantum error correction, 2005. URL `http://dx.doi.org/10.1117/12.608548`.

[38] C.-K. Li, M. Nakahara, Y.-T. Poon, N.-S. Sze, and H. Tomita. Recovery in quantum error correction for general noise without measurement. *ArXiv e-prints*, February 2011. URL `http://arxiv.org/abs/1102.1618`.

[39] B. Horstmann, J. I. Cirac, and G. Giedke. Noise-driven dynamics and phase transitions in fermionic systems. *Phys. Rev. A*, 87:012108, Jan 2013. URL `http://link.aps.org/doi/10.1103/PhysRevA.87.012108`.

[40] R. Laflamme, C. Miquel, J. P. Paz, and W. H. Zurek. Perfect quantum error correcting code. *Phys. Rev. Lett.*, 77:198–201, Jul 1996. URL `http://link.aps.org/doi/10.1103/PhysRevLett.77.198`.

[41] H. F. Trotter. On the product of semi-groups of operators. *Proceedings of the American Mathematical Society*, 10:545 – 551, 1959. URL `http://www.ams.org/journals/proc/1959-010-04/S0002-9939-1959-0108732-6/`.

[42] W. Janke and T. Sauer. Properties of higher-order Trotter formulas. *Physics Letters A*, 165(3):199 – 205, 1992. ISSN 0375-9601. URL `http://www.sciencedirect.com/science/article/pii/037596019290035K`.

[43] A. Y. Kitaev. Fault-tolerant quantum computation by anyons. *Annals of Physics*, 303 (1):2 – 30, 2003. ISSN 0003-4916. URL http://www.sciencedirect.com/science/article/pii/S0003491602000180.

[44] R. Alicki, M. Fannes, and M. Horodecki. On thermalization in Kitaev's 2D model. *Journal of Physics A: Mathematical and Theoretical*, 42(6):065303, 2009. URL http://stacks.iop.org/1751-8121/42/i=6/a=065303.

[45] F. Pastawski, A. Kay, N. Schuch, and J. I. Cirac. Limitations of passive protection of quantum information. *Quantum Info. Comput.*, 10(7):580–618, July 2010. ISSN 1533-7146. URL http://dl.acm.org/citation.cfm?id=2011373.2011376.

[46] S. Bravyi and B. Terhal. A no-go theorem for a two-dimensional self-correcting quantum memory based on stabilizer codes. *New Journal of Physics*, 11(4):043029, 2009. URL http://stacks.iop.org/1367-2630/11/i=4/a=043029.

[47] R. Alicki, M. Horodecki, P. Horodecki, and R. Horodecki. On thermal stability of topological qubit in Kitaev's 4D model. *ArXiv e-prints*, November 2008. URL http://arxiv.org/abs/0811.0033.

[48] F. L. Pedrocchi, A. Hutter, J. R. Wootton, and D. Loss. Enhanced thermal stability of the toric code through coupling to a bosonic bath. *Phys. Rev. A*, 88:062313, Dec 2013. URL http://link.aps.org/doi/10.1103/PhysRevA.88.062313.

[49] S. Bravyi and J. Haah. Quantum self-correction in the 3D cubic code model. *Phys. Rev. Lett.*, 111:200501, Nov 2013. URL http://link.aps.org/doi/10.1103/PhysRevLett.111.200501.

[50] H. Bombin, R. W. Chhajlany, M. Horodecki, and M. A. Martin-Delgado. Self-correcting quantum computers. *New Journal of Physics*, 15(5):055023, 2013. URL http://stacks.iop.org/1367-2630/15/i=5/a=055023.

[51] E. Majorana. Teoria simmetrica dell'elettrone e del positrone. *Il Nuovo Cimento*, 14 (4):171–184, 1937. ISSN 0029-6341. URL http://dx.doi.org/10.1007/BF02961314.

[52] F. Wilczek. Majorana returns. *Nature Physics*, 5:614 – 618, 2009. URL http://www.nature.com/nphys/journal/v5/n9/abs/nphys1380.html.

[53] D. A. Ivanov. Non-Abelian statistics of half-quantum vortices in p-wave superconductors. *Phys. Rev. Lett.*, 86:268–271, Jan 2001. URL http://link.aps.org/doi/10.1103/PhysRevLett.86.268.

[54] A. Kitaev and C. Laumann. Topological phases and quantum computation. *ArXiv e-prints*, April 2009. URL http://arxiv.org/abs/0904.2771.

[55] C. W. J. Beenakker. Search for Majorana fermions in superconductors. *Annual Review of Condensed Matter Physics*, 4(1):113–136, 2013. URL `http://www.annualreviews.org/doi/abs/10.1146/annurev-conmatphys-030212-184337`.

[56] J. D. Sau, R. M. Lutchyn, S. Tewari, and S. Das Sarma. Generic new platform for topological quantum computation using semiconductor heterostructures. *Phys. Rev. Lett.*, 104:040502, Jan 2010. URL `http://link.aps.org/doi/10.1103/PhysRevLett.104.040502`.

[57] J. D. Sau, C. H. Lin, H.-Y. Hui, and S. Das Sarma. Avoidance of Majorana resonances in periodic topological superconductor-nanowire structures. *Phys. Rev. Lett.*, 108:067001, Feb 2012. URL `http://link.aps.org/doi/10.1103/PhysRevLett.108.067001`.

[58] R. M. Lutchyn, J. D. Sau, and S. Das Sarma. Majorana fermions and a topological phase transition in semiconductor-superconductor heterostructures. *Phys. Rev. Lett.*, 105:077001, Aug 2010. URL `http://link.aps.org/doi/10.1103/PhysRevLett.105.077001`.

[59] Y. Oreg, G. Refael, and F. von Oppen. Helical liquids and Majorana bound states in quantum wires. *Phys. Rev. Lett.*, 105:177002, Oct 2010. URL `http://link.aps.org/doi/10.1103/PhysRevLett.105.177002`.

[60] V. Mourik, K. Zuo, S. M. Frolov, S. R. Plissard, E. P. A. M. Bakkers, and L. P. Kouwenhoven. Signatures of Majorana fermions in hybrid superconductor-semiconductor nanowire devices. *Science*, 336(6084):1003–1007, 2012. URL `http://www.sciencemag.org/content/336/6084/1003.abstract`.

[61] M. T. Deng, C. L. Yu, G. Y. Huang, M. Larsson, P. Caroff, and H. Q. Xu. Anomalous zero-bias conductance peak in a Nb–InSb nanowire–Nb hybrid device. *Nano Letters*, 12(12):6414–6419, 2012. URL `http://pubs.acs.org/doi/abs/10.1021/nl303758w`.

[62] C.-H. Lin, J. D. Sau, and S. Das Sarma. Zero-bias conductance peak in Majorana wires made of semiconductor/superconductor hybrid structures. *Phys. Rev. B*, 86:224511, Dec 2012. URL `http://link.aps.org/doi/10.1103/PhysRevB.86.224511`.

[63] S. Das Sarma, J. D. Sau, and T. D. Stanescu. Splitting of the zero-bias conductance peak as smoking gun evidence for the existence of the Majorana mode in a superconductor-semiconductor nanowire. *Phys. Rev. B*, 86:220506, Dec 2012. URL `http://link.aps.org/doi/10.1103/PhysRevB.86.220506`.

[64] D. Roy, N. Bondyopadhaya, and S. Tewari. Topologically trivial zero-bias conductance peak in semiconductor Majorana wires from boundary effects. *Phys. Rev. B*, 88:020502, Jul 2013. URL `http://link.aps.org/doi/10.1103/PhysRevB.88.020502`.

[65] M.-C. Bañuls, J. I. Cirac, and M. M. Wolf. Entanglement in systems of indistinguishable fermions. *Journal of Physics: Conference Series*, 171(1):012032, 2009. URL `http://stacks.iop.org/1742-6596/171/i=1/a=012032`.

[66] F. Hassler. Majorana qubits. *ArXiv e-prints*, April 2014. URL `http://arxiv.org/abs/1404.0897`.

[67] F. Hassler, A. R. Akhmerov, and C. W. J. Beenakker. The top-transmon: a hybrid superconducting qubit for parity-protected quantum computation. *New Journal of Physics*, 13(9):095004, 2011. URL `http://stacks.iop.org/1367-2630/13/i=9/a=095004`.

[68] F. Buscemi. All entangled quantum states are nonlocal. *Phys. Rev. Lett.*, 108:200401, May 2012. URL `http://link.aps.org/doi/10.1103/PhysRevLett.108.200401`.

[69] A. Einstein, B. Podolsky, and N. Rosen. Can quantum-mechanical description of physical reality be considered complete? *Phys. Rev.*, 47:777–780, May 1935. URL `http://link.aps.org/doi/10.1103/PhysRev.47.777`.

[70] D. Poulin. Stabilizer formalism for operator quantum error correction. *Phys. Rev. Lett.*, 95:230504, Dec 2005. URL `http://link.aps.org/doi/10.1103/PhysRevLett.95.230504`.

[71] M. Herold, E. T. Campbell, J. Eisert, and M. J. Kastoryano. Cellular-automaton decoders for topological quantum memories. June 2014. URL `http://arxiv.org/abs/1406.2338`.

[72] E. H. Lieb and D. W. Robinson. The finite group velocity of quantum spin systems. *Communications in Mathematical Physics*, 28(3):251–257, 1972. ISSN 0010-3616. URL `http://dx.doi.org/10.1007/BF01645779`.

[73] S. Bravyi, M. B. Hastings, and F. Verstraete. Lieb-Robinson bounds and the generation of correlations and topological quantum order. *Phys. Rev. Lett.*, 97:050401, Jul 2006. URL `http://link.aps.org/doi/10.1103/PhysRevLett.97.050401`.

[74] B. Nachtergaele and R. Sims. Much ado about something: Why Lieb-Robinson bounds are useful. *IAMP Bulletin*, pages 22–29, Oct 2010. URL `http://www.iamp.org/bulletins/old-bulletins/201010.pdf`.

[75] M. Cheneau, P. Barmettler, D. Poletti, M. Endres, P. Schausz, T. Fukuhara, C. Gross, I. Bloch, C. Kollath, and S. Kuhr. Light-cone-like spreading of correlations in a quantum many-body system. *Nature*, 481:484–487, Jan 2012. URL `http://dx.doi.org/10.1038/nature10748`.

[76] D. Poulin. Lieb-Robinson bound and locality for general Markovian quantum dynamics. *Phys. Rev. Lett.*, 104:190401, May 2010. URL `http://link.aps.org/doi/10.1103/PhysRevLett.104.190401`.

[77] M. B. Hastings. Decay of correlations in Fermi systems at nonzero temperature. *Phys. Rev. Lett.*, 93:126402, Sep 2004. URL `http://link.aps.org/doi/10.1103/PhysRevLett.93.126402`.